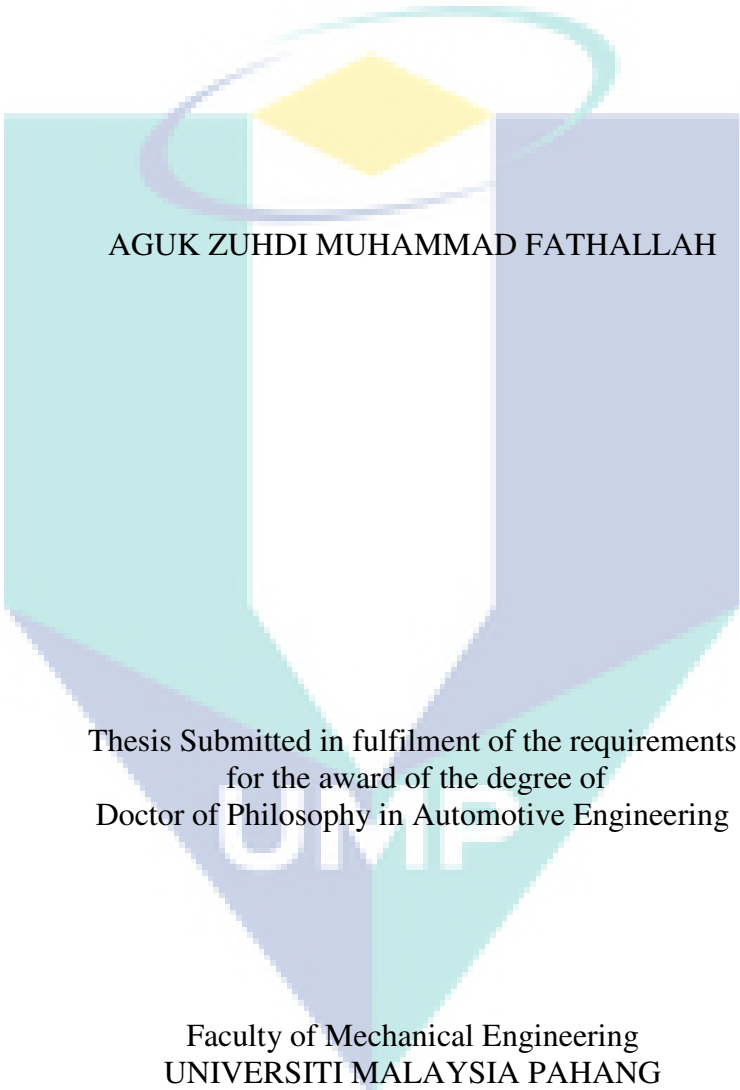


DESIGN AND SIMULATION OF A SINGLE CYLINDER HIGH SPEED SPARK
IGNITION LINEAR ENGINE WITH SPRING SYSTEM

The logo of the University of Malaysia Pahang (UMP) is a shield-shaped emblem. It features a central white vertical stripe. The left side of the shield is light blue, and the right side is a darker blue. At the top center, there is a yellow diamond shape. A stylized, glowing ring in shades of blue and green encircles the yellow diamond. The text 'AGUK ZUHDI MUHAMMAD FATHALLAH' is printed across the middle of the shield.

AGUK ZUHDI MUHAMMAD FATHALLAH

Thesis Submitted in fulfilment of the requirements
for the award of the degree of
Doctor of Philosophy in Automotive Engineering

Faculty of Mechanical Engineering
UNIVERSITI MALAYSIA PAHANG

MARCH 2011

SUPERVISOR'S DECLARATION

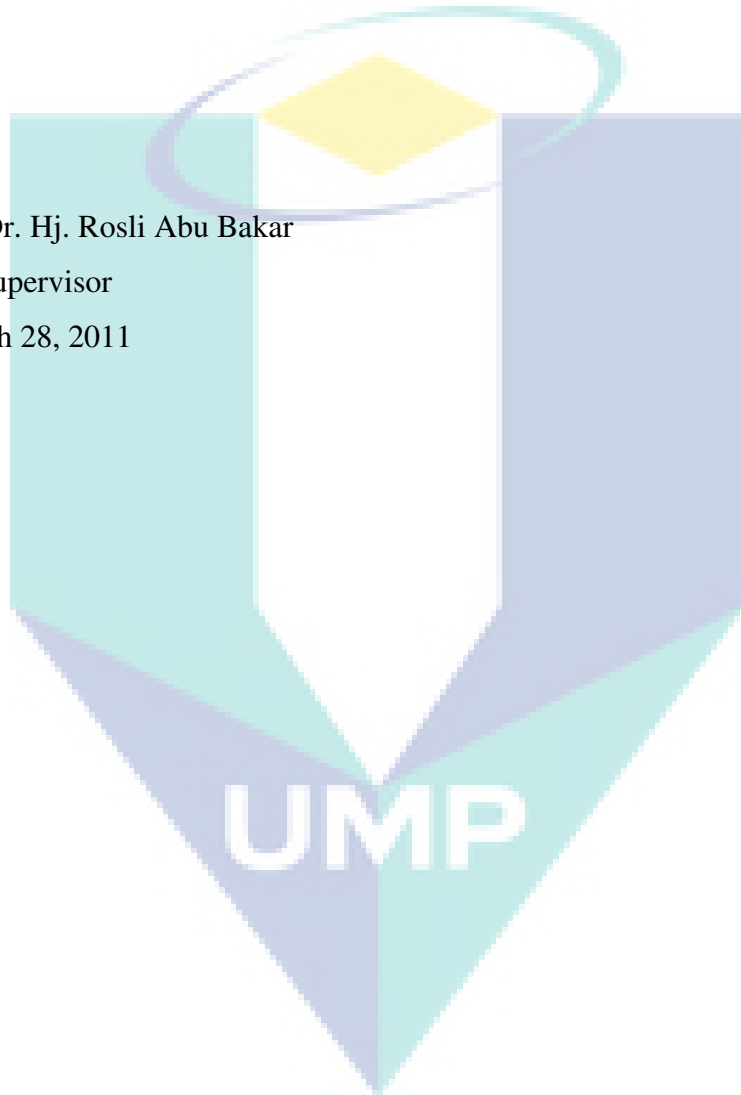
I hereby declare that I have checked this thesis and in my opinion, this thesis is adequate in terms of scope and quality for the award of the degree of Doctor of Philosophy in Automotive Engineering.

Signature

Professor Dr. Hj. Rosli Abu Bakar

Position: Supervisor

Date: March 28, 2011



STUDENT'S DECLARATION

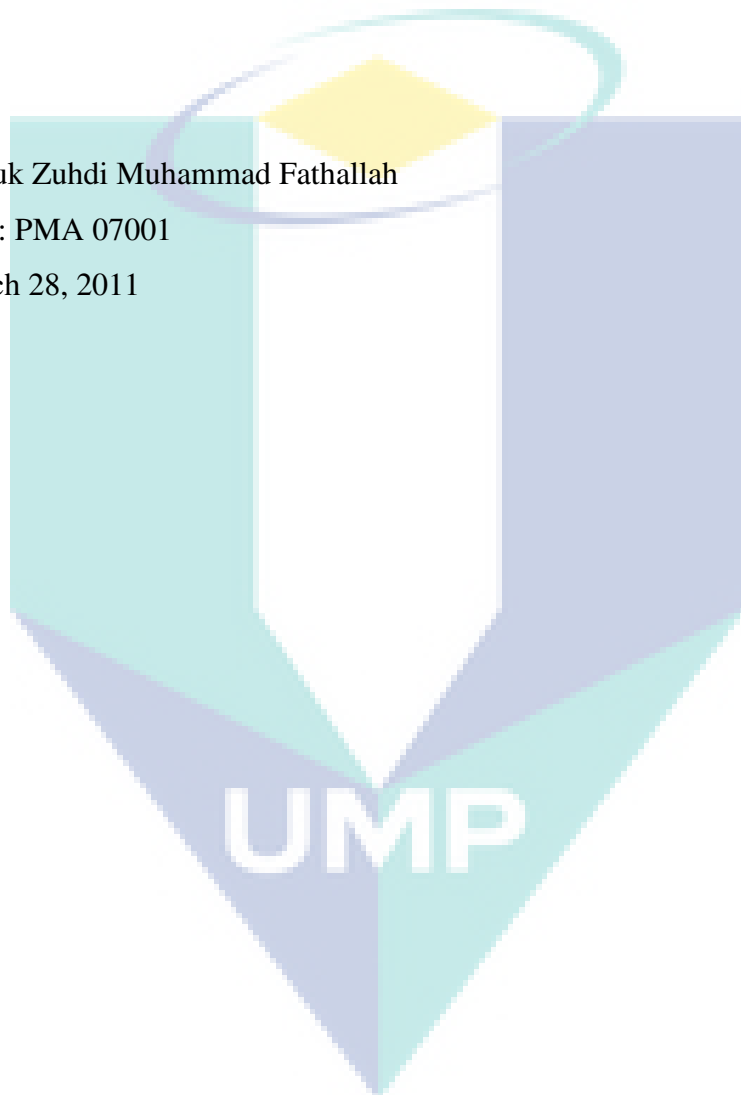
I hereby declare that the work in this thesis is my own except for quotations and summaries which have been duly acknowledged. The thesis has not been accepted for any degree and is not concurrently submitted for award of other degree.

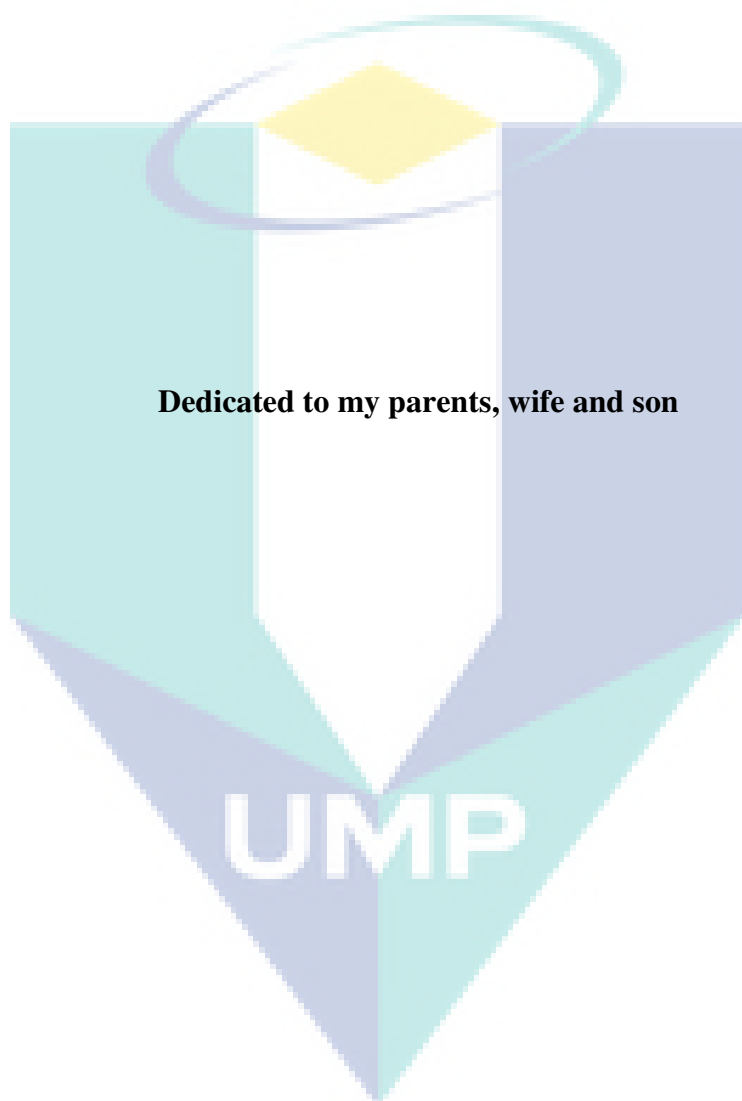
Signature

Name: Aguk Zuhdi Muhammad Fathallah

ID Number: PMA 07001

Date: March 28, 2011



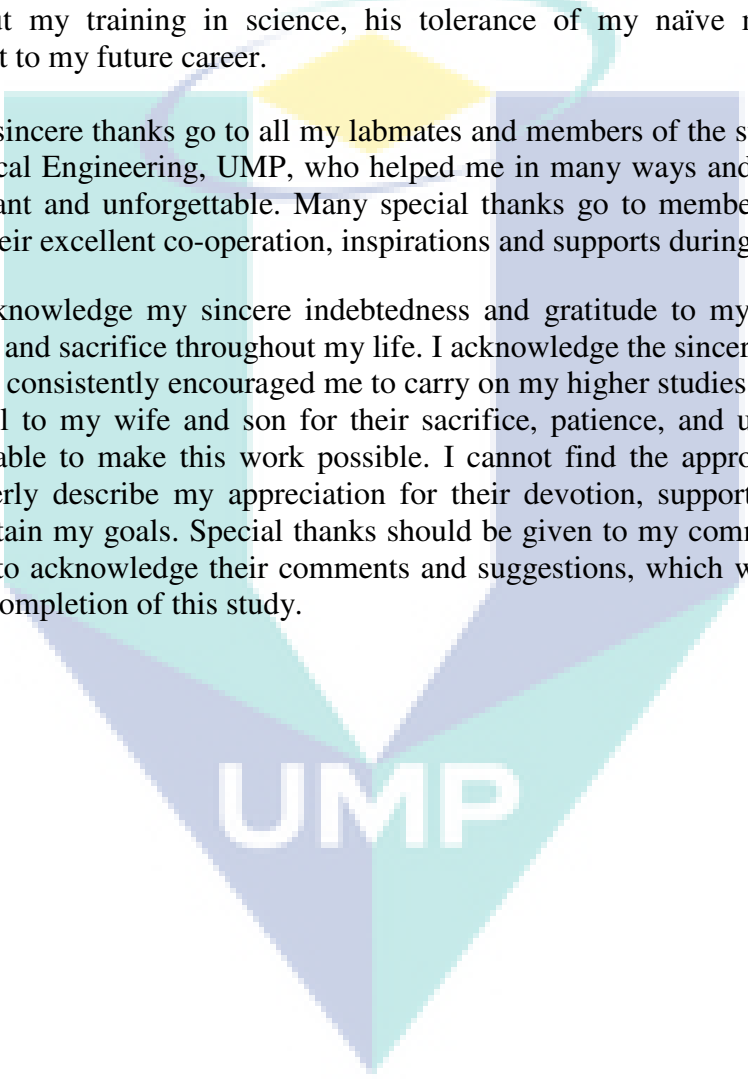


ACKNOWLEDGEMENTS

I am grateful and would like to express my sincere gratitude to my supervisor Professor Dr. Hj. Rosli Abu Bakar for his germinal ideas, invaluable guidance, continuous encouragement and constant support in making this research possible. He has always impressed me with his outstanding professional conduct, his strong conviction for science, and his belief that a PhD program is only a start of a life-long learning experience. I appreciate his consistent support from the first day I applied to graduate program to these concluding moments. I am truly grateful for his progressive vision about my training in science, his tolerance of my naïve mistakes, and his commitment to my future career.

My sincere thanks go to all my labmates and members of the staff of the Faculty of Mechanical Engineering, UMP, who helped me in many ways and made my stay at UMP pleasant and unforgettable. Many special thanks go to member engine research group for their excellent co-operation, inspirations and supports during this study.

I acknowledge my sincere indebtedness and gratitude to my parents for their love, dream and sacrifice throughout my life. I acknowledge the sincerity of my parents-in-law, who consistently encouraged me to carry on my higher studies in Malaysia. I am also grateful to my wife and son for their sacrifice, patience, and understanding that were inevitable to make this work possible. I cannot find the appropriate words that could properly describe my appreciation for their devotion, support and faith in my ability to attain my goals. Special thanks should be given to my committee members. I would like to acknowledge their comments and suggestions, which was crucial for the successful completion of this study.

The logo of Universiti Malaysia Perlis (UMP) is a large, stylized 'V' shape composed of several overlapping triangles in shades of teal, light blue, and yellow. The letters 'UMP' are written in a bold, white, sans-serif font across the center of the 'V' shape.

UMP

ABSTRACT

This thesis deals with the design of a single cylinder high-speed spark ignition linear engine with a spring system return cycle. The main objective of the research is to design and analyse a free piston linear engine that is easy to start, easy to maintain and easy to control. The unique design of the spring as a return cycle in a free piston linear engine is presented and its effects on engine performance and motion are discussed. The engine performance has been predicted the aim is to design a linear engine particularly for the spring system. The spring design has been optimised by using a multilevel optimization approach. Based on the optimisation of the spring design, the linear engine geometry design has been conducted. The performance of the linear engine design has been measured and the results compared with the predicted performance. Besides which the motion of the linear engine has been studied; however, friction affect show the rotated of the piston. It is necessary to modify the spring mechanism to ensure that the scavenging process works properly. Two scenarios such as the removal of the bottom part of the piston skirt and adding a lock to the connecting rod are recommended, based of structural stress and thermal-structural stress analysis. Software has been used in the research to analyse the design of the free piston linear engine with a spring system, including GT-Power, SolidWorks, Matlab, Algor, and Spread-Sheet. The model has been built using GT-Power to predict the engine performance. To validate the model, it has been assessed with the original engine manual and experimentally. Three step multilevel optimisation of the spring geometry has been carried out by using Matlab and Spread-Sheet. SolidWorks has been used to design all of the components and for the assembly of the linear engine. Cosmos motion, which is a part of the SolidWorks facility, has been used to analyse the piston dynamics of the linear engine. Once again, GT-Power has been used to analyse the effect of the spring design on the linear engine performance. For the modification of the design of the spring system, Algor has been used to analyse the thermal-structural stress of the piston and the connecting rod. Through step by step considerations started from building model to predict the performance of linear engine, to optimize the spring geometry design then continued build the free piston linear engine with spring system including design, analyses and modified. The result is a design which predicts the performance and the dynamics of piston motion. Only 50% of the 12 speeds sampled worked correctly. The rotation of the piston on the Z-ordinate can be fixed through modification of the piston or connecting rod. A design of a single cylinder high-speed spark ignition linear engine with spring system as return cycle has been carried out. Although the range of speeds was narrow compared to a conventional engine, the maximum power output is still higher. The final design result was 1.03 kW at 3.6 m/sec.

.

ABSTRAK

Tesis ini berkaitan dengan merencanakan sebuah mesin pencucian bunga api berkelajuan tinggi yang berbentuk mesin linier dengan menggunakan sistem pegas sebagai kitar kembali. Tujuan utama kajian ini adalah untuk merencanakan dan mengkaji mesin linier putaran bebas yang mudah dimulakan, mudah dibuat penyenggaraan dan senang dikawal. Keistimewaan pegas sebagai kitaran kembali didalam mesin linier piston bebas telah ditunjukkan dan pengaruhnya keatas prestasi mesin dan pergerakannya dibincangkan. Prestasi mesin telah diramalkan mengikut rekabentuk mesin linier terutama menggunakan mekanisme pegas. Rekabentuk pegas telah dioptimumkan dengan pendekatan pengoptimum secara berperingkat. Berdasarkan keputusan optimasi rekabentuk pegas, geometri daripada rekabentuk mesin linier telah dapat dilakukan. Prestasi rekabentuk mesin linier telah dikaji dan hasilnya dibandingkan dengan prestasi ramalan. Selain itu, daripada pergerakan mesin linier yang telah dipelajari geseran dapat ditunjukkan dengan pengaruh pusingan piston. Dengan itu pergerakan mekanisme pegas perlu ditukar untuk dapat memastikan proses menghapus sisa boleh bekerja dengan baik. Dua keadaan yang mana pemotongan bahagian bawah dinding piston dan penambahan kekunci pada rod penyambung dicadangkan mengikut kajian ketegangan struktur dan ketegangan terma-struktural. Beberapa perisian telah digunakan kerana untuk mengkaji rekabentuk mesin linear piston bebas dengan sistem pegas, iaitu GT-Power, SolidWorks, Matlab, Algor, dan Spread-Sheet. Sebuah model telah dibina dengan menggunakan GT-Power untuk meramal prestasi mesin. Untuk pengesahan model ini telah dibuat pemeriksaan dengan menggunakan buku panduan asli dan eksperimen. Dengan menggunakan Matlab dan Spread-Sheet untuk mendapat optimum peringkat ketiga bagi merencanakan geometri pegas. SolidWorks telah digunakan untuk merencanakan semua bahagian dan pemasangan mesin linier. Cosmos Motion yang merupakan sebahagian daripada kemudahan SolidWorks telah digunakan untuk mengkaji dinamik piston daripada mesin linier. GT-Power telah digunakan sekali lagi untuk mengkaji kesan daripada rekabentuk pegas pada prestasi mesin linier. Untuk mengubahsuai rekabentuk sistem pegas, Algor telah digunakan untuk mengkaji tegangan terma-struktural daripada piston dan rod penyambung. Melalui langkah demi langkah bermula daripada pertimbangan pembentukan model untuk meramal prestasi mesin linier, untuk optimasi perancangan geometri pegas seterusnya membina mesin linier piston bebas dengan sistem pegas, iaitu merencanakan, mengkaji dan mengubahsuai. Hasilnya adalah sebuah rekabentuk yang telah diramal prestasi dan gerak dinamik daripada piston nya. Dari 12 kelajuan sebagai pembolehubahnya hanya 50% kelajuan boleh bekerja dengan baik. Putaran piston pada paksi Z boleh diperbaiki dengan pengubahsuaian dari piston atau rod penyambung. Rekabentuk mesin pencucian bunga api berkelajuan tinggi mesin linier dengan menggunakan sistem pegas sebagai kitar kembali telah dilakukan. Walaupun kelajuan mesin menurun berbanding dengan mesin konvensional, tetapi output kuasa maksimum masih lagi tinggi. Keputusan rekabentuk akhir adalah sebanyak 1.03 kW pada 3.6 m/saat.

TABLE OF CONTENTS

	Page
SUPERVISOR’S DECLARATION	ii
STUDENT’S DECLARATION	iii
ACKNOWLEDGEMENTS	v
ABSTRACT	vi
ABSTRAK	vii
TABLE OF CONTENTS	viii
LIST OF TABLES	xiii
LIST OF FIGURES	xvi
LIST OF SYMBOLS	xxiv
LIST OF ABBREVIATIONS	xxviii
CHAPTER 1 INTRODUCTION	
1.1 Back Ground	1
1.2 Problem Statement	2
1.3 Objectives	3
1.4 Scope and Limitations	3
1.4.1 Scope	3
1.4.2 Limitations	4
CHAPTER 2 LITERATURE REVIEW AND THEORITICAL BACKGROUND	
2.1 Introduction	5
2.2 Paper Reviews	5
2.2.1 Historical Perspective	5
2.2.2 Basic Concept of Linear Engine	8
2.2.3 Researches Development	10
2.2.3.1 Research Development Base Applications	11
2.2.3.1.1 Free-Piston Hydraulics Pump Researches Development	11

2.2.3.1.2	Free-Piston Air Compressor Researches Development.	13
2.2.3.1.3	Free-Piston Alternator Researches Development	14
2.2.3.2.	Research Development Base Designs Configuration	16
2.1.3.2.1.	Free Piston Research Development Based Single Piston Combustion Chamber	17
2.1.3.2.2.	Free Piston Research Development Based Dual Piston	19
2.1.3.2.3.	Free Piston Research Development Based Opposed Piston	24
2.2.3.3.	Research Development Base Research Groups	25
2.2.3.3.1.	The National Aeronotical and Space Administration (NASA)	26
2.2.3.3.2.	West Virginia University (WVU)	27
2.2.3.3.3.	Solo Kleinmotorn	29
2.2.3.3.4.	Sandia National Laboratories	30
2.2.3.3.5.	Royal Institute of Technology	32
2.2.3.3.5.	Sunpower Inc	33
2.2.3.3.6.	Inas B.V.	34
2.2.3.3.7.	Aerodyne Research Inc. (ARI).	36
2.3	Theoretical Background	38
2.3.1	Design Method.	38
2.3.2	Heat Release	38
2.3.3	Friction Force	40
2.3.4	Optimization of Spring Design	42
2.3.5.	The Dynamic Model for Motion Studies	47
2.4	Conclusions	49

CHAPTER 3 RESEARCH METHODS

3.1	Introduction	50
3.2	Flow Chart, Model and Validation	51
3.2.1	Flow Chart of the Research	51
3.2.2	Model and Validation Technique	53
3.3	Method for Prediction of the Engine's Performance	54

3.4	Spring Design Optimization Method	55
3.5	Linear Engine Design Method	57
3.6	Effect of Spring Design on Linear Engine Performance Analyses Method	58
3.7	Dynamic Motion Analysis Method	59
3.8	Analysis Methods for Spring System Modification	60
3.9	Conclusion	61

CHAPTER 4 RESULTS AND ANALYSES

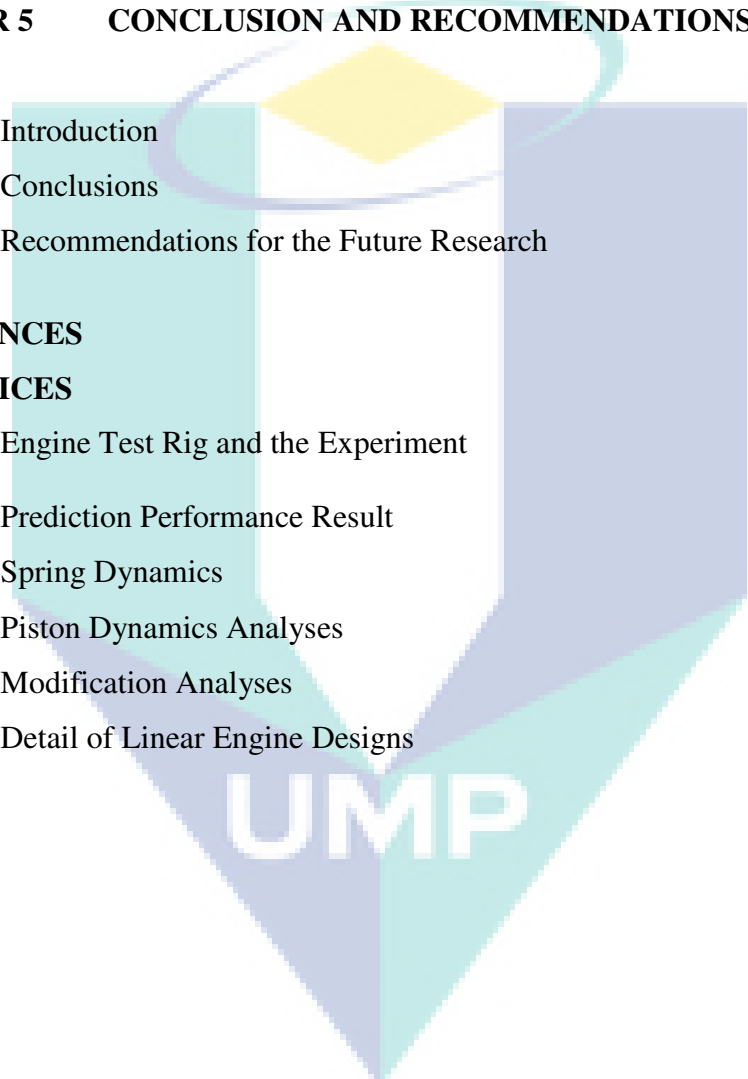
4.1	Building Model and Validation	63
4.1.1	D GT-Power Engine Simulation Model	63
4.2.1	Back Pack Brush Cutter	64
4.2.2	Model	65
4.1.2	Validation	67
4.3.1	Validation with Back Pack Brush Cutter Guide Manual	67
4.3.2	Validation with Experimental data	69
4.1.3	Summary	71
4.2	Prediction Studies for the performance of a single cylinder high speed spark ignition linear engine with spring system	73
4.2.1	Engine Dynamics	73
4.2.2	Prediction method	75
4.2.2.1	Friction Force	76
4.2.2.2	Modification of Model	78
4.2.3	Results	79
4.2.4	Discussion	87
4.2.5	Summary	88
4.3	Design and Optimization of Spring for Two Stroke Single Cylinder Spark Ignition Linear Engine	90
4.3.1	Material and Spring Design Optimisation Method	91
4.3.2.	Basic Equation for Spring of Round Wire	94
4.3.2	Results	104
4.3.3	Discussion	109
4.3.4	Summary	110
4.4	Linear Engine Design	111
4.4.1	Process of Design	111
4.4.2	Results	112

	4.4.2.1 Linear Engine Design Configuration	113
	4.4.2.2 Oscillation Control System	113
	4.4.2.3 Isometric View Design	116
	4.4.3 Discussion	118
	4.4.4 Summary	118
4.5	Analyses Studies of Linear Engine Design	119
	4.5.1 Effect of Spring System Design on the Engine's Performance	119
	4.5.1.1 Effect of Spring System on Linear Engine Performance Studies	120
	4.5.1.2 Effect of Spring System on Linear Engine Performance	123
	4.5.1.3 Discussion	126
	4.5.2 Effect of Spring System Design on Piston Dynamics	128
	4.5.2.1 Numerical Simulation of Linear Engine	129
	4.5.2.2 Engine Model and Dynamics Simulation Methods	131
	4.5.2.3 Effect of Spring System on Piston Dynamics Results	134
	4.5.2.3.1 Basic Considerations	134
	4.5.2.3.2 Effect of Friction on Piston Dynamics	135
	4.5.2.3.3 Effect of Spring Design on Piston Dynamics	138
	4.5.3 Discussion	142
	4.5.3 Summary	144
4.6	Design Modification	146
	4.6.1 Scenario of Design Modification	146
	4.6.2 Modifications Analyses Methods	149
	4.6.2.1 The Basics of Finite Element Technique and Software	151
	4.6.2.2 Governor Equations	152
	4.6.2.2.1 Heat Transfer Analysis	153
	4.6.2.2.2 Elasticity Analysis	155
	4.6.2.3 Model and Discretization	160
	4.6.3 Results of the Analysis Modifications	163
	4.6.3.1 Structural Stress of Pistons	164

4.6.3.2	Thermal Stress of Pistons	165
4.6.3.3	Thermal-Structural Stress of Pistons	168
4.6.3.4	Structural Stress of Connecting Rod	170
4.6.4	Discussion	172
4.6.5.	Summary	173
4.7	Conclusion	174

CHAPTER 5 CONCLUSION AND RECOMMENDATIONS

5.1	Introduction	175
5.2	Conclusions	175
5.3	Recommendations for the Future Research	177
	REFERENCES	178
	APPENDICES	186
A	Engine Test Rig and the Experiment	187
B	Prediction Performance Result	196
C	Spring Dynamics	217
D	Piston Dynamics Analyses	227
E	Modification Analyses	238
F	Detail of Linear Engine Designs	256



UMP

LIST OF TABLES

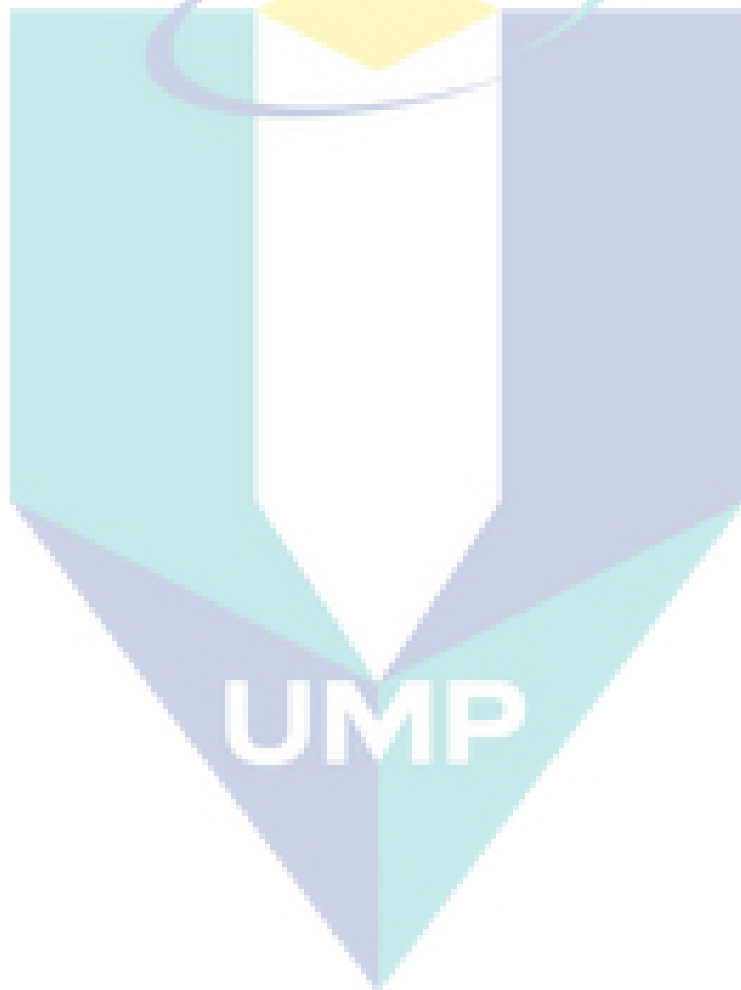
Table No.	Title	Page
4.1.1	Back pack brush cutter engine specification	65
4.3.1	Speed, IMEP and thrust force of engine performance	93
4.3.2	Springs Design Result	95
4.5.1	Geometry of spring design	122
4.5.2	Effect spring design on performance engine	123
4.5.3	Effect of decreasing of IMEP on spring deflection	126
4.6.1	Solid mesh statistics	162
4.6.2	Material design characteristics	163
A.1	Calibration of angular velocity	192
A.2	Calibration of volt-metre	193
A.3	Calibration of Ampere-metre	193
A.4	Result of engine speed for 1000 rpm	195
A.5	Result of engine speed for 2000 rpm	195
A.6	Result of engine speed for 3000 rpm	196
A.7	Result of engine speed for 4000 rpm	196
A.8	Result of engine speed for 5000 rpm	197
A.9	Result of engine speed for 6000 rpm	197
A.10	Comparison results between experiment and simulation	198
B.1.A	Friction Losses in Rotation Engine	200
B.1.B	Friction Losses in Linear Engine	201
B.1.1	Prediction of performance rotation engine at 500 rpm	202

List of Table: Continue

B.1.2	Prediction of performance linear engine at 500 rpm	203
B.2.1	Prediction of performance rotation engine at 1000 rpm	204
B.2.2	Prediction of performance linear engine at 1000 rpm	205
B.3.1	Prediction of performance rotation engine at 1500 rpm	206
B.3.2	Prediction of performance linear engine at 1500 rpm	207
B.4.1	Prediction of performance rotation engine at 2000 rpm	208
B.4.2	Prediction of performance linear engine at 2000 rpm	209
B.5.1	Prediction of performance rotation engine at 2500 rpm	210
B.5.2	Prediction of performance linear engine at 2500 rpm	211
B.6.1	Prediction of performance rotation engine at 3000 rpm	212
B.6.2	Prediction of performance linear engine at 3000 rpm	213
B.7.1	Prediction of performance rotation engine at 3500 rpm	214
B.7.2	Prediction of performance linear engine at 3500 rpm	215
B.8.1	Prediction of performance rotation engine at 4000 rpm	216
B.8.2	Prediction of performance linear engine at 4000 rpm	217
B.9.1	Prediction of performance rotation engine at 4500 rpm	218
B.9.2	Prediction of performance linear engine at 4500 rpm	219
B.10.1	Prediction of performance rotation engine at 5000 rpm	220
B.10.2	Prediction of performance linear engine at 5000 rpm	221
B.11.1	Prediction of performance rotation engine at 5500 rpm	222
B.11.2	Prediction of performance linear engine at 5500 rpm	223
B.12.1	Prediction of performance rotation engine at 6000 rpm	224
B.12.2	Prediction of performance linear engine at 6000 rpm	224

List of Table: Continue

C.1	The Performance of Spring design with 6 mm of wire diameter	225
C.2	The Performance of Spring design with 6.5 mm of wire diameter	227
C.3	The Performance of Spring design with 7 mm of wire diameter	229
C.4	The Performance of Spring design with 7.5 mm of wire diameter	231
C.5	The Performance of Spring design with 8 mm of wire diameter	233



LIST OF FIGURES

Figure No.	Title	Page
2.1	Basic Concept of Free Piston Engine	9
2.2	General layout of a free piston engine for use in hybrid electrical vehicles	10
2.3	Loads compatible with free-piston engines. Please note that the diagrams are not drawn to scale and that the shaded regions represent equal areas	12
2.4	Solo Stirling 161 tests fired with biomass	30
2.5	The Innas free-piston engine. (a) The working principle of the Innas free-piston engine. (b) Photograph of the engine	35
2.6	MICE Generator Design	36
3.1	General flow chart of research methods	52
4.1.1	Back pack brush Cutter type BG- 328	64
4.1.2	GT-Power model of two stroke SI BG-328 engine	66
4.1.3	GT-Power model engine performance prediction result and hand calculation	68
4.1.4	Power output characteristics of both simulation and experiment	70
4.1.5	Torque characteristics between simulation and experiment	70
4.1.6	Specific fuel consumption both experiment and simulation	71
4.2.1	Single cylinder rotation engine	74
4.2.2	Single cylinder linear engine	74
4.2.3	Flow chart of the model design analysis	76
4.2.4	Friction formulas for conventional engine	77
4.2.5	Friction formulas for linear engine	78
4.2.6	Modification technique to replace the friction force	78

List of Figures: Continued

4.2.7	Log P-log V diagram at different engine speeds	80
4.2.8	P-V diagram at critical characteristics	81
4.2.9	Comparison of friction loss between rotation and linear engine	81
4.2.10	Comparison of brake power between rotation and linear engine	82
4.2.11	Torque of both linear and rotation engines on variable speeds	83
4.2.12	Effect of mechanical efficiency at both linear and rotation engines with different engine speeds	83
4.2.13	Comparison of brake specific fuel consumption between rotation and linear engine	84
4.2.14	Effect of brake efficiency of linear and rotation engines at different engine speeds	85
4.2.15	The characteristics engine on maximum pressure of variable speed	86
4.3.1	Flow chart of linear engine with spring system	92
4.3.2	PV diagram of variable speed	93
4.3.3	Block diagram of multilevel optimization approach	94
4.3.4	States of the spring according to the index of basic states of springs	95
4.3.5	The most common types of spring end designs	98
4.3.6	Seating types of the springs	99
4.3.7	Curves of permitted deformation according to the type of seating of the spring	100
4.3.8	The ultimate tensile strength- EN	101
4.3.9	Fatigue diagram for shot-peened chrome-vanadium alloy steel wire SAE 6150, d=7 mm	103
4.3.10	Optimization imep	105
4.3.11	Effect of engine load and speed on spring deflections	107

List of Figures: Continued

4.3.12	Characteristics of critical speed of spring design	107
4.3.13	Resonance effect on variable spring speeds	108
4.3.14	Dynamic safety level of different spring wire diameters at different operating speeds	109
4.4.1	Flowchart of linear engine process design	112
4.4.2	Configuration design of linear engine	114
4.4.3	Oscillation control system	115
4.4.4	Isometric view of linear engine without top casing	117
4.4.5	Isometric view of full assembly	117
4.5.1	Design of linear engine with spring mechanism	121
4.5.2	Flow chart of the model design analysis	122
4.5.3	Effect spring design on PV diagram at 1 m/sec speed	124
4.5.4	Effect spring design on PV diagram at 4.1 m/sec speed	124
4.5.5	Effect spring design on PV diagram at 4.6 m/sec speed	125
4.5.6	Spring system design for linear engine	129
4.5.7	Redesign of conventional engine type BG-328.	131
4.5.8	Design of linear engine with spring mechanism with/without top casing	132
4.5.9	Flow chart of motion analysis technique	132
4.5.10	Displacements of linear and conventional	134
4.5.11	Velocity of linear and conventional engines	135
4.5.12	Acceleration of linear and conventional	136
4.5.13	Acceleration of linear engine with friction trend	136
4.5.14	Acceleration trend with and without friction	137
4.5.15	Angular momentum with and without friction at Z ordinate	137

List of Figures: Continued

4.5.16	Photograph of linear engine at certain frames	138
4.5.17	Displacement trend of predicted and designed at 16.67 Hz	139
4.5.18	Displacement trend of predicted and designed at 66.67 Hz	139
4.5.19	Velocity of predicted and designed at frequency 16.67 Hz	140
4.5.20	Velocity of predicted and designed at frequency 66.67 Hz	140
4.5.21	Acceleration trend of predicted and designed at frequency 16.67 Hz	141
4.5.22	Acceleration trend of predicted and designed at frequency 66.67 Hz	142
4.6.1	Design configuration of linear engine before modification	147
4.6.2	(A) Original piston. (B) Modified piston	148
4.6.3	(A) Original Connecting rod. (B) Modified Connecting rod	148
4.6.4	Flow chart for stress analyses	150
4.6.5	A Three-dimensional domain Ω , its boundary Γ with unit normal \hat{n} , and a typical three-dimensional finite element	155
4.6.6	Piston models. A: Originals model. B: Modification model	160
4.6.7	Connecting rod with pin and piston models. A: Original design model. B: Improvement model	161
4.6.8	Piston mesh generated in Algor FEMPRO. A: Mesh of original piston. B: Mesh of modification piston	161
4.6.9	Connecting rod meshes assembly with piston and pin. A: The mesh of original design. B: The mesh of improvement design	162
4.6.10	Structure stress analysis of the original piston. A: Front site of stress analysis of the original piston. B: Inner site of stress analysis of the original piston	164
4.6.11	Structure stress analysis of the piston modification. A: Front site of stress analysis of the piston modification. B: Inner site of stress analysis of the piston modification	165

List of Figures: Continued

4.6.12	Thermal distribution of original piston. A: Front site of thermal distribution of original piston. B: Bottom site of thermal distribution of original piston	166
4.6.13	Thermal distribution of modified piston. A: Front site of thermal distribution of modified piston. B: Bottom site of thermal distribution of modified piston	166
4.6.14	Thermal stress of original piston. A: Front site of thermal stress of original piston. B: Bottom site of thermal stress of original piston	167
4.6.15	Thermal stress of modified piston. A: Front site of thermal stress of modified piston. B: Bottom site of thermal stress of modified piston	168
4.6.16	Thermal-structural stress of original piston. A: Front site of thermal-structural stress. B: isometric site of thermal-structural stress	169
4.6.17	Thermal-structural stress of modified piston A: Front site of thermal-structural stress of modified piston. B: Isometric site of thermal-structural stress of modified piston	170
4.6.18	Structural stress of first design of connecting rod	171
4.6.19	Structural stress of the modified connecting rod	171
A.1	Front view photograph of engine test rig	190
A.2	Instruments and tools	191
A.3	Front view of engine test rig with electric circuit load	191
D.1.1	Displacements of Linear and Conventional Engines	235
D.1.2	Velocity of linear and conventional engines	236
D.1.3	Acceleration of linear and conventional engines	237
D.1.4	Multi-cycles of acceleration of linear engine with friction trend	238
D.1.5	Multi-cycle of acceleration trend with and without friction trend	239
D.2.1	Multi-cycles of displacement trend of predicted and designed at 16.67 Hz	240

List of Figures: Continued

D.2.2	Multi-cycles of velocity of predicted and designed at frequency 16.67 Hz	241
D.2.3	Multi-cycles of acceleration trend of predicted and designed engine at frequency of 16.67 Hz.	242
D.3.1	Multi-cycles of displacement trend of predicted and designed at 66.67 Hz	243
D.3.2	Multi-cycles of velocity of predicted and designed at frequency 66.67 Hz.	244
D.3.3	Multi-cycles acceleration trend of predicted and designed engine at frequency of 66.67 Hz	245
E.1.A	Front site of structural stress analysis of the original piston	246
E.1.B	Isometric sites (non pinhole area) of structural stress analysis of original piston	246
E.1.C	Bottom site of structural stress analysis of the original piston.	247
E.1.D	Top site of structural stress analysis of the original piston	247
E.1.E	Back site of structural stress analysis of the original piston	248
E.1.F	Inner site of structural stress analysis of the original piston	248
E.2.A	Front site of structural stress analysis of the modified piston	249
E.2.B	Isometric sites (non pinhole area) of structural stress analysis of modified piston	249
E.2.C	Bottom site of structural stress analysis of the modified piston	250
E.2.D	Top site of structural stress analysis of the modified piston	250
E.2.E	Back site of stress analysis of the modified piston	251
E.2.F	Inner site of stress analysis of the modified piston	251
E.3.A	Front site of thermal distribution of original piston	252
E.3.B	Bottom site of thermal distribution of original piston	252
E.3.C	Front site of thermal stress of original piston	253

List of Figures: Continued

E.3.D	Bottom site of thermal stress of original piston	253
E.3.E	Left isometric site of thermal stress of original piston	254
E.3.F	Isometric site of thermal stress of original piston	254
E.4.A	Front site of thermal distribution of modified piston	255
E.4.B	Bottom site of thermal distribution of modified piston	255
E.4.C	Front site of thermal stress of modified piston	256
E.4.D	Bottom site of thermal stress of modified piston	256
E.4.E	Left isometric site of thermal stress of modified piston	257
E.4.F	Isometric site of thermal stress of modified piston	257
E.5.A	Front site of thermal-structural stress of original piston	258
E.5.B	Left isometric site of thermal-structural stress of original piston	258
E.5.C	Top site of thermal-structural stress of original piston	259
E.5.D	Bottom site of thermal-structural stress of original piston	259
E.5.E	Back site of thermal-structural stress of original piston	260
E.5.F	Isometric site of thermal structural stress of original piston	260
E.6.A	Front site of thermal-structural stress of modified piston	261
E.6.B	Left isometric site of thermal-structural stress of modified piston	261
E.6.C	Top site of thermal-structural stress of modified piston	262
E.6.D	Bottom site of thermal-structural stress of modified piston	262
E.6.E	Back site of thermal-structural stress of modified piston	263
E.6.F	Isometric site of thermal structural stress of modified piston	263
F.01	Assembly	264
F.02	Casing	265
F.03	Piston	266

List of Figures: Continued

F.04	Head	267
F.05	Connecting Rod	268
F.06	Carburator	269
F.07	Journal Bearing	270
F.08	Connecting rod-Pin-Piston	271
F.09	Spring Preload	272
F.10	Piston Ring	273
F.11	Screw Casing	274
F.12	Exhaust Screw	275
F.13	Nat Casing	276
F.14	Starter Handle	277
F.15	Exhaust	278
F.16	Inlet Manifold Gasket	279
F.17	Exhaust gasket	280
F.18	Cylinder Washer	281

A large, semi-transparent watermark logo for UMP is centered on the page. It features a stylized shield shape with a yellow diamond at the top, a teal oval, and the letters 'UMP' in white at the bottom. The shield is composed of teal and light blue sections.

UMP

LIST OF SYMBOLS

α	Coefficient of thermal expansion
β	Coefficient of convection
δ	Displacement, deflection of the spring
γ	Gas specific heat ratio (C_p / C_v)
ρ	Density of material
ε	Strain
σ	Stress
τ	Shear Stress
τ_{\max}	The maximum of shear stress
Δ	different
ΔT	Temperature different
Ω	Domain
Ω_e	The element of domain
Γ	The boundary of surface
Γ_1, Γ_2	The boundary of surface on the portions 1 and 2 respectively
a	The parameter of Wiebie
A	Area
b	Cylinder bore,
$Bmep$	Break mean effective pressure
C	Constant
C_b	Patton proportional constant of bearing (3.03×10^{-4} kPa-min/rev-mm)

List of Symbols: Continued

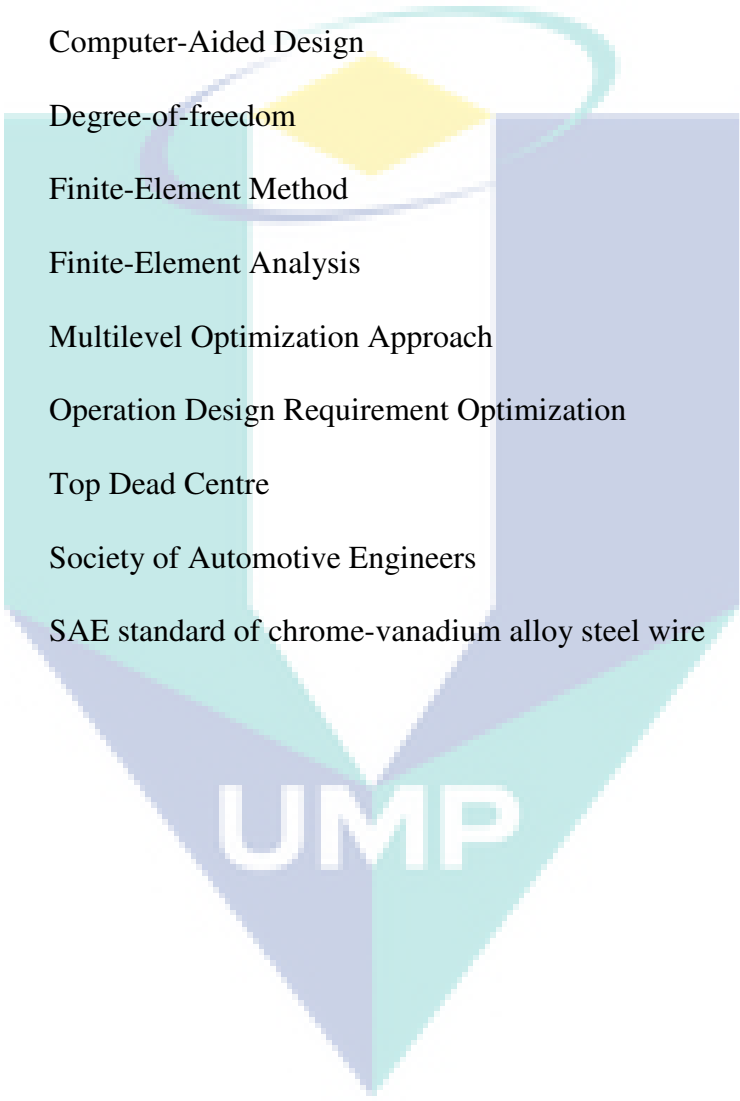
C_g	Bishop gas load constant ($C_g=6.89$)
C_{ps}	Patton proportional constant of skirt (294kpa-mm-s/m)
C_{pr}	Patton proportional constant of rings (4.06×10^4 kPa-mm ²)
C_s	Patton proportional constant of seals (1.22×10^5 kPa-mm ²)
d	Wire diameter
D	The mean of diameter of coil
D_{as}	The accessory or balancing shaft bearing diameter
D_{cb}	The connecting rod bearing diameter
D_{mb}	The main bearing diameter
f	Frequency
f_n	The natural frequency
f_{mep}	The friction of mean effective pressure
F	Force, Loading of spring
F_c	The force of combustion
F^e	The element load vector
F_f	The force of the friction
F_l	The force of the loads
F_s	The force of the spring
g	Acceleration gravity, The internal heat generation per unit volume in a three-dimensional domain
G	The shear modulus
$k_x k_y k_z$	The conductivities of an orthotropic solid
K	The stress constrain factor

List of Symbols: Continued

K	Bishop friction K constant (0.14 for spark ignition engines and 0.29 for diesel engines)
K^e	The stiffness matrix
L	The free length of spring
L_b	The length of bearing
L_{mb}	The total main bearing length per number f cylinders
L_{cb}	The rod bearing length
L_{as}	The total length of all accessory shaft bearing per number of cylinders
m	The parameter of Wiebe
m	The number of pistons per rod bearing
m	mass
M^e	The element mass matrix
mps_f	The mean piston speed factor
$mpss_f$	The mean piston speed square factor
n	The number of active coil
n_b	The number of bearing
n_c	The number of cylinders
n_r	The number of cylinder
N	The engine speeds
P	Pressure
P_a	The atmospheric pressure
P_f	The peak cylinder pressure factor
P_f	The fiction power
P_i	The intake manifold pressure

List of Symbols: Continued

Q	Heat release
Q	The number of inactive coil
Qe	The vector of internal force
r	Compression ratio
s	The piston stroke
S	Spring deflection
S_f	Safety level
t	The time variable of combustion
t_{comb}	The period of combustion
T	Temperature
T_∞	The ambient temperature ambient
U	A characteristic velocity
\bar{U}_p	The average of instantaneous piston speed
V	Volume
V_d	The displacement volume
w	The weight function
W	The rate of heat release
x	The displacement of the piston assembly
X	The mass fraction burnt
X	The design vector
X_{max}	The maximum of mass fraction burnt

LIST OF ABBREVIATIONS

BDC	Bottom Dead Centre
BG	Brush Cutter
CAD	Computer-Aided Design
DOF	Degree-of-freedom
FEM	Finite-Element Method
FEA	Finite-Element Analysis
MOA	Multilevel Optimization Approach
ODRO	Operation Design Requirement Optimization
TDC	Top Dead Centre
SAE	Society of Automotive Engineers
SAE6150	SAE standard of chrome-vanadium alloy steel wire

UMP

CHAPTER 1

INTRODUCTION

1.1 BACKGROUND

Alternative engines have been developed at the University Malaysia Pahang (UMP) for several years. A single cylinder high-speed linear spark ignition (SI) engine is one of the projects in the Faculty of Mechanical Engineering, UMP (Fathallah & Bakar, 2009). Many studies of linear engines have been conducted by researchers. However, the research results are too unreliable to produce an engine in the near future. Most linear engine research was of high technology product design, especially control systems. They used electronic automatic control systems. The weakness of the linear engine is its high production cost which makes it uncompetitive with traditional engine products. Therefore, more effort is needed to design a new system for competitive linear engines.

The advantage of a linear engine compared with a conventional engine is that it is simpler and more efficient. The concept of a linear engine rests on reducing the friction factor to increase the power output. Three common models have been developed for the free-piston linear engine system, such as both chambers being combustion chambers, one chamber being a combustion chamber while the opposite chamber is used for air kick back, and only having one chamber for combustion while using spring for return back force piston movement (Fonna, Mohamed & Ariffin, 2005).

The main problems with linear engine design that are difficult to solve are the return cycle, system control, maintenance, and others (Goertz and Peng, 2000; Nag, 2002). The difficulty in controlling the piston motion, in particular stroke length and compression ratio, has been proven. This is due to the fact that the combustion process in one cylinder has a high influence on the next compression (Mikalsen & Roskilly, 2007). A single cylinder free-piston linear engine is an alternative to eliminate, in general, the weakness of linear engines. The spring has been developed to conduct the return cycle. Spring technology, which is used as part of the dynamic forces of linear

engines, could be adopted because spring techniques can be incorporated from cam valve devices. It is expected that this method will reduce the difficulties with the start and control systems.

The difficulty of designing the spring for a linear engine system is not only due to the fact that the load is dynamic, but also that the design has some constraints such as fatigue, buckling, shear stress and natural frequency. Moreover, since there were two objective functions of the minimisation of weight and dimensions and maximisation of spring work for certain engine performance services, it makes the design more complicated.

The engine should be operated at variable speeds and under variable loads. For an electrical generator, the load is important because it always changes with time. The engine load will affect the performance, including combustion process and pressure in the combustion chamber. The pressure in the combustion chamber produces a thrust force; this force will transfer to the spring. The spring compression force will be divided by the spring constant (k) to obtain the engine stroke ($x = F/k$). The small load results in a small pressure in the combustion chamber, because k is constant, the stroke will be small. On the other hand, if the load increases, it will increase the engine stroke. For that reason, the spring needs to be designed precisely, otherwise the scavenging process cannot work effectively.

The purpose of this research is to design and simulate a single cylinder high speed SI linear engine with spring system. The scope of the work that has already been done is described in the section introducing the scope and limitations of the problem. Preliminary design analysis results show the existence of interference from the scavenging system on the combustion process. Therefore, it is necessary to modify the design and to analyse the construction with respect to the impact of stress on the structure. Two recommendations in the modifications have been proposed at the end of this thesis.

1.2 PROBLEM STATEMENT

The main problem of the research is how to design, simulate and study the performance of a linear engine which is easy to start, easy to maintain and can also be controlled easily. The spring system has been adopted as the return cycle. The main task

is the design of a two-stroke, single cylinder, SI Linear engine with a spring system. Nevertheless, the system arrangement should be easy to repair and maintain. Another problem is how to adopt the mixture scavenging system and ignition timing system of a conventional engine in a linear engine system. Finally, the performance of the newly designed engine is an important factor.

1.3 OBJECTIVES

The main objectives of the research is to design a free-piston linear engine which is easy to start, maintain and control. Details of the research objective are listed below:

1. To design a free-piston linear engine with spring system.
2. To analyse the effect of a spring system design result of a free-piston linear engine on piston motion.
3. To study the performance of the new design of the free-piston linear engine with spring system.

1.4 SCOPE AND LIMITATIONS

Due to the scope of the problem being very broad, and the limited ability of science, not all the design problems relating to the design of a linear engine with spring system will be completed in this thesis. To facilitate settlement of the problems it is necessary to limit the scope of the work and restrict the problem. The discussion regarding the scope and limitations of the problem are as follows:

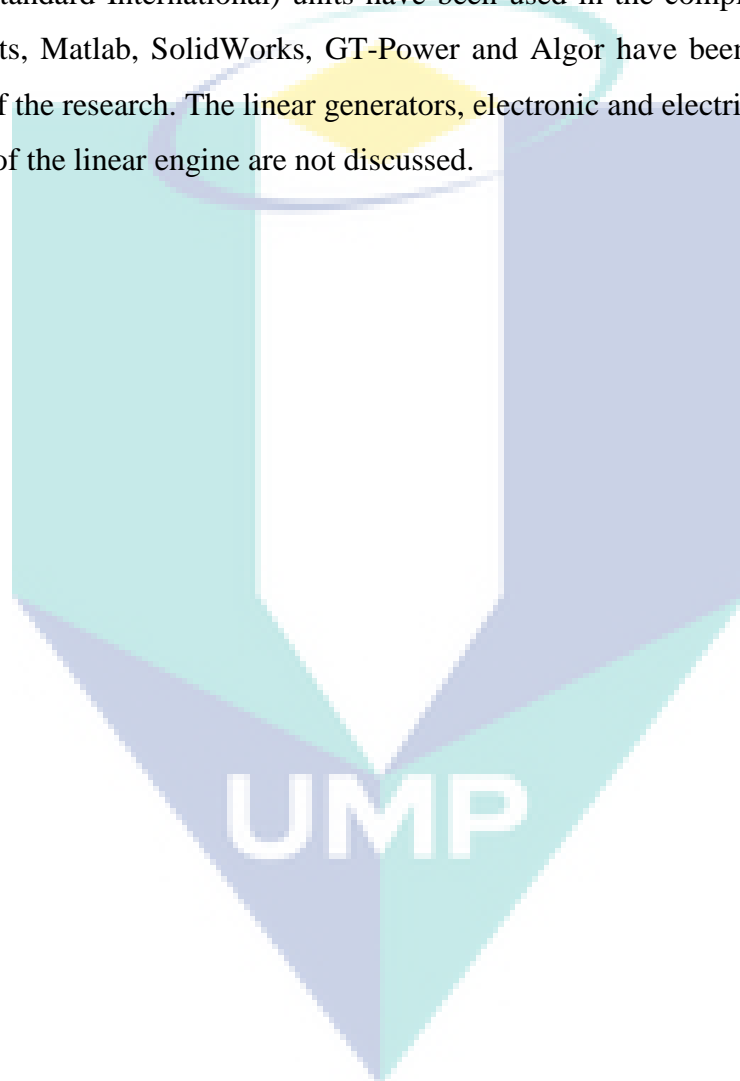
1.4.1 Scope

The scope starts with building a model and its validation. Secondly, a prediction is made to study for the performance of a single cylinder high-speed spark ignition linear engine with spring system. Thirdly, the design and optimisation is carried out for the spring for a two-stroke single cylinder high-speed spark ignition linear engine with spring system. Fourthly, a linear engine with spring system is designed. The analysis

studies the effect of the spring system design on piston motion. Finally an analysis of the design modifications, if it necessary, will be conducted.

1.4.2 Limitations

The engine used as a reference is a Back Pack Brush Cutter engine, type BG-328. SI (Standard International) units have been used in the completion of the thesis. Spreadsheets, Matlab, SolidWorks, GT-Power and Algor have been used to solve the problems of the research. The linear generators, electronic and electrical systems used in the design of the linear engine are not discussed.



CHAPTER 2

LITERATURE REVIEW AND THEORETICAL BACKGROUND

2.1 INTRODUCTION

This chapter is mainly focused on the literature review and theoretical background. In the literature review, the discussion of some subjects is separated in terms of items such as the history of the linear engine, basic concepts of linear engines and the research development of linear engines. The theoretical background explains the theory, especially the formulas which are used in this research.

2.2 LITERATURE REVIEW

2.2.1 Historical Perspective

Research and development of free-piston linear engine started in the 1920's. According to history, research and development into free-piston linear engines can be divided in a number of periods. The first generation of free-piston linear engines was in the 1922–1940 period. The free-piston engine concept was first presented by Pescara (1928), and since then a number of free-piston designs have been proposed. The piston motion is not restricted by the motion of a rotating crankshaft, as in conventional engines. As a result, the piston is free to move between its endpoints. It is only influenced by the gas and load forces acting upon it. This gives the free-piston engine some distinct characteristics, the most important being the variable stroke length and high control requirements. The original Pescara patent describes a single piston spark ignited air compressor. Pescara started his work on free-piston engines around 1922 and he developed prototypes with spark ignition in 1925 and diesel combustion in 1928. The latter led to the development of the Pescara free-piston air compressor (Underwood, 1957). Pescara continued his work on free-piston

machinery, and also patented a multi-stage free-piston air compressor engine in 1941 (Noren and Erwin, 1958).

The second period was in between 1941–1960. The different applications of free-piston engines were carried out during that period. The use of free-piston engines supplying gas to drive a turbine for automotive applications was presented by Underwood (1957), while Flynn (1957) investigated the performance, power, economy and reliability of free-piston engines over the more conventional diesel engines. An automotive-size free-piston engine with matching turbine was designed, built and tested by Frey et al (1957). Besides which, a simulation of linear engines was also conducted during this second period. Due to very complicated analysis, the University of Michigan simulated a free-piston engine using an analogue simulation technique. The feasibility of using an electronic analogue computer for computing the transient and steady state performance of a free-piston engine was demonstrated (Larowe & Spancer, 1958).

The third period, called the patent period, occurred in 1980-1990. However, after about two decades vacuumed, at that time many research results were patented by researchers. Significant patents were presented by Nerstrom (1985), Iliev et al (1985), Allais (1984), Heintz (1989), Rittmaster et al (1982), Galitello (1989) and Buck (1991). These patents emphasised different applications of free-piston engines, as well as the advantages of reduction the of moving parts, like the connecting rods and crankshafts of an engine, thereby leading to a greater ease of maintenance, reduced cost and lower frictional losses, bringing about a higher mechanical efficiency of the engine.

Heintz (1989) has disclosed a free-piston engine pump system. The device consists of a pair of opposite pistons connected by a common rod, operating a hydraulic pump. The free-piston engine pump has double acting power pistons attached, and pumping pistons as the main reciprocating member and movable in housing. The housing itself moves for purposes of mass balance. The engine is spark ignited, and stroke control is provided by a valve system. Air is supplied and the exhaust products are removed from the two combustion chambers by common intake and outlet valves. These valves are operated by a common actuator in response to the position of the main reciprocating member.

A spark ignition linear engine connected to a hydraulic power system has been presented by Rittmaster et al (1982). Hydraulic fluid is stored and maintained under pressure in two pressurisation chambers on opposite sides of the pistons, forming an internal combustion engine. A set of proximity detectors are used in order to time the operation of the engine, located around the connecting rod. The hydraulic fluid flow in the two pressurisation chambers is controlled by a set of cross-over valves. A hydraulic motor is interposed downstream of the cross-over valves in order to convert the flow of the fluid into the rotation of a shaft. The cylinders of the engine have electronically operated intake and exhaust valves. A flywheel is attached to the shaft of the hydraulic motor to dampen the pulsation induced by the shifting of the cross-over valves and to store the energy of the pistons between reciprocation.

Iliev et al (1985) presented a linear engine coupled to an electrical alternator. The engine operates on a two-stroke cycle and is spark ignited. The engine is controlled by an electronic module, which also controls the linear alternator. The spark timing is regulated, based on the quality of fuel and the electrical load. According to the inventors, the engine is designed to operate at high frequencies, thereby attaining a high thermal efficiency.

Galitello (1989) proposed a linear engine controlled by a computer. The engine is a two-stroke compression ignition engine. According to the inventor, the engine operates at ultra-high speeds and is vibration free. During engine start, ignition assist is provided by spark plugs. The engine can be connected to an electric generator or to a hydraulic power system.

The fourth period (1990–present), is the period in which the application of free-pistons in hybrid generation systems has been developed. Kos (1991) patented a hybrid engine that uses a reciprocating piston controlled by an electromagnetic transducer. A piston-rod magnet unit, constrained to move translationally in one axis by means of bearings, was used to generate an electric current in the windings of the yoke of the transducer. The motion of the piston and magnet was controlled using an impedance-based computer control system. The two-stroke cycle engine was designed for multi fuel operation and could be spark ignited or compression ignited. Fuel injection, valve timing, and ignition

timing were computer controlled. The stroke was adjusted using the computer, and an opposed piston arrangement using a common link rod was also deemed operational.

With the introduction of modern control methods, the free-piston engine has again attracted interest among present-day engineers seeking to reduce engine emissions and increase efficiency. A free-piston engine for a linear electric generator is being investigated by, amongst others, researchers at the University of West Virginia. The main applications of the units are hybrid-electric vehicles (Clark et al, 1998). The most successful linear engine is the hydraulic free-piston engine, where the Dutch company, Innas BV, has reported performance advantages over conventional technology (Achten et al, 2000). A number of other research groups are also working on this type of engine, which is used for off-highway vehicles such as forklift trucks and earth-moving machines.

2.2.2 Basic Concept of the Linear Engine

The basic concept of the free-piston engine is introduced by Mikalsen and Roskilly (2008). The term free-piston engine or linear engine comes from the purely linear piston motion that is not restricted by a crank mechanism. It means that free-piston engine is a crankless internal combustion engine, in which the piston motion of the free-piston engine is not controlled by the crankshaft as in a conventional engine. There are a number of variations of free-piston engine configuration, such as the single piston free-piston engine and many other, but the main parts of the engine are a combustion cylinder, a bounce chamber cylinder and a linear electric machine. Figure 2.1 shows the basic concept design of a free-piston engine.

Free-piston engines are usually divided into three categories, based on the piston/cylinder configuration. A fourth category, free-piston gas generators, identifies engines where the load is extracted purely from an exhaust turbine and not from a load device mechanically coupled to the engine (Mikalsen & Roskilly, 2007). A single piston free-piston engine essentially consists of three parts, a combustion cylinder, a load device and a rebound device to store the energy required for compressing the next cylinder charge. In the engine shown in Figure 2.1, the hydraulic cylinder serves as both the load and

rebound device, whereas in other designs these may be two individual devices, for example in an electric generator and a gas-filled bounce chamber.

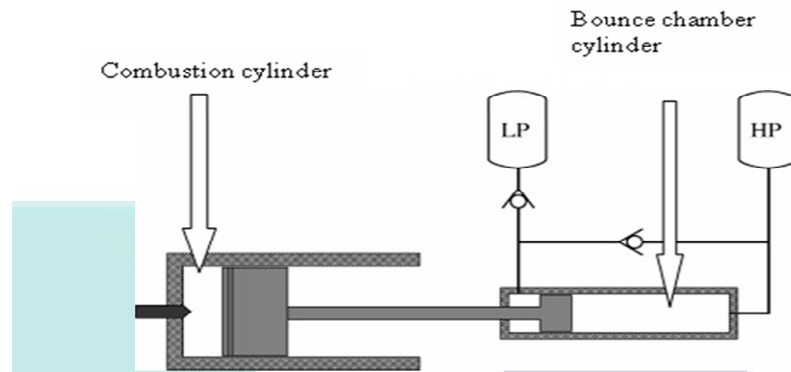


Figure 2.1: Basic concept of a free piston engine

Source: Mikalsen and Roskilly (2007).

The general design consists of two opposing combustion cylinders with an integrated linear alternator in-between. The general layout can be seen in Figure 2.2. The pistons of each cylinder are connected by a shaft on which permanent magnets are mounted. A two-stroke cycle and combustion in alternating cylinders pushes the shaft back and forth through the alternator coils, inducing an electric current for power generation. The alternator is also used to control the shaft's motion and start-up (Klemann, Dabadie & Henriot, 2004).

The advantages of free-piston engines originate in their compact and modular design and the lack of mechanical linkage, thus allowing for a variable compression ratio while reducing friction losses. Some problems with the dual piston design have, however, been reported. The control of piston motion, in particular stroke length and compression ratio, has proven difficult. This is due to the fact that the combustion process in one cylinder conditions the compression in the other, and small variations in the combustion will have great influence on the next compression (Mikalsen & Roskilly, 2007).

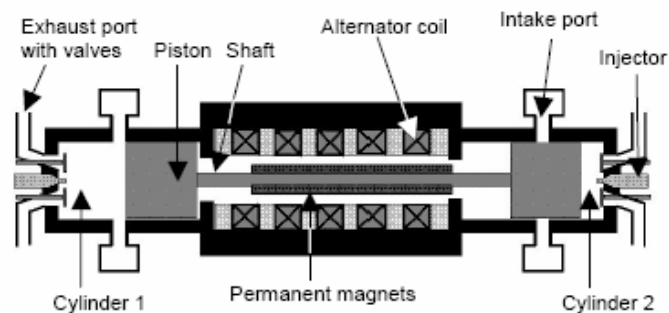


Figure 2.2: General layout of a free-piston engine for use in hybrid electrical vehicles

Source: Klemann, Dabadie and Henriot (2004).

2.2.3 Research Development

Free-piston research development can be divided into three parts, development based applications, development based designs and development based research groups. Research development based applications can be further separated into applications including to generate alternator, air compressors and hydraulic pumps. Research development based design can be categorised into single piston, dual piston and opposed piston. Chiefly, free-piston development is under investigation by research groups. There are numerous research groups, such as NASA, Sandia National Laboratory, ARI (Aerodyne Research, Inc), Innas BV, Solo Kleinmotorn, Czech Technical University, West Virginia University, Case Western Reserve University, FEV Engine Technology, Helsinki University of Technology, IFP France, Japanese Aerospace, MIT, University of Newcastle upon Tyne, Royal Institute of Technology, Sunpower, Shinhua University, The University of Minnesota, Korea Institute of Energy, Shanghai Jiaotong University. There are also some universities in Malaysia that have formed a research group.

2.2.3.1 Research Development Based Applications

Free-piston engines based applications are under investigation by a number of researchers due to their potential advantages in terms of fuel efficiency and engine emissions. Some prototypes have emerged, mainly aimed at vehicle propulsion and hydraulic power generation (Mikalsen & Roskilly, 2008, 2007). The compatibility load of a free-piston linear engine was discussed by Aichlmayr (2002). However, a simple explanation can be seen in Figure 2.3. The hydraulic pump has the simplest force-position characteristic because the working fluid is incompressible. The air compressor force-position curve is discontinuous because it is essentially a polytropic compression process followed by a constant pressure discharge process. The linear alternator force-position characteristic is slightly more complicated because the resisting force is assumed to be proportional to the piston velocity. The linear engine used in conjunction with a linear alternator offers an interesting choice for use in hybrid vehicles. The linear motion of the pistons is directly converted into electricity by the alternator, and the result is a compact and efficient energy converter that only has one moving part (Fredriksson & Denbratt, 2004). The free-piston with linear alternator is the most prospective application, because hybrid vehicles and stationary power systems will undoubtedly be powered by electric generators. For that reason, extensive development of free-piston electric generators that are capable of high conversion efficiencies and very low exhaust emissions is needed.

2.2.3.1.1 Free-Piston Hydraulics Pump Research Development

A free-piston hydraulic pump application has been developed by Issakson (2000), Achten et-al. (2000), and Swatkaomeng (2008). The hydraulic industry is relatively young, and when hydraulic pumps and motors arrived on the market, the crankshaft engine, mechanical drives and the electric motor had already defined a quasi-standard: the rotating shaft. The hydraulic industry had to adapt to this “standard”, especially since in most cases the hydraulic systems were seen as an accessory, leaving the main drive functions to gears, chains and belts. Furthermore, the diesel engine had already been produced in large

quantities, and there was no reason to construct a new engine for the small hydraulic market. Although this new hydraulic engine-pump combination could be simple, the effects it would have on production lines, retailing, after-sales and service would have been rather complex (Achten et al, 2000).

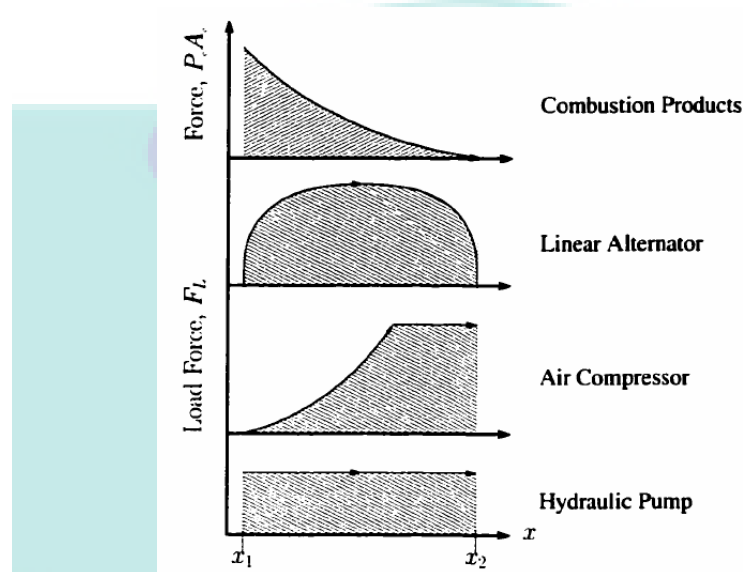


Figure 2.3: Loads compatible with free-piston engines. Please note that the diagrams are not drawn to scale and that the shaded regions represent equal areas

Source: Aichlmayr (2002).

There are many different concepts of free-piston engines. Even those concepts for hydraulic applications are different depending on each hydraulic pump application. Achten et al (2000) developed the CHIRON, which belongs to the family of single piston engines; there is only one piston and one combustion cylinder. The CHIRON is designed for application in common pressure rail systems (Issakson, 2000), and developed a dual free-piston hydraulic pump for use in heavy duty appliances such as tractors in which propulsion is not the main objective, or where the continuous running of the engine is not necessary. However, Swatkaomeng (2008) proposed four designs that combined a free-piston engine

and a single acting pump, free-piston engine and double acting pump, dual free-piston engine with a double acting pump, and a free-piston engine with a single acting pump.

2.2.3.1.2 Free-Piston Air Compressor Research Development

The first generation of free-piston linear engine research development was based on compressor appliances. Historical details of free-piston air compressor development have been explained by Aichlmayr (2002A). Pescara's first air compressor prototype was completed in 1925 and utilised spark ignition. The second prototype was completed in 1928 and utilised diesel combustion (Pescara, 1928). Pescara also patented a free-piston type three-stage motor compressor (Pescara, 1941). The four-stage Junkers free-piston air compressor is one of the most widely recognised examples of free-piston machinery. The Junkers free-piston air compressor uses a rack and pinion synchronisation mechanism (London and Oppenheim, 1952).

Braun and Schweitzer (1973) developed the single-piston free-piston air compressor. This machine delivers 2.94 kg/min of air at 690 kPa. This is a fixed-output machine and air retained in the compressor clearance volume provides the rebound force. At full load, it operates at 1350 cycles/min and it develops an indicated power of 16 kW. When compared to other free-piston air compressors, the Braun machine has several unique features. For example, it employs spark ignition combustion, loop scavenging, a single piston and air cooling. Consequently it is approximately 80% lighter than the asymmetric compressor.

A modern free-piston air compressor concept has been presented by Aichlmayr, Kittelson and Zachariah (2002 A), and Aichlmayr, Kittelson and Zachariah (2002 B). A concept for a 10 W miniature free-piston engine-compressor and various considerations for its design has been studied comprehensively. Not only that, the operational maps for crankshaft-equipped miniature homogeneous charge compression ignition (HCCI) engines are established using performance estimations, detailed chemical kinetics and diffusion models for heat transfer and radical loss. In small scales, the free-piston HCCI engine-compressor is a promising alternative, while traditional combustion schemes generally are infeasible due to quenching effects (Aichlmayr, Kittelson & Zachariah, 2002 A).

HCCI combustion was modelled using detailed chemical kinetics in a variable-volume batch reactor, while small-scale effects were incorporated via diffusion-based sub-models for heat and mass transfer. Operational maps were found to feature distinct boundaries between feasible and unfeasible designs; a lengthy analysis followed. Additionally, size limitations for miniature HCCI engines were explored by considering power outputs of 1 and 0.1 W (Aichlmayr, Kittelson & Zachariah, 2002 B).

2.2.3.1.3 Free-Piston Alternator Research Development

A linear alternator is the most interesting equipment developed by researchers. The applications have been developed starting from small to large power output. The diverse applications include general appliances, aerospace, military and hybrid vehicles. The monumental generation of linear generator application has been proposed by Kos (1991). He granted a patent which covers linear engines for electrical power generation for hybrid vehicles. Since then many researchers have continued developing them in certain applications. However, the hybrid vehicle is dominates research. For example, Van Blarigan, Paradiso and Goldsborough (1998) proposed a free-piston linear alternator to generate approximately 30 kW and use HCCI. Efficiency is the over-arching reason for them choosing this combination of engine configuration and combustion mode. They expected to attain an essentially ideal Otto cycle efficiency and to generate negligible quantities of regulated emissions, such as NO_x.

Atkinson et al (1999) proposed a two-stroke linear engine-alternator combination for a hybrid electric vehicle. A small-bore working prototype of a two-stroke spark ignited linear engine-alternator combination has been designed, constructed and tested and has been found to produce as much as 316 W of electrical energy. This engine consists of two opposed pistons (of 36 mm diameter) linked by a connecting rod with a permanent magnet alternator arranged on the reciprocating shaft. The same prototype, a linear alternator-engine for hybrid electric vehicle applications has been developed by Cawthorne et al (1999). Although the present prototype system is not optimally designed, it has provided a platform to demonstrate and test the linear engine and alternator concept. The experimental results

have been presented and are extremely promising. It showed that with a larger bore engine, the output power of the existing alternator can be increased to levels that are more suitable for hybrid vehicle propulsion. Cawthorne et al (2001) improved on the linear alternator by using a tubular brushless permanent magnet linear alternator in conjunction with a linear internal combustion engine, which offers a number of advantages over the conventionally used rotary systems for electrical power generation. In rotary configuration, the linear force imparted to the piston rod by the engine must be converted to a rotary torque through a crankshaft mechanism. This rotary energy is then transmitted to a conventional rotary generator. The linear system is capable of directly utilising the linear piston force without the need of additional mechanical components that are necessary in a rotary configuration. The result is more compact due to the absence of a crank housing, and more reliable since the linear configuration has only one moving part. Additionally, the linear system should prove to be more efficient as the frictional losses associated with the crank and rod bearings are eliminated.

Hoshino (2003) has been closely studying solar thermal energy applications in space. One of his studies is on a solar heat transport system, which supplies solar heat to a bottoming system with minimal energy loss. Since 1997, research on a solar heat transport system composed of a cavity solar absorber, thermal energy storage and heat pipes have been conducted. The study seeks to establish the basic technology for space experiments using solar thermal energy. In addition, Stirling engine converters have been developed as heat-to-electricity power converters. Several types of Stirling generators have been fabricated and experimentally evaluated. These prototype converters, called the NALSEM series, are semi-free-piston Stirling machines with moving magnet linear alternators. The performance test results of the NALSEM 500 indicated a thermodynamic efficiency of 35% and overall efficiency of 22%. After that, an improved Stirling engine converter, NALSEM 700, was designed and evaluated. This engine has an opposed piston configuration in order to minimise mechanical vibrations. Based on these achievements, a basic model of a free-piston Stirling engine converter was designed. The converter was called the NALSEM200 and was designed to achieve an overall efficiency of 20 % or more with an electrical output power of 200 W.

Brandhorst (2007) developed a 5 kW free-piston Stirling space convertor funded by NASA. A nominal 5 kW convertor allows two of these units to be dynamically balanced. A group of three dual-convertor combinations would yield the desired 30 kW. The status of this program will be presented later. Brandhorst's goals include a specific power in excess of 140 W/kg at the convertor level, a lifetime in excess of five years and AC output. The initial step is the design and development of a nominal 5 kW per cylinder Stirling Convertor Assembly (SCA), which will serve as a prototype for one or more SCAs that will make up the final 30 kW Stirling Convertor Power System.

Annen, Stickler and Woodroffe (2003) replaced battery technology as a primary power source with a free-piston linear engine technology for the objective force warrior require portable power. The objective is to improve the efficiency. Mechanical power technologies have the potential to meet the need for portable power, having much higher energy densities than rechargeable and primary batteries. The major issues, especially at a millimetre scale, of internal combustion (IC) engines have presented. Calculations showing the effect of leakage, combustion quenching and heat transfer as a function of size are presented. An assessment of the efficiency of the two-stroke IC engine as a function of size from the 1 W to 1000 W scale was given. Besides that, linearly-oscillating Miniature IC Engine (MICE) technology was described. MICE is a free-piston system with a two-stroke engine, a spring and a linear alternator. A key feature of MICE is the ability to operate without oil lubrication. Data from early tests and recent net power tests are presented. A 20 W MICE system is projected to have an energy density of 1200 W hr/kg for an 8-hour operation period, and potentially 2400 W hr/kg is achievable for an advanced design for a 72-hour operation period.

2.2.3.2 Research Development Based Design Configuration

The descriptions of different categories of free-piston engines are single piston, dual piston and opposed piston. Achten et al (2000), Pohl and Graf (2000), Ariffin et al (2006) and Annen, Stickler and Woodroffe (2008) have developed free-piston linear engines with single cylinder based. Atkinson et al (1999), Van Blarigan (1999), Deutsch and Visoky

(2006), Isaksson (2000) and many others developed free-piston engine based dual piston. While London and Oppenheim (1952), Hu and Hibi (1990), and Hibi and Ito (2004) have developed free-piston opposed systems.

2.1.3.2.1 Free-piston Research Development Based Single Piston Combustion Chamber

Free-pistons with a single piston is a unique system. The main problem of this system is the return cycle. Since there is only one combustion chamber, it is necessary to design return systems for the next cycles. There are some systems that have been developed by researchers including Achten et al (2000), Pohl and Graft (2005), Arifin et al (2006), Annen, Stickler and Woodroffe (2008), and Fathallah and Bakar (2009). Achten et al (2000) developed a return cycle based hydraulic system. Pohl and Graf (2005) and Ariffin et al (2006) have used compressed air; they called it an air spring or air kick back. However, Annen, Stickler and Woodroffe (2008) and Fathallah and Bakar (2009) have used spring systems, but they have developed different designs and techniques.

Achten et al (2000) have developed a single piston, diesel powered, hydraulic free-piston engine, intended as an alternative to conventional engines and hydraulic pump systems in off-highway vehicles. By design, characteristics within a net effective power output 17 kW have been implemented in modern hydraulic systems for a forklift truck. This research could be used as a barometer for modern research development among free-piston linear engines. Accordingly, Mikalsen and Roskilly (2007) are regarded as some of the leading researchers within free-piston technology today. They reported on a linear engine is based on a single piston configuration. Stepped hydraulic piston with three piston areas are compression piston, hydraulic piston pump delivery and rebound piston pump. The compression piston is for supplying the compression energy to the piston. The pump piston delivers part of the effective hydraulic power. However, the rebound piston delivers the other parts of the hydraulic power and limits the bouncing movement of the piston in the bottom dead centre due to the compressibility of the oil.

Pohl and Graf (2005) have developed a hardware demonstrator to investigate the functionality of the free-piston linear alternator. In parallel with the hardware components, a dynamic simulation model of the complete system is developed using Modelica software. This software can be used to study the piston motion of a linear engine. A Modelica library was outlined to provide basic and advanced components for free-piston engine modelling. A major scope is compatible with Modelica standard libraries and with future standards of thermodynamic modelling.

The free-piston linear alternator model can be built from library components. The control systems, the thermodynamic models of a combustion cylinder and gas spring are shown. The electrical system consists of the linear alternator and the power electronics. On a sub-layer the physical effects are modelled in detail, i.e. the mass flows in and out of the cylinders can be observed, the combustion process is modelled, heat transfer effects are investigated and the thermodynamic properties describe the state of the cylinders. The linear engine is a based single piston configuration. Although it has two pistons it is still called a single cylinder because this linear engine only has one combustion chamber and the function of another piston is for cycle return.

Arifin et al (2006) simulated a two-stroke free-piston linear engines motion consisting of combustion and air-kickback chambers. The models are two-stroke spark ignition engines. The free-piston linear engine consists of five main parts, i.e. combustion chamber, scavenging chamber, kickback chamber, generator housing and slider piston. The term slider-piston is used to describe the unification of combustion piston, kickback piston, connecting rod and permanent magnet. The rod connects the two oppositely placed pistons, and also acts as a prime mover for the linear engine. The permanent magnet is placed at a certain position along the rod. The two opposing pistons have different diameters. The kickback piston diameter is larger than the combustion piston diameter to ensure the generated force in the kickback chamber is adequate to push the slider-piston back.

2.1.3.2.2 Free-piston Research Development Based Dual Piston

The free-piston with dual piston was intensely developed by researchers for several decades. Nakumar (1998) designed, constructed and tested a prototype spark ignited dual piston linear engine coupled with an alternator, and successfully tested it under various operating conditions. The cycle-to-cycle variations in pressure were studied and led to the conclusion that the addition of load and retarding of timing would be highly beneficial in improving the engine's drivability. Atkinson et al (1999) continued the work in the modelling of the operation of linear engines. The engine's computational model combined dynamic and thermodynamic analysis. The dynamic analysis performed consisted of an evaluation of the friction forces and the load applied to the shaft by the alternator. The thermodynamic analysis consisted of an evaluation of each process that characterised the engine cycle, including scavenging, compression, combustion and expansion, based on the first law of thermodynamics. The Wiebe function based on time was used to express the mass fraction burned for the combustion process of dual free-piston engines, while the combustion model used a single-zone.

Van Blarigan, Paradiso and Goldsborough (1998) approached the utilisation of a free-piston in a double-ended cylinder, or what is also called a dual piston free-piston engine. A new approach to the free-piston linear engine such as HCCI combustion could be used to solve the problems of burn duration, and allow for an ideal Otto cycle operation to be more closely considered. In this combustion process a homogeneous charge of fuel and air is compression heated to the point of auto ignition. Numerous ignition points throughout the mixture can ensure very rapid combustion. Very low equivalence ratios (f is about 0.3) can be used since no flame propagation is required. Furthermore, the useful compression ratio can be increased as higher temperatures are required to auto ignite weaker mixtures. In general, HCCI combustion has been shown to be faster than spark ignition or compression ignition combustion. A much leaner operation than in SI engines is possible, while also resulting in lower NO_x emissions.

Computation design studies also have been conducted by Kleemann, Dabadie and Henriot (2004). They studied a high efficiency and low emissions prototype of a dual piston

free-piston engine. The method has been developed based on an iteration between zero-, 1-D and Simplified Computational Fluid Dynamic (CFD) simulation to define the operating conditions and overall geometrical parameters which offer the best engine performance. Based on these findings, more detailed 3-D CFD calculations have been used to specify the optimal intake and exhaust port configurations and injection characteristics. The results have been characterised in terms of scavenging and trapping efficiencies. However, scavenging efficiency predictions reach a 2% lower value, while trapping efficiency is 9% higher than the first stage result. The effect of injection timing and spray cone angle on combustion has been studied. The best results have been obtained for a SOI of 260° CA. An indicated efficiency of 52% is reached, combined with nearly zero NO_x and low soot emissions.

Fredriksson and Denbratt (2004) used BOOST and SENKIN to investigate the engine performance of a two-stroke free-piston engine dual piston for different fuels. A dynamic model of the complete free-piston engine was created that predicts the piston motion and frequency. The gas exchange was simulated with the commercial 1-D code BOOST, which solves the gas dynamic equations. The high pressure cycle of the commercial 1-D code BOOST was replaced by detailed chemistry calculations in the SENKIN code. The modelled engine runs on two-stroke cycles, since each downward stroke needs to be a power stroke. To obtain the best possible scavenging, uniflow scavenging is employed. There are four exhaust valves in the cylinder head and scavenge ports around the circumference at the bottom end of the cylinder. The results show that the piston motion of the free-piston engine differs substantially from the piston motion in a conventional internal combustion engine. The pressure rise due to combustion will lead to the piston experiencing accelerations of more than three times that of a crankshaft engine in extreme cases. The high accelerations are not considered a problem when running at frequencies as low as those predicted.

In order to find the specifications and design guidelines for the electrical machine, a simplified model of the combustion process has been carried out by Arshad et al (2002). Specifications for the electrical machine are discussed, and different electrical machine topologies are outlined. A layout suggesting the use of the free-piston generator in a series-hybrid vehicle is presented and discussed briefly. Arshad et al (2003) used a dual piston

free-piston generator in transverse-flux machines (TFM) in a free-piston generator in order to find an electrical machine solution for the free-piston generator that would meet the requirements. It was found that further improvements to conventional TFM designs were required to meet the demands on the electrical machine. Several design modifications for the surface-mounted designs were investigated. Unfortunately, all these designs failed during the 3-D-FEM verification. This was mainly due to the incorrect estimation of 3-D armature-flux leakage during the analytical design phase. For the buried magnets designs it was found that an improvement in the design was quite possible. This improvement allowed some of the permanent defects in a TFM to be overcome, i.e. armature-flux leakage, flux fringing and magnet-flux leakage.

Research development into free-piston dual piston engines is not only carried out for the internal combustion engine itself, but also linear generators. For free-piston energy converters to develop optimum system performance, and reduce their size and cost, such investigations are necessary. One important system issue is the interaction between the generator force, the translator dynamics and the driver system. The generator force affects the size of the power converters, the size of the electrical machine, the amplitude of the generated power pulsations and thus the size of energy storage. This makes the force a critical parameter for system design and performance control (Hansson, Leksell & Carlsson, 2005).

Hansson et al (2005) found that the losses in a free-piston energy converter during start up, stop and idle periods affected the energy consumption and power required from the supply system. Therefore, to make efficient use of the free-piston energy converter (FPEC) in a hybrid electric vehicle (HEV), it is desirable to know which operational mode the FPEC should be in, and what cost that mode is associated with. Furthermore, to design the electrical system supply for optimal performance, the required energy and power for each mode must be known. The results indicate that the electrical machine efficiency is the most critical factor during start up. By closing the correct amplitude of the starting force, energy consumption during start up can be reduced. When it comes to idling, friction is the most significant energy loss factor. Nevertheless, by compensating the mechanical loss for short

time intervals using the generator force, the reciprocating motion can be kept alive for a rapid start without major energy consumption.

Finally, Hansson and Leksell (2006) tested the performance of a series of hybrid electric vehicles with a free-piston energy converter. The research aim was to investigate the performance gain of utilising the FPEC in a medium-sized series hybrid electric vehicle (SHEV), compared to a conventional diesel-generator. Firstly, they utilised optimisation to determine a lower limit on the SHEV's fuel consumption for a given drive cycle. In addition, they developed a control strategy based on the ideas of Equivalent Consumption Minimization (ECM) proposed earlier in the literature. The results show a potential decrease in fuel consumption of up to 19% compared to a diesel-generator SHEV. The ECM control strategy behaves as desired, and a 13% reduction in fuel consumption compared to a traditional load-following strategy is achieved.

The control problem is multi-level, with usually three levels in the case of FPG used in hybrid vehicles. The top level is in charge of the energy management of the vehicle, which determines the use of the on-board energy sources – batteries (or super capacitors) and hydrocarbon-electricity converter (FPG in this case). This level is not considered at this time. The middle level controls the amount of the fuel-air mixture to burn, according to the power demand. This is done by controlling the fuel injectors, throttle and spark position. It is also responsible for emissions and keeping the lambda ratio equal to 1 (approx). The bottom level controls the movement of rod-connected pistons by keeping the maximum efficiency of energy drain. It is done by the adequate control of an Insulated Gate Bipolar Transistor (IGBT) Power Bridge. This level is also responsible for overcoming misfires (prevent stopping of FPG due to a misfire) and avoiding collisions between pistons and cylinder heads (Němeček & Vysoký, 2007).

Němeček and Vysoký, (2007) studied the Free-Piston Generator (FPG) model and its control for achieving steady operation. An FPG is a special type of combustion engine representing a new approach concerning the conversion of the chemical energy of hydrocarbon fuel into electrical energy. The FPG prototype employs two 50 cm³ cylinders with direct fuel injectors. The linear motor generator is a product of the VUES Company and is driven through the 3-phase power bridge with IGBT transistors. With the new control

system described above, long-term steady operation was achieved. Many new experimental results were obtained. Unfortunately, without appropriate equipment we were not able to identify the combustion engine parameters. Therefore, the results are mainly concerned with the electric motor-generator and the global behaviour of the FPG.

Xia, Pang and Grimble (2006) have modelled and controlled a hybrid-system based free-piston energy converter (FPEC). A hierarchical hybrid controller is then designed based on the FPEC model. The main control objective of the free-piston energy converter is to maintain the piston steady, avoiding collision between the piston and the cylinder head, which would cause a catastrophic failure. In terms of energy balance, the energy absorbed through compression of the gas charge and the energy removed electrically must be equal to the energy of the system after combustion. In common with all combustion processes, cycle-by-cycle variations exist in many parameters, including the released combustion energy.

One critical task in the operation of the linear machine (work in dual piston) is the initial process of starting the engine. (Zulkifli, Karsiti & Aziz 2008A, 2008 B, 2009). To start a free-piston linear engine generator involves reciprocating a freely moving piston-magnet-translator assembly between two oppositely placed engine cylinders in order for combustion to occur. To produce the required motion the machine is a brushless linear motor. Because the peak compression force is very large and, on the other hand, the current rating of the stator coils is limited and insufficient motor force constant, it is not possible to drive the translator end to end in a cycle. For that reason, it compressed air needs to be utilised to start the engine.

Zulkifli, Karsiti and Aziz (2008A) discussed a starting problem and its mechanical aspects for a specific linear generator configuration, and built a mechanical model and presented simulation results on the viability of a starting strategy using different values of constant-magnitude motoring force. Zulkifli, Karsiti and Aziz (2008B) discussed the electrical aspects of starting strategy, considered control possibilities, built a model of an electrical system, and presented simulation and validation tests of integrated models to start the investigation. Zulkifli, Karsiti and Aziz (2009), also discussed simulation and experiments, and they showed that motoring the linear generator with a rectangular current commutation and open-loop does not produce cycles of increasing amplitude, but instead

steady-state operation after the very first cycle. So that every DC bus voltage level, certain fixed cyclic amplitude, speed and compression pressure would be resulted. Thus, using a sufficiently high DC bus voltage, the linear generator can be reciprocated at the required amplitude for starting instead, since the compression pressure and cyclic speed is much higher than required.

A permanent magnet linear engine generator was designed by Ping, Arof and Wijono (2006). There are two types of linear generator design, such as a long translator type and a long stator type. In the long translator generator, the translator (mover) is longer than the stator, alternatively, in the long stator it is vice versa. The long translator type always activates all windings in every generator motion, on the other hand, in the stator type only a part of the stator is activated. From a machine efficiency point of view, the long type translator generator will be the best choice. Although, selection of the generator type may also depend on the space provided in the generator system.

The fabrication and testing of a linear electric generator for a free-piston engine have been conducted by Hew et al (2003). A linear electric generator is capable of generating 5 kW of power. The performance was evaluated using test bed drives by an induction motor via a crank slider. During the test, all coils are connected in series and the no-load induced voltage is measured. From the results obtained, it is proven that the constructed linear generator is functional, and this proves that the theoretical concept works. Linear electric generators can be fabricated using commonly available manufacturing techniques and commercially available materials in Malaysia.

2.1.3.2.3 Free-piston Research Development Based Opposed Piston

An opposed piston free-piston engine essentially consists of two single piston units with a common combustion chamber. Each piston requires a ribbon device and a load device may be coupled to one or both of the pistons. Usually, a mechanism system is necessary to synchronise in an opposed piston free-piston engine. The main advantage of the opposed piston configuration is the perfectly balanced and vibration free design. This feature is not shared by any of the other free-piston configurations, which need alternative means to

control vibrations. A further advantage of the opposed piston design is reduced heat transfer losses due to the opposed piston cylinder (elimination of cylinder head), and this also allows uniflow scavenging to be used, resulting in a high scavenging efficiency (Mikalsen & Roskilly 2007).

An opposed piston free-piston engine is rarely found in modern free-piston engines because it needs a piston synchronisation mechanism. London and Oppenheim (1952) began to develop the old generation of opposed piston free-piston engine. The modern opposed piston free-piston engine has been reported on by Hu and Hibi (1999) and Ito (2004). For a clearer explanation about opposed piston free-piston engines we recommended reading the dissertation of Aichlmayr (2002).

A fundamental test apparatus of a hydraulic opposed piston free-piston internal combustion engine was conducted by Hu and Hibi (1990). In order to eliminate the vibration of the system, an opposed piston design has been constructed in the experiment. The features of the test apparatus are fuel injection, compression ignition, uniflow scavenging, two-stroke and single cylinder. The engine design was not intended to be a mechanical synchronised system. Synchronisation of the opposed piston was achieved by positioning both pistons at mirroring positions before the start of the gas cycle.

2.2.3.3 Research Development Base Research Groups

The reason for discussing the research groups in this subchapter is to develop a networking interest. There are currently many research groups working on linear engines scattered all over the world, such as in the United States, Europe and Asia. The contributors could come from industries, governments and universities. Since there are so many research groups, it is very difficult to discuss them all individually at the present time, and only a number of the research groups are discussed in this research.

2.2.3.3.1 The National Aeronautical and Space Administration (NASA)

The National Aeronautics and Space Administration (NASA) Lewis Research Center (LeRC) have been working on free-piston Stirling engine activities since the 1980s. These include (1) a generic free-piston Stirling technology; the project has conducted developing technologies generic to both space power and terrestrial heat pump applications in a cooperative, cost-shared effort with the Department of Energy (DOE)/Oak Ridge National Laboratory (ORNL), and (2) a free-piston Stirling space power technology feasibility demonstration project that has the supported of the Defense Advanced Research Projects Agency (DARPA), DOE, NASA, SP-100 project. The generic technology effort includes extensive parametric testing of a 1 kW free-piston Stirling engine (RE-1000), development of a free-piston Stirling performance computer code, design and fabrication under contract of a hydraulic output modification for RE-1000 engine tests, and a 1000-hour endurance test, under contract, of a 3 kWe free-piston Stirling/alternator engine. The newly initiated space power technology feasibility demonstration effort addresses the capability of scaling a free-piston Stirling/alternator system to about 25 kWe, developing a thermodynamic cycle efficiency >70 percent of Carnot at temperature ratios in the order of 1.5 to 2.0, achieving a power unit specific weight of 6 kg/kWe, operating with non-contacting gas bearings, and cable dynamic balancing of the system. Planned engine and component design and test efforts are described in Slaby (1984).

In the 1990s, NASA developed a 25 kW free-piston Stirling Space Power Demonstrator Engine for the SP-100 program. Since that time, NASA has shown continued interest in free-piston Stirling conversion systems. As part of the NASA Radioisotope Power Systems program, DoE has been developing the Stirling Radioisotope Generator (SRG110). using dual 55 W Stirling convertor systems for use with radioisotope heat sources. Engineering and qualification units are being produced, and multiple dual-generator system tests are ongoing. Test times over 20,000 hrs have been accumulated on the one set of Stirling convertors at NASA GRC. In addition, the testing of a pair of 55 W Stirling convertors in a thermal vacuum environment at NASA GRC in order to advance the technology readiness level is underway (Brandhorst, 2007).

The NASA Vision for Space Exploration of the moon may someday require a nuclear reactor coupled with a free-piston Stirling converter at a power level of 30–40kW. Recently, NASA began a new project with Auburn University to develop a 5kW, single converter for potential use in a lunar surface reactor power system. The goals of this development program include a specific power in excess of 140 W/kg at the converter level, lifetime in excess of five years and a control system that will safely manage the converters in the case of an emergency. Auburn University has awarded a subcontract to Foster-Miller, Inc. to undertake the development of the 5 kW Stirling converter assembly (Brandhorst & Chapman, 2008).

2.2.3.3.2 West Virginia University (WVU)

West Virginia University is one of leading research institutions in free-piston linear engines. At the beginning, studies have concentrated on the use of a small bore, two-stroke cycle, linear gasoline engines in conjunction with a linear alternator for the generation of electrical power (Clark, Nankumar & Famouri, 1999; Clark et al, 1998A, 1998B; Atkinson et al, 1999). A two-stroke engine prototype, with a 36.5 mm bore and a maximum stroke of 50 mm, operating in a gasoline-fuelled spark-ignited mode, was successfully tested under varying externally applied loads and ignition timing conditions (Nankumar, 1998). It was found by analysis of the pressure volume diagrams that the ignition timing had to be highly advanced in the no-load (or idling) case in order to perform the adverse work required to slow the piston near the end of the compression stroke. As the load on the engine was increased (initially through the application of a friction brake, and later with an electrical alternator load), the ignition timing was required to be retarded, thus reducing and finally eliminating the adverse work, while concomitantly increasing the net positive work output of the engine.

Cawthorne et al (1999) developed an overall system design as well as subsystems, including the engine and alternator. A dynamic simulation is then presented which utilises the developed model to determine the output characteristics of the system. The prototype system was successfully tested, and experiment results are also included. Accordingly, after

the design was completed, the linear alternator and engine were constructed, and load testing was performed to evaluate the performance of this prototype. The motoring action of the linear alternator was used as a starting device, which is automatically disengaged after the engine exceeds a certain reciprocation frequency. The load testing was conducted using a purely resistive variable load. The load testing was terminated because the engine stalled as the load was increased over the value used in the final test.

Atkinson et al (1999) continued this research using a simulated engine model connected with a linear alternator. The engine consists of two opposed pistons, connected by a common connecting rod that is allowed to oscillate back and forth between the two end-mounted cylinders. The cylinders are ported in such a manner so as to utilise a loop scavenging process, although this process was not optimised. The fuel is supplied to each cylinder by two pulse width-modulated gasoline fuel injectors. In order to keep the engine temperature within a reasonable operating range, water is forced through the cylinder heads.

West Virginia University also developed a diesel two-stroke linear engine (Houdyschell, 2000). A diesel linear engine prototype has been developed for electrical power generation. The operation of a linear engine is different from that of a conventional slider-crank mechanism engine as the motions of the two horizontally opposed pistons are not externally constrained. The two-stroke engine prototype with a bore of 75 mm and a maximum stroke of 71 mm has been developed. The diesel prototype engine was tested several times with varying results. As the testing progressed, the engine control unit (ECU) design and other parts were updated to improve the performance of the engine. The improvements have led to an engine that would fire but it has not fired, at the present time it runs in sustained operation. No attempt to collect data from the in-cylinder pressure transducers has been made because the engine has not run in a sustained mode of operation.

A conceptual design of a four-stroke linear engine based on the numerical simulation of the operation of this type of linear engine has been presented by Petreanu (2001). The engine consists of four opposed pistons linked by a connecting rod to a linear alternator. A series of numerical simulations was developed and employed to investigate the operation and performance of this crankless, four-stroke linear engines. Two numerical models permit the simulation of the four-stroke linear engine employing a direct injection compression

ignition mode and a HCCI mode. The engine computational model combines dynamic and thermodynamic analyses. A detailed analysis of the engine operation range allows results to be obtained from a parametric study. The parametric study was performed to predict the engine behaviour over a wide operating range, given intake parameters, variations in fuel combustion properties, reciprocating mass of the piston shaft assembly, frictional load and the externally applied load, and injection and valve timing. Based on the parametric study, a conceptual design for a 15 kW linear engine was developed, showing the effects of reciprocating mass and air to fuel ratio on the frequency of operation, power output, and efficiency. The engine operating in direct injection compression ignition permitted high efficiency, with values between 46% and 49% corresponding to a compression ratio range between 17 and 35, respectively.

2.2.3.3.3 Solo Kleinmotorn

Solo Kleinmotorn, a German producer of small engines for different applications, has been working in the design and field test of a single acting V-1 Stirling engine for several years. Its main applications is in 9 kW/24 kW CHP units with natural gas and later biomass fuel, as well as for solar concentrators. The engines produce electric energy via an alternator and work stationary; the design and development history were described in earlier ISEC papers. The main advantages of the Stirling are its multi fuel capacity, low emissions and long service and lifetime. Since 1996, several Stirling engines called “Solo Stirling 161” were built and used for testing. The majority operate as small CHP-units for heat and electric energy production in buildings. Some engines are working in parabolic concentrators for solar energy. Others are used for tests woodchips. One machine is tested for be used as a refrigerator. In total, more than 150,000 operating hours of reliable work for stationary applications with extremely long service and lifetime have been logged. Now, more than 6,000 operating hours before service and a lifetime of at least 40,000 hours can be achieved.

De-centralised Power-Heat Co-Generation is recognised as an effective way to reduce CO₂ emissions. A politically desired reduction of 25% by the year 2005 requires the

doubling of electrical energy from combined heat/power stations. A large potential exists for the expansion of Co-Generation, particularly with small units ranging from 5-10 kW producing the basic heat demand in buildings. Presently, the technical standard is set by gas driven Otto engines with catalysts which operate in parallel with the heating system. For a smaller capacity range below 10 kW, the Stirling engine presents an attractive solution with the advance of up to 8000 maintenance free operating hours, 5000 hours in excess of the time period offered by gas driven Otto Engines. A service frequency similar to a heating system is possible (Baumuller & Schmierder, 2001). Figure 2.4 below shows the Solo Stirling 161 tests fired with biomass.

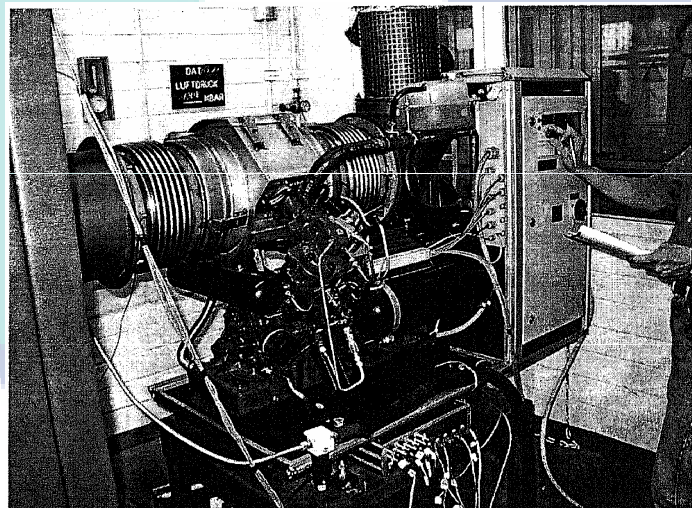


Figure 2.4: Solo Stirling 161 tests fired with biomass

Source: Baumuller and Schmierder (2001)

2.2.3.3.4 Sandia National Laboratories

Sandia National Laboratories has been consistently developing linear engines since 1998. The laboratory has been investigating a new, integrated approach to generating electricity with ultra low emissions and very high efficiency for low power (30 kW) applications such as in hybrid vehicles and portable generators; the approach utilises a free-piston in a double-ended cylinder. Combustion occurs alternately at each cylinder end, with

intake/exhaust processes accomplished through a two-stroke cycle. A linear alternator is mounted in the central section of the cylinder, serving both purposes; generation of useful electrical power and control of the compression ratio by varying the rate of electrical generation. Thus, a mechanically simple geometry results in an electronically controlled variable compression ratio configuration (Van Blarigan, Paradiso, & Goldsborough, 1998).

Sandia National Laboratories is developing a combustion-driven generator set for application in both transportation and stationary power systems. The goal is to maximise the thermal efficiency at a particular operating point while releasing essentially zero emissions. The operating principle is to ignite and burn lean (fuel/air equivalence ratio (ϕ) \sim 0.4) homogeneous charge mixtures, thereby improving the indicated thermal efficiency, whilst reducing the peak cylinder temperatures to a level where essentially no NO_x is formed. Based on measured engine-out emissions from a rather conventional, but optimised for hydrogen, four-stroke cycle spark ignition engine, the project complies with the California Air Resources Board's (CARB) proposed standard for equivalent zero emissions vehicles, when the generator set is integrated into a series type hybrid power train for a standard sized automobile (Van Blarigan, 1999).

Van Blarigan (2002) continued the Sandia National Laboratories program by using hydrogen. The objective of this project is to provide a high efficiency means of renewable hydrogen-based fuel utilisation. The development of a high efficiency, low emissions electrical generator will lead to establishing a path for renewable hydrogen-based fuel utilisation. A full-scale prototype will be produced in collaboration with industrial partners. The electrical generator is based on already developed internal combustion reciprocating engine technology. It is able to operate on many hydrogen-containing fuels (e.g. H_2 , CH_4O , NH_3 , Biogas, etc.). The efficiency and emissions are comparable to fuel cells (50% fuel to electricity, \sim 0 NO_x). This electrical generator is applicable to both stationary power and hybrid vehicles. It also allows specific markets to utilise hydrogen economically and painlessly.

Goldsborough and Van Blarigan (2003) continued the research on optimising the scavenging system for a two-stroke cycle, free-piston engine for high efficiency and low

emissions. To ensure that the engine's performance goals can be achieved, the scavenging system was configured using computational fluid dynamics (CFD), zero- and 1-D modelling, and single step parametric variations. A wide range of design options were investigated, including the use of loop, hybrid-loop and uniflow scavenging methods, different charge delivery options, and various operating schemes. Parameters such as the intake/exhaust port arrangement, valve lift/timing, charging pressure and piston frequency were varied. Operating schemes including a standard uniflow configuration, a low charging pressure option, a stratified scavenging geometry, and an over-expanded (Atkinson) cycle were studied.

2.2.3.3.5. Royal Institute of Technology

Sweden Universities such as the Royal Institute of Technology have developed integrated free-piston generators sponsored by the Swedish Energy Agency. The free-piston generator integrates a combustion engine with an electrical generator (as shown in Fig. 1). The rod that connects the two oppositely placed combustion chambers also acts as a prime mover for the generator. The reciprocating, ignition and compression processes in the two chambers causes the connecting rod to have an oscillating motion. Now, if this rod is placed in a magnetic field (containing coils), and if the movement of the rod causes a disturbance of the field, an electromagnetic force (EMF) will be induced in the coils. This is the principle of the free-piston generator, producing electricity directly from the linear motion of the pistons. The crankshaft, which is normally required in conventional hybrid concepts, is therefore eliminated (Arshad et al, 2002, 2003; Chen et al, 2004).

Most work concerning FPECs has focused separately on the mechanical parts of the converter, the combustion process, and the linear generator design or control. There has been little research at a system level of the FPEC. To optimise system performance and reduce the size and cost such investigations are necessary. One important system issue is the interaction between the generator force, the translator dynamics and the drive system. The generator force affects the size of the supplying power converters, the size of the electrical machine, the amplitude of the generated power pulsations and thus the size of energy

storage. This makes the force a critical parameter for system design and performance (Hansson, Leksell & Carlsson, 2005).

2.2.3.3.6 Sunpower Inc

Sunpower have in fact developed free-piston Stirling engines since the 1990's. However, prototype free-piston Stirling machines (engines, coolers, and cryocoolers) accumulated thousands of hours of maintenance free operation and tens of thousands of stop-start cycles. Free-piston (linear) compressor designs are also proving reliable as well as efficient, and are nearing commercial availability. This work proposes a design that builds on these maturing technologies. This design promises to increase the feasible electric output of generators based on free-piston Stirling engines (FPSE). Sunpower designed free-piston Stirling engines with 3 kW and 1.1 kW output in the context of the design challenges of conventional, kinetic Stirling engines. The free-piston designs use an effective and efficient power control system, non-contact gas bearings and seals, and a robust, relatively inexpensive heat exchanger design (Lane & Beale, 1997).

Sunpower continue with the preliminary design of a 7 kWe free-piston Stirling engine with rotary generator output. The design combines several features of prototype free-piston machines that are nearing commercial production. This approach promises to extend the commercially practical range of free-piston Stirling engines/electric generators. The Stirling driver is comprised of two conventional, displacer type, free-piston engines configured as a dynamically balanced opposed pair. Using the outer face of its power piston, each engine drives a single-acting blower. The single turbine/generator uses a commercial unit and it is separated from the engines and connected by ductwork. The engines and turbines utilise the same helium working fluid (Wood, Lane & Beale, 2001).

More recently, Sunpower has been working on two development programs involving small Free-Piston Stirling Engine (FPSE) converters, ultimately intended for space power applications. NASA is interested in Stirling converters because of their high efficiency which could reduce the amount of Plutonium-238 required in Radioisotope Power Systems (RPS) by approximately a factor of four (Wood & Lane, 2004).

2.2.3.3.7 Inas B.V.

The Dutch company Inas BV is among the research leaders within free-piston technology at the present time. A single piston, diesel powered, hydraulic free-piston engine has been developed, intended as an alternative to conventional engine and hydraulic pump systems in off-road vehicles (Achten et al, 2000). With heavily fluctuating fuel prices, the total cost of ownership of loaders, excavators, and other off-road machines is nowadays strongly influenced by fuel costs. Moreover, there is growing concern about CO₂ emissions caused by the burning of fossil fuels, as well as in the long-term availability of these fuels. The fuel economy and efficiencies of the drive train and the hydraulic implements have therefore become extremely important parameters in the design of future off-road machines (Achten, 2009).

The Inas free-piston engine has 17 kW power output, and indicated efficiencies of around 50% are reported. The engine uses the pulse pause modulation control principle. The fuel consumption is 20% lower than a conventional engine-pump unit, and at low load even 50% lower (Mikalsen & Roskilly, 2007). The contraction of the engine is shown in Figure 2.5. However, the engine utilises a complex hydraulic control system.

Inas is currently working on a series hydraulic hybrid driven trains (Achten, 2009). Hybrid transmissions are normally not considered to be a solution for off-road machines. Hybrid drive trains are foremost developed for passenger cars where they can benefit from the recuperation of brake energy. But for many off-road vehicles, brake energy recuperation is not an option. Furthermore, hybrid electric vehicles need sophisticated electric transmissions with delicate and expensive inverters, converters and batteries. Taking the extreme power transients in mobile machinery and the rough operational conditions of off-road drive trains into account, it is questionable whether the delicate hybrid electric drive trains can be considered a viable, inexpensive and robust option for off-road applications.

In this new concept, the complete mechanical transmission of a car is replaced by a full hydrostatic transmission, allowing energy recuperation and efficient engine operation. The concept requires extremely efficient hydrostatic pumps, motors and transformers, which have recently been developed. The idea comes from the fact that cars are commonly not

always operated at close maximum continuous rating. In fact when one drives a car in cities there is a high traffic density resulting in high average fuel consumption. The internal combustion engine delivers all its energy to a constant displacement pump. The engine torque is directly related to the pressure in the high-pressure accumulator and can consequently only vary between 50% (at 200 bar) and 100% (at 400 bar) of the maximum torque. Operation of the engine at low loads is therefore completely avoided. In the hybrid, each wheel has its own hydraulic motor. These motors act as a pump when braking, thereby recuperating brake energy and storing it in the high pressure accumulator. The torque of the in-wheel motors is controlled by means of the hydraulic transformers, one for each axis. The system has a variable traction control for the front and rear axis. The pumps, motors and transformers in the Hybrid are of the new “floating cup” type (Innas, 2010).

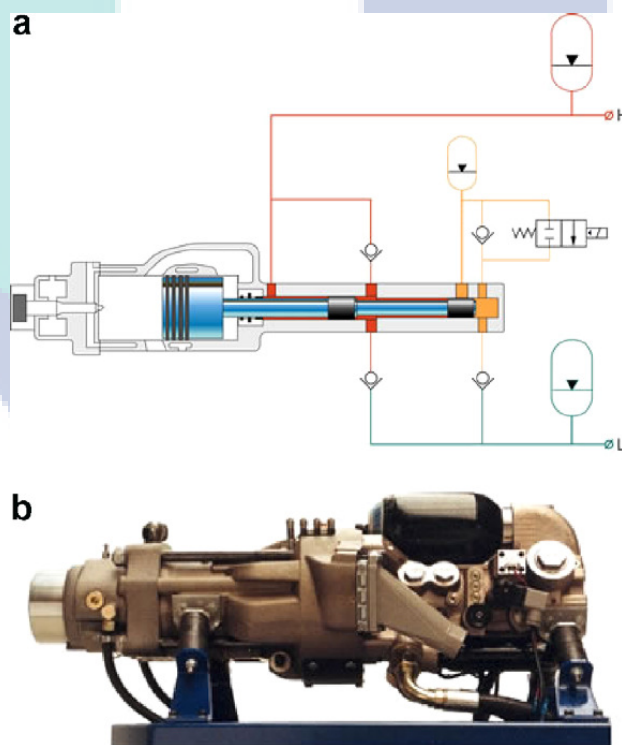


Figure 2.5: The Innas free-piston engine. (a) The working principle of the Innas free-piston engine. (b) Photograph of the engine.

Source: Mikalsen and Roskilly (2007).

2.2.3.3.7 Aerodyne Research Inc. (ARI).

A linear-oscillating miniature internal combustion engine, the so called MICE, has recently been developed by Aerodyne Research Inc. (ARI) (Annen et al, 2003). Portable electric power is an essential element in modern technologies. Applications range from electronic products such as laptops and cell phones, to cordless devices such as power tools and “dustbusters”, to a wide range of military items such as night-vision goggles and communications equipment. In almost all cases, this power is currently supplied by batteries, though the low energy density of batteries significantly limits the duration of use and represents a substantial fraction of the weight of these systems.

ARI is developing an innovative motor-generator, consisting of a miniature linear engine coupled with a linear electric alternator, which takes advantage of the high energy content of hydrocarbon fuels while eliminating most of the parts found in a standard internal combustion engine-generator set. The MICE generator has been developed by ARI into a patented design (Annen et al, 2003). The configuration of MICE can be seen in Figure 2.6.

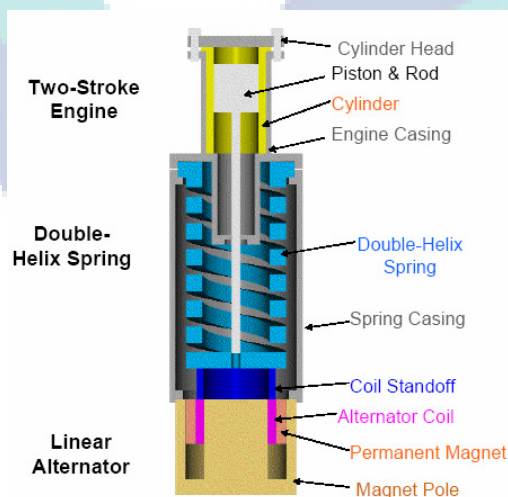


Figure 2.6: MICE Generator Design

Source: Annen et al (2003, 2008).

The basic MICE design consists of a free-piston two-stroke engine, a spring, and an alternator in a linearly oscillating configuration. MICE is inherently an electric power generator, since there is no mechanical linkage with which to extract power. Pure linear motion is ensured by the use of a unique double helix or multiple helix spring. The pure linear oscillation provides sliding motion with no side forces. Thus, MICE has low frictional losses since there are no bearing surfaces with a direct load. The complexity and cost of the rotary components in the conventional crankshaft-rod-piston arrangement are eliminated, thus also removing the typical failure point in small engines. The low friction characteristics and absence of stresses generated by direct loads allow MICE to operate at very high cycle speeds, leading to high energy and power density, particularly at smaller sized scales. The pure linear motion, in addition to having low frictional losses, may allow operation with little or no oil lubricant, instead using a solid film lubricant (Annan et al, 2008).

According to Annan et al (2008) ARI has developed the MICE generator in three power ranges, the 5 - 10 W, 300-500 W and 100 W. The 5-10 W MICE generator, is developed as an alternative power source for micro air vehicles, next to the 300-500 W MICE generator which is designed to use both heavy (JP-8, diesel) and light (propane, butane) fuels. The 100 W MICE generator was designed to operate with a butane or propane fuel cartridge. This design is connected with a military BB-390 battery (5 inch height) for relative size comparison. The 100 W unit has a diameter of 36 mm (1.4") and a height of 130 mm (5.1"). Operation of JP-8 will be possible at this size scale with further development. A 100-hour test of the 100 W spring and alternator components was recently completed, and combustion testing of the 100 W MICE generator is currently in progress. The MICE generator has demonstrated full operation from cold start up to steady state operation on Jet-A fuel in 300 W scale in laboratory tests. The MICE generator has also shown the capability of quiet operation, demonstrating 71 dBA at 1 ft in laboratory tests with much lower levels achievable with an improved acoustic design. The MICE generator technology has the potential to meet the portable power needs of US military forces. With additional development to TRL levels of 6 or 7, these high performance characteristics can be demonstrated and quantified.

2.3 THEORETICAL BACKGROUND

2.3.1 Design Method

Two approaches to the design and development of linear engine are full design of all components and modification from conventional engine. The case of full design is a simpler process than modification, but has a higher cost, is more time consuming, and requires increased equipment support. The advantages of modification are a reduced research budget and the fact that comparative studies of both designed systems (conventional engine and linear engine) can be made. This research is to be carried out to develop a linear engine based on conventional engines (engine modification technique).

2.3.2 Heat Release

To predict engine performance without conducting tests is called modelling (Stone, 1997). GT-Power has been used for the simulation. Conceptually, a prediction of engine performance by simulation is quite different from conducting an engine experiment. In the experiment, the pressure diagram is collected first and followed by heat release analysis. The reverse is true for a simulation technique. There are two theories of heat release, namely, chemical theory and mathematical modelling using the first law of thermodynamics. Both theories will be adopted in this research. The Wiebe combustion model is chemical theory based, where the mass fraction burnt profile is represented as:

$$x = 1 - \exp \left[a \left(\frac{t}{t_{comb}} \right)^{m+1} \right] \quad (2.1)$$

After differentiation of Equation 2.1, the rate of heat release $dt/d(t/t_{comb})$ is expressed as:

$$W = a(m+1) \left(\frac{t}{t_{comb}} \right)^m \exp \left[a \left(\frac{t}{t_{comb}} \right)^{m+1} \right] \quad (2.2)$$

where t_{comb} is period of combustion, t is time variable of combustion process $0 \leq t \leq t_{comb}$, and a , m are parameters. The parameter of a is a characteristic of the completeness of combustion, while m is the rate of combustion. Wiebe assumed $W_{max} = 0.990$, and hence $a = 6.908$ (Kowalewicz, 1984). Values of $a = 5$ and $m = 3$ have been reported to fit well with the experimental data (Ferguson & Kirkpatrick, 2001; Heywood, 1988). Using the Wiebe combustion model, the first law of thermodynamics was used to substitute heat energy for the pressure gradient of the gas at combustion space. Equation 2.3 is an expression of the first law of thermodynamics

$$\frac{dp}{dt} = -\gamma \frac{P}{V} \frac{dV}{dt} + \frac{\gamma-1}{V} \left(\frac{dQ}{dt} \right) \quad (2.3)$$

This is a first order differential equation of the form $dP/dt = f(t, P, Q)$ for cylinder pressure as a function of time t , pressure P , and heat release Q . By using formula 2.3, the pressure diagram of the combustion process in linear engines could be established.

The characteristics of pressure in the combustion chamber in a rotational engine and linear engine are exactly the same. The difference lies in its dynamics which result in a different power output. The engine friction reduces the work of an engine, and its difference between the indicated work and the brake work at power output. The friction process in an internal combustion engine can be categorised into three components which are the mechanical friction, the pumping work, and the accessory work (Stone, 1997; Ferguson & Kirkpatrick, 2001; Heywood, 1988).

2.3.3 Friction Force

Many methods have been developed to measure engine friction loss, including experimental and simulation techniques. Power output of linear engines can be predicted through simulation. Hence predicting friction loss is a very important exercise. Great efforts have been made by researchers in the development of comprehensive and accurate mechanical loss models and different model approaches have been proposed (Ferguson & Kirkpatrick, 2001; Heywood, 1988). Arsie et al (1998) have proposed an excellent formula, however the circumstances of these studies cannot be adopted. Although the formulas have a high precision level, they are difficult to break down in some parts, especially for the prediction of friction loss through the crank shaft, pin and bearing. In the case of linear engines, some devices could be ignored except for the connecting rod, piston and journal bearing.

According to the GT-Power manual (Gamma, 2004) the engine friction is calculated using the attribute as follows:

$$fmep = C + (pf \cdot P_{\max}) + (mpsf \cdot \bar{U}_p) + (mpssf \cdot \bar{U}_p^2) \quad (2.4)$$

where C is a constant part of the friction mean effective pressure ($fmep$), pf is the peak cylinder pressure factor, and $mpsf$ represents the peak cylinder pressure factor. $mpssf$ represents the mean piston speed squared factor. Looking at this expression, it is difficult to break it down into parts of friction components, but it is possible to use separate calculations using another expression. If $fmep$ is known, then this data is used directly by inputting the data into a constant part of $fmep$, because $fmep$ is a part of the calculations of the performance engine in GT-Power.

Atkinson et al (1999) introduced a simple equation for calculating the $fmep$ of linear engines. The developed expression is based on friction from contact between piston and cylinder liner. In fact, the effects of the cylinder pressure and main bearing still

occurred. For that reason the formula of Atkinson et al (1999) will not be adopted in this research. The preceding component analysis can be combined to form an overall engine *f_{mep}* model. The component equations are summarised by Ferguson and Kirkpatrick (2001) and have been used to develop a *f_{mep}* model in this research. Some component equations including valve train, pumping and accessory were not adopted in our two-stroke engine design (Gamma, 2004). Although the type of main bearing is different between rotational and linear engines; however, this expression is closer to the prediction of the friction losses of linear engines than the formula of Atkinson et al (1999). The following equations are used in *f_{mep}* modelling design simulation.

$$\text{Main bearings} \quad f_{mep_{bearings}} = c_b \frac{n_b N D_b^2 L_b}{n_c b^2 s} \quad (2.5)$$

$$\text{Seal} \quad f_{mep_{seals}} = c_s \frac{D_b}{n_c b^2 s} \quad (2.6)$$

$$\text{Connecting rod bearing} \quad f_{mep_{bearing}} = 41.37 K \left(\frac{b}{s} \right) \left(\frac{N}{1000} \right) \quad (2.7)$$

$$\text{and } K = \left(D_{mb}^2 L_{mb} + \frac{D_{cb}^2 L_{cb}}{m} + D_{as}^2 L_{as} \right) \frac{1}{b^3} \quad (2.8)$$

$$\text{Skirt} \quad f_{mep_{skirt}} = c_{ps} \frac{\bar{U}_p}{b} \quad (2.9)$$

$$\text{Rings} \quad f_{mep_{rings}} = c_{pr} \left(1 + \frac{1000}{N} \right) \frac{1}{b^2} \quad (2.10)$$

$$\text{Gas pressure} \quad f_{mep_{gasload}} = c_g \frac{P_i}{P_a} \left[0.088r + 0.182r^{(1.33-K\bar{U}_p)} \right] \quad (2.11)$$

Equations (2.5) through (2.11) are normally used for two-stroke rotation spark ignition engines. For a linear engine, some parts could be eliminated. In this research Equation (2.5) will be used to predict friction losses in the main bearing, Equation (2.6) for the seal, Equation (2.9) for the piston rings, and Equation (2.10) for the gas pressure. The friction losses at the connection rod bearing and skirt will be ignored.

2.3.4 Optimisation of Spring Design

Any practical design that has a large number of elements or subsystems will involve a number of variables and constraints, especially under multiple load conditions. The optimisation problem becomes improperly large and the solution process becomes too costly and can easily saturate even the largest computers available. The multilevel optimisation is a decomposition technique in which the problem is reformulated into several smaller sub-problems (one for each sub-system) to preserve the coupling among the sub-problems (sub-systems) (Rao, 1996).

An approach to this problem can be divided into single-level optimisation approaches and multilevel approaches. In the former, only a single optimisation problem is solved for the inter system, while in the latter, optimisation problems are solved within the disciplines as well as for the system as a whole (Balling & Safieszcznski-Sobieski, 1994). In such cases, the optimisation problem can be broken into a series of smaller problems using different strategies (Rao, 1996).

The multilevel optimisation approach is presented as a non-hierarchical multidisciplinary system. However, all disciplines are on the same level, thus the analysis and optimisation associated with the coordination of the system are implied. Each discipline in this system has an associated analysis program which computes the output function values from input values from the variables. One of the tasks of the single-level or multilevel optimisation approach is to satisfy the coupling constraints which enforce equality between each coupling variable and its corresponding coupling function. Each step contains objective

functions, these represent factors such as the maximisation of benefits and the minimisation of costs (Balling & Safieszcznski-Sobieski, 1994).

Optimisation of springs has been considered by Agrawal (1978), Pardes, Sarfor and Masclet (2001), Ahn and Jeong (2000). Agrawal (1978) developed a spring design with geometric programming techniques. However, Pardes, Sartor and Masclet (2001) have developed a numerical method of an optimisation process for extension spring design. A spreadsheet is implemented for the optimisation of processes to be applied in industrial applications. A more specific optimisation of the spring design parameters of circuit breaker to satisfy the specified dynamic characteristics has been developed by Ahn and Jeong (2004).

In the case of spring design, especially for dynamic loading, fatigue limit is the most important constraint. There is so many fatigue research related to spring design, including DeLlano-Viscaya et al (2006), Ruzicka and Doubrava (2005) and Yamada et al (2000). Improved fatigue strength by the application of a new fine shot peening technology is advantage research for spring design in special cases. In the special case of advanced spring design, it is usual to have unique constraints and object functions. For those cases, a specific spring material with a high fatigue limit is needed.

For engine performance optimisation, especially under dynamic load, it is impossible for static compilers to analyse the whole program. Adaptive dynamic optimisation is the most effective technique to solve dynamic problems (Bruening, Garnet & Amarashinghe, 2003). Dynamic code optimisations can produced stable, possibly phased, behaviour exhibited by a running application, and can thereby utilise information not available to a static optimiser. Furthermore, new code deployment techniques, such as dynamically linked libraries, create barriers for traditional optimisers, but are agreeable for dynamic optimisation (Fahs et al, 2001).

The spring has to be presented so that its design and mechanism of combustion requirements are met for linear engines. The objective functions of the spring design of a linear engine system are the minimisation of spring weight and maximisation of operation area for the spring on variable speeds and load on linear engines. To conduct the best optimisation results based on the objection functions, the multilevel optimisation approach

has been adapted. The three methods used for the spring design are nonlinear, geometric and dynamic programming methods. The first step is to use nonlinear 1-D minimisation methods. The first step in spring design is to predict the ideal force (Gotoh & Imaizumi, 2000). Force data can be estimated by GT-power simulation. The objective function of the optimisation is to minimise the force difference between the minimum and maximum values. The second step is using geometrical programming techniques. Agrawal (1978) applied this technique to solve a design optimisation problem for the minimum weight of torsion coil springs. The last step is using dynamic programming techniques. This method tries to maximise the operational area of the spring mechanism. Variable speed on full load condition data is used to measure deflection performance of the spring mechanism as an objective function.

A geometric programming technique has been adopted for a part of spring design optimisation. It is used to minimise functions that are in the form of polynomials subject to constraints of the same type. It differs from other optimisation techniques. In essence, it places relative magnitudes of the objective function rather than variables. Instead of finding the optimal values of the design variables at the beginning, geometric programming first finds the optimal value of the objective function. To formulate the minimum weight design of a helical spring under axial load as a geometric programming problem, we should consider the constraints on shear stress, natural frequency and buckling of the spring (Rao, 1996). By selecting the mean diameter of the coil and the diameter of the wire as design variables, the design vector is introduced as in Equation 2.12.

$$X = \begin{Bmatrix} x_1 \\ x_2 \end{Bmatrix} = \begin{Bmatrix} D \\ d \end{Bmatrix} \quad (2.12)$$

where D is the mean diameter of the coil and d is the wire diameter.

The objective function (weight) of the helical spring can be expressed as shown in Equation 2.13.

$$f(X) = \frac{\pi d^2}{4} (\pi D) \rho (n + Q) \quad (2.13)$$

where n is the number of active coils, Q is the number of inactive coils, and ρ is the weight density of the spring material. If deflection of the spring is δ , we obtain a formula as shown in Equation 2.14.

$$\delta = \frac{8PC^3 n}{Gd} \text{ or } n = \frac{Gd\delta}{8PC^3} \quad (2.14)$$

where G is the shear modulus, P is the axial load on the spring, and C is the spring index ($C = D/d$). Substitution of Equation 2.13 into Equation 2.12 gives Equation 2.15.

$$f(X) = \frac{\pi\rho G\delta}{32P} \frac{d^6}{D^2} + \frac{\pi\rho Q}{4} d^2 D \quad (2.15)$$

If the maximum shear stress in the spring (τ) is limited to τ_{\max} , the stress constraint can be expressed as Equation 2.16.

$$\tau = \frac{8KPC}{\pi d^2} \leq \tau_{\max} \text{ or } \frac{8KPC}{\pi d^2 \tau_{\max}} \leq 1 \quad (2.16)$$

where K denotes the stress constraint factor, which is defined by Equation 2.17.

$$K \approx \frac{2}{C^{0.25}} \quad (2.17)$$

The use of Equation 2.17 in Equation 2.16 will produce Equation 2.18.

$$\frac{16P}{\pi\tau_{\max}} \frac{D^{3/4}}{d^{1/4}} \leq 1 \quad (2.18)$$

To avoid fatigue failure, the natural frequency of the spring (f_n) is restricted to be greater than $(f_n)_{\min}$. The natural frequency of the spring is given by Equation 2.19.

$$f_n = \frac{2d}{\pi D^2 n} \left(\frac{Gg}{32\rho} \right)^{1/2} \quad (2.19)$$

where g is the acceleration due to gravity. Using $g = 9.81 \text{ m/s}^2$, $G = 8.56 \times 10^{10} \text{ N/m}^2$, and $f_n = 13$, Equation 2.19 becomes Equation 2.20.

$$\frac{13(f_n)_{\min} \rho G d^3}{288,800 P D} \leq 1 \quad (2.20)$$

Similarly, in order to avoid buckling, the free length of the spring is limited as dictated by Equation 2.21.

$$L \leq \frac{11.5(D/2)^2}{P/K^1} \quad (2.21)$$

Using the relationships of Equations 2.22 and 2.23 below:

$$K^1 = \frac{Gd^4}{8D^3 n} \quad (2.22)$$

$$L = nd(1 + Z) \quad (2.23)$$

and $Z = 0.4$, then Equation 2.20 can be expressed as Equation 2.24.

$$0.0527 \left(\frac{G\delta^2}{P} \right) \frac{d^5}{D^5} \leq 1 \quad (2.24)$$

It can be observed that the problem posed by the objective function of Equation 2.15 and the constraints of Equations 2.17, 2.19 and 2.24 are geometric programming problems.

2.3.5 The Dynamic Model for Motion Studies

Motion studies for linear engines have been conducted by many researchers. From the numerous reviews conducted, it was found that different designs of linear engines introduced different characteristics. Certain methods and software are also available to investigate the motion studies of linear engines. Mikalsen and Roskilly (2008) used the open source computational fluid dynamics toolkit OpenFoam, written in C++ programming language and released under GNU general public license. Fonna, Mohamed and Arifin (2005) built an engine model that was created in MSC Adams software. Frederiksson and Denbratt (2004) have used three different tools for simulation, such as Matlab/Simulink, boost and Senkin. Matlab/Simulink was used to simulate piston dynamics, for simplified modes of scavenging, ignition and combustion. Gas exchange was computed by the 1-D commercial code boost and chemistry was simulated with Senkin. Qingfeng, Xiao and Huang (2008) also have used three software applications to investigate the performance of the novel development of a two-stroke free-piston engine for electrical power generation. They used Matlab/Simulink, Senkin and finite element methods (FEM) to simulate the motion of a linear engine.

The modelling starts with a dynamic analysis of the linear engine. They consider the case of a linear engine with spring system that oscillates back and forth in a left-to-right motion with a fixed inlet scavenging port. The expansion is conducted by combustion pressure, while the compression force is the reacting spring force. A system of coordinates was chosen with their origin at the outermost point of the left cylinder. Considering a mechanical system represented by the piston assembly in motion, this system obeys Newton's second law. This formula was also adopted by some researchers (Ahmad et al,

2006; Nik et al, 2006; Saiful et al, 2008; Mikalsen & Roskilly, 2008; Christopher et al, 1999).

$$m \frac{d^2 x}{dt^2} = \sum_i F_{ix} \quad (2.25)$$

where x represents the displacement of the piston assembly, and $\frac{d^2 x}{dt^2}$ is the acceleration of the piston. The right hand side of Equation 2.25 represents the summation of the forces that act in the plane of motion.

The only forces considered to act on the moving assembly are the resultant pressure forces given by the difference between the pressures in the two cylinders, a frictional force, the inertial force and the load.

Equation 2.25 can be written as:

$$m \frac{d^2 x}{dt^2} = F_C - F_f - F_s - F_L \quad (2.26)$$

$$F_C = (p_1 - p_2) \frac{\pi D^2}{4} \quad (2.27)$$

where F_C is the resultant of the combustion pressure forces, F_f is the friction force, F_s is the spring force, F_L is the load applied to the shaft, D is the piston diameter, and p_1 and p_2 are the corresponding in-cylinder pressures.

In order to determine the solution of this differential equation, it is necessary to integrate it twice with respect to time. The analytic integration is somewhat complicated to evaluate due to the complex variation in the three forces with respect to space and time.

However, the thrust force of the combustion process is expressed by a pressure diagram which results from a 1-D GT-power simulation analysis.

2.4 CONCLUSION

A literature review and theoretical background have been studied in this chapter. The objective of the relevant papers is to trace the study of research problems and theoretical background to solve the problems of the research. The review of the papers starts from the history of the development of linear engines from beginning to the present. Trends in research development of free-piston linear engines and related studies including control systems and linear generator have been examined in this chapter.

Most research development concentrates on the dual piston. Thus, many papers and research groups work in this area. The research developments include the design, development and simulation of linear engines. Linear generators have also been developed for dual piston free-piston engines. The start system is very important for the dual piston system; however, it needs to extend into more advanced research development. Spring systems have rarely been looked at closely until recent time. For this reason, the present research is a very important exploration of different techniques and different applications. This research is carried out in order to design a linear engine by the modification of a conventional engine for a small linear generator application. Two-stroke single cylinder free-piston linear engines with spring system strongly contribute to the development.

CHAPTER 3

RESEARCH METHODS

3.1 INTRODUCTION

This chapter mainly explains a business strategy to conduct research and methods to design a single cylinder two-stroke linear engine with a spring as the return cycle. The contents include strategy, methods, prediction of engine performance, spring design optimisation method, linear engine design method, effect of spring design on linear engine performance analysis method, dynamic motion analysis method, and an analysis method for spring system modification.

As explained in the theoretical background, the main concern of the research is to design a linear engine based on a conventional engine, or as we called it an engine modification technique; since complete data are important to conduct a design-based modification technique. The two approaches for collecting data, experimentation and simulation; however due to having a small budget, in this research a simulation approach has been used.

The business strategy for designing a single cylinder high-speed spark ignition (SI) linear engine starts with the prediction of the engine performance. Due to optimisation of the spring design, this step is very an important one. Before conducting the design of a linear engine, it is first necessary to design the spring, and then continue to the design of components of the linear engine. The possibility of developing a single cylinder high-speed SI linear engine can be carried out when all requirements have been accepted, for that reason analyses are necessary. The analyses include the effect of the designed spring on engine performance and engine dynamics. Modification of the designed linear engine, if necessary, will also be conducted.

To obtain the best results of the research, complete data are very important. Some professional software has been used in this research, but a validation process is necessary. Since engine performance prediction is the key factor for the success of the research, the validation should be carefully conducted. In this study the model

validation is done in two ways, first following the manual of the original conventional engine, and second, by conducting experiments. Using manual validation is a very simple and trustworthy method but only one point result could be a proof. To find out about all the aspects concerning the process, experimentation is needed.

3.2 FLOWCHART, MODEL AND VALIDATION

3.2.1 Flowchart of the Research

To obtain an acceptable design, the following steps are needed, the prediction of the engine's performance, linear engine design, design analysis, modification spring system, and lastly a final design. A spring is chosen as a return force source for the piston movement. The uniqueness of using a spring as a return cycle is the main characteristic of this engine. However, the stroke of the engine is not constant, as in a conventional engine. The problem is that the expansion stroke depends on the thrust force of the piston. On the other hand, the engine needs to be operated at suitable variable speeds and loads. A constraint of using a spring as the return cycle for a linear engine is that it is very sensitive to thrust force. For that reason, prediction of the engine performance is very important.

The engine performance prediction should begin by building a model. The model is a scale from the original components of the main combustion system of the conventional engine. The arrangement also should be the same as the original one. A 1-D GT-Power software application has been used in this study. This software could not predict linear engine performance but, with a small modification by following the GT suite manual, it is possible to predict the performance of the linear engine.

The second step is to design a linear engine including spring design optimisation, connecting rod, casing and bearing. Some components have been used from the original engine. The step starts with the optimisation of the designed spring, then continues with the other components. Some different types of software have been used in this step, including SolidWorks and a spreadsheet. SolidWorks is a drawing application and the spreadsheet is used to design the spring. The spring was designed using a multilevel optimisation approach. The detail of the approach can be seen in the

theoretical background in Chapter 2. Besides which, the topic is also explained in a specific sub chapter.

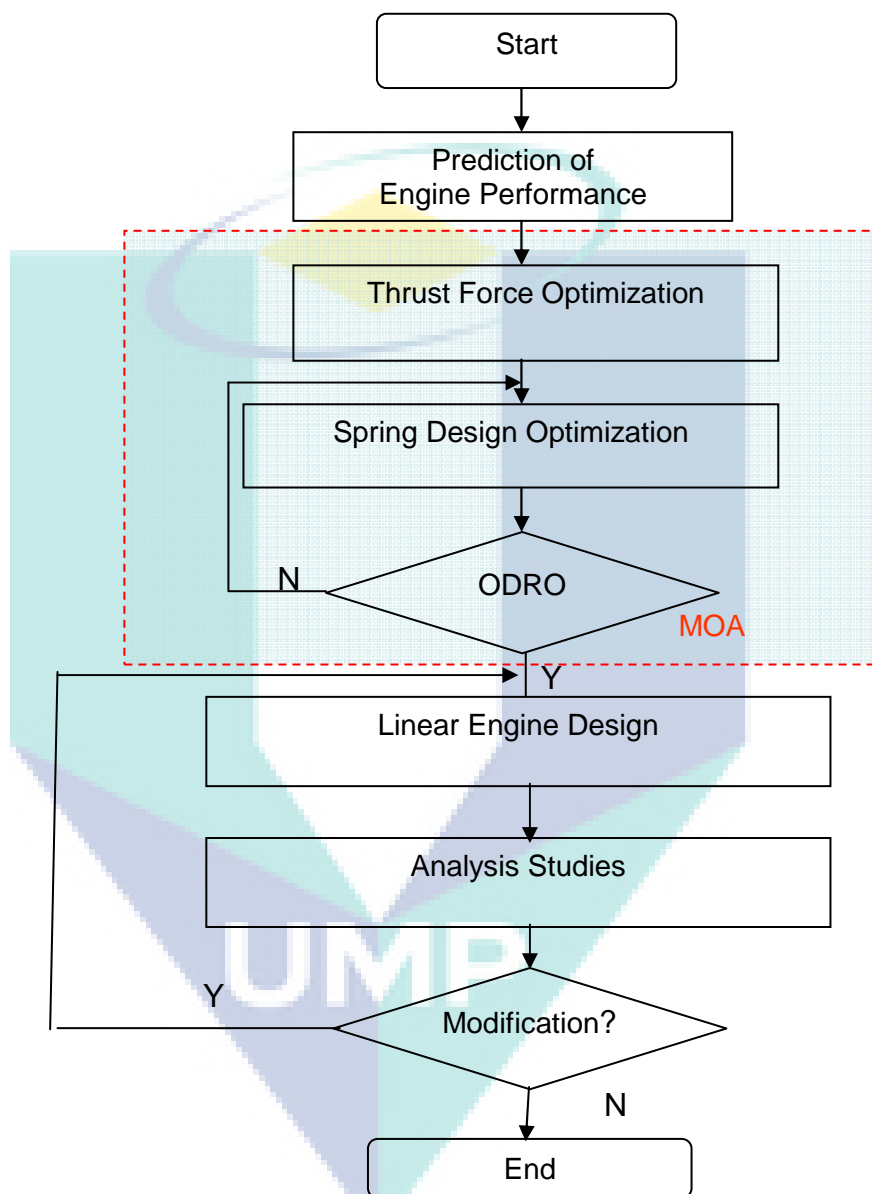


Figure 3.1: General flowchart of research methods

The third step is the analysis of the designed linear engine, including combustion and engine performance and spring system dynamic motion. It is necessary since the linearisation of a conventional rotational engine could have different characteristics. However, the resulting designed spring strongly influences the characteristics of the linear engine. There are two cases to be considered for analysis, namely the effects of

the spring design on the engine performance and the piston dynamics. A modification of the engine is necessary if the design cannot work properly.

Figure 3.1 shows the general flowchart of the research, where ODRO stands for Operation Design Requirement Optimisation and MOA for Multi Level Optimisation Approach. There are five steps required to conduct the research, and they have been explained in five subsection. Subchapter 4.1 concerns building a model and its validation. The model is used to predict the performance of the engine. Since the data is used for designing the linear engine, the model should be precise. For that reason, the validation is very important. Subchapter 4.2 covers the prediction of the engine performance. This chapter discusses a comparison between a conventional rotation engine and a linear engine with the same combustion chamber design. Subchapter 4.3 presents a design for the spring, and subchapter 4.4 discusses the design of a single cylinder two-stroke linear engine with spring system. Subchapter 4.5 discusses the analyses of the effect of the spring design, which in some cases that could influence the running of the linear engine. In Subchapter 4.6, the modification of the spring system design based on the results of the analysis is discussed.

3.2.2 Model and Validation Technique

1D-GT Power, part of the software of the GT Suite, has been used to predict the engine's performance and its results are used to modify the linear engine. Before building a model, all real components related to the combustion system should be measured precisely. For that purpose, the real engine is overhauled and every component is measured. A Back Pack Brush Cutter BG-328 has been used as the model. All components in the crank case should be extracted one by one and measured. After all the engine parts are measured, the engine model is constructed using the GT-Power software. At this level, all of the elements in the simulation model should be inserted with the measured values.

There are also some constants in the element that have to be defined. In order to simulate single piston free-piston linear engines in GT-power software, it is necessary to modify the friction factor of the engine. In a linear engine, the friction is small due to a lower number of parts in the engine. Some parts in the conventional engine are replaced by only the connecting rod. The frictions that have to be considered are at the

crankshaft's main bearing, crankshaft-seal, piston-ring and the piston-gas pressure. The equations used are shown in the literature review section in subchapter 2.3.3.

To obtain accurate data, a validation process is necessary. Two validation methods have been used in this research. Firstly, the model is validated with the specification from the engine in the manual. However, the specification of the engine is only shown at full load. Partial loads are also important for this research. For that reason, experiments are needed to validate the partial load conditions. Therefore, for the second validation an experiment should be conducted. However, power output, torque and specific fuel consumption are available to validate the model.

Accordingly, validation is only conducted for conventional rotational engines. However, the difference between conventional rotation engines and linear engines lie conceptually in their friction loss. By modifying the GT-Power facility, both types can be successfully predicted after the model is validated. Detailed modifications of the model are explained in Chapter 4.

3.3 METHOD FOR PREDICTION OF THE ENGINE PERFORMANCE

To predict the engine's performance GT-Power is used. The pressure characteristics in the combustion chamber are the same in both the rotation engine and linear engine. The differences are in the dynamics and result in different power outputs. The engine friction reduces the work of an engine, and it is the difference between the indicated work and the brake work at the power output. The friction process in an internal combustion engine can be categorised into three components, namely the mechanical friction, the pumping work and the accessory research. In the case of linear engines, the mechanical friction part can be reduced because it does not involve rotation motion and only leaves the piston ring and gas pressure components with friction (Fathallah & Bakar, 2009).

To predict the power output of linear engines through simulation, the predicted friction loss is very important. Many methods have been developed to measure the engine friction loss by means of experimental and simulation techniques. Great effort has been made by researchers in developing comprehensive and accurate mechanical loss models. Different model approaches have been proposed by Ferguson and

Kirkpatrick (2001). In the case of linear engines, some devices could be ignored, except for the connecting rod, piston and journals bearing.

The engine friction model is used to model the friction in the engine. GT-Power uses a Chen-Flynn model and the friction is calculated using the attributes of peak cylinder pressure factors, mean piston speed factor, mean piston speed squared factor and mean piston speed (Bos, 2007). Following that expression, it is difficult to break the friction components into parts, but it is possible to use separate calculations using another expression. If the *f_{mep}* is known, then we can use this data directly by inputting the data into a constant part of *f_{mep}*. The preceding component analysis can be combined to form an overall engine *f_{mep}* model (Fathallah & Bakar, 2009). The component equations are summarised by Ferguson and Kirkpatrick (2001), and have been used to develop a *f_{mep}* model in this research. However, some component equations, such as valve train, pumping and accessories were not adopted in the present two-stroke engine design. More detail information is given by Fathallah and Bakar (2009).

3.4 SPRING DESIGN OPTIMISATION METHOD

There are requirements that we should comply with in order to optimise the spring design for the cycle of the linear engine mechanism. First, the mechanism in combustion cycles should work properly. The deflection of the spring is dependent on the load. If the travel is not sufficient then the intake scavenging port cannot open. As a result, combustion in linear engine will not occur. For that reason, spring design should require the operation of linear engine mechanisms at variable speeds and loads. Another requirement is the criteria of the dynamic loading of the spring design. It should be checked at the spring stage for the possibility of fatigue. Moreover, it should be free from shock, spring resonance and spring mass system resonance.

The main objective of the spring mechanism in linear engines is the return of the cycle. However, the spring is not only there to actuate on the load for the shaft work from the Top Dead Centre (TDC) to the Bottom Dead Centre (BDC), but also to compress the mixture from BDC to TDC with a certain compression ratio. In this case, the compression ratio design is 1:9. It is a sophisticated design problem because there

are many constraints. On one side, there is a need for a strong spring design with dynamic loads, and on the other the deflection should properly open the inlet of the scavenging port at variable speeds and loads. Therefore, to achieve the best spring design, it requires compromise during optimisation.

The first step in the spring design process is selecting a material that suits the loads and deflections required for the design. According to a linear engine spring design, the work parameter is fatigue loading based. Environmental conditions can be set to non-corrosion category by designing a lubricated system design. The surrounding temperature of a spring working inside a linear engine casing can be assumed to be 100°C. This spring has to work under heavy-duty load with a wide deflection area, so it needs the best material for the finishing of the surface. To improve fatigue properties, a shot peening technology is adopted. According to Yamada et al (2000) the fatigue strength of wave springs, in terms of amplitude stress, is increased by almost twice. A chrome-vanadium alloy wire SAE 6150 has been used as the material in the spring mechanism of the linear engine. This material is suitable as spring valve material. However, spring systems of linear engines have a similar work area to spring valves.

There are some techniques to spring design and software with many kinds of approaches available. This research assumes that the engine performance applies in particular to a known Indicated Mean Effective Pressure (IMEP). This data is very important in designing spring loads. GT-Power is used to produce some data at variable speeds and loads. The IMEP maximum is not used as an input to the design, because affected on some part load do not work properly. For that reason, the IMEP performance data needs to be optimised, and the optimisation is carried out by using the numerical integration technique of Matlab. Spreadsheet is used to optimise the spring design; however, trial and error methods could be carried out more easily by hand. All criteria regarding dynamic loads of the spring design are required. Trial and error starts with the smallest wire diameter and then the diameter is increased gradually. Some design results are tabulated and analysed. There are important criteria when optimising spring design, namely:

- Spring working stroke should close to 30.5 mm
- Service strength (fatigue life)
- Compact dimensions with optimum weight

The engine load effects on the spring's performance are also analysed. It is important to study the engine's performance and spring performance itself. There are some criteria that affect the engine performance tests, such as:

- Deflection should meet inlet scavenging port design operation
- Critical velocity should meet a velocity of engine speed (critical velocity should be greater than the engine speed)
- Natural frequency of vibration should be at least 13 times (Rao, 1996).

According to the optimisation methods, there are some approaches to designing a spring. A spring system in a linear engine is a very specific device. The objective functions of the spring design are to minimise the spring dimensions and to maximise the spring operation work. There are so many constraints for both objective functions. A simpler method for optimising a linear engine spring system is to use a multilevel optimisation approach. The detailed concept has been introduced by Wei, Zhang and Nakhla (1993) and Balling and Safieszcznski-Sobieski (1994). The approach used three steps in series with different techniques, including nonlinear, geometric and dynamic programming methods. The detail of the method is available in subchapter 2.3.4

Spring manufacturers require an estimate of the fatigue life for dynamic load spring design. In the prediction of a component's life, the most powerful presentation of the fatigue life test is the modified Goodman diagram (Jurnival & Marshek, 2006). The strength check of a spring exposed to fatigue loading is conducted by comparison of the maximum fatigue strength of the material for the given loading with the corrected stress of the spring in a fully loaded state. If the design spring has to meet the strength check at the full extent, the resulting level of safety must be higher than or equal to the desired level of safety (in this design S_f was 1.05). The value has been chosen according to mechanical, industrial and technical calculations for chrome-vanadium alloy steel wire SAE6150 with the peened process (Miroslav, 2009).

3.5 LINEAR ENGINE DESIGN METHOD

After the best suitable spring design for the linear engine has been achieved, design of the linear engine in the obvious next step. As mentioned before, the linear engine design of this research is designed based on a conventional two-stroke engine.

New connecting rod, journal bearing and spring, all of which is called the spring mechanism, has been designed to replace the crankshaft system. Removing the crankshaft, crankcase, connecting rod, bearing and seal components, and replacing them with a spring mechanism makes the linear engine casing bigger than a conventional engine. Some components have been adopted from conventional engines, such as the Back Pack Brush Cutter (BG – 328). The components include piston, piston pin, cylinder head, carburettor and exhaust system.

All components, including new and original conventional engine components, have been drawn by SolidWorks. The original component's dimensions are measured and duplicated as design components. However, the rod, journal bearing, crank case and bearing were designed as new components. All components were stored in a database, categorised into groups and later fully assembled in the form of the single cylinder linear engine design. Professional software such as SolidWorks have been used to design and assemble the engine.

3.6 EFFECT OF SPRING DESIGN ON LINEAR ENGINE PERFORMANCE ANALYSES

To study the single cylinder SI linear engine's performance, simulation has been used. GT-Power has been used for simulation purposes. This simulation technique is similar to the one used by Fathallah and Bakar (2009) with few modifications. The modifications of the GT-Power model are the cylinder geometry, scavenging port, intake port and exhaust port. The assembly should be modified at each change of the spring deflection. The cylinder geometry is changed in a stroke and compression ratio. The angle at the start of the port overlap and the angle at the last closed port are also modified depending on the spring deflection. In a similar manner, the scavenging ratio is modified and should be justified by the spring deflection. The crank angle array and area array at the intake and exhaust ports are modified and should match the deflection angle of the spring.

After the assembly is modified, data continues being collected including combustion characteristics and engine performance. PV diagrams have been used to compare the combustion process and power output in order to compare the engine's performance. This research is focused on 1, 4.1 and 4.6 m/sec speeds, since according to

the results of linear engine design the spring does not deflect properly at those speeds. The assembly should be modified every time the speed is changed. All data are recorded and compared with predicted data.

The Indicated Mean Effective Pressure (IMEP) has been examined using Hook's law. If a spring cannot deflect higher than 25 mm, then the intake scavenging port is not open. It results in an engine misfire. Equation (3.1) shows the formula to calculate spring deflection, which was adopted from Miroslav (2009):

$$s = \frac{8FnD^3}{Gd^4} \quad (3.1)$$

Accordingly, the spring system of a linear engine force is the sum of the minimum load and combustion pressure load. The minimum load is the force of the compression cycle (F_{min}); according to the original conventional engine, the design of compression ratio is 1:9. However, the force of the combustion pressure (F_{IMEP}) depends on the result of the Indicated Mean Effective Pressure (IMEP). Equation (3.2) is used to calculate the piston force:

$$F = F_{min} + F_{IMEP} \quad (3.2)$$

The force is found by multiplying the pressure by the piston's cross-sectional area. The formula is shown in Equation (3.3)

$$F = PA \quad (3.3)$$

where P is the pressure within the combustion chamber. The pressure (P) pushes the piston with cross-sectional area (A). The force (F) causes the deflection of the spring (s).

3.7 DYNAMIC MOTION ANALYSIS METHOD

In order to compare linear engines with conventional ones, an original conventional engine has been redesigned. All components have been drawn and

assembled using SolidWorks. Some components of the conventional engine are used in the design, including piston, head, carburettor and exhaust system. The most important component is the spring mechanism of the return cycle. However, for optimisation purposes, the geometry of spring has been designed with multilevel optimisation.

Three different tools have been used for the simulations. Design and assembly used SolidWorks, where physical models can be seen in linear engine design results. The geometry of the spring has been optimised by using Spread Sheet with multilevel optimisation. In order to simulate linear engine motion, the spring in the real design has been removed and replaced by a flexible spring, which is available in SolidWorks' motion analyses. GT-Power is used to calculate the combustion pressure. However, dynamic pressure versus time has been used as the cubic interpolated force in motion analysis. The motion study properties have been set to 1000 frames per second. The 3-D contact resolution accuracy is 0.0001. The integrator type is GSTIFF, maximum iteration is 100 with initial integrator step size of 0.0001. The minimum integrator size is 0.0000001 and the maximum is 0.01.

In order to examine the effect of friction on a linear engine's motion, 3-D material contact modes have been utilised in this study. There are three contact points, such as friction contact between piston rings with the cylinder liner and between the two journal bearings with the linear rod, these have been set in specified materials with greasy modes.

3.8 ANALYSIS METHODS FOR SPRING SYSTEM MODIFICATION

Due to the modification of the spring mechanism, two scenarios have been developed, the first is the modification of the piston, and the second the modification of the connecting rod. The first scenario is to cut the bottom part of the piston skirt. The objective in removing this part is to eliminate the effect of piston rotation on the scavenging process. The mixture is still flowing properly into the combustion chamber through the scavenging inlet port. However, the effect of removing part of the piston skirt needs to be analysed. The second scenario is to add a connecting rod lock. The objective of this is to fix the piston rotation in the Z direction.

For the analyses of both the piston and connecting rod, a finite element method has been adopted. Stress and thermal stress have been used for the piston analysis.

However, the connecting rod is unnecessary for thermal stress analysis. The modification models such as piston and connecting rod have been compared with the original design. There are three kinds of software that have been adopted in the research, GT-Power, SolidWorks and Algor. GT-Power has been used to collect the data, SolidWorks has been used to build the models and assemblies, and Algor has been used to solve and analyse the problems.

For the analysis of thermal stress, the piston has been analysed separately. However, the connecting rod has been assembled with a piston and piston pin. The objective is to place a load equal with piston analysis. The steps of the analysis began with building the mathematical model, building the finite element model, solving the finite element model and analysing the results.

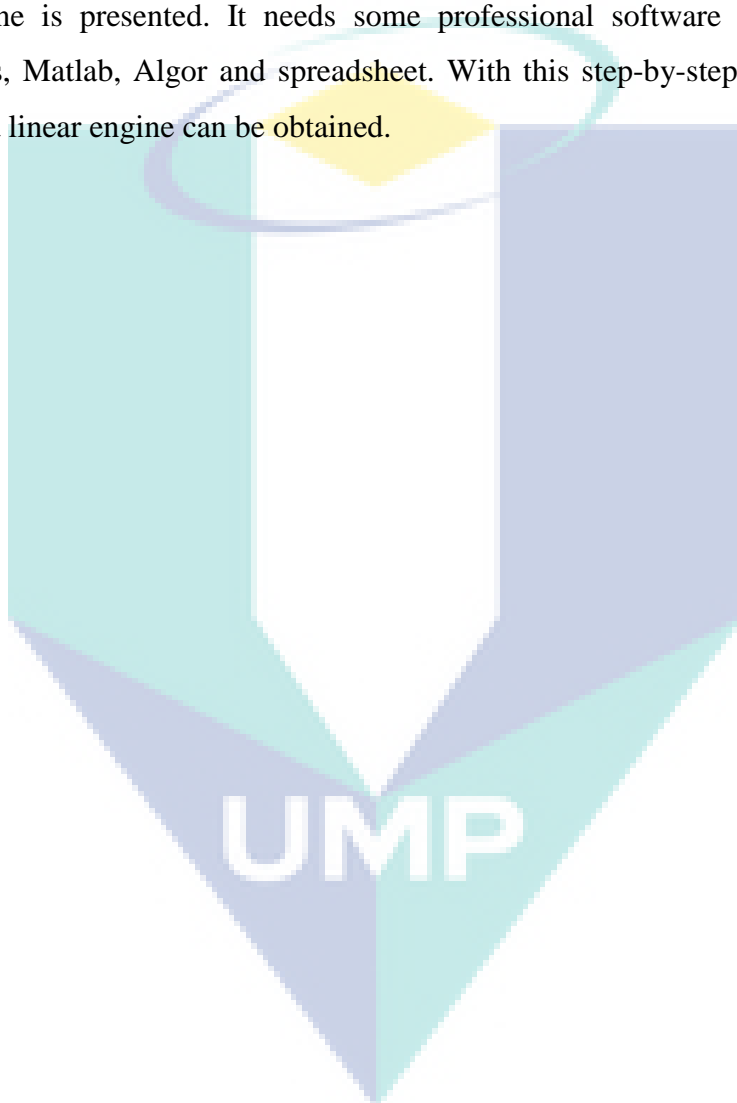
The mathematical model is built starting from the geometry represented by the SolidWorks model a part and assembly. The components are piston, pin and connecting rod, which include a modified piston and connecting rod. The geometry should be reliable to mesh into a correct and reasonably small finite element mesh. The requirement of the mesh ability has very important implications. It must ensure that the CAD geometry is indeed meshed and that the produced mesh provides the correct solution for the stress and thermal stress.

Building an element model through a process of discretisation is known as meshing. The mesh model has been set to automatic, which combines bricks and tetrahedral bodies. The analysis type is static stress with linear material models. However, for the thermal stress process, analysis consists of two basic steps. The first is distribution temperature with steady state heat transfer. In it the resulting temperature is taken directly as load in a structural analysis to determine the stress caused by the temperature loads. The second step is to define materials, loads, constraints and analysed models.

3.9 CONCLUSION

Research methods have been discussed in this chapter. The discussion began with considering the strategy for completing the research. Design through modification of conventional engines has been selected due to cost and facility constraints. A design modification begins by determining the accuracy of the data and designing the spring

system as a return cycle. In order to do this engine operation data are used to predict the engine performance. The engine performance data is used in the optimisation of the spring design. The second step is the design of the free-piston linear engine, beginning with the design of the spring and the system. The analysis continues with an examination of the influence of the spring design on the performance of the engine, the piston motion and scavenging. Finally, the modification of the design of the free-piston linear engine is presented. It needs some professional software such as GT-Suite, SolidWorks, Matlab, Algor and spreadsheet. With this step-by-step technique, a great design for a linear engine can be obtained.



CHAPTER 4

RESULTS AND ANALYSES

4.1 MODEL BUILDING AND VALIDATION

The strategy followed to design a single cylinder two-stroke free-piston linear engine with a spring as a return cycle is to modify a conventional engine. Accurate data is very important in the research, and needs financial backing. If there is a lack of funding, then the simulation technique is the most appropriate method to conduct the research. This chapter has two objectives, namely building a model for the simulation and validation of the model. Building a model and its validation are interrelated and cannot be separated. Although GT-Power is a good software application, it is just a tool to solve problems and validation is still necessary. Validation of the model is done by including specifications of the conventional engine manual and carrying out experiments. Experiments are needed since the spring design should use optimisation processes, and part-load performance data are very important.

4.1.1 1D GT-Power Engine Simulation Model

GT-Power is an application included in the GT-Suite developed by Gamma technologies Inc. GT-Power is used by many engine/vehicle manufactures and developers to simulate and analyse the working principles of engines. It can be combined with several other simulation software packages. However, this software uses 1-D gas dynamics to represent the flow and heat transfer in the components of the engine model. These components are linked with connected objects; it is what we call a model. Within the components, the properties must be defined by the user. Engine performance can be studied by analysing the mass and energy flow between individual engine components and the heat and work transfers within each component. Simulation of 1-D flow involves the solution of the conservation equations, mass, energy and

momentum, in the direction of the mean flow. Details of the theoretical background are presented in Chapter 2.

To build a model, the configuration of a real engine must be known in detail. Precise measurements can result in excellent performance prediction. Before building the model, a real engine is dismantled and all parts are measured. Connection arrangements of the model correspond to the actual engine. GT-Power provides a template for all engine components in the template library. To build a component, we can copy it from the library and then adjust it to the size of the existing data from the actual engine. Then all the components are connected to form a model which tries to represent the actual engine.

4.1.1.1 Back Pack Brush Cutter

The engine used in this study is the Back Pack Brush Cutter, which is shown in Figure 4.1.1. For model building purposes, this engine is stripped apart and all components are measured. The dimension is used as input for each component that has been copied from the library on the GT-Power software.



Figure 4.1.1: Back Pack Brush Cutter type BG- 328

The engine's main specification is shown in Table 4.1.1. The specification is adopted from the Back Pack Brush Cutter BG-328's manual. It can be seen that the

maximum power output is 0.81 kW at 6000 rpm. Maximum power output is used as a comparison for the model validation. It is necessary to conduct an experiment to verify the part-load power output for the validation.

Table 4.1.1: Back Pack Brush Cutter engine specification.

Model Engine	BG-328
Type	2 cycle, single cylinder, forced air cooled, gasoline engine
Displacement	30.5 cc
Max. Output	0.81 kW/ 6000 rpm
Carburettor	Float type
Ignition system	IC Ignition (Solid state)
Ignition plug	BM-7A or CHAMPION CJ6
Fuel	Mixed fuel of gasoline and 2 cycle oil at 25:1
Fuel tank capacity	1.2 litres
Body	
Drive	Flexible shaft, drive shaft, pinion and gear
Rotational direction of cutter (viewed from the top of the cutter)	Counter clockwise
Dimension (Length x Width x Height)	345 x 280 x 401 mm (back loaded part only)
Dry weight	9.4 kg

4.1.1.2 Model

The model has been built following the GT-Power manual. The steps have already been explained at the beginning of subchapter 3.2.2. The model building sequence begins with the inlet port and ends with the exhaust port. The same order is not always followed when building components of a model, but it should be arranged sequentially according to the actual composition of the real engine. There are not many components in the original engine and there is little electronic control. This makes the model quite simple. Although the model is simple, building the model is not easy. Therefore, the engine's cylinder, engine's crank train and engine's crank case needs to be built carefully. Besides that, we also need to pay attention to the valve-port-connections (inlet and exhaust ports). Determining the crank angle versus area arrays must be done carefully, because the inlet and exhaust ports will characterise the

scavenging phenomena. Combustion and heat transfer are also affected by the inlet and exhaust ports arrangement, so building valve-port-connections is very important. The power output of the engine is small. If the data input of the model are not accurate, then the result is incorrect. Figure 4.1.2 shows the simulation model.

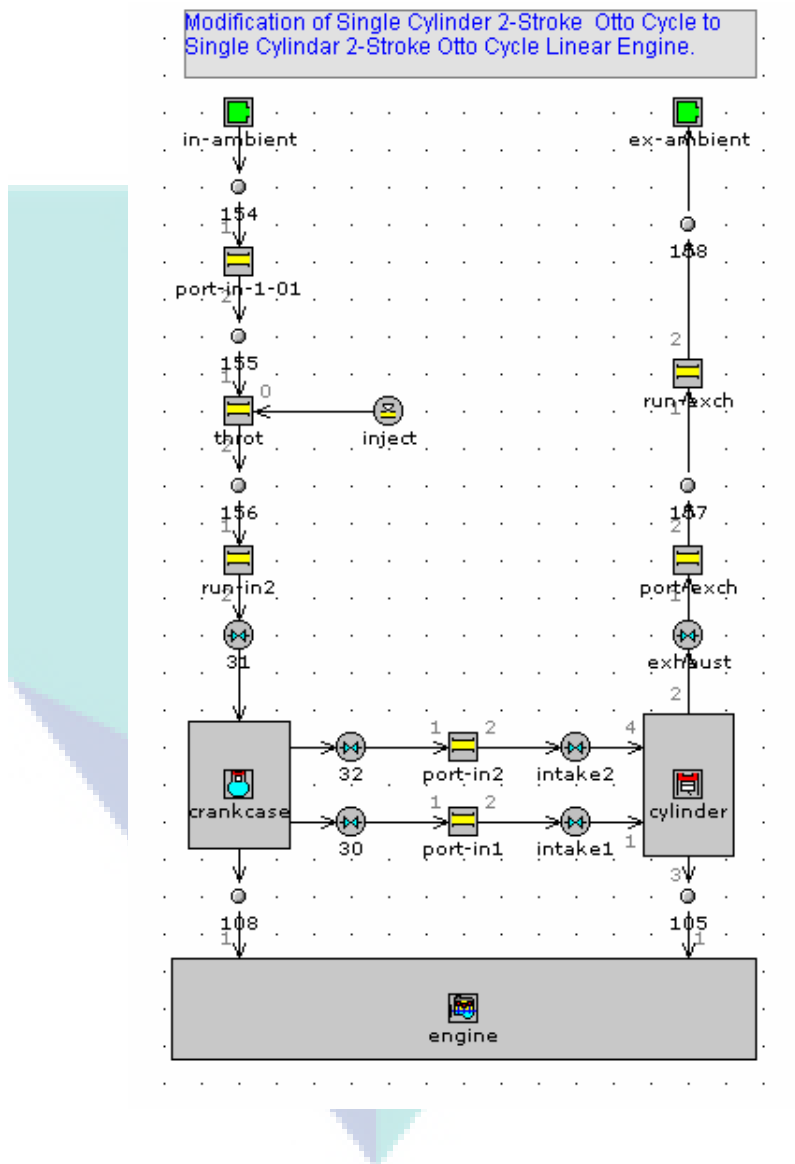


Figure 4.1.2: GT-Power model of two-stroke SI BG-328 engine

GT-suite software is used to simulate the conventional engine and, with a little modification, it allows the simulation of a linear engine. Issakson (2000) has used GT-Power to simulate a two-stroke compression ignition hydraulic free-piston engine. The motion analysis of the free-piston engine was done by modifying the piston motion object at Eng-Cyl-Geom-User. To predict the linear engine performance, it is possible to

run the modification of engine crank train. Conceptual differences between conventional engines and linear engines can be found in the crank mechanism.

The purpose of the free-piston linear engine is to reduce friction in the crank mechanism by removing and replacing it with linear oscillation. With this technique, the friction at the crank systems can be significantly reduced. As a result, the power output increases. GT-Power was not provided with a formula to reduce the friction on the crank mechanism. However, the manual of GT-Power provides the opportunity to enter friction data for the experiment. This means that in the same way we can use another formula for free-piston linear engine simulation. With the formulas presented in Chapter 2, the performance of the linear engine can be predicted.

4.1.2 Validation

The purpose of conducting the engine performance test is to collect some parameters that can be used in the free-piston linear engine design. In order to achieve this, it is necessary to validate the model. In this study, the validation is planned to be used in two ways, firstly validation for complying with the specifications in the manual and the secondly by conducting an experiment. There is only data for one power given in manual. More data on power is required since the spring design optimisation is done under part-load conditions. The experiments conducted can provide the data. These data will be used for simulation validation.

4.1.2.1 Validation with Back Pack Brush Cutter Manual

The model shown in Figure 4.1.2 was validated with the Buck Pack Brush Guide manual. The specification of the engine can be seen in Table 4.1.1. The maximum load occurred at 6000 rpm, and the model should be setup under the same conditions. The simulation has been running successfully, and opening of the GT-Spot has been done. The results are seen in Figure 4.1.3. The weakness of the GT-Suite software lies in the result of the power output with only one decimal place. Such results are less favourable for the simulation of a small engine such as a Back Pack Brush Cutter engine. The accuracy of the results are lower for the SI unit in kW within one digit of accuracy.

However, it can be recalculated using other data, the results of which, as well as the formula used (Equation 4.1.1), are presented in Figure 4.1.3.

$$P = \frac{B_{mep} V_d N}{n_R} \quad (4.1.1)$$

where P is the brake power, B_{mep} is the brake mean effective pressure, V_d is the volume displacement, N is the engine speed and n_R is the number of cylinders.

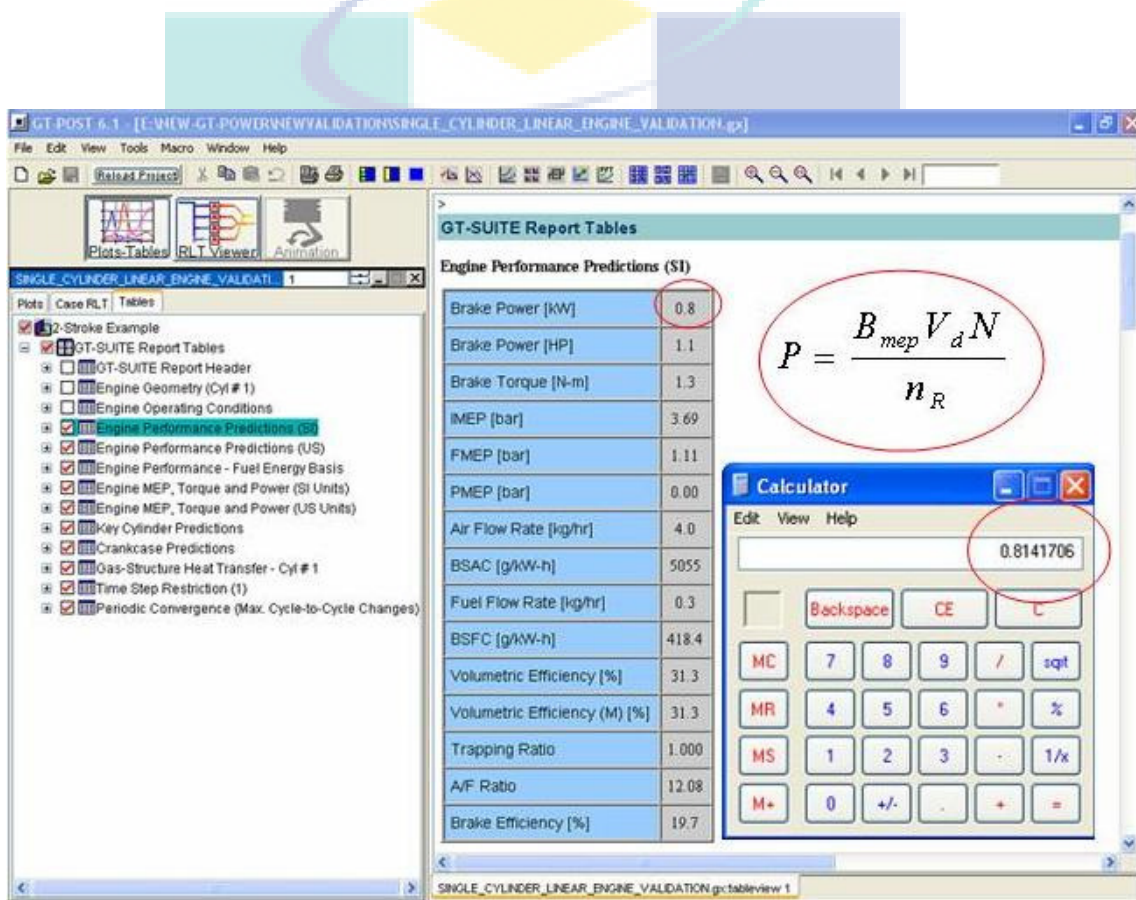


Figure 4.1.3: GT-Power model engine performance prediction result and hand calculation.

Using GT-Power provides a power output of 0.8 kW. Using Equation 4.1.1 will produce a power output of 0.8141704 kW. This closely matches the value stated in the engine's manual. The relative error the between power maximum specified and the

maximum power calculated is given by Equation (4.1.2). However, the relative error is -0.51 %. The formula has been adopted from Bos (2007).

$$\text{Relative error} = \frac{x - x_0}{x} 100\% \quad (4.1.2)$$

Referring to the validation results using the manual for the engine, the model result is good and acceptable. It means that the model is precise under fully loaded conditions. However, the accuracy is not always the same at part-load. Therefore, it needs to be reviewed under part-load conditions by using the experimental technique.

4.1.2.2 Validation with Experimental Data

The experimental data is the actual data of the engine's performance. The data could be used as a reference for model validation. To conduct the engine performance test requires a dynamometer. An alternator has been used as a DC dynamometer in this experiment. An engine test rig was designed and shown in appendix A. The experiment data was conducted at similar speeds to simulation conditions. The speeds of the engine were 1000, 2000, 3000, 4000, 5000 and 6000 rpm. Every engine speed was run under variable loads, and trough analysis of the full engine load at certain speeds could be determined.

Figures 4.1.4, 4.1.5, 4.1.6 show the relationships between power output, torque, and specific fuel consumption against engine speed, respectively. All those performances are measured at full load for all speed conditions. The trends of the power output at variable speeds are similar between the experiment and simulation. The relative error is between -0.8% to -10.77% with the average of -5.45%. Likewise, trends in the torque and specific fuel consumption present a similar performance with the power output.

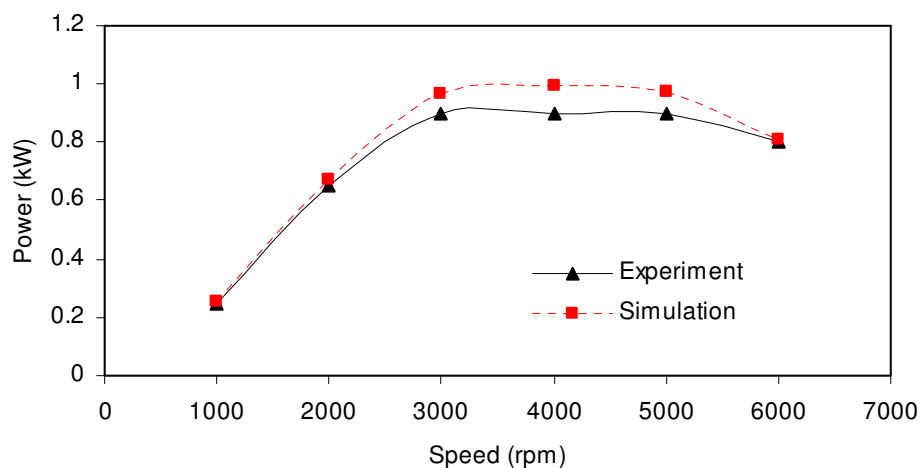


Figure 4.1.4: Power output characteristics of simulation and experiment

Performance at 1000 rpm and 6000 rpm of both the simulation and experiment are good. However, at 4000 rpm, the performance is slightly different but can still be accepted as a good performance. From a power output characteristics point of view of the model, the performance is good and can be used as a simulation tool in linear engine design. Since all partial load data showed a very good trend, this model is adopted for determining the characteristics of a linear engine.

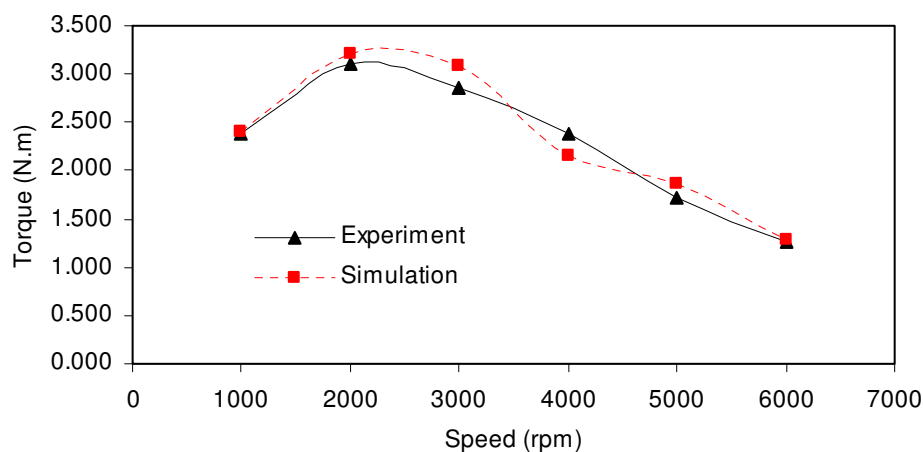


Figure 4.1.5: Torque characteristics between simulation and experiment.

Figure: 4.1.5 shows the torque characteristics of the simulation and experiment. Unlike the characteristics of power output, the torque has a slightly different trend,

especially at the speed of 4000 rpm. The torque in simulation is lower than the experimental results. Nevertheless, the difference between the simulation and the experimental values is very small. Relative errors are between -0.11% and 9.99% with an average error of -1.84%.

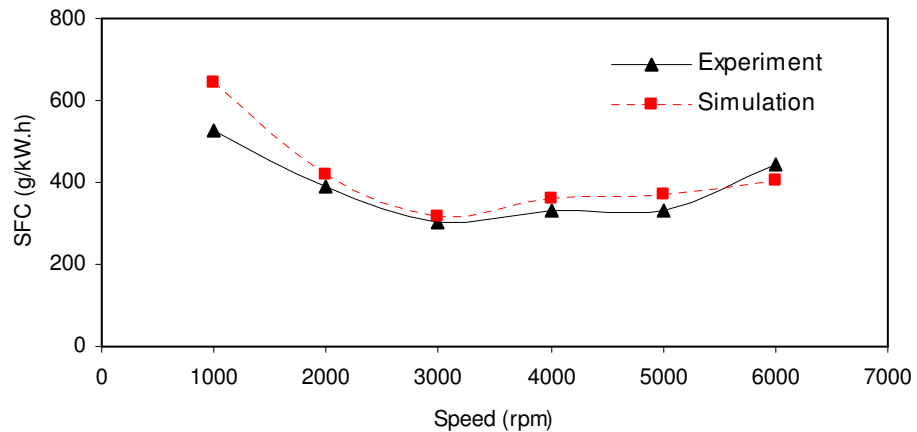


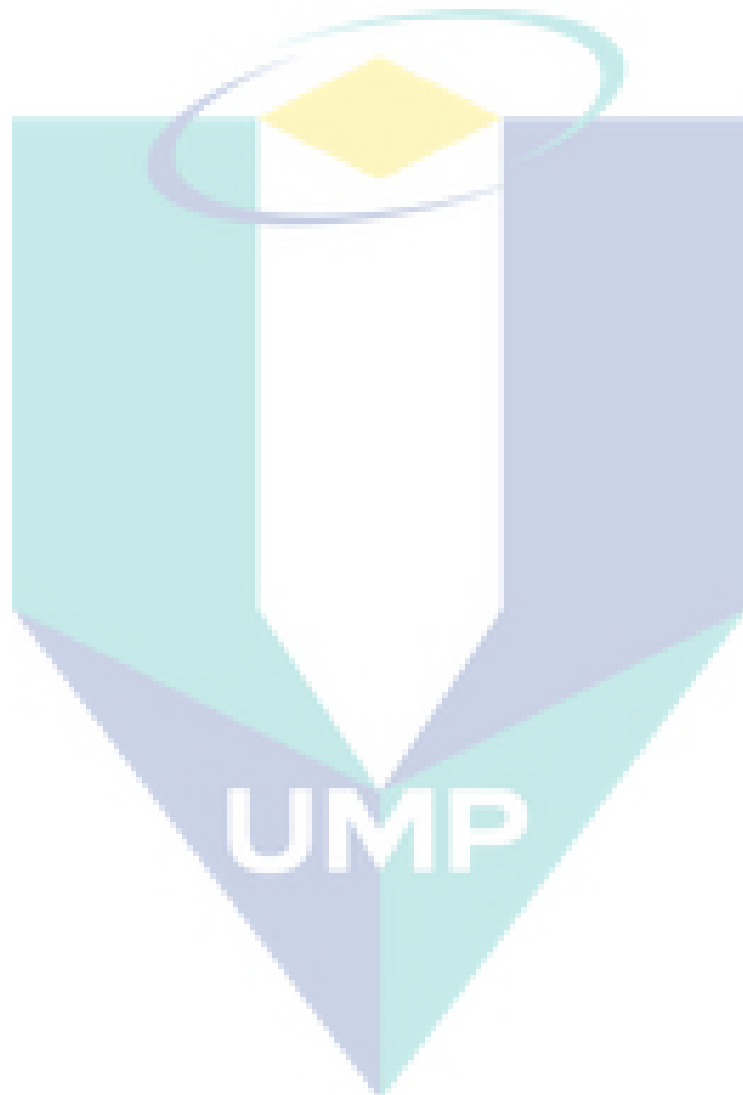
Figure 4.1.6: Specific fuel consumption for experiment and simulation.

Figure 4.1.6 shows the specific fuel consumption for the simulation and experiment. Theoretically, the results of the experiment should be greater than the simulation results. At an engine speed of 6000 rpm, the result correctly meets the assumption. The validity of the model is relatively good as far as the trends are concerned. The relative error of the graphs lies between -22.86% and 8.25%, and the average error is -8.00%. Based on fuel consumption, the validation of the model can be accepted.

4.1.3. Summary

Model building and validating strategies have been presented in this chapter. GT-Power was used to simulate the free-piston linear engine. Simulation of the engine performance requires some modification to the engine crank train. GT-Power is a tool to estimate engine parameters, and it is necessary to validate the model. In this research, model validation is carried out by comparing data with the manual and conducting

experiments. The analysis showed that the model is good and can be used to simulate the engine at a variety of loads.



4.2 PREDICTION STUDIES FOR THE PERFORMANCE OF A SINGLE CYLINDER HIGH-SPEED SPARK IGNITION LINEAR ENGINE WITH SPRING SYSTEM

Engine performance data are very useful for linear engine design, especially when modifications are involved. This chapter describes the performance prediction of a single cylinder high-speed spark ignition linear engine with a spring mechanism as a return cycle. To enlighten the engine's performance phenomena, an original conventional engine has been studied and compared. To predict the performance of the engine, 1-D GT-Power software has been employed. The model has been validated, and can be seen in Chapter 4.1. Here, a small modification is needed to predict the performance of a linear engine.

4.2.1 Engine Dynamics

In order to investigate the dynamics of reciprocating engines, it is necessary to analyse the dynamic forces, moments and torques in a machinery system, even if it is a simple mechanism. The actual mechanism is quite complex in terms of the dynamic consideration necessary to design for high-speed operation (Norton, 2004). The difference between a single cylinder rotational reciprocating engine with a linear engine is the process of returning back to the top dead centre. A basic mechanism for rotational engines consists of a crank, a connection rod and a piston. On the other hand, the linear engine consists of a spring, a connecting rod and a piston. This basic design has a large impact on the engine's performance. Figures 4.2.1 and 4.2.2 show schematic diagrams for the single cylinder rotational engine and linear engine respectively.

In the internal combustion engine, the energy is delivered from exploding gases during the power stroke of the cycle. The piston must return to the top dead centre on its own momentum before it can receive another push from the next explosion. In fact, for rotational engines, the energy must be stored in the crankshaft merely to carry it through the top dead centre and bottom dead centre points. In the case of single cylinder linear engines the energy should be stored in the spring.

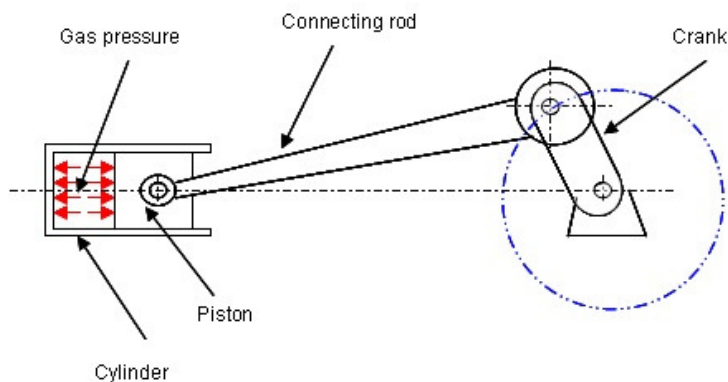


Figure 4.2.1: Single cylinder rotation engine

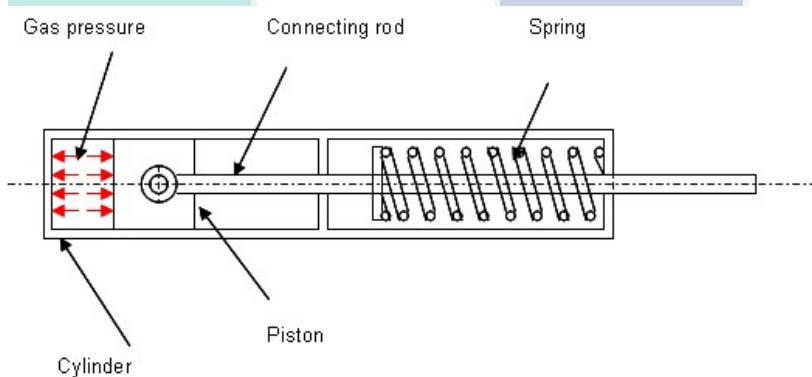


Figure 4.2.2: Single cylinder linear engine

In linear engine designs, the spring is the most crucial component and needs to be analysed carefully. In rotational engines, the stroke is always the same under many operating conditions. The displacement of the spring is dependent on the force. This spring should be travelling from the bottom dead centre to top dead centre as needed under operating conditions. Thus, a part or all of the intake manifold should be opened in order to transfer the air-fuel mixture. If this fails to happen, the explosion in the combustion chamber will not happen. The spring displacement is affected by piston speed and engine load. Both variables were detrimental explosion in combustion chamber. Unwanted explosions can cause the thrust forces to vary. As a result, the displacement of the piston would be erratic.

The engine works as two-stroke spark ignition and does not need any valve, however to increase its efficiency it is sometimes provided with a passive (pressure differential operated) valve at the intake port. It requires only two strokes, to complete one cycle. There is a passageway, called a transfer port, between the combustion chamber above the piston and below the crankcase. There is also an exhaust port on the side that moves up and down. The crankcase is sealed and the carburettor mounts on it, also serving as the intake manifold. The combustion process of a two-stroke spark ignition linear engine is exactly the same as rotational two-stroke engines. For that reason, it is not necessary to explain the detail of the process.

The usable output torque is created from the explosive gas pressure generated within the cylinder. The magnitude and shape of this explosion pressure curve will vary with the engine design, stroke cycle, fuel used, speed operation and other factors related to the thermodynamics of the system. For the purpose of analysing the mechanical dynamics of the system, the gas pressure function is kept constant while other design parameters are varied in order to compare the results of the linear engine design.

4.2.2 Prediction Method

GT-Power has been used to predict the performance of both conventional and linear engines. Details of formulas and procedures have already been explained in Chapter 2. Based on the concept of linear engines, the power output is increased by reducing the friction force at the shaft power. For engine simulation performance, GT-Power is limited and so the model needs to be modified. Figure 4.2.3 shows a prediction method flowchart. The modification is done by replacing the GT-Power formula with a formula adopted from Ferguson and Kirkpatrick (2001). More detailed information can be found in Chapter 2. The friction force can be evaluated using a spreadsheet. The value of the friction force can be replaced at the engine crank train. Figures 4.2.4 and 4.2.5 present the friction force of conventional and linear engines respectively.

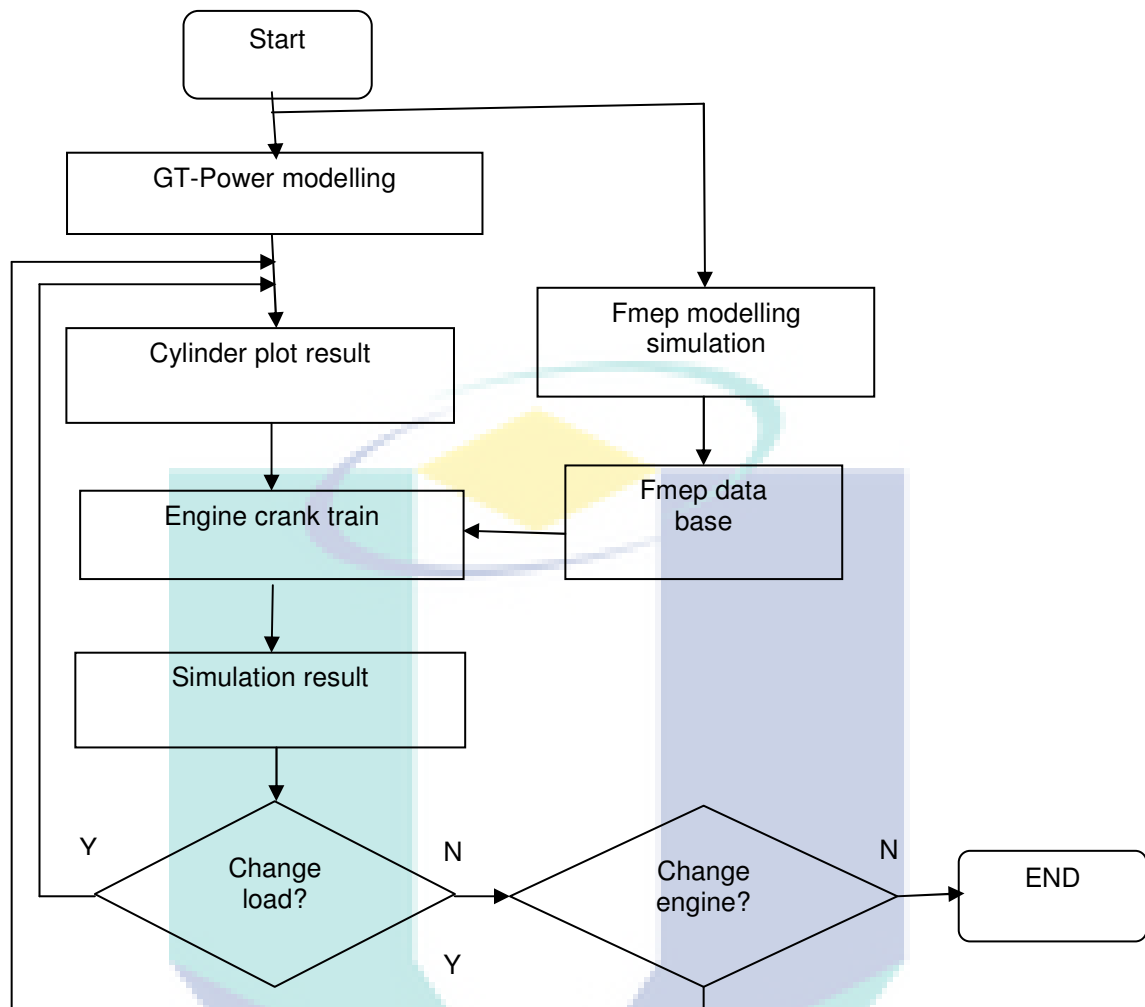


Figure 4.2.3: Model design analysis flowchart

4.2.2.1. Friction Force

According to the GT-Power manual, the model makes use of experimental friction data by modifying the engine friction coefficient factor in the template of the edited object of friction. The location of the template is at the engine crank train. It is called the engine template (see Figure 4.1.2, Chapter 4.1). In GT-Power, the engine friction coefficient factor is a function of the mean effective pressure friction constant, peak cylinder pressure factor, mean piston speed factor, and mean piston speed squared factor. Details of the formula for engine friction have been explained in Chapter 2. To replace with experimental data, it is assumed that all components are ignored except for the constant of friction mean effective pressure. The constant can be written with

experimental data. Using the same technique, our own formula can be used after being calculated using a spreadsheet.

$$f_{mep_{gasload}} = c_g \frac{P_i}{P_a} \left[0.088r + 0.182r^{(1.33 - K\bar{U}_r)} \right]$$

$$f_{mep_{skirt}} = c_{ps} \frac{\bar{U}_p}{b}$$

$$f_{mep_{rings}} = c_{pr} \left(1 + \frac{1000}{N} \right) \frac{1}{b^2}$$

$$f_{mep_{seals}} = c_s \frac{D_b}{n_c b^2 s}$$

$$f_{mep_{bearing}} = 41.37K \left(\frac{b}{s} \right) \left(\frac{N}{1000} \right)$$

$$f_{mep_{bearings}} = c_b \frac{n_b N D_b^2 L_b}{n_c b^2 s}$$

Figure 4.2.4: Friction formulas for conventional engine

Figure 4.2.4 presents a single cylinder rotation engine with friction formulas. These formulas have been adopted from Ferguson and Kirkpatrick (2001). The results calculated using a spreadsheet are shown in Appendix B. Figure 4.2.5 shows a linear engine complete with operating formulas. Some formulas (friction of skirt, friction of connecting rod bearing and friction of main bearing) are removed since the return cycle is linear. The frictions only occur in-between the piston ring with cylinder liner, gas load, seals and bearings. Theoretically, the combustion process in the combustion chamber is similar. However, it differs since the dynamics of the connecting rod in rotating and linear engines are different. The power outputs are also different since the frictional forces are different.

$$f_{mep_{gasload}} = c_g \frac{P_i}{P_a} \left[0.088r + 0.182r^{(1.33-K\bar{U}_p)} \right]$$

$$f_{mep_{seals}} = c_s \frac{D_b}{n_c b^2 s}$$

$$f_{mep_{rings}} = c_{pr} \left(1 + \frac{1000}{N} \right) \frac{1}{b^2}$$

$$f_{mep_{bearings}} = c_b \frac{n_b N D_b^2 L_b}{n_c b^2 s}$$

Figure 4.2.5: Friction formulas for linear engine

4.2.2.2. Modification of Model

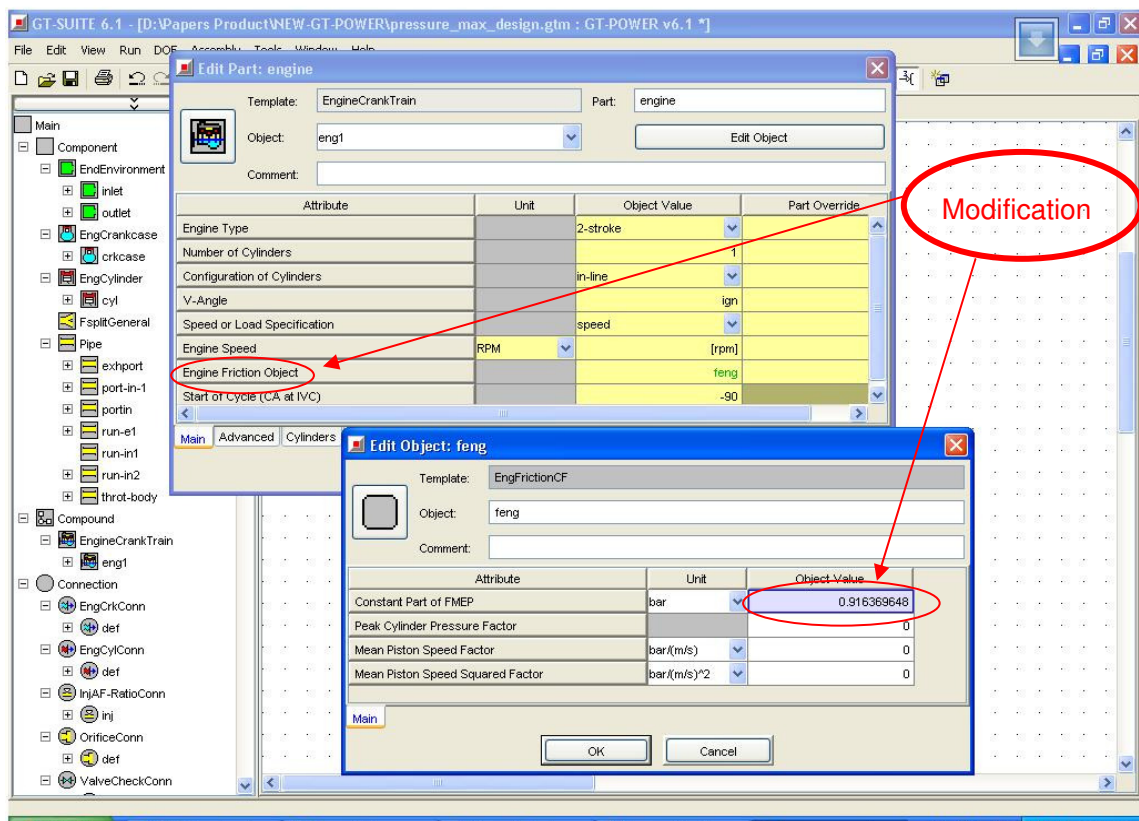


Figure 4.2.6: Modification technique to replace the friction force

Physically, the model is the same as shown in Figure 4.1.2, except for a small modification in the frictional values at the engine crank train. This value cannot run automatically, however, after setting the value at certain speeds and loads, the model should then be assembled. Figure 4.2.6 shows the modification technique to replace the value of friction force. The method followed the GT-Power manual, in the same manner replacing friction value with experimental data. First of all, the template of the engine crank train must be opened, and secondly the template of engine friction object is opened. Then input a value of zero into all components, except for the constant value of f_{mep} . The constant frictional value has been independently calculated using a spreadsheet.

4.2.3. Results

The main concern of the research is to calculate linear engine performance and to design a real engine based on a real rotation engine. The advantages of modifying rotational engines into linear engines are in reducing the research budget and being able to study and compare both system designs. The performance differs at a given value of friction mean effective pressure (f_{mep}). Note that the performances in the combustion chamber are exactly the same in both engines. In this research, the parameter profiles of dynamics aspects are presented according to researchers' conventions, but the data is displayed in cycles. This is due to the linear engine, even though the researchers also examine the rotational engine for comparative study.

Logarithmic and P-V diagrams are used to express the pressure diagrams. The logarithmic scale provides a rational interpretation of the profile. Their data are expressed in terms of analytic functions. The polytropic exponents are evaluated. The least square fit regression for the compression and expansion profile processes are shown to be linear (Antoni, 2006). According to Heywood (1988), the start of combustion can be identified by the departure of the curve from the straight line. The end of combustion can be approximately located in a similar fashion.

Figure 4.2.7 shows a logarithmic diagram showing $\log P$ versus $\log V$ at variable speeds. With the same initial conditions, the engine pressure increases to 2 m/sec of speed, then decreases again at 6.1 m/ sec of speed. The pressure degradations after 2 m/sec of speed are smaller than before 2 m/sec of speed. Figure 4.2.8 shows a

comparison of the P-V diagram at critical characteristics. The figure shows a PV cyclic process at different speeds. When the speed is 6.1 m/sec, the pressure at the end of the stroke is still high. This means that energy is still high at the end of the stroke. However, the exhaust port has already opened and this results in the volumetric efficiency reduction. From Figure 4.2.8, it can be shown that maximum pressure starts from 36.34 bar at 0.5 m/sec then increases to 45.79 bar at 2 m/sec, and finally drops to 26.56 bar at 6.1 m/sec. There is a large contrast between the maximum and minimum pressures. Figure 4.2.9 shows a comparison of frictional losses between a rotational engine and linear engine at different engine speeds. The frictional loss in the rotational engine reaches a minimum value at 1.5 m/sec before increasing dramatically. For the linear engines, it decreases systematically from the beginning before stabilizing when the speed reaches 4.1 m/sec.

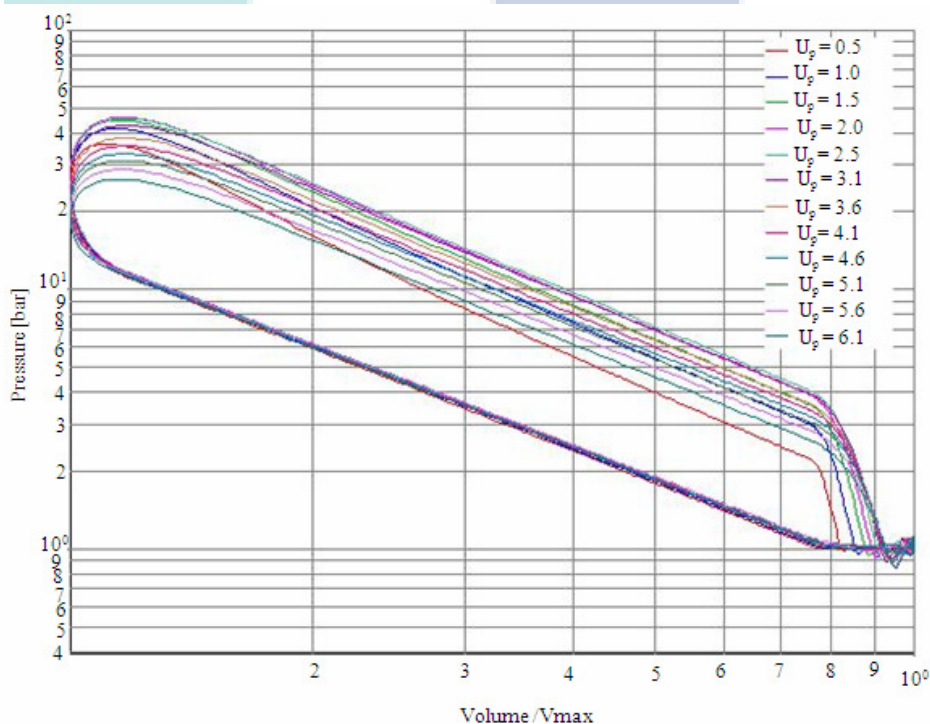


Figure 4.2.7: Log P-log V diagram at different engine speeds

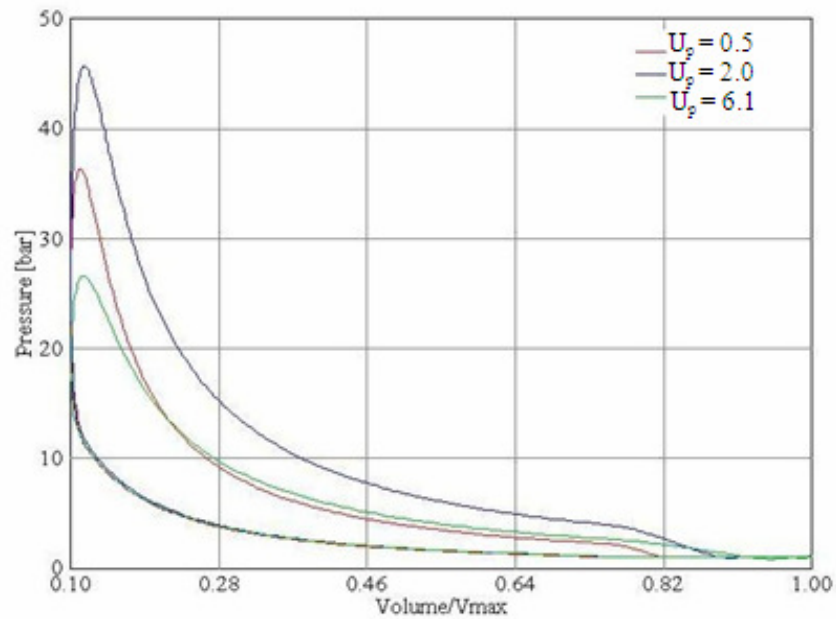


Figure 4.2.8: P-V diagram at critical characteristics

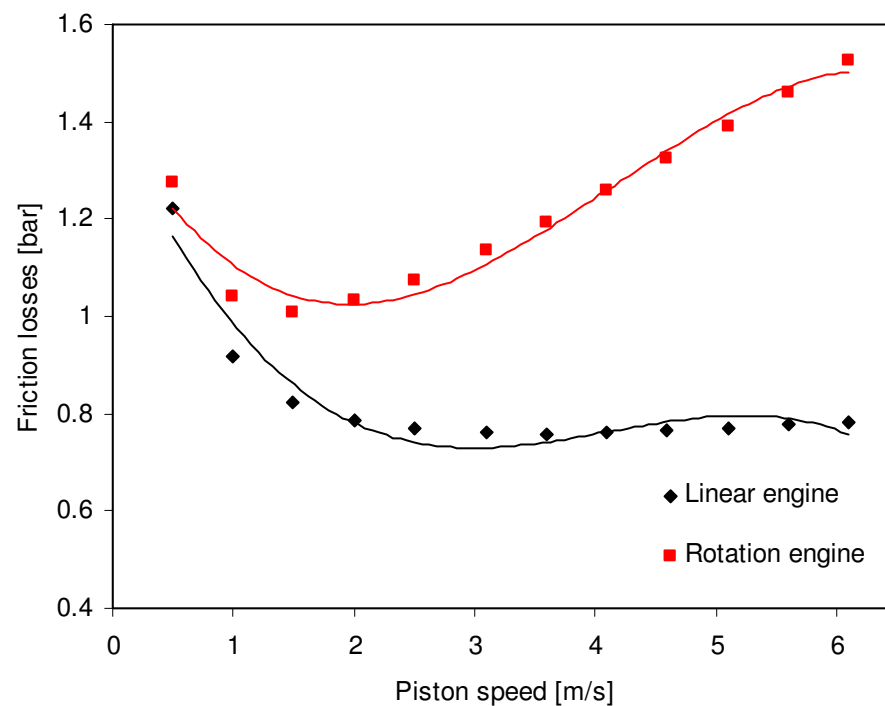


Figure 4.2.9: Comparison of friction loss between rotation and linear engines

The brake power was obtained by deducting the frictional losses from the indicated power. The characteristics of the engines are shown in Figure 4.2.10. At low speed, the difference between the rotational and linear engine is not significant, but when the speed reaches 1.5 m/sec the gap between both lines widens. For the rotational

engine, when the speed reaches 4.1 m/sec the power drops systematically. In the case of linear engines, the brake power starts to drop after 5.1 m/sec. This performance, caused by friction losses after the speed of 4.1 m/sec, is stable. As a result, the drop in power is small.

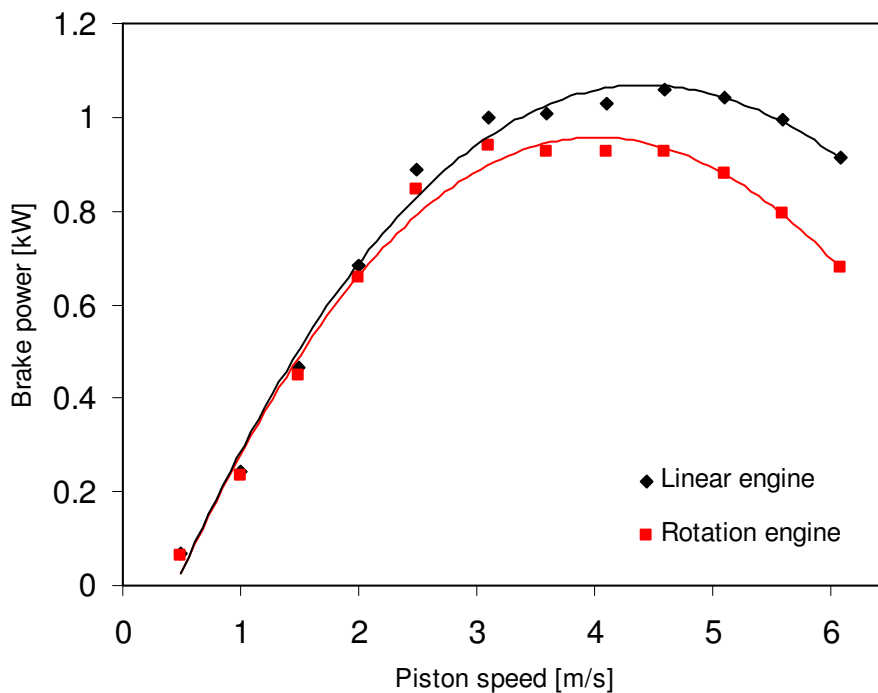


Figure 4.2.10: Comparison of brake power between rotational and linear engine

The torque is a good indicator of an engine's ability to do work. The characteristics of both linear and rotational engines are shown in Figure 4.2.11. It was shown that both the linear and rotational engines present the same trend. The point of maximum torque is at a piston speed of 2.5 m/sec, with the torque of the linear engine being higher than that of the rotational engine.

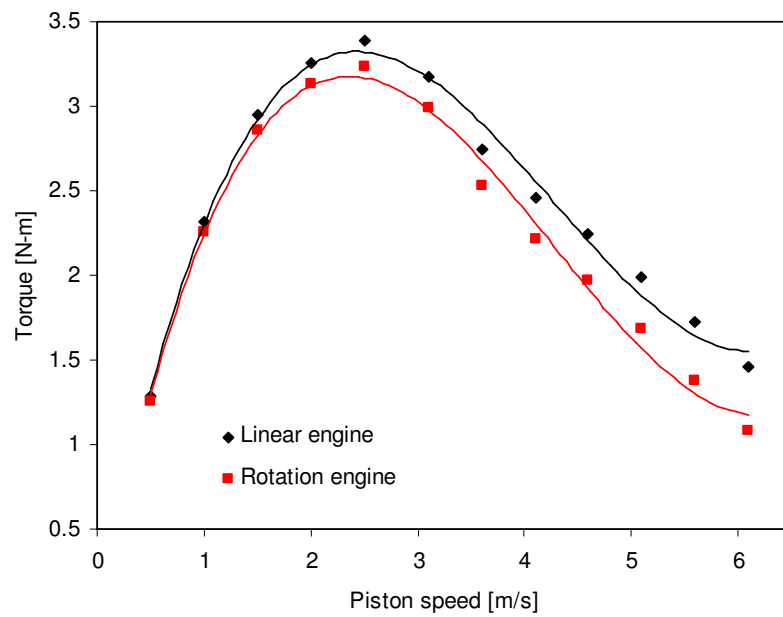


Figure 4.2.11: Torque of both linear and rotation engines at variable speeds

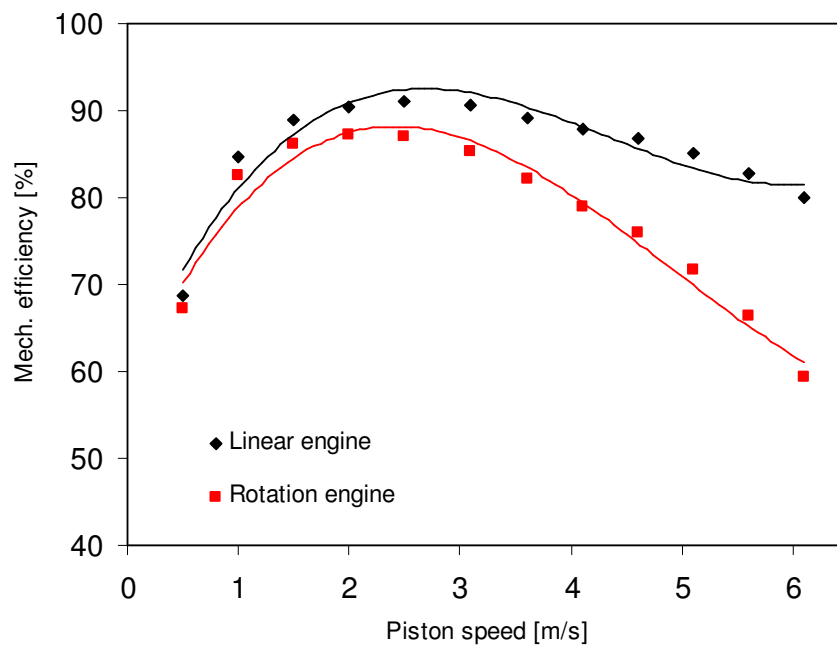


Figure 4.2.12: Effect of mechanical efficiency on both linear and rotation engines at different engine speeds

Mechanical efficiency is determined by the ratio of brake work at the crankshaft to the indicated work in the combustion chamber. Excluding parasitic loads, the

mechanical efficiency of the rotational engine is between 59.4–87.1%. It begins from 67.2% at a piston speed of 0.5 m/sec, then it increases to 87.1% at 2 m/sec. After this point, it gradually decreases to 59.4% at a speed of 6.1 m/sec. The mechanical efficiency of a linear engine is between 68.8–91.1%. It begins from 68.8% at a speed of 0.5 m/sec and increases to 91.1% at a speed of 2.5 m/sec, and then drops to 79.9% at a speed of 6.1 m/sec. Figure 4.2.12 shows the characteristics of mechanical efficiency of both the rotation and linear engines. The energy losses are at their greatest when the engine works at high-speed, which reduces the mechanical efficiency, while the heat loss is the greatest loss at low speeds (Willard, 2004).

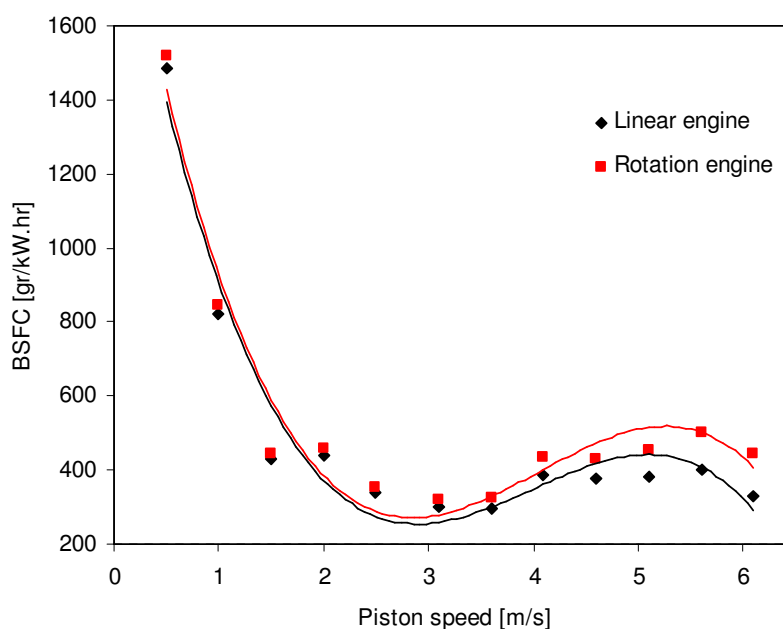


Figure 4.2.13: Comparison of brake specific fuel consumption between rotation and linear engines

Fuel consumption is one of the most important characteristics of engine performance. If one can improve consumption, then the engine design would be better. Figure 4.2.13 shows the comparison between the brake specific fuel consumption of rotational and linear engines. As found earlier, the characteristics of fuel consumption for a linear engine is better than for a rotational engine. Improvement in brake specific fuel consumption lies between 3.2–25.7%. The average improvement is about 11.2%.

The economic area of the linear engine is in between 2–5.1 m/sec and 2–4.1 m/sec for rotation engines. The minimum oil consumption is about 297.9 g/kWh for linear engines and 323.6 g/kWh for rotation engines. The improvement in fuel consumption is due to the reduced friction on the spring system.

The brake efficiency of both linear and rotational engines is shown in Figure 4.2.14. The greatest brake efficiency is at a piston speed of 3.6 m/sec. After that the brake efficiency drops, when the piston speed is 5.6 m/sec the efficiency increases again. This phenomenon, caused by a mass flow of fuel and power, decreases at a piston speed of 6.1 m/sec. However, the trend of both parameters is not parallel. As a result, brake efficiency increases. Decrease in fuel consumption on the piston speed at 6.1 m/sec also impacts on the decline of the imep. Since the decline is not parallel with the decrease of the bmep, the brake efficiency increases.

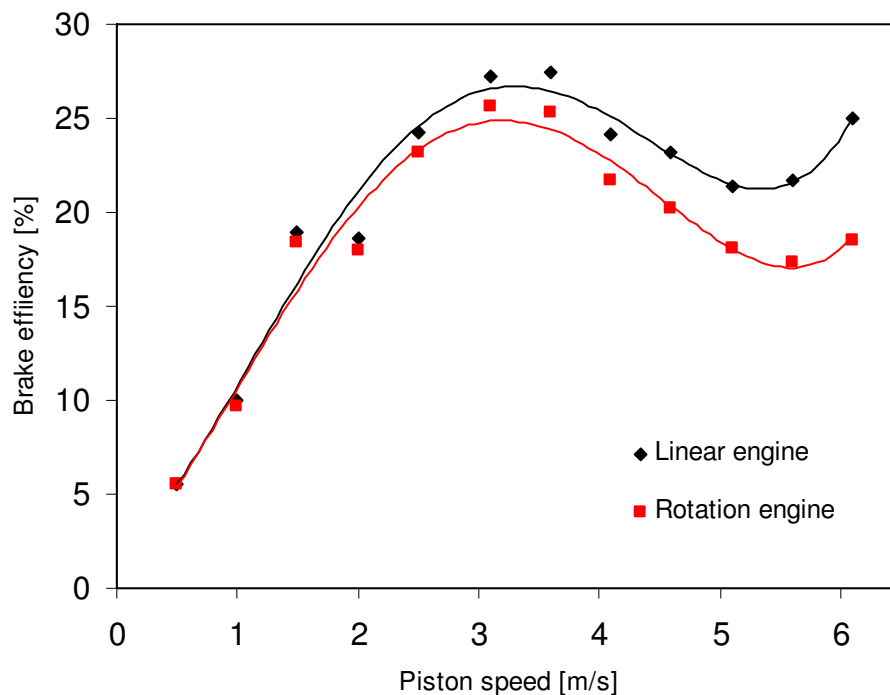


Figure 4.2.14: Effect of brake efficiency of linear and rotation engines at different engine speeds.

The focus of this research is to design a real linear engine with a spring as return cycle. To design the spring, the thrust force of the piston needs to be optimised. Figure

4.2.15 shows a prediction of the maximum pressure when the engine speed is at full load. At the start, the maximum pressure is 36.3 bar, then it reaches a maximum about 45.8 bar at 2 m/sec, and then falls until 26.7 bar at 6.1 m/sec. There are many theories effecting performance and characteristics of the engine. Pressure could be related to the crank angle at which this maximum pressure occurs, the maximum pressure rises and many correlations could be analysed. The pressure rate of change is substantially affected by the rate in change cylinder volume, as well as the rate of burning. It is changed during the combustion process (Heywood, 1989). Slow burning and fast burning are related to speeds and loads. They have also been correlated with maximum pressure. The quantity of fuel burnt in premixed combustion also contributes to the maximum pressure. Figure 4.2.15 shows that the maximum pressure occurred at 2 m/sec. It is much affected by the quantity of fuel burnt in premixed combustion that is the highest one, as a result of the highest maximum pressure. On the other hand, combustion rates at high speed decreased gradually and resulted in a smaller maximum pressure.

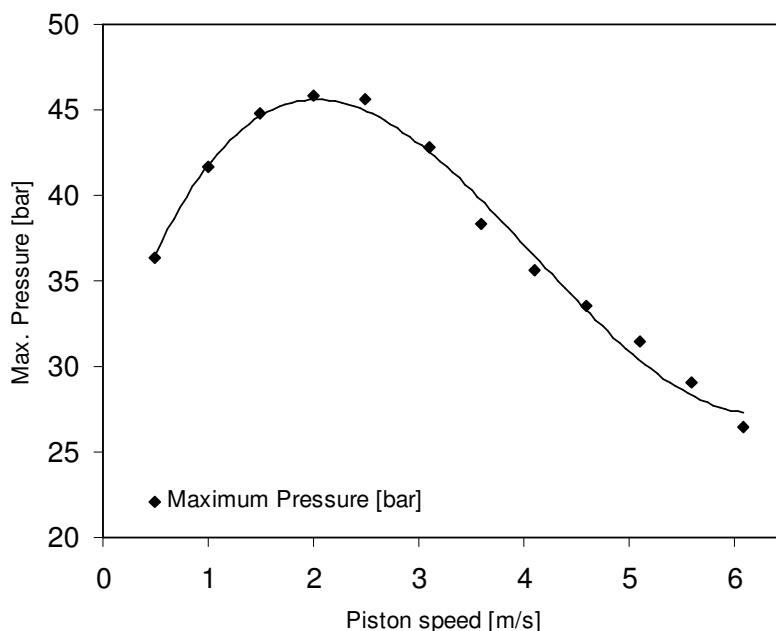


Figure 4.2.15: The characteristic engine at maximum pressure at variable speeds

4.2.4 Discussion

Combustion pressure is one of the important performances to be discussed. In relation to the performance of combustion pressure, the study shows that the difference between minimum and maximum pressure is high. This is because it is affected by many variables. In relation to combustion pressure performance result is complicated. This parameter is important for designing the spring of a return cycle in linear engines. The pressure trend can be described as diffuse; being small at low and high speeds, and high at medium speeds. The optimisation of spring design for a linear engine needs to be analysed carefully.

Friction work is defined as the difference between the work transferred to the piston from the gas contained inside the cylinder and the work available at the drive shaft. The analysis of friction losses has to be considered during the design due to its role in differentiating between a good and average engine design (Macro, 1998). Figure 4.2.9 compares the friction between linear and rotational engines. The piston skirt caused the frictional losses to be different. The friction loss of a skirt depends on the average velocity of the piston. According to Ferguson and Kirkpatrick (2001), and see also Equation 2.9 in the paper review in Chapter 2, that formula is correlated with the boundary lubrication viscosity, bore of the piston, and average velocity of the piston. Patton, Nitschke and Heywood (1989) suggested a proportionality constant $C_{ps} = 294$ kPa mm sec/m. In the case of the linear engine, the skirt friction is ignored because the engine does not work on a rotational bases. However, in general the design of the piston assembly has no skirt connector in linear engines (Achten et al, 2000). In a linear engine, the piston and rod is connected rigidly. Pin holes are not necessary. Because the movement of the engine is linear, there is no friction between the skirt and the cylinder liner.

The main objective of developing a linear engine is to increase brake power as clearly shown in Figure 4.2.10. Compared with another research results, both trends show similar performances (Atkinson et al, 1999). Heywood (1988) and Stone (1997) also reported that the performance characteristics of a small two-stroke engine has maximum power at about 4.1 m/sec, and smaller motor cycle engines can achieve slightly higher bmep and higher speeds. According to the engine specification in Table 4.1.1, the maximum power is different. The maximum engine power is 0.81kW at 6000

rpm (6.1 m/sec). In this research, the maximum power is 0.93 kW at 4.6 m/sec. For a rotational engine, at a speed of 6.1 m/sec, is it about 0.7 kW. In the case of a linear engine's maximum power, the target is to increase power output of the engine. The improvement power output increases between 2.3–34.6% and the average improvement is about 13.8%. In this study, an excellent improvement is obtained at high-speed engine performance. However, at low speeds the improvement is not as good.

Normally, brake specific fuel consumption is a function of the engine speed. The brake specific fuel consumption decreases as the engine speed increases; it reaches a minimum and then increases at high speeds. The fuel consumption increases at high speeds because of greater friction loss. At low engine speeds, the longer time per cycle allows for more heat loss, and fuel consumption increases (Willard, 2004). According to Figure 4.2.9, the friction loss of rotational engines is high at high speeds and this causes fuel consumption to increase. The brake specific fuel consumption is also affected by fuel equivalence ratios. Based on the research results, the fuel equivalence ratio is between 2.5–6.1 m/sec where it fluctuates unsystematically. The impacted brake specific fuel consumption at high speeds is shown in Figure 4.2.13.

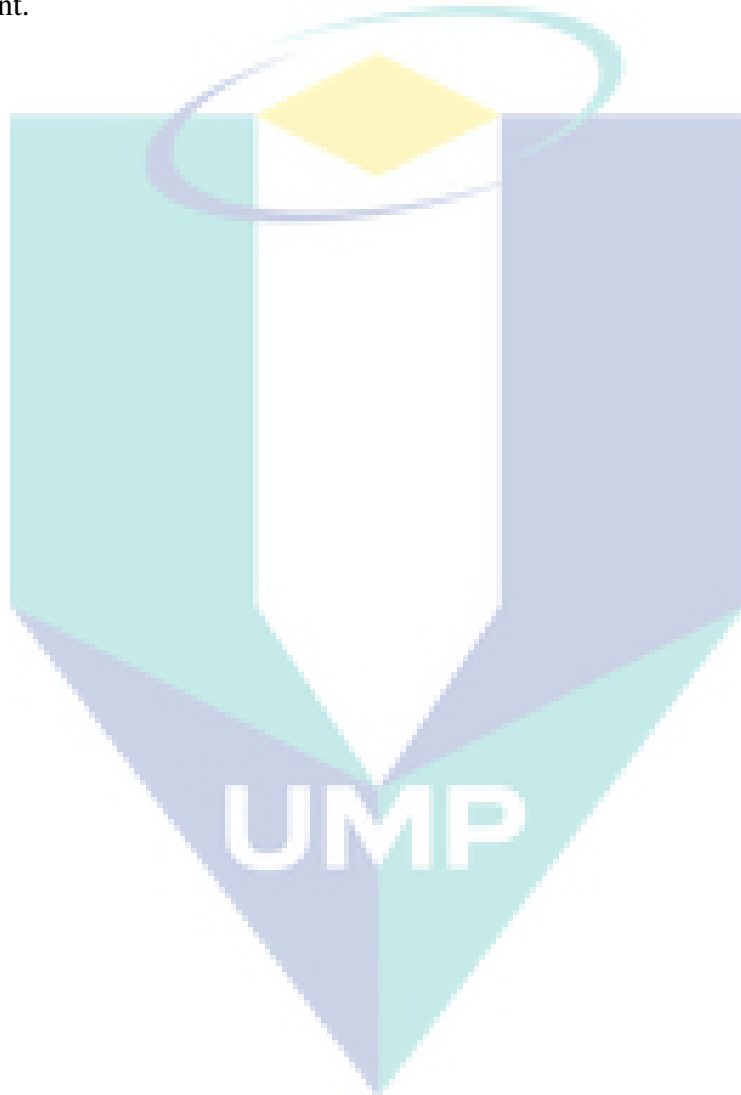
Brake efficiency in Figure 4.2.14 shows that the trend is different when compared to Mikalsen and Roskilly (2008). The free-piston engine has a slight efficiency advantage over the conventional engine at low speeds, but the efficiency drops as the speed increases. This could be compromised because the performance of an engine can be affected by the configuration of engine design.

4.2.5 Summary

The performance of linear engines with spring prediction has been studied in this research. The friction losses are simulated separately using GT-Power software. When compared to rotation engines, all performances introduce strong improvements, especially in high-speed operation. Friction losses could be reduced appropriately which means the power output could be increased. Specific fuel consumption also could be reduced, especially under high-speed operation. This phenomenon is caused by reducing friction losses and changing the energy to contribute to the power output of the engine.

The prediction of combustion pressure at variable speeds is a very important result in this research. Although the point of maximum pressure is fairly different, it is still possible to design a spring as return cycle in the linear engine.

In general, the results of the research could be adapted to design a real linear engine, especially when springs as the return cycle are simulated. With the predicted weakness in the original engine design, it is possible to modify the system design for improvement.



4.3 DESIGN AND OPTIMISATION OF A SPRING FOR TWO-STROKE SINGLE CYLINDER SPARK IGNITION LINEAR ENGINES

There are some techniques for the optimisation of a spring for linear engines. The main objective of this research is to design a linear engine in which the spring design is part of the linear engine design. For that reason, a simpler method has been used in this research. The trial and error method with spreadsheet and multilevel optimisation approach is an excellent choice for designing springs for linear engine applications. The multilevel optimisation is a decomposition technique in which the problem is reformulated as several sub-problems (one for each subsystems) and a coordination problem (at system level) to preserve the coupling among the subsystems (Rao, 1996). In the case of dynamic spring design, fatigue is an important phenomenon, especially for infinite life spring design. Metal fatigue is the failure of a component as a result of cyclic stress. The failure occurs in three phases: crack initiation, crack propagation and catastrophic overload failure. The duration of each of these three phases depends on many factors, including fundamental raw material characteristics, magnitude and orientation of applied stress, processing history and many others (Julivan & Marshek, 2006).

To meet safety requirement, the fatigue life can be estimated using a Goodman diagram (Shigley, Mischke & Budynas, 2004). To predict a component's life span, a modified Goodman diagram is presented. This diagram is presented in a variety of formats. The most common format used in the spring industry has the minimum operating stress represented along the x-axis, while the maximum operating stress is found along the y-axis. Many tests have been conducted to develop modified Goodman diagrams specifically for helical compression springs. To use this diagram, a designer must first know the spring's application. Specifically, the minimum and maximum Wahl corrected stress must be known for the spring's operating range (Julivan & Marshek, 2006).

The problem encountered is establishing an optimum spring design for a linear engine. The criterion for selecting a suitable solution with the lowest weight of spring is one of the objective functions of the optimisation of spring design. Another objective function is the maximisation of spring work. To fulfil both objectives' functions,

primary data were needed. For that reason, the engine performance simulation should be conducted first. To obtain the best optimisation results based from the objective functions, the multilevel optimisation approach has been adopted. There are three methods that have been used for spring design, namely nonlinear, geometric and dynamic programming methods. Through the three steps of the multilevel optimisation approach, spring design with specific deflection and high safety in fatigue can be achieved. However, the spring design results affect the linear engine performance especially during the scavenging process.

4.3.1 Material and Spring Design Optimisation Method

A multilevel optimisation approach has been used to design the linear engine spring. The theory of spring design has already been explained in Chapter 2, and the steps of the optimisation techniques are explained in Section 3.5. Figure 4.2.2 shows a sketch of a linear engine with a spring mechanism and Figure 4.3.1 presents the flowchart of the spring design. There are three steps involved in the optimisation of spring design. The first step is to optimise the thrust force as one of the input data. This piece of data is the most important in spring design with dynamic loading. Optimisation of thrust force data is necessary because if the resulting maximum force is used the engine does not work, especially at lower and higher areas. To minimise improper engine performance, the thrust force is optimised. The second step is to optimise the spring design. There are some requirements when designing dynamic load springs. The final step is to optimise the effect of spring design on engine load operation, especially in engine scavenging.

The data of thrust force performance is calculated using GT-Power. Table 4.3.1 shows the linear engine performance at variable speeds under full load. The values of imep are taken from Figure 4.3.2.

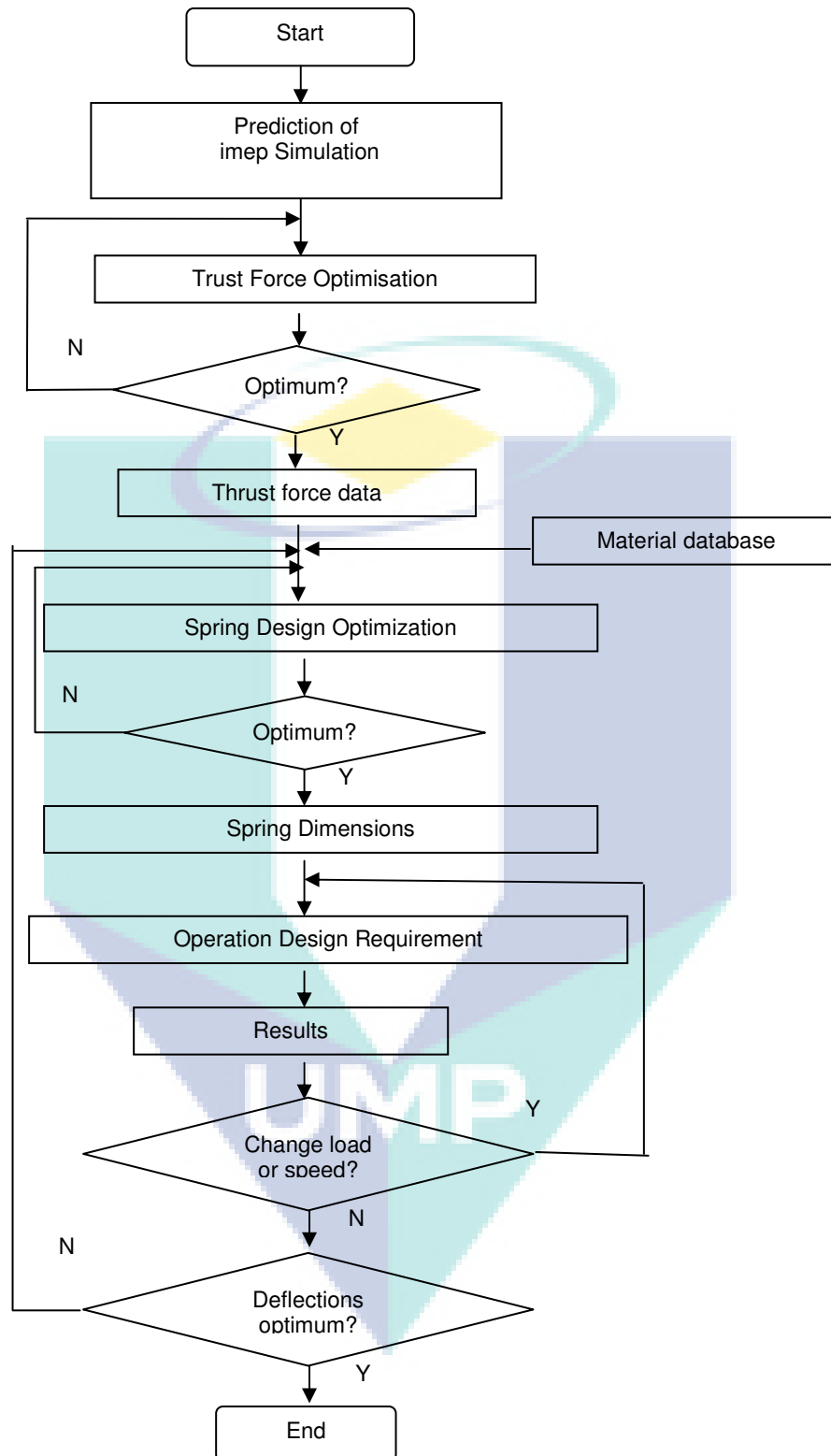
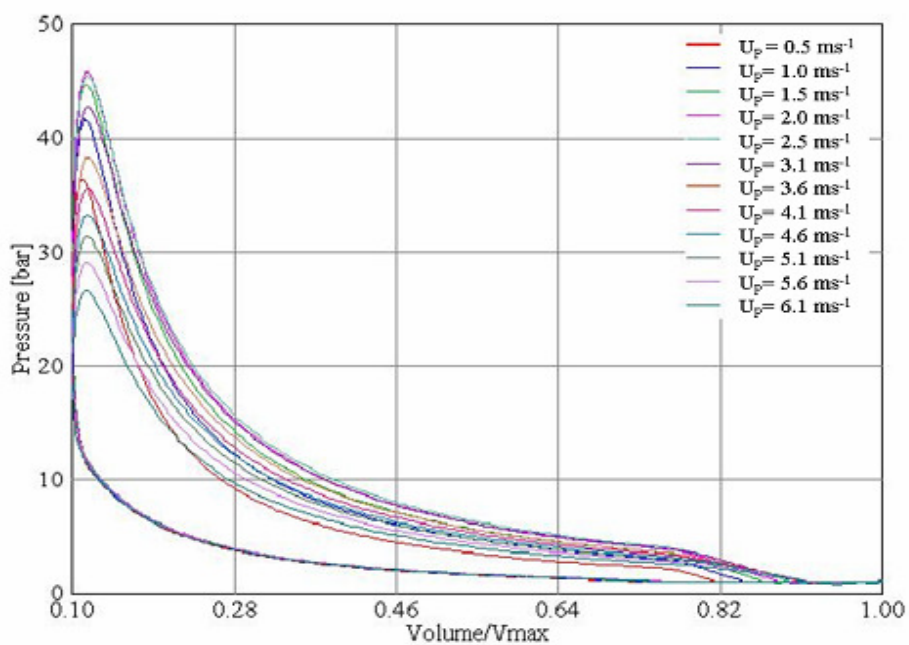


Figure 4.3.1: Flowchart of a linear engine with spring system

Table 4.3.1: Speed, imep and thrust force of engine performance

No	Speed (m/sec)	imep (bar)	F _o (N)
1	0.5	0.378	1370.2
2	1	5.54	1551.79
3	1.5	6.7	1671.48
4	2	7.78	1731.32
5	2.5	7.52	1756.09
6	3.1	7.09	1711.72
7	3.6	6.23	1622.99
8	4.1	5.66	1564.18
9	4.6	5.24	1520.84
10	5.1	4.74	1469.2
11	5.6	4.21	1414.57
12	6.1	3.68	1357.88

**Figure 4.3.2:** PV diagram of variable speeds

Before optimising the thrust force performance as data input, it is first necessary to establish a polynomial equation. Later the results were used for data input into an optimisation procedure by using a numerical integration technique. By using Matlab, the thrust force data could be calculated. The data of speed versus imep is shown in Table 4.3.1 and is used to obtain a function by means of curve fitting with the polynomial high order. Finally using a numerical integration technique, the optimisation can be concluded.

The second step is to optimise spring geometries. The objective function of the spring design is the minimisation of the spring material. The fatigue loading, shock, resonance of the spring and resonance of the spring mass system are constrained for spring design optimisation. The other criterion for the spring should be deflection, which is close to 30.5 mm. Wire diameter of the spring can be calculated by using a spreadsheet with a geometric approach. These results should be continued to a third step, such as spring dynamics optimisation using a dynamic approach. A block diagram of the multilevel optimisation approach is shown in Figure 4.3.3.

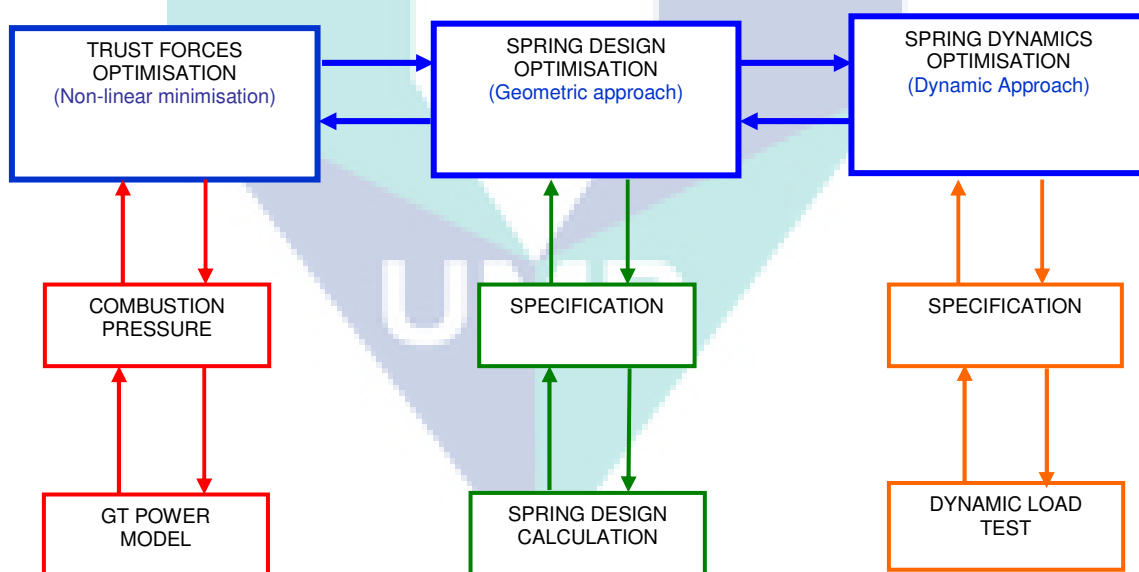


Figure 4.3.3: Block diagram of multilevel optimisation approach

4.3.2. Basic Equation for Round Wire Spring

Springs are constructional elements designed to retain and accumulate mechanical energy, working on the principle of the flexible deformation of material. A

compression spring is a helical cylindrical spring with a constant spacing of active coils and an approximately constant stiffness, which is able to receive external forces acting against each other in its axis. In view of the spring's function, there are four basic states of springs, which include free load, preloaded, fully loaded and limiting. In the Table 4.3.2, the mentioned indexes are used in the calculation to specify the individual parameters of the spring related to the given state of the spring. Figure 4.3.4 provides a specification of the individual parameters of the spring.

Table 4.3.2: Indexes in the calculation

State of the spring	Description of states of a spring	index
free	the spring is not loaded	0
preloaded	the spring is exposed to minimum operational loading	1
fully loaded	the spring is exposed to maximum operational loading	8
limiting	the spring is compressed to full contact of coils	9

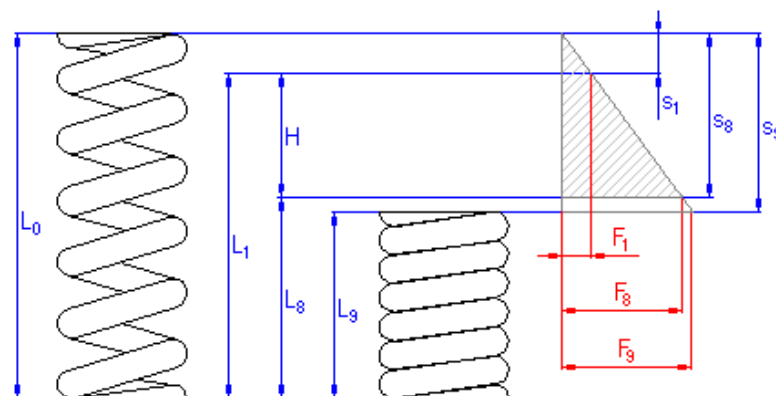


Figure 4.3.4: States of the spring according to the index of basic states of springs
(Petele, 2009)

a. Basic Equation

According to Juvinall and Marshek (2006), the torsional stress of the spring material (τ) is calculated by:

$$\tau = K_s \cdot \frac{8.F.D}{\pi.d^3} \quad (4.3.1)$$

where K_s is the curvature correction factor, F is the loading of spring (N), D is the mean spring diameter (mm), and d is the wire diameter (mm).

For fatigue loading, the equation for corrected stress includes the complete Wahl factor:

$$\tau = K_w \cdot \frac{8.F.D}{\pi.d^3} \quad (4.3.2)$$

where K_w is the Wahl factor.

The analysis involving the derivation of the equation for the Wahl factor can be multiplied to give the total resultant shear stress on the inside of the coil:

$$K_w = \frac{4.C-1}{4.C-4} + \frac{0.615}{C} \quad (4.3.3)$$

where C is the spring index.

When the loading on a spring is essentially static, the view is usually taken that the first term of Equation (4.3.3), which accounts for the curvature effect, should not be used because it is essentially a stress concentration factor. This can usually be ignored with static loading of ductile materials (Juvinall & Marshek, 2006). Setting this term equal to unity gives a correction factor:

$$K_s = 1 + \frac{0.615}{C} \quad (4.3.4)$$

Curvature correction factor is the coil bending causes additional bending stresses in coil springs. Therefore the calculation uses the correction coefficient to correct the tension. For springs of round section wire, the correction coefficient is determined with the given spring coiling ratio by several empirically defined formulas (Petele, 2009). This calculation uses the following relation:

$$K_s = 1 + \frac{0.5}{C} \quad (4.3.5)$$

where C the is spring index, and can formulated with the equation below:

$$C = \frac{D}{d} \quad (4.3.5)$$

where D is the mean spring diameter (mm), and d is the wire diameter (mm).

Derivation of the equation for helical spring deflection (s) is most readily accomplished using Casigliano's method, assuming that the contribution of transverse shear to deflection is negligible and only the torsional load needs to be considered. The detailed derivation can be read from Juvinal and Marshek (2006), below is the result of the spring deflection equation:

$$s = \frac{8FD^3N}{d^4G} \quad (4.3.6)$$

where F (N) is the force load, N is the active coil number and G is the modulus of elasticity in shear (MPa).

The spring rate (also called the spring constant or spring scale with units of Newton per millimetre) is commonly designated as k , where

$$k = \frac{F}{s} = \frac{d^4G}{8D^3N} \quad (4.3.7)$$

b. Design of spring ends

In the case of compression springs, several various designs for spring ends are used. These differ in number of ends and machined coils and designs of the supporting surfaces of the springs. End coils are edge coils of the spring, co-axial with the active coils, whose angle pitch does not change during the functional deformation of the spring. End coils create a supporting surface for the spring, and with compression springs one end coil is usually used at both ends of the spring. Ground coils are edge coils of the spring, machined to a flat surface perpendicular to the spring axis, usually machined from three-fourths or half of the end coil up to its free end. Machined coils are commonly only used with springs with diameters of wires $d > 1$ mm (Petele, 2009).

The four standard end designs used with compression helical springs are illustrated in Figure 4.3.5.

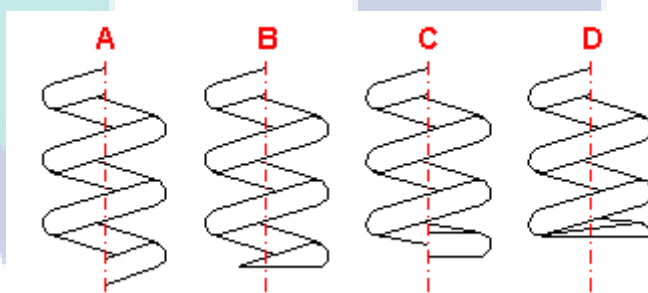


Figure 4.3.5: The most common types of spring end designs (Petele, 2009)

- A. Open ends not ground: the edge coil is not bent to the next one, the supporting surface is unmachined
- B. Open ends ground: the edge coil is not bent to the next one, the supporting surface is machined to a flat end perpendicular to the spring axis
- C. Closed ends not ground: the edge coil is bent to the next one (it usually adjoins its free end), the supporting surface is unmachined
- D. Closed ends ground: the edge coil is bent to the next one, the supporting surface of the spring is machined.

c. Buckling Analysis.

The possibility of the buckling effect in the compression action of helical springs must be considered, particularly for large ratios of free length to mean diameter (Juvinal & Marshek, 2006). The check is performed by comparison of the maximum working deformation of the spring with the permitted deformation. The value of the permitted deformation is determined empirically for the given slenderness ratio of the spring L_0/D and the type of seating of the spring. The mode of seating of the spring has a significant effect on its possible side deflection. Figure 4.3.6 shows the seating types of the spring.

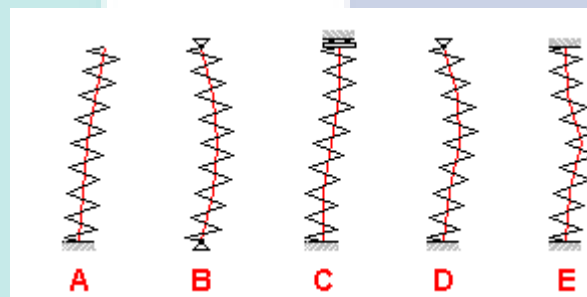


Figure 4.3.6: Seating types of the springs (Petele, 2009)

A spring which cannot be designed as secured against side deflection is usually installed on a pin or inside a sleeve. If there is danger of damage to the spring due to friction, the spring can be divided into several shorter springs arranged in series (Petele, 2009). Figure 4.3.7 shows the curves of permitted deformation according to the type of seating of the spring. Curves B and C represent the most common deformations. If buckling is indicated, the preferred solution is to redesign the spring. Otherwise, the spring can be supported and hence prevented from buckling by placing it inside a cylinder that provides a small clearance (Juvinal & Marshek, 2006).

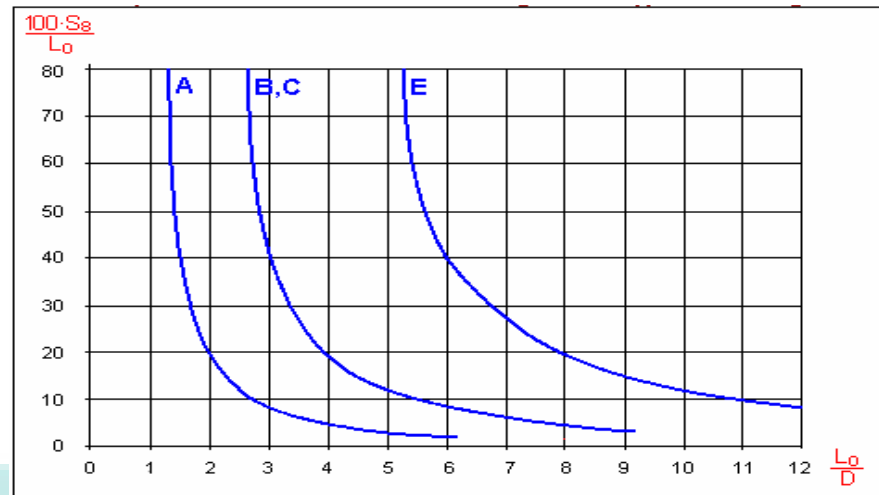


Figure 4.3.7: Curves of permitted deformation according to the type of seating of the spring (Petele, 2009)

d. Fatigue loading

Springs exposed to oscillating (dynamic) loading, i.e. with cyclical changes of loading, with the requirement of a service life from 10^5 working cycles upwards, require fatigue analysis. Two fields of the fatigue loading of springs can be distinguished with springs exposed to fatigue loading. In the first field, with the limited service life of springs (lower than approx. 10^7 working cycles), the fatigue strength of the spring decreases with an increasing number of working cycles. In the field of unlimited service life (the desired service life of the spring is higher than 10^7 working cycles), the fatigue limit of the material and thus the strength of the spring remains approximately constant.

The level of safety gives the minimum permissible ratio between the fatigue strength in torsion of the spring and the actual maximum working stress τ_8 in the spring coils. For a non-corrosive atmosphere and working temperature in the immediate vicinity of the spring of up to 80 °C, and with regards to the course and mode of loading, it is advisable to choose a level of safety of compression for springs in the interval from 1.05 to 1.25. When determining the level of safety, it is also necessary to consider the suitability of the selected material for fatigue loading. With materials unsuitable for fatigue loading, it is advisable to increase the desired level of safety by up to 20%. Springs working at higher temperatures or in a

corrosive environment should be designed with higher levels of safety. Corrosion in particular significantly decreases the service life of a spring exposed to fatigue loading (Petele, 2009).

There are some methods to analysis fatigue, and one of them is the Goodman diagram. In this diagram the alternating stresses are on the y-axis and the mean stresses are on the x-axis. The value for the endurance limit is then placed on the alternating stress axis and the ultimate tensile strength on the mean stress axis. These are then connected with the Goodman line (infinite life). A line drawn from the origin to the endurance limit, with a slope equal to the alternating stress, is the load line. To find the life of the spring one finds the point located by the mean stress and the alternating stress (this should be on the load line) (Porteiro, 2010).

In predicting the life of a component, a more useful presentation of fatigue life test data is the modified Goodman diagram. These diagrams, while still limited by specimen geometry, surface condition and material characteristics, allow the user to predict the life at any stress ratio. To determine satisfactory spring geometry, fatigue loading should be analysed. Design analyses begin from perform strength characteristics of the material. Figure 4.3.8 is the ultimate tensile strength for the given material and wire size.

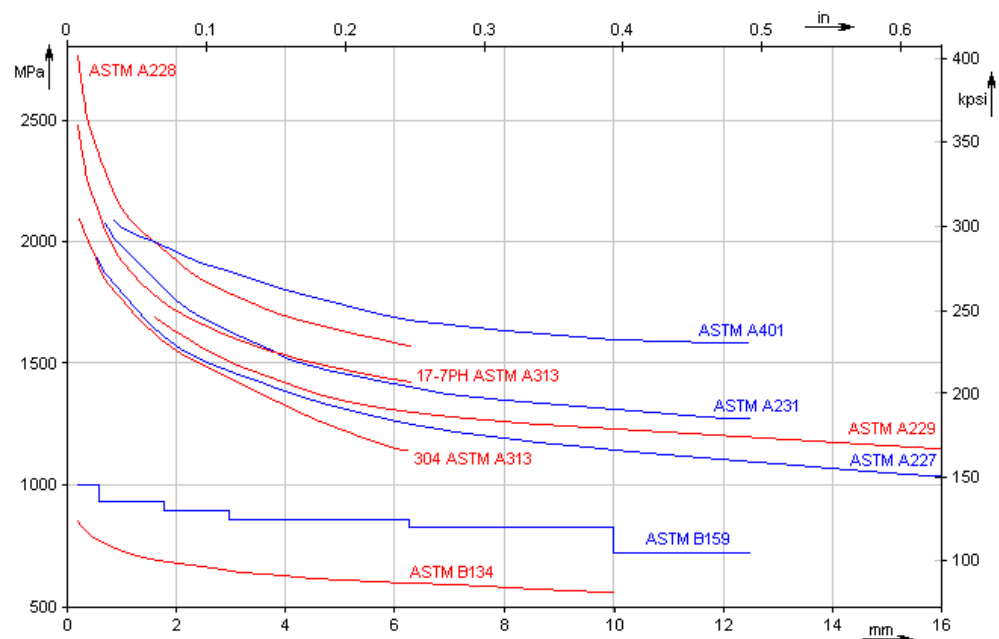


Figure 4.3.8: The ultimate tensile strength- EN (Petele, 2009)

The ultimate fatigue strength in shear (τ_e) is:

$$\tau_e = 0.36S_u \quad (4.3.8)$$

According to Petele (2009), shot peening of the spring increases the fatigue limit by approximately 15 to 25%. In case of springs with shot peening exposed to fatigue loading, this allows users to reduce the consumption of material used in the production of the spring, to reduce its dimensions and installation space, increase the working stroke or increase the protection of the spring against fatigue breaks. Therefore, it is advisable to apply the technical requirement of shot peening to all springs exposed to oscillating loading.

The permissible torsional stress (τ_A) associated with a 2 percent long-term set is:

$$\tau_A \leq S_u \quad (3.3.8)$$

According to Juvinall and Marshek (2006) the ultimate shear strength (S_{us}) is approximated as:

$$S_{us} = 0.8S_u \quad (3.3.8)$$

An estimated torsional fatigue strength curve for infinite life is plotted in Figure 4.3.9, and Table 4.3.3 presents the calculated data for shot-peened chrome-vanadium alloy steel wire SAE 6150, d=7 mm.

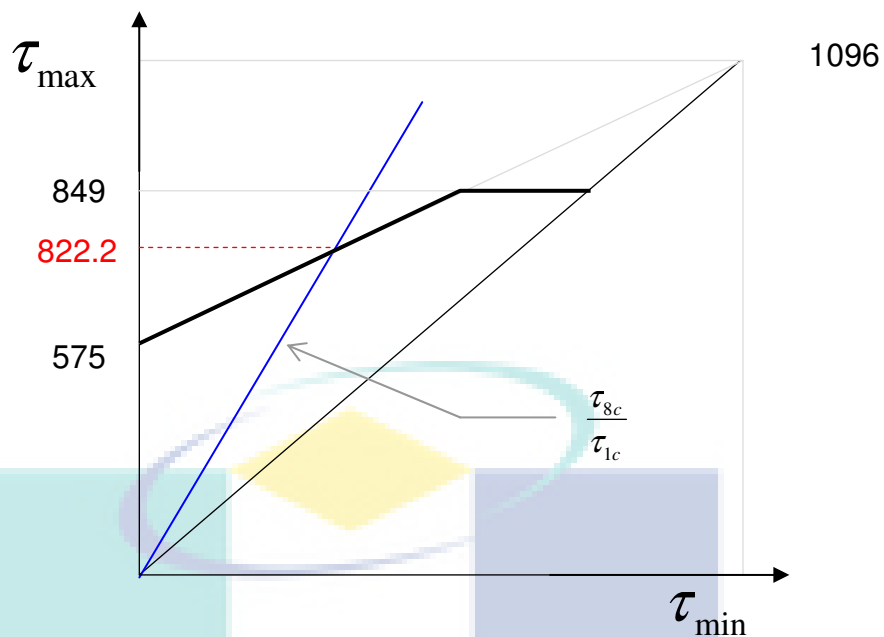


Figure 4.3.9: Fatigue diagram for shot-peened chrome-vanadium alloy steel wire SAE 6150, $d=7$ mm.

Table 4.3.3: Calculated data for Figure 4.3.9

No	Description	Symbols	Values
1	Curvature correction factor	K_f	1.2059
2	Corrected stress of preloaded spring (MPa)	τ_{1c}	419.88
3	Corrected stress of fully loaded spring (MPa)	τ_{8c}	663.86
4	Ultimate shear strength (MPa)	S_{us}	1096
5	Permissible torsional stress (MPa)	τ_A	849
6	Ultimate fatigue strength in shear (MPa)	τ_e	575
7	Fatigue strength for the given loading (MPa)	τ_f	822.2
8	Level of safety factor	-	1.239

4.3.2 Results

There are three main optimisation results, namely thrust force engine performance, spring design and the effect of the engine load on spring characteristics. As many as 12 thrust force engine performances obtained from GT-power are optimised using nonlinear programming with a numerical integration technique. The objective function is to establish an optimum load based performance for spring design by minimisation of the differences between the maximum and minimum forces. It needs the compromise of load for the majority of engine load operations. After some iterations with a trial and error technique, 6 wire diameters of the same material were established. Selection of the design is necessary for the spring mechanism of linear engine systems. Finally, the best spring design for the two objective functions is chosen. The functions considered are minimised spring weight and maximised spring range workload.

The optimisation of the spring design load data started with the modelling of variable speed versus imep. From here, the thrust force engine performances then followed with the optimisation result of the imep. The polynomial of Equation 4.3.1 is a modelling result. However, a 5 degree model is the best equation for conducting the optimisation of imep.

$$y = -0.0112X^5 + 0.1715X^4 - 0.7987X^3 + 0.4601X^2 + 3.8383X + 1.8439 \quad (4.3.1)$$

Figure 4.3.10 shows the optimisation results of imep. The optimum imep is about 5.1439 bar. With this optimum imep, the spring is designed and the optimum thrust force was obtained.

Table 4.3.4 shows the spring design results, these design conducted based thrust force and wire spring material data in variable wire diameter. Spring wires of 6.5 mm, 7 mm, 7.5 mm and 8 mm in diameter are examples which require the criteria of a spring design based geometric program approach. If the spring design carried out is based only on geometric optimisation, then a spring diameter of 6.5 mm is lighter and safer from fatigue. If consideration is needed as to how the spring works under dynamic loads, the speeds and loads need to be changed. In a dynamic optimisation based approach, a spring with 7 mm diameter wire is the best. Most of the speed can be served with the spring without any problem with respect to fatigue. A spring wire with a

diameter of 7 mm is available on the market as a cold formed spring. For that reason, the 7 mm diameter spring is the final choice. Although it is heavier than the 6.5 mm diameter spring, it should be a good compromise.

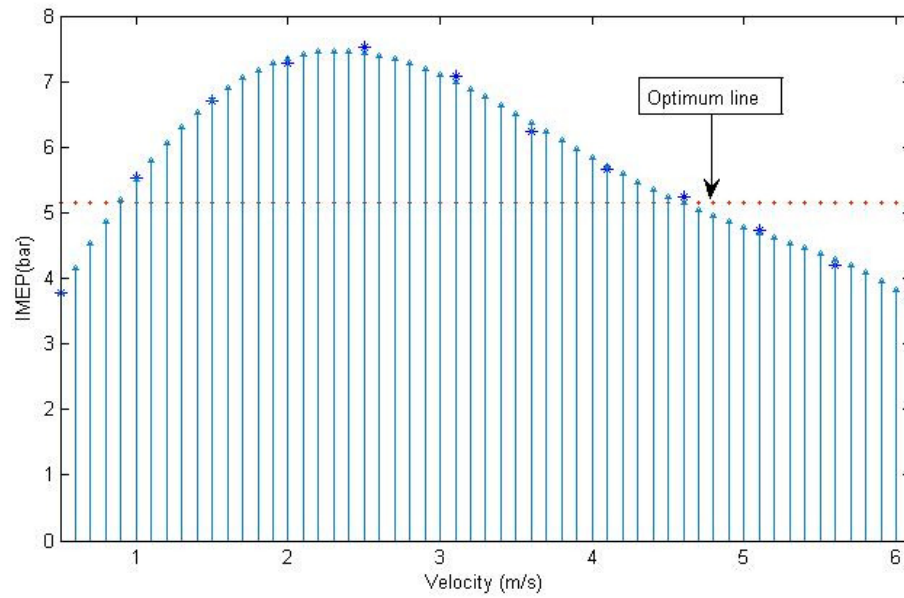


Figure 4.3.10: Optimization imep

The spring dynamics, especially deflection characteristics, have an impact on the engine performance. The engine load and engine speed can influence the imep performance, and automatically thrust force of piston movement could exchange. If the thrust force is too small, the spring deflects slightly. This would result in the intake scavenging port not opening and a misfire would occur. Figure 4.3.11 shows the correlation between engine speed and working stroke. It is shown that not all engine speeds can deflect the spring properly. Normally springs should be deflected 30.5 mm, in this condition the scavenging port intake opens 100%. In the original conventional engines, the height of intake the scavenging port is designed at 7.5 mm. If the spring is deflected less than 22.5 mm then the mixture cannot pass through to the combustion chamber. However, 25 mm of spring deflection is acceptable in this research, where the intake scavenging port would only be able to open 33.3%.

Table 4.3.4: Spring design result

Spring material :	Chrome-vanadium alloy steel wire SAE 6150					
Direction of coil winding	Right					
Surface treatment	Shot-peened springs					
Wire diameter	d	6	6.5	7	7.5	8
Number of active coils	n	12	12	10	9	9
Outer spring diameter	D_e	44	48.4	57.7	65.1	70.8
Inner spring diameter	D_i	32	35.4	43.7	50.1	54.8
Free spring length	L_f	200	200	200	200	205
Preloaded spring length	L_i	150.69	152	147.32	147.24	152.18
Fully loaded spring length	L_o	122.01	124.09	116.7	116.58	124.31
Theoretical spring limit length	L_t	84	91	84	82.5	88
Minimum working loading [N]	F_i	928.6	928.6	928.6	928.6	928.6
Maximum working loading [N]	F_o	1468.6	1468.6	1468.3	1468.3	1418.6
Theoretical spring limit loading [N]	F_s	2184.3	2108.8	2044.6	2068	2056.9
Spring deformation energy [J]	W_8	57.27	55.74	61.16	61.25	57.24
Critical spring speed [m/s]	V_k	9.25	7.18	6.26	6.02	5.75
Natural spring frequency [Hz]	f_n	121.68	108.42	95.7	88.26	79.2
Developed wire length [mm]	l	1702	1877	1947	2028	2211
Spring constant [N/mm]	k	18.83	19.35	17.63	17.6	17.58
Spring weight [kg]	m	0.378	0.489	0.588	0.703	0.872
Permissible torsional stress [MPa]	t_A	967	961	954	947	940
Static level of safety		1.362	1.563	1.615	1.742	1.994
Fatigue strength for the given loading	t_{max}	743	740	737	734	746
Dynamic level of safety		0.912	1.052	1.107	1.206	1.417

Figure 4.3.11 shows that spring wires of 7 and 7.5 mm can work properly when the speed is between 1 m/sec to 4.5 m/sec. This is the optimum performance result of the working stroke for the linear engine design. However, at 4.6 m/sec the deflection of spring wires of 6.5 mm and 8 mm are 24.64 and 24.59 mm respectively. Both deflections were close to the requirement, but they were rejected.

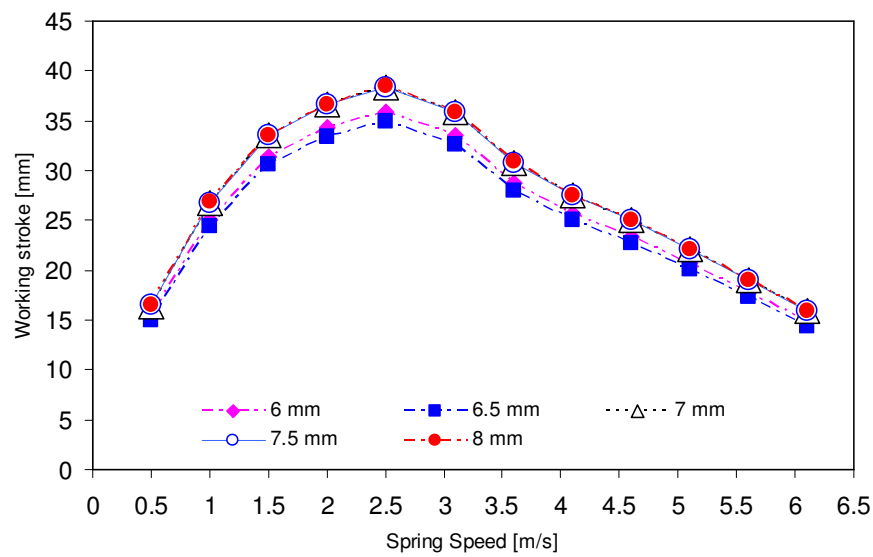


Figure 4.3.11: Effect of engine load and speed on spring deflections

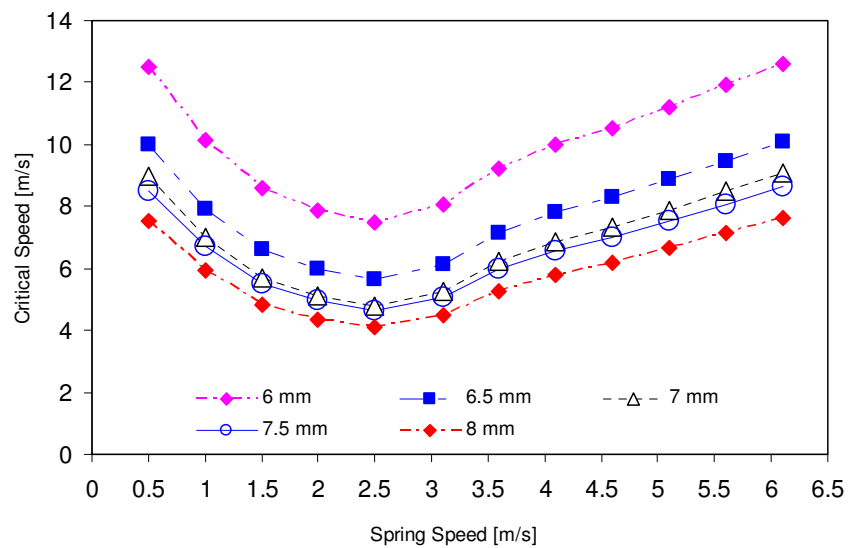


Figure 4.3.12: Characteristics of critical speed of spring design

Figure 4.3.12 shows the critical speeds of the spring design at different wire diameters. Reducing the spring diameter may increase the critical speeds. This is shown that all wire diameters could be accepted based on the requirement of the critical speed effects on the spring speed works area.

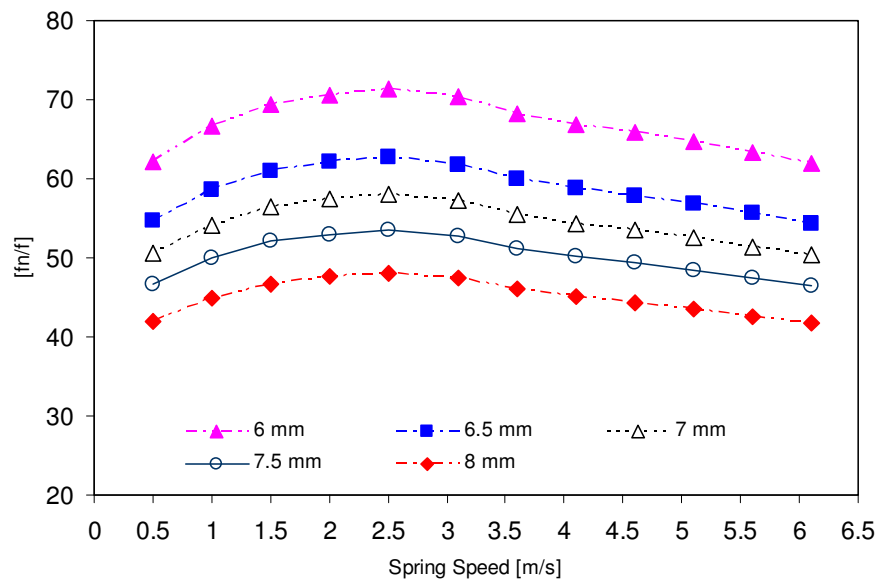


Figure 4.3.13: Resonance effect on variable spring speeds

Figure 4.3.13 shows the natural frequency divided operation frequency of the spring against variable speeds for different spring wire diameters. Increasing the spring wire diameter could have an impact on the decreasing dependency of resonance effect. However, all spring wire diameters are safe if based on the requirements of the dynamic loading-resonance effect. According to Rao (1996), in order to avoid the resonance, the natural frequency of springs should be at least 13 times the operating frequency.

Figure 4.3.14 presents the dynamic safety level of different spring wire diameters at different working speeds. The effect of dynamic safety level is a very important constraint in spring design, especially for spring systems of linear engines. In this case, the linear engine spring should be durable at different speeds and loads. Through iteration techniques, dynamic safety levels could be obtained. Figure 4.3.14 shows that a spring speed of 2.5 m/sec is crucial, and some of the spring wire diameters cannot meet the requirement. Only spring wires that meet the requirement are accepted, such as diameters of 7 mm, 7.5 mm and 8 mm.

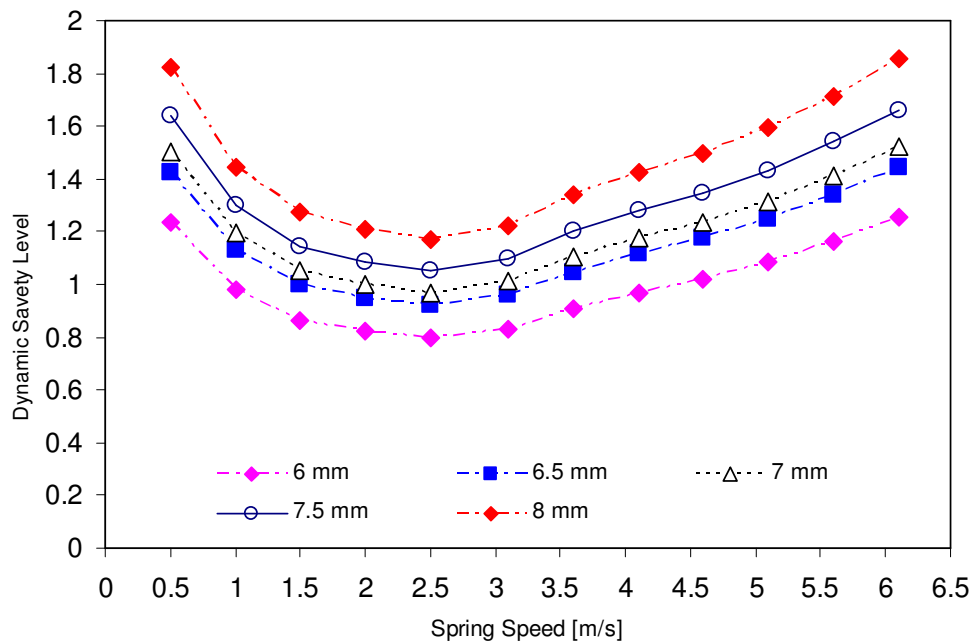


Figure 4.3.14: Dynamic safety level of different spring wire diameters at different operating speeds

4.3.3 Discussion

The three steps of the multilevel optimisation approach form the simplest method for solving the spring problem of a linear engine design. The thrust force engine performance is very important because it leads to the final geometry of the spring. Equation 4.3.1 is the key for the optimisation step for the thrust force of engine performance. The compromised thrust force can be obtained from this formula; for example the optimum imep is 5.1439 bars.

The tables and figures of the results in Chapter 4.3.2 are the product of the three step multilevel optimisation approach. If the linear engine is operated at constant speed and load, the best spring wire is 6.5 mm. However, the objective of the research is not only to minimise spring weight but also to maximise the operation area of spring work. So, the spring should be accepted at certain speeds and loads for a performance engine trend. For that reason, the last step in the multilevel optimisation approach is conducted by using a dynamic programming technique. In these steps, the spring deflection in Figure 4.3.11 and dynamic safety level in Figure 4.3.14 are the most important parameters. The deflection characteristic of a spring wire 6.5 mm in diameter is similar

to the operating areas of spring wires of 7 mm, 7.5 mm and 8 mm in diameter. However, the dynamic safety is very weak and at certain spring speeds, such as 2 m/sec, 2.5 m/sec and 3 m/sec, less than 1.05. A spring wire diameter of 7 mm is the best choice, according to this research, because it is accepted based on all requirements. The deflect inion of the spring could open a scavenging port between 1 m/sec to 4.6 m/sec speed; and the dynamic safety levels of the spring are accepted based on the requirements.

Although scavenging ports could only be opened fully by spring deflection, there are some speeds that cannot open the port. The spring should deflect 30.5 mm to fully open the scavenging port. In the case of a 7 mm diameter spring wire, there are some conditions under which the port cannot open; i.e. when the engine speed is less than 1 m/sec and at engine speeds higher than 4.6 m/sec. So, at certain speeds, a misfire at the combustion chamber happens. Besides that, at certain speeds it is also predicted that engine performance decreases, such as at engine speeds of 1 m/sec, 4.1 m/sec and 4.6 m/sec. The percentage of the decreasing performance is dependent on the opening of the scavenging port area. However, 56.4% scavenging port could open at 1 m/sec speed, 66.6% at 4.1 m/sec, and 31.1% at 4.6 m/sec. Incomplete deflection of the spring does not only affect the scavenging port function, but also the compression ratio of the engine. The compression ratio of the engine also decreases depending on the characteristics of the spring deflection.

4.3.4 Summary

A design of the spring for single cylinder spark ignition linear engine has been conducted in this research, and a multilevel optimisation approach is an excellent technique to adopt. Shot-peened, chrome-vanadium alloy steel wire SAE 6150 of 7 mm diameter is an excellent cold process spring design. The spring works very well under dynamic load services, and they are accepted based on all safety level requirements. Besides, they also provide the best operating work at certain speeds and loads. Incomplete deflection of the spring could impact on the combustion process, including scavenging ports that would not be able to open properly, and decreases the pressure ratio.

4.4 LINEAR ENGINE DESIGN

The essence of the research is to design a linear engine. Although less attractive, the results of a design configuration using CAD must be discussed in terms of scientific analysis. This chapter shows the design method and the results of preliminary design. For the final result, further discussion is needed on the analysis, such as on the influence of spring design on the performance of the engine, piston dynamics and scavenging. This will be discussed in the next chapter. This chapter introduces the results that indicate that all components have been assembled as a whole with sufficient explanation. The steps in the assembly are also presented. The detailed components are given in Appendix F.

4.4.1 Process of the Design

As already discussed in previous subchapters, the design method has been chosen for the modification of a conventional engine. Some of the components are taken from a conventional engine, and some are created as new components. The geometry of the components is measured in a conventional engine, and then redrawn to the same size. The new components are designed based on results of the analysis, and this forms a preliminary design. Depictions are recreated in accordance with its original size. The new component is illustrated based on the earlier calculations on which the analysis has been conducted. The size of the connecting rod and casing are adjusted based on the results of the spring design optimisation.

All components are drawn using professional software, called SolidWorks. After all the components are drawn precisely at their original size, they are assembled using the same software. The assembly is not performed as one unit, but in the form of certain parts, such as the carburettor, connecting rods, casing, cylinder heads and exhaust systems. Then these parts are assembled into an whole system.

The results of the assembly should meet the predetermined requirements; if it does not happen then the components are modified. The next step is the analysis of the design which has become a unit of the linear engine design. This step will be discussed in the next subchapter. If no problems are encountered in the analysis stages, then the

design of the linear engine is considered as being well performed. Figure 4.4.1 shows the flow diagram of design process of a linear engine.

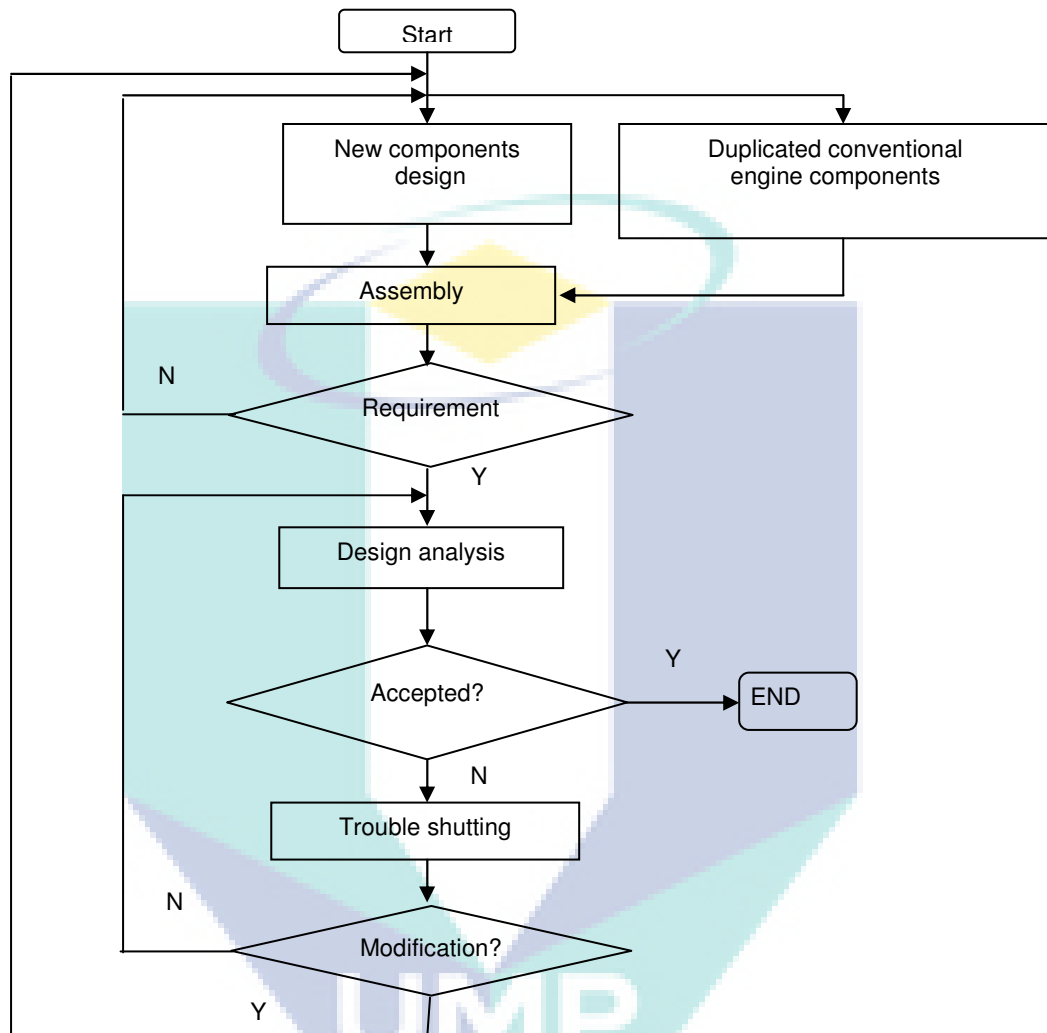


Figure 4.4.1: Flowchart of linear engine process design

4.4.2 Results

Designing a linear engine must be based on optimum results of the spring design. This is followed by the design of the connecting rod configuration as well as the design of a journal bearing. By combining the movement of the piston oscillation with the design of the connecting rod, one can design a casing which is the final part of the design of the linear engine. In designing new components, special attention is given to the geometry of components which are adopted from a conventional engine.

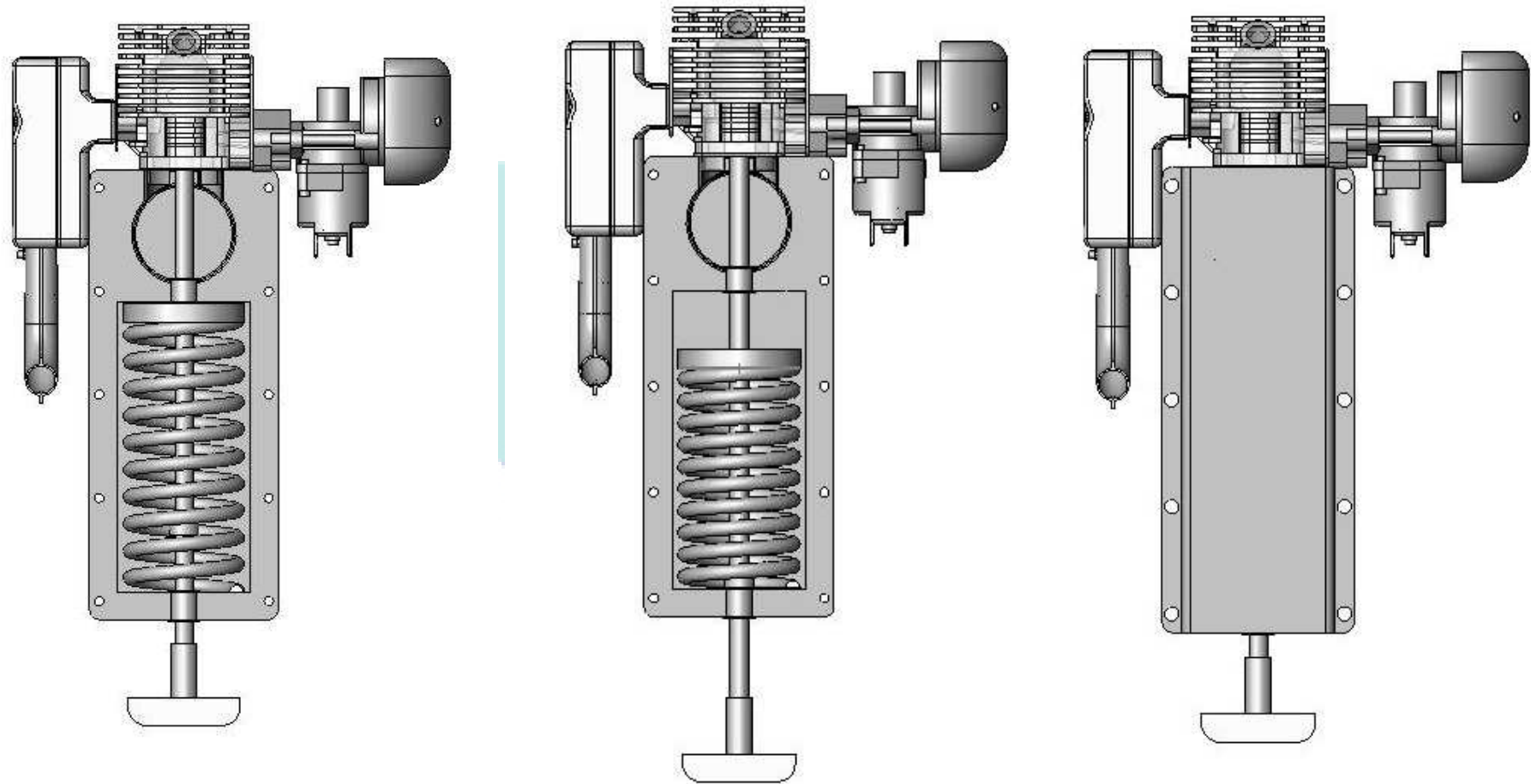
4.4.2.1 Linear Engine Design Configuration

Figure 4.4.2 presents the configuration of a linear engine design with a spring mechanism as a return cycle. Figure 4.4.2(A) shows the preloaded conditions at the top dead centre (TDC) position. Even without the load, the spring should be able to compress with a pressure ratio of 1:9. When it is stopped, the linear engine is always TDC position. Figure 4.4.2(B) shows the full load condition at the bottom dead centre (BDC). In this state, the spring is compressed as deep as 30.5 mm. Figure 4.4.2(C) is a front view of the full assembly of a linear engine.

Figures 4.4.2(A) and (B) show the diametric clearance of the spring with the engine casing wall of $0.1D$, where D is mean spring diameter of the spring. The clearance gives the spring a considerable space allowing it to expand, and this can avoid friction and wear on the spring from rubbing against engine casing wall. The $0.1D$ clearance is a commonly recommended diametric clearance in spring design (Petele, 2009).

4.4.2.2 Oscillation Control System

In order to make a linear engine work as desired, a simple control device is needed. The spring follows Hooke's law, in which oscillation motion is due to the work of pressure.



(A) Preloaded condition

(B) Fully loaded condition

(C) Front view of full assembly

Figure 4.4.2: Configuration design of linear engine

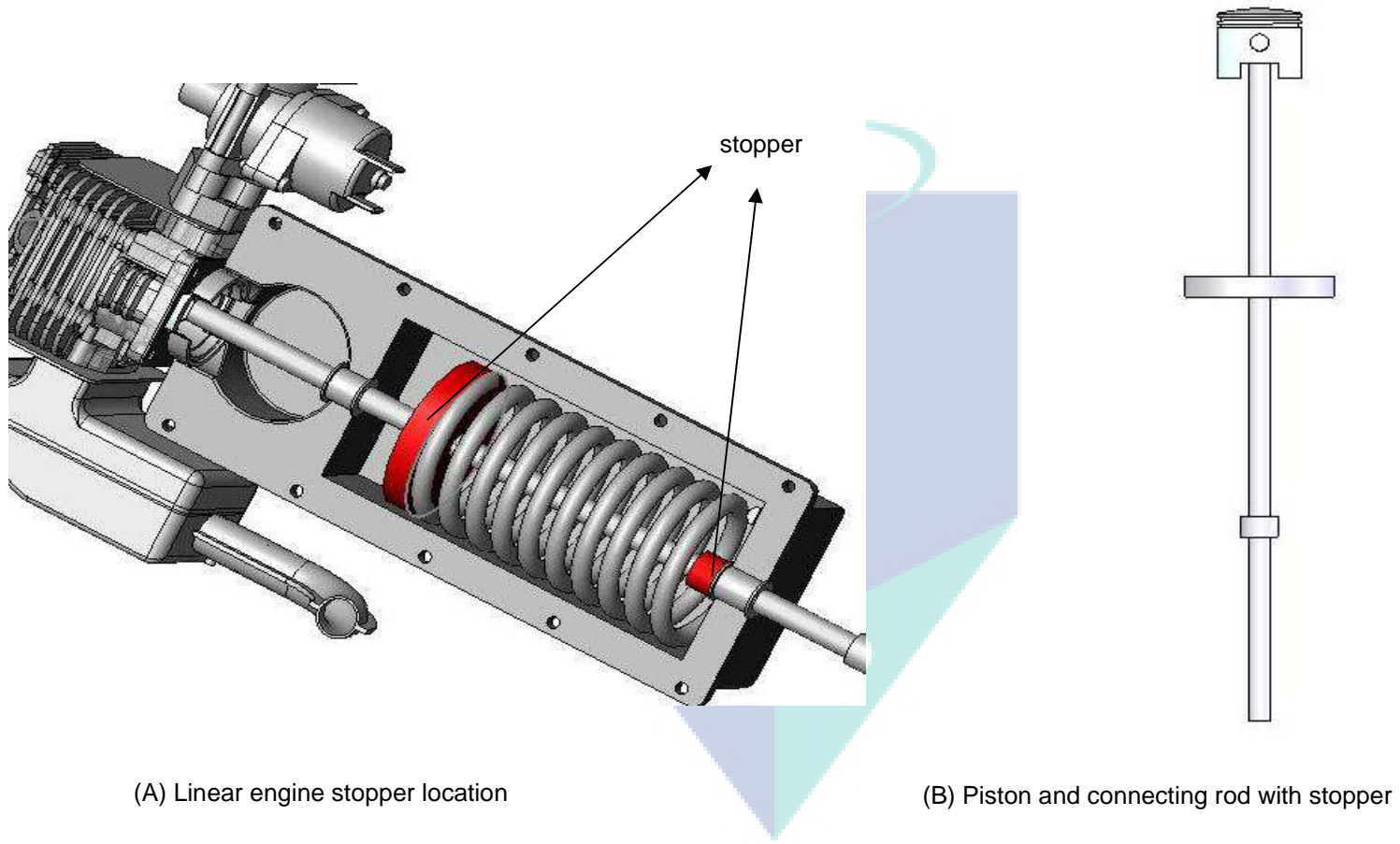


Figure 4.4.3: Oscillation control system.

At high pressure, the spring will be deflected very deep via versa. Under too-high pressure conditions, stoppers are used to control displacement. If the pressure is too small, misfire will occur because the scavenging port cannot be opened.

Figure 4.4.3 shows an oscillation control system where the oscillations move excessively. When the piston deflects more than 30.5 mm to the bottom dead centre (BDC) it will be retained by the bottom stopper. Conversely, if the combustion chamber pressure is overly small, the spring force cannot be arrested by the combustion chamber pressure, the piston movement will be stopped by the top stopper. If there is no stopper to hold, the oscillation movement of the piston cannot be controlled. In certain circumstances, the piston can slip out of the cylinder liner. Using this technique, a linear engine is expected to work well.

Collision between the bottom stopper and the casing will occur when the working pressure exceeds the optimum load. When the combustion chamber pressure is lower than the designed value, then the top stopper will collide with the casing. Collision is just a state when the engine does not work normally. Figure 4.4.3(A) presents the location of the stopper in a spring of a linear engine system. The red colour identifies the location of the top and bottom stoppers. Figure 4.4.3(B) shows the physical form of the connecting rod that is assembled with a piston.

4.4.2.3 Isometric View Design

Figures 4.4.4 and 4.4.5 show the isometric view of linear engine design. Figure 4.4.4 shows an isometric view of a linear engine when the top casing is opened. This image shows the spring system design. The geometry depends on the results of the spring design. So excessively large dimensions of a linear engine result in the geometry of a spring that cannot be reduced. The linear engine geometry is larger than a conventional engine.

Ergonomics is another concern when designing a linear engine. The technique for assembling, repairing and the maintenance of systems should be considered. This engine is designed for use as the driver of a linear generator. Usually, the linear generator is designed together with the connecting rod. The advantage of this system is that it is very compact, and it will be very easy repair or maintain the components. Here the linear generators and engines are designed separately for ease of repair and

maintenance. Ergonomically, the design is quite nice and simple. It gives the impression of being easy-care and cheap.

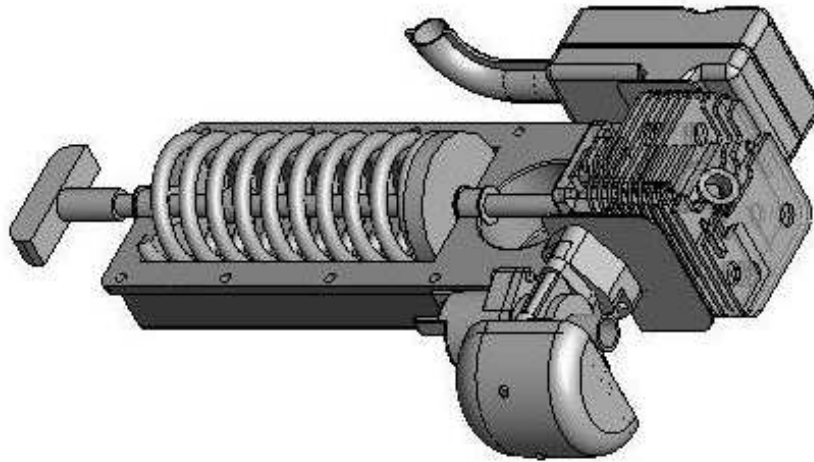


Figure 4.4.4: Isometric view of linear engine without top casing

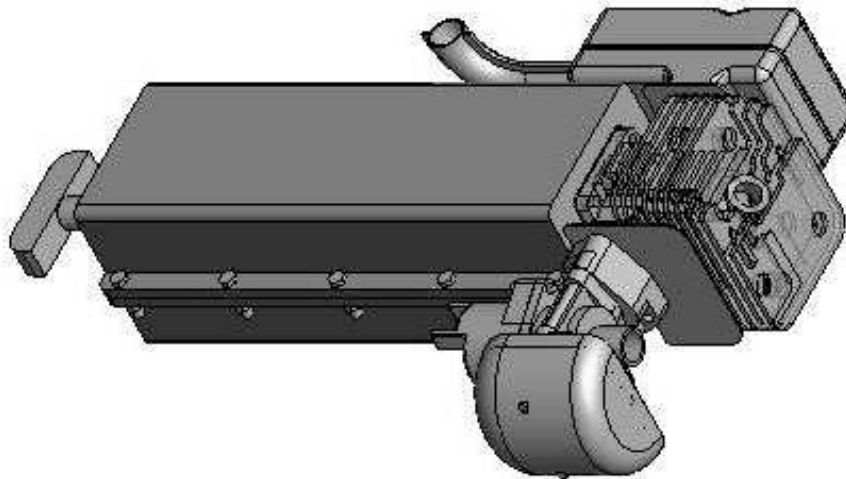


Figure 4.4.5: Isometric view of full assembly

4.4.3 Discussion

Physical design of linear-based engines and modification of conventional engines are easy tasks. Nevertheless, they require detailed analysis that must be adjusted from the original engine. The spring is used as a return cycle. Hence the spring design may affect the performance of the engine. The spring follows Hooke's law, in which the deflection depends on the thrust force of the piston. At the same time, the linear engine must be able to work under variable speeds and loading. Considering all these factors, a compromise must be achieved.

The weakness in the modification method is limited by the original engine configuration. The motion of oscillation, scavenging and characteristics of the original engine limit the modification. For example, the design geometry of the spring means that some engine speeds will not be supported, or the weak deflection meaning that the scavenging port will not open. As a result, misfire occurs. This can happen because the characteristics of the engine are not in line with the Hooke's law of the spring.

The result of the linear engine design is interesting to study, because the change in the predicted performance is not linear with the original performance. For example, the maximum power and torque are obtained at different speeds, which are a result of the design of the spring. Although the physical design of the linear engine has been realised, it has not yet been developed. Modification of the ignition system is needed here. Technically, the ignition system of a rotational engine can be adopted in a linear engine and controlled through a connecting rod.

4.4.4 Summary

Design of a linear engine with a spring as a return cycle has been carried out. Although the physical design has been realised there is still room for further analysis. Some parts need to be developed in more detail to ensure the design is satisfactory. The spring design influences the design of the linear engine characteristics. Before physically building the engine, it is necessary to study the influence of the spring design on the performance of the engine and dynamic motion.

4.5 ANALYSIS OF A LINEAR ENGINE DESIGN

This subchapter explains the analyses carried out for a linear engine design. The study should be conducted before the linear engine is developed. The analyses will focus on certain conditions, such as engine speeds of 1 m/sec, 4.1 m/sec and 4.6 m/sec. It has been predicted that the engine will not work properly and the scavenging port will not open fully since it is affected by an imperfect deflection of the spring.

The analyses of the problems have been discussed separately; starting with the effect of the spring system design on the performance of a linear engine, continuing with the piston dynamics and finally considering scavenging. In the analyses, the effect of the spring system design has been compared with the original conventional engine. The goal is to determine the performance of the designed product. Differences in achieved results are also included in the analysis of the design of the linear engine with a spring mechanism as a return cycle.

4.5.1 Effect of Spring System Design on the Engine's Performance

The effects of optimisation on the spring design of the linear engine with spring mechanism and its performance and combustion processes have been examined. However, under certain conditions the engine cannot properly work as predicted. This occurs because the displacement of the engine stroke depends on thrust forces from the combustion process in the cylinder of the engine. Moreover, the pressure ratio also decreases depending on the deflection of the spring force. This research is carried out to examine the performance of an engine under certain conditions in which the displacement of the spring does not work normally, at speeds such as 1 m/sec, 4.1 m/sec, and 4.6 m/sec. It is necessary to examine this performance because at those speeds the intake scavenging port does not open properly. A solution is presented here using a simulation technique. The combustion pressure and power output are compared with the predicted results. The results are given in terms of the indicated mean effective pressures (imep), which drops significantly, and impacted reduced of the power output. Normally the linear engine works at a speed of 1 m/sec.

4.5.1.1 Effect of Spring System on Linear Engine Performance Studies

The configuration of the linear engine design is shown in Figure 4.5.1. The linear engine design starts with a prediction of the engine's performance, optimising the spring geometry and finally designing the linear engine with a spring as a return cycle. The optimisation of the spring design is necessary because the linear engine should work on variable speeds and loads, as would occur in the original conventional engine. According to predicted results, there is a very large range of imep. The prediction starts with the smallest pressure and continues with the largest pressure, where the low pressure is at maximum speed while the minimum speeds and largest pressure achieve the maximum torque. As a result, the spring geometry becomes complex as it should be able to accommodate various speeds and loads.

Figure 4.5.1(A) shows the piston position at the Top Dead Centre (TDC). In this position, the spring force is the smallest. After combustion occurs, the pressure increases rapidly and then expands into the volume of the cylinder, compresses the spring and deflects to the Bottom Dead Centre (BDC). According to the original conventional engine, the oscillation of the piston is 30.5 mm. At that operation, scavenging is working properly. However, the Hooke's law of the spring affects the displacement of the piston. If the imep is too low then the deflection of the spring should be small, and if the imep is too high then the deflection should be large. For that reason, a stopper is needed when the deflection is higher than 30.5 mm. Figure 4.5.1 (B) illustrates a stopper design for a spring system in a single cylinder SI linear engine.

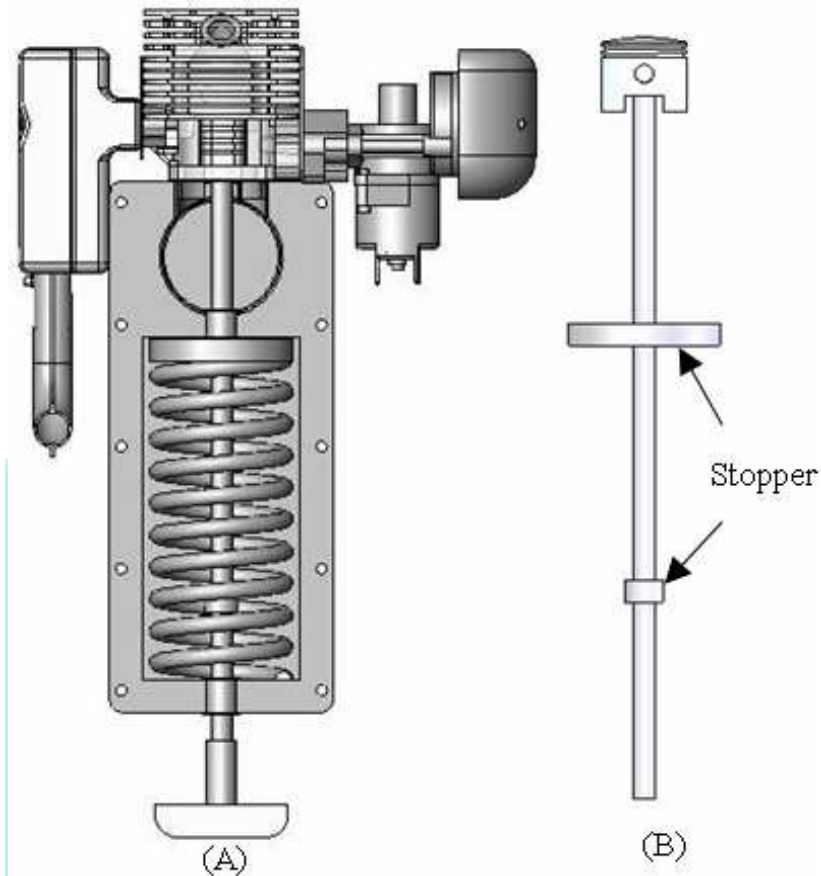


Figure 4.5.1: Design of linear engine with spring mechanism

To study the single cylinder SI linear engine's performance, a simulation has been used. GT-Power has been used to simulate the performance of the linear engine based design. The simulation technique is similar to that used in the prediction of the linear engine's performance in Chapter 4.2, in the midst of a small modification. Figure 4.5.2 presents a flowchart of the model design analysis. A real engine specification has been used in this study. The main specifications of the engine are shown in Table 4.1.1, and the geometry of spring design optimisation results are shown in Table 4.5.1.

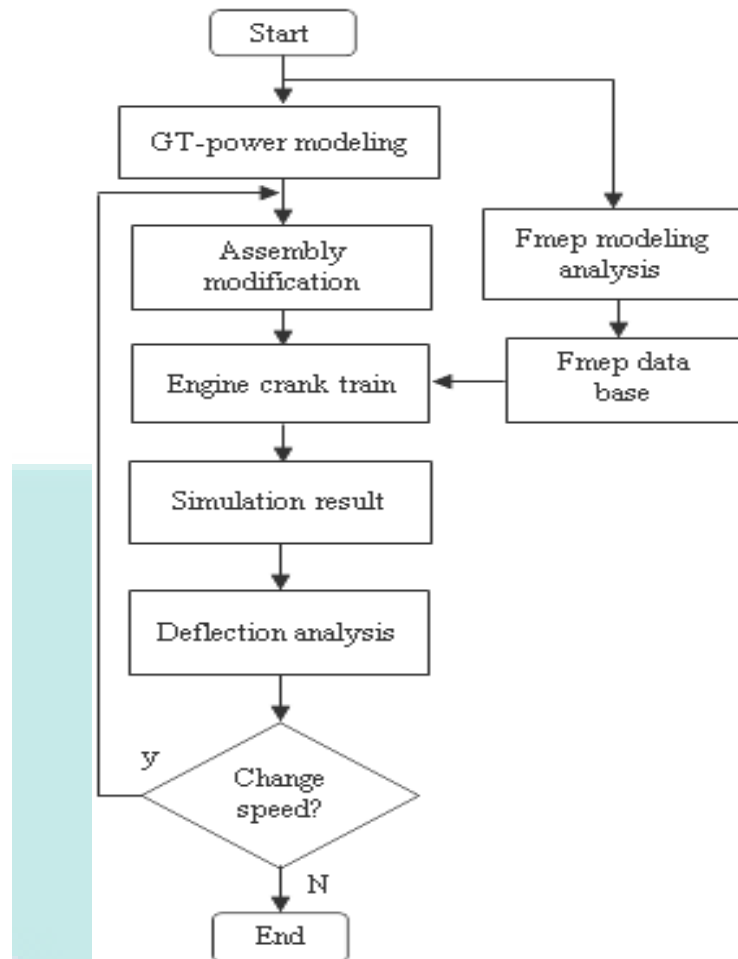


Figure 4.5.2: Flowchart of the model design analysis

Table 4.5.1: Geometry of spring design

Spring material :	Chrome-vanadium alloy steel wire SAE 6150	
Direction of coil winding:	Right	
Surface treatment:	Shot-peened springs	
Wire diameter (mm)	D	7.00
Number of active coils	N	10.00
Outer spring diameter (mm)	D_e	57.70
Inner spring diameter (mm)	D_i	43.70
Free spring length (mm)	L_f	200.00
Preloaded spring length (mm)	L_i	147.32
Fully loaded spring length (mm)	L_o	116.70
Theoretical spring limit length (mm)	L_t	84.00

Modifications to the GT-Power simulation model are made for cylinder geometry, scavenging port, intake port and exhaust port. The assembly should be modified for each change in spring deflection. As a result "*cylinder geometry*" is changed with respect to stroke and compression ratio, and "*angle at start of port overlap*" and "*angle at last port closed*" were also modified depending on the spring deflection. This is because the deflection of the spring is not normal. The scavenging ratio is modified and should be justified with spring deflection. The crank angle array and area array at the intake port and exhaust port are modified and should match the deflection angle of the spring system.

4.5.1.2 Effect of Spring System on Linear Engine Performance

The research is to study the effect of the designed spring on the linear engine performance and combustion process. The results of the comparison study are shown in Table 4.5.2. The different trends of the combustion process are shown in Figures 4.5.3 to 4.5.5. Figure 4.5.3 presents a PV diagram for both the predicted and designed combustion processes at 1 m/sec speed. However, Figures 4.5.4 and 4.5.5 show different trends in the pressure at speeds of 4.1 m/sec and 4.6 m/sec, respectively.

The intake scavenging port only opens 56.4% at 1 m/sec speed, 66.6% at 4.1 m/sec and 31.1% at 4.6 m/sec. The other speeds do not need to be observed as they worked properly.

Table 4.5.2: Effect of spring design on performance engine

	1 m/sec		4.1 m/sec		4.6 m/sec	
	Predicted	Designed	Predicted	Designed	Predicted	Designed
Brake Power [kW]	0.24	0.23	1.03	0.51	1.60	0.13
Brake Torque [N-m]	2.20	1.90	2.40	1.10	2.20	0.30
imep [bar]	5.54	5.30	5.66	3.18	5.24	0.73
Air Flow Rate [kg/hr]	2.00	1.40	4.30	2.30	4.40	0.70
BSAC [g/kW-h]	8565.00	7365.00	4243.00	4960.00	4251.00	4785.00
BSFC [g/kW-h]	690.60	595.90	347.10	412.40	351.00	301.40
Volumetric Efficiency [%]	92.50	75.70	50.00	28.80	45.70	8.40
Trapping Ratio	0.798	0.954	1.00	1.00	1.00	1.00
A/F Ratio	12.40	12.36	12.23	12.03	12.11	15.88
Brake Efficiency [%]	11.90	13.80	23.80	20.00	23.50	27.40

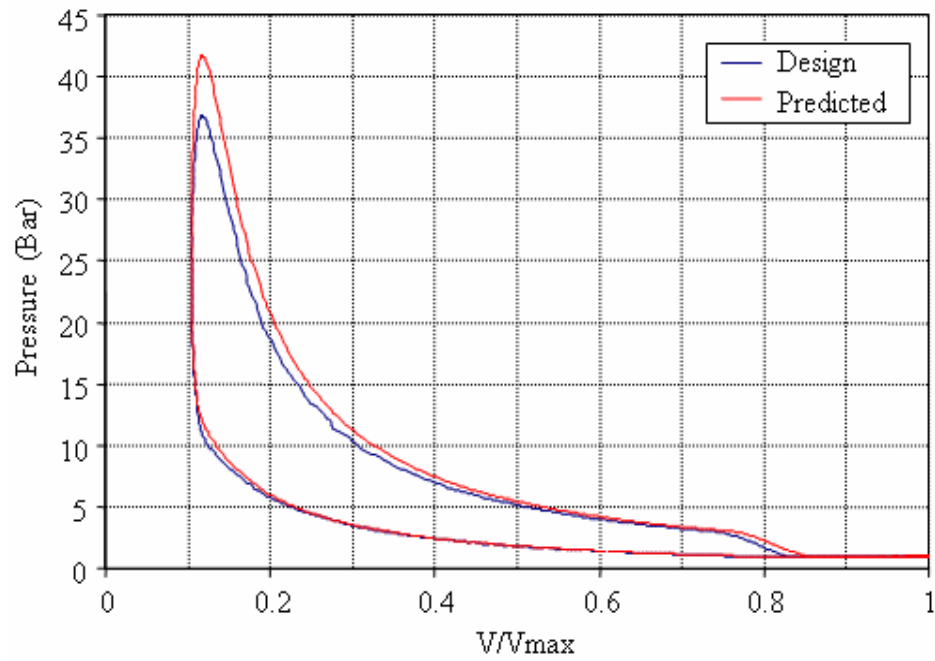


Figure 4.5.3: Effect of spring design on PV diagram at 1 m/sec

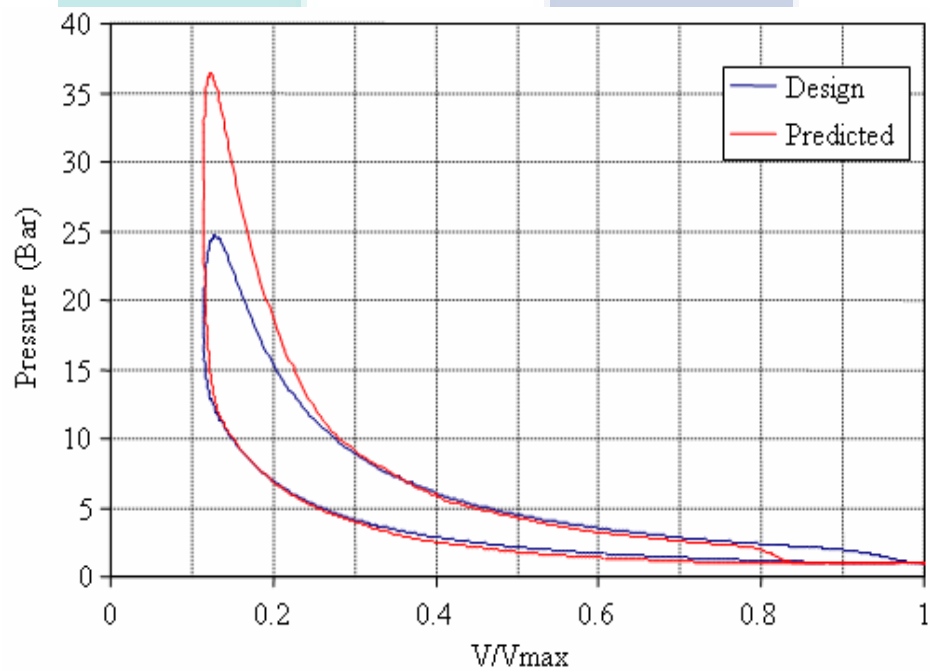


Figure 4.5.4: Effect of spring design on PV diagram at 4.1 m/sec

Table 4.5.2 showed that the difference in power output between the predicted and designed results at 1 m/sec decreased slightly from 0.24 to 0.23 kW. However, at a

speed of 4.1 m/sec, the difference is doubled and decreases dramatically at 4.6 m/sec. A similar trend was found for the brake torque, imep, air flow rate and volumetric efficiency. The performance in brake specific fuel consumption and brake efficiency were inconsistent. The design result of the brake efficiency at 1 m/sec and 4.6 m/sec was higher than the predicted values. The opposite result was found at a speed of 4.1 m/sec. The predicted value at this speed is higher than the design value. BSFC also presents the same trend with respect to brake efficiency.

Figure 4.5.3 shows a different trend in the PV diagram at a speed of 1 m/sec. The maximum pressure drops slightly, and so does the imep value. The prediction of imep at 1 m/sec is 5.54 bar. Compared to the design value the imep decreases to 5.2 bars. The imep decreases by about 6.1% at a speed of 1 m/sec.

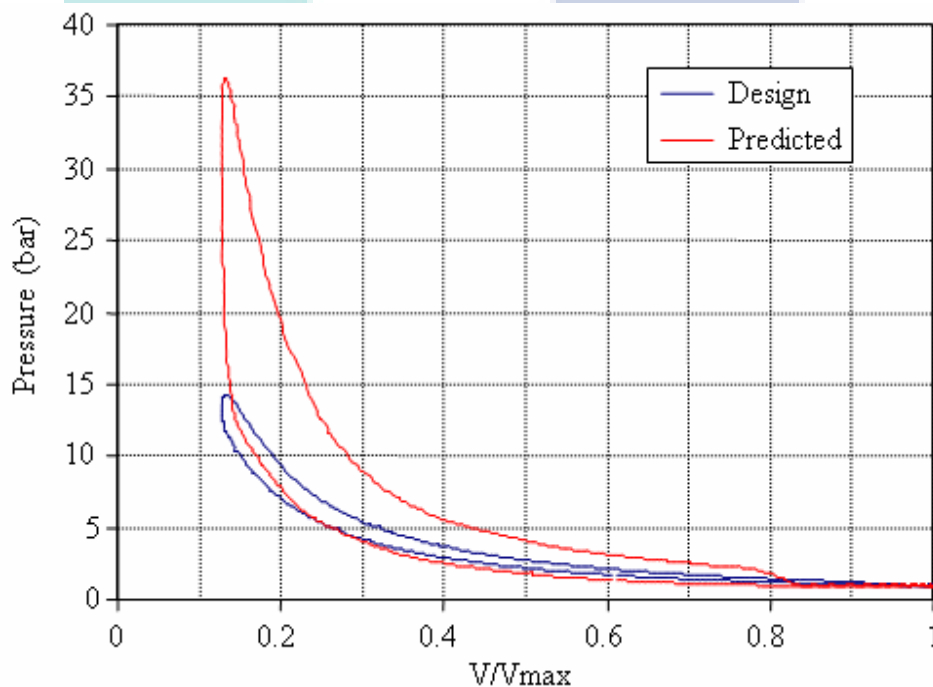


Figure 4.5.5: Effect of the spring design on PV diagram at 4.6 m/sec

Figure 4.5.4 presents the PV diagram at a speed of 4.1 m/sec. The maximum pressure decreases from 36.34 bars to 24.57 bars. The imep also decreases from 5.66 bars to 3.18 bars. More sophisticated degradable characteristic is at an engine speed of 4.6 m/sec. The maximum pressure decreases from 36.34 bars to 14.19 bars, and imep decreases from 5.24 bars to 0.73 bars. This is because of insufficient air-fuel mixture in

the combustion chamber. Figure 4.5.5 shows the PV diagrams of the predicted and the designed springs at a speed of 4.6 m/sec.

Table 4.5.3: Effect of decreasing imep on spring deflection

No	Piston Speed [m/sec]	Deflection (mm)	
		Predict	Design
1	0.50	16.57	0.00
2	1.00	26.95	25.36
3	1.50	33.79	33.79
4	2.00	36.87	36.87
5	2.50	38.63	38.63
6	3.10	36.09	36.09
7	3.60	31.02	31.02
8	4.10	27.66	18.75
9	4.60	25.18	4.30
10	5.10	22.24	0.00
11	5.60	19.11	0.00
12	6.10	15.98	0.00

4.5.1.3 Discussion

In order to run a large range of speeds in a linear engine, it is necessary to optimise the spring design. Hooke's law must be taken into consideration. The engine performance and the combustion process of a linear engine are very sensitive to the spring characteristics. Interaction between thrust forces, which are produced from the combustion process the with spring, could change the engine's dynamic performance. The interaction between the spring and combustion has an impact on the basic performance of the linear engine.

The design performance is lower than the predicted performance because of matching problems between the best engine performances with spring characteristics. The decrease in engine performance is caused by factors including an imperfect scavenging process and decrease in pressure ratio. Unstable oscillations in piston movement cause the intake scavenging port not to open properly. This disturbs the supply of mixture to the combustion chamber. Moreover, decreasing oscillation of the piston also creates a reduction in the compression ratio, as the penalty is a lower

efficiency. The indicated mean effective pressure also decreases (Heywood, 1988). Table 4.5.2 shows the difference between the predicted and designed performance. The compression ratio is also affected by compression energy (Mikalsen & Roskilly, 2008). The oscillation energy is produced by the thrust force of the combustion product. If the deflection is small, the pressure ratio will decrease and will linearly reduce the thrust force.

The air flow rate is very important for the combustion process. Insufficient air supply could cause imperfect combustion and result in a smaller imep. In Table 4.5.2, it can be seen that the predicted air flow rate increases with rising engine speeds. On the other hand, air flow rate decreases at design conditions. This phenomenon is due to an improper scavenging process, resulting in a smaller of imep performance. Figures 4.5.3, 4.5.4 and 4.5.5 clearly show that the predicted PV diagrams are higher than designed ones. According to the mass fraction definition, burn duration should increase with an increase in engine speed (Heywood, 1988). Similar results were obtained by researchers such as Atkinson et al (1999), who worked at constant load, resulting in an increase in peak pressure. The theory is more clearly explained by Ferguson and Kirkpatrick (2001).

In two-stroke engines, performance and combustion stability strongly depend on the scavenging process, in which burned gases are flushed out from the cylinder and replaced by the intake mixture (Kleemann, Dabadie & Henriot, 2004). A lack of intake scavenging port is a high contributor to reduced performance and combustion processes. The smaller the space provided for the intake scavenging port, the greater the degradation of the performance and the combustion process. Figures 4.5.3 to 4.5.5 clearly show that the combustion process is affected by improper intake scavenging. Table 4.5.3 also shows clear results of engine performance. The correlation between air flow rate with imep, torque and power output is very strong.

Improper scavenging processes at speeds of 1 m/sec, 4.1 m/sec and 4.6 m/sec affect the imep characteristics. A smaller imep results in smaller thrust forces at the piston spring system. Therefore, the spring deflection decreases; if the spring oscillation is less than 25 mm then the intake scavenging port does not open and it results in a misfire in the combustion chamber. According to Table 4.5.3, although the deflection at 1 m/sec decreases, it can still open the intake scavenging port. However, this does not provide enough deflection for speeds of 4.1 m/sec and 4.6 m/sec, therefore

resulting in misfires. Finally, only 50% of the range of speeds works properly. According to the predicted performance, the best power output is 1.06 kW at a speed of 4.6 m/sec (Fathallah & Bakar, 2009). The real design result is 1.03 kW at 3.6 m/sec. Although the optimum design result is only 1.03 kW, it is better than the performance of a conventional engine. The best performance of a conventional engine is was 0.93 kW at 4.6 m/sec.

4.5.2 Effect of Spring System Design on Piston Dynamics

A spring system as a return cycle has been developed for a linear engine since it is a simple technique to be applied. Although the system is simple, some aspects related to the system need to be analysed. Currently, the motion of a linear engine with single cylinder spark ignition and a spring mechanism have been examined. The linear engine has been modified from a conventional engine. For that reason, the motion analyses are compared between linear and conventional engines. The effects of the spring design on the motion of a linear engine are also included in this study.

The optimisation of the spring design has a very strong effect on the motion of the linear engine. The geometry of the spring could affect the combustion continuity of the engine. Deflection of the spring is influenced by the thrust force of the combustion of an engine. According to Hooke's law, if the force is strong then the spring will be further deflected. A small deflection will occur if the force is weak. Hence it is very important to study the effect of the spring design on the motion of the linear engine.

Although it is believed that a linear engine has lower friction compared to a conventional engine, it is, however, difficult to ignore it until zero point. The effect of the spring on the piston motion has also been studied in this research. According to the design of a linear engine with a spring mechanism, the friction sources are caused by piston rings and journal bearings. The friction between the piston rings and cylinder liner is very important and cannot be ignored. The friction in bearings also has a contribution in this linear engine.

There are three main aims of the research. First, is to compare the motion between conventional and linear engines in basic motions such as displacement, velocity and acceleration. Secondly, is to study the effect of a spring design on engine motion. The final aim is to study the effect of friction on engine motion. The second and

the third aims are very important, because they could influence the design of the linear engine.

4.5.2.1 Numerical Simulation of a Linear Engine

The spring system is rarely used to generate a linear engine system. However, in this case the compression spring has been used to absorb expansions cycle energy and a part of energy to return the compressions process. Figure 4.5.6 shows the spring system configuration used to create a single cylinder linear engine.

The numerical model is developed for a spark ignited linear engine, but can be easily adapted for the case of a compression ignition linear engine. The numerical analysis also allows a parametric study of the operation of this type of engine. The engine modelling has been validated using results from the existing works on linear engines. The numerical model represents an idealised case based on the assumptions made, while allowing a parametric study to be performed.

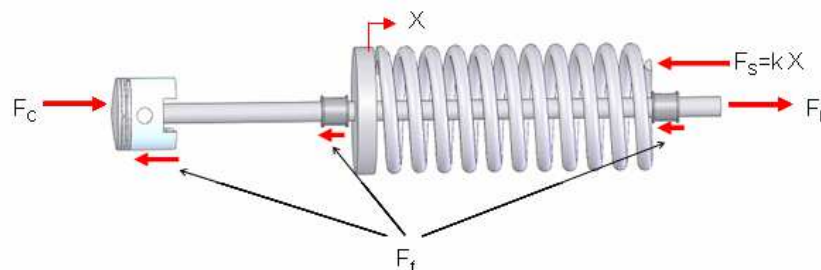


Figure 4.5.6: Spring system design for a linear engine

Basic theories of dynamic models have been explained in the paper review in Chapter 2. The numerical model used in this section is the same model as for Equations 2.25, 2.26 and 2.27. The numerical model has been developed from Newton's second law, which is formulated from the spring system of the linear engine as shown in Figure 4.5.6.

The friction forces in the engine are a consequence of hydrodynamic stresses in oil films and metal to metal contact. Since friction losses are a significant fraction of the power produced in an internal combustion engine, the minimisation of the friction has been a major consideration in engine design and operation. The frictional processes in

internal combustion engines can be categorised into three main components, the mechanical friction, the pump work and the accessory work (Ferguson & Kirkpatrick, 2001). The mechanical friction includes the friction of internal moving parts such as the crank shaft, piston, rings and valve train. The pumping work is the net work that is done during the intake and exhaust strokes. The accessory work is the work required for the operation of accessories such as the oil pump, fuel pump, alternator and fan. In this case, a simple two-stroke engine does not have a pump or accessory work. For that reason, the effect of both frictions can be ignored (Fathallah & Bakar, 2009).

The dependence of the mechanical friction mean effective pressure on the friction force, F_f , and other engine parameters depends on the friction regime and the lubrication surface geometry, such as sliding or rotating surfaces. The friction force, F_f , is the product of the friction coefficient f and the normal force F_n , and the friction power P_f is the product of friction force F_f and a characteristic velocity U :

$$F_f = fF_n \quad (4.5.1)$$

$$P_f = F_f U \quad (4.5.2)$$

Therefore, the mechanical friction mean effective pressure scale is

$$mf_{mep} \approx \frac{P_f}{NV_d} \approx \frac{F_f U}{NV_d} \approx \frac{F_f U}{n_c N b^2 S} \quad (4.5.3)$$

where N is the engine speed, V_d is the displacement volume, b is the cylinder bore, S is the piston stroke, and n_c is the number of cylinders.

The preceding component analysis can be combined to form an overall engine f_{mep} model. It should be noted that the component equations are likely to depend on the type of engine for which the friction regime is available. Usually f_{mep} for a simple two-stroke conventional engine, such as the friction from a crankshaft mechanism and piston components, includes the main bearings, seals, connecting rod bearings, skirts, rings and gas pressure. However, for two-stroke linear engines, it is only the left piston rings, gas pressure and journal bearing. The detail of the components for both conventional and

linear engines models have been explained by Fathallah and Bakar, (2009). Their engine models have also been adopted in this research. However, the seal formula has been ignored since the design of the linear engine does not use oil seals.

4.5.2.2 Engine Model and Dynamic Simulation Methods

The model has been developed from a conventional engine. One of the objectives of the research is to investigate the difference between linear engines and rotating engines. The original engine needs to be redesigned. Figure 4.5.7 shows the result of the redesign of the original machine in 3-D. All components are drawn one by one and then assembled into one unit using SolidWorks. The original engine in Figure 4.5.7, as shown in Figure 4.1.1 in subchapter 4.1, was drawn in the opposite direction. Figure 4.5.8 shows the result of the modification of the linear engine which will be used to analyse the dynamics of the piston.

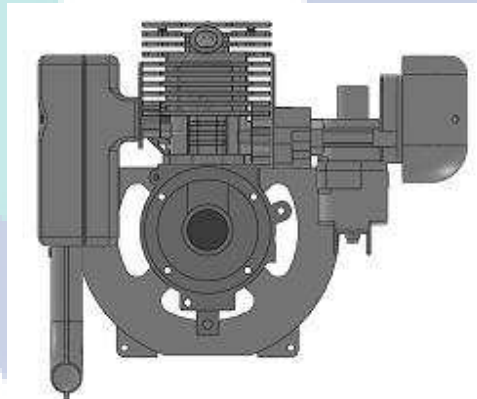


Figure 4.5.7: Redesign of a conventional engine type BG-328.

Two models are used for the dynamic analyses. Both models differ in the return cycle only, and the combustion systems and accessories used are the same. Since all systems are in the same condition, except for the return cycle system, then the validity of the comparison of both engines can be assumed.

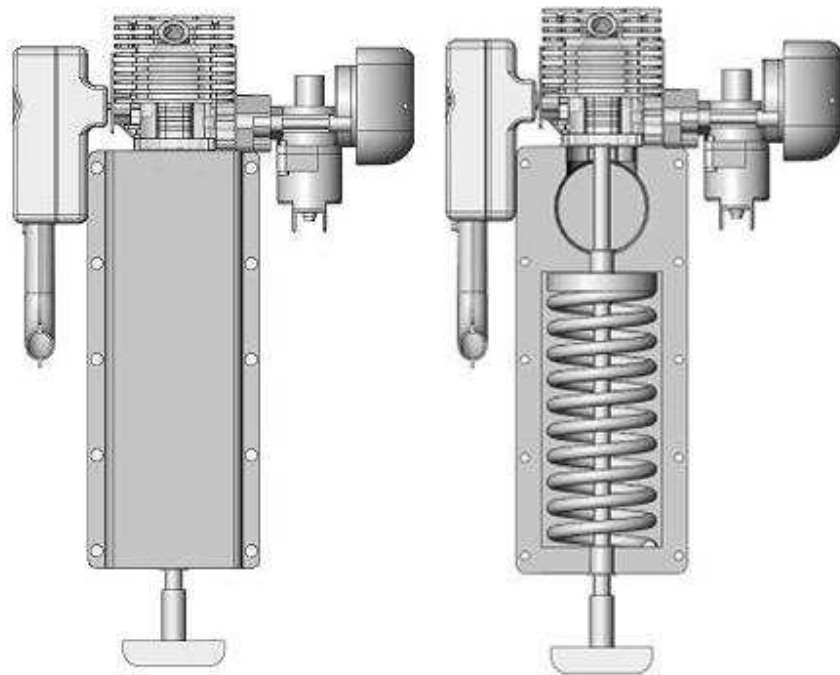


Figure 4.5.8: Design of linear engine with spring mechanism with/ without top casing.

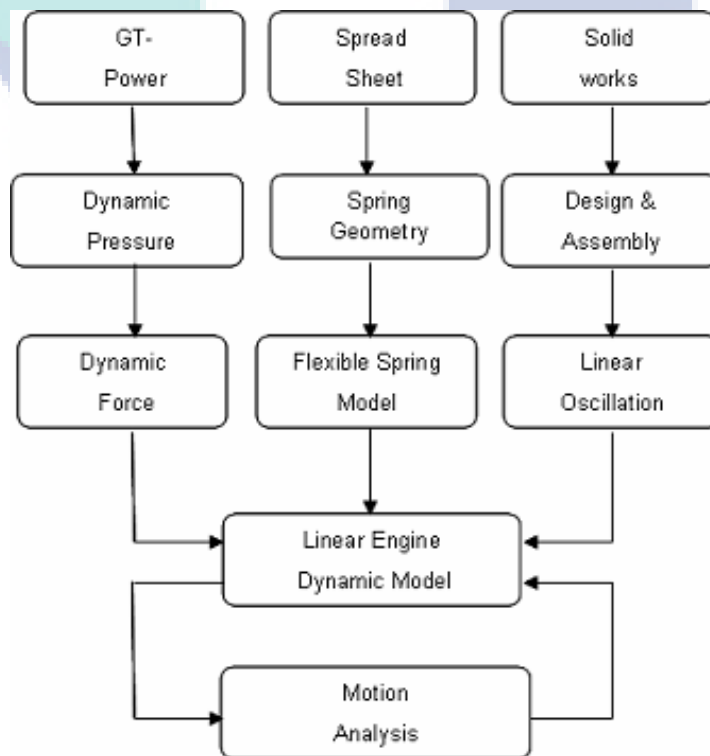


Figure 4.5.9: Flowchart of motion analysis technique.

Figure 4.5.9 presents a flow diagram of the dynamic analysis techniques which are used in this study. GT-Power, a spreadsheet, SolidWorks and Cosmos are used to support the dynamic model analysis. GT-Power is used to gradually supply the pressure that is generated from the combustion process to provide input on the system's dynamic force of the spring. The spreadsheet is used to design the spring in accordance with the engine. The spring of the model must be exchanged with a flexible spring that is available from the Cosmos software database.

To simulate the friction of the piston with the cylinder liner, or between the journal-bearings with a rod, contacting surfaces are needed. Then it should define based of material, friction, or elastic properties. For the study of the dynamic friction of a piston, this simulation has been chosen to specify the material, namely friction between aluminium and steel which is greasy. The oscillation motion is simulated by choosing a linear motor whose oscillating pattern has been selected according to displacement and frequency and can be adjusted to suit the desired simulation. Once the linear engine dynamics model can function properly, then an analysis of the motion can be conducted.

The modelling of the rotational engine is quite simple. Pressure data generated from the combustion processes are the same as the data used for the linear engines. It requires changing the linear motion to rotation by removing the linear motor and replacing it with a rotary motor. The dynamic model in this rotation is only used to study the basic movements, so the friction element of the piston is not studied in this research.

There are three objectives in this research, which are the basic considerations, the effect of friction and the effect of the spring design. The basic consideration is only needed due to the limitations of Cosmos motion at 1000 frames per second, as it is not good enough to simulate high-speed engines. A basic consideration is to understand the basic movements of the piston, especially to study the effect of friction on the piston's dynamics. Secondly, the dynamics of the piston at high-speed are studied. The effect of friction is also studied. Engines that run at 60 rpm or 1 Hz is need learning purposes in the case of the basic consideration.

4.5.2.3. Effect of Spring System on Piston Dynamics

4.5.2.3.1 Basic Considerations

In basic considerations, different characteristics of conventional and linear engine motion, such as piston displacement, velocity and acceleration, are considered. The motion study runs in multi-cycles mode. The differences between both engines are shown in a single cycle. The speed of the engines have been set to slow speed.

Figure 4.5.10 shows the trend of displacement of conventional engines and linear engines. The oscillation journey and elapse time are the same; however, a linear engine is slimmer than the conventional engine. Both engines have been running under the same conditions although they have different characteristics.

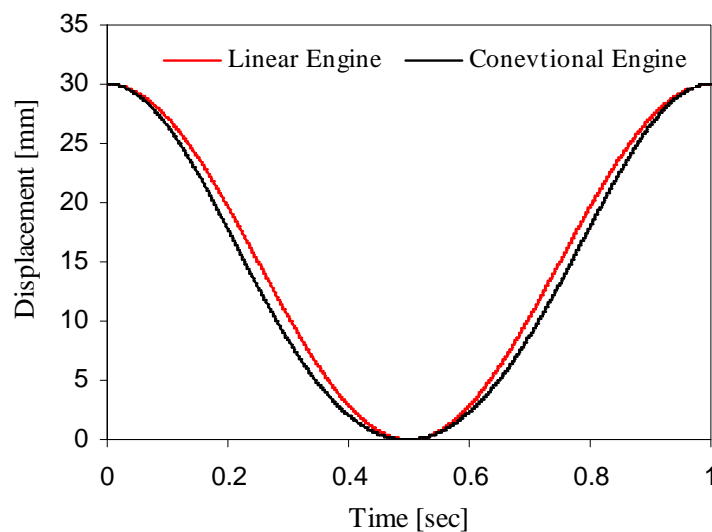


Figure 4.5.10: Displacement of linear and conventional engines

Figure 4.5.11 presents the comparison between the trends of speed. Both engines have been simulated at 5 cycles with 1000 frames per cycle. However, on all cycles, each engine has a similar trend, although both engines have different characteristics. The conventional engine has faster and higher oscillations. On the other hand, is the oscillations are lower and wider than a linear engine. Somehow, both engines have the same elapsed time for every cycle.

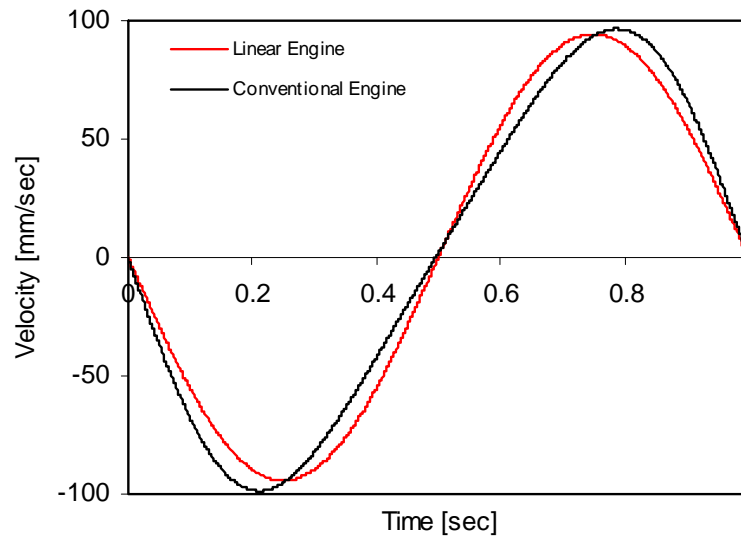


Figure 4.5.11: Velocity of linear and conventional engines

Figure 4.5.12 shows the acceleration of both linear and conventional engines. The difference in characteristics between both engines is very clear. The acceleration of a conventional engine is ‘fatter’ than the linear one. The time period at the TDC is longer, and then bends dramatically to the BDC. On the other hand, the BDC is slim. The characteristics of linear engines are different compared to conventional engines. The oscillation acceleration is consistent at the TDC and BDC. Whilst it might not be clear in one cycle, but in multi-cycles this is very clear as shown in Figure D.1.2 in Appendix D.

4.5.2.3.2 Effect of Friction on Piston Dynamics

Friction has been studied and does not seem to affect trends in displacement and velocity. Friction strongly influences the acceleration, as shown in Figure 4.5.13. The effect is very strong at the TDC and BDC. The fluctuation, frame by frame, in the frictions is high at the TDC and BDC. If compared to non-friction, it is very clear that the difference is a small part of the total. This figure has been observed at low speed and the recording is at 1000 frames per second. Because the recordings of data are good, then the result is very smooth and the trend graphs as well. Fluctuations of the frictions between piston and cylinder liner are also good choice of study to analyse.

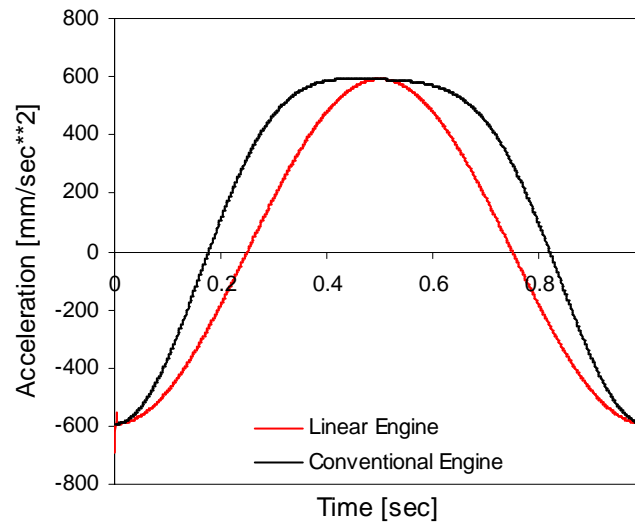


Figure 4.5.12: Acceleration of linear and conventional

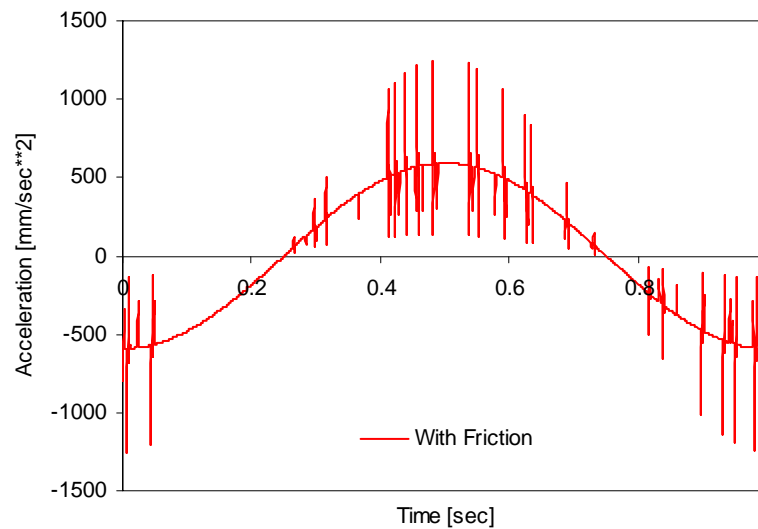


Figure 4.5.13: Acceleration of linear engines with friction trend.

Figure 4.5.14 presents a comparison of the acceleration trend between non-friction and friction, the bold black line is non-friction while the red line shows the friction trend. The differences between both trends are at fluctuation zones caused by friction forces. However, close to the TDC, large fluctuations are observed, and the BDC also has the same trend. Figure 4.5.15 illustrates the angular momentum both with

and without friction on the z-axis. There is no angular momentum when the friction force is not enforced. The amount of angular momentum is always shown on the z-ordinate as long 5 times oscillations. A large angular momentum occurs when friction is applied. The angular momentum is fluctuating, and the trend below the z-ordinate is possibly influenced by the force of gravity.

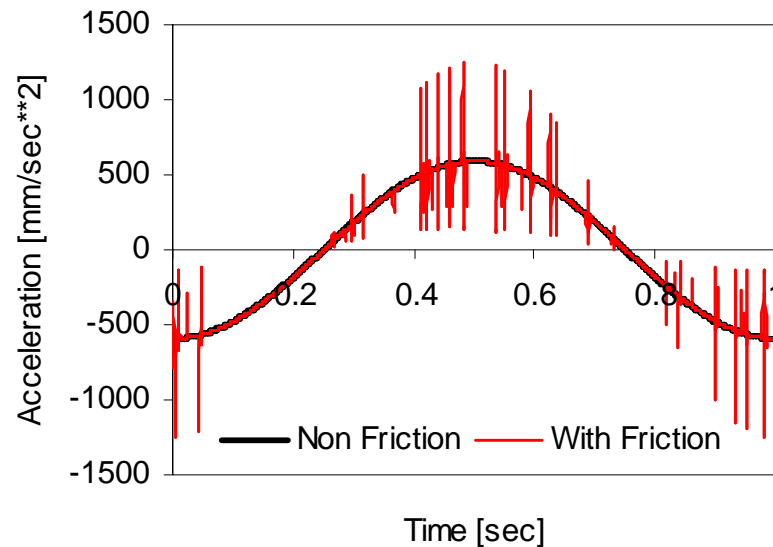


Figure 4.5.14: Acceleration trend with and without friction

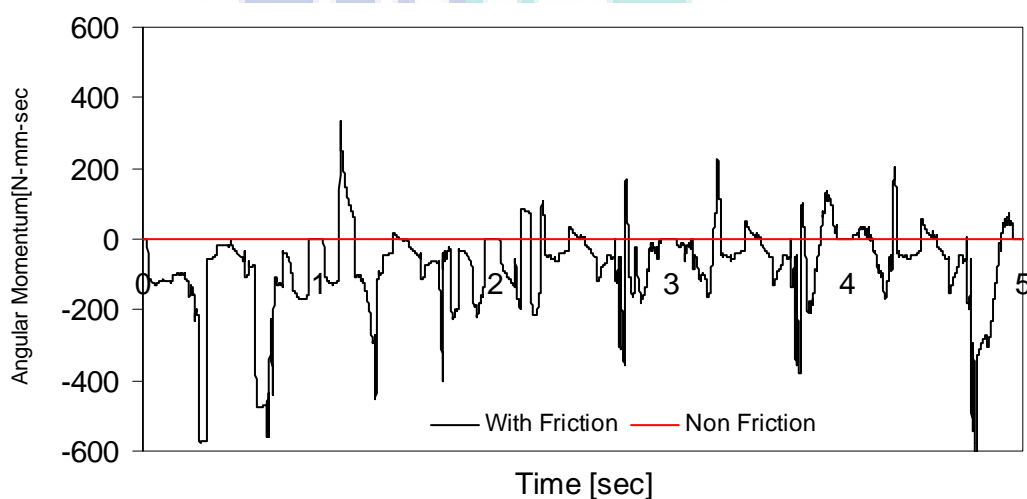


Figure 4.5.15: Angular momentum with and without friction at the z-ordinate

Figure 4.5.16 shows an image of real motions studies frames. In this work, the movements of the piston, cylinder head and other components at the top have been hidden. The images show the start of the first oscillation and every 1000 frames are selected and collected until the finish. The images also introduce rotary motion of the piston. The piston is rotated by about 90 degrees, which can be seen from the piston pin-hole which starts at the front in frame number 1 (F 1) and then moves every 1000 frames until finally it is displaced by about 90 degrees in frame number 5000 (F 5000).

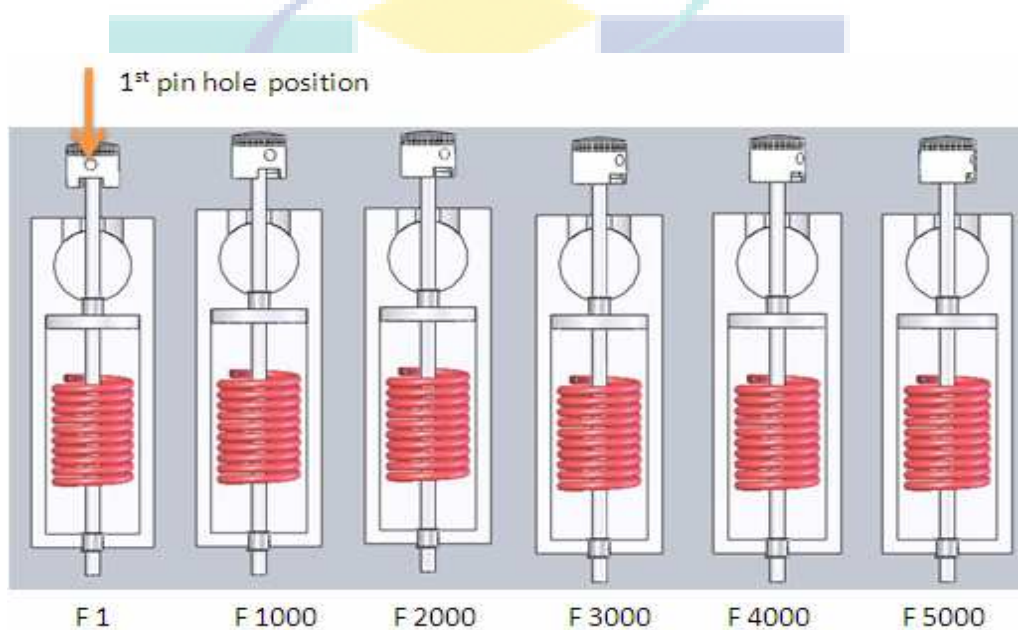


Figure 4.5.16: Image of linear engine at specific frames

4.5.2.3.3 Effect of Spring Design on Piston Dynamics

Accordingly, the geometry of the spring design has been optimised using multilevel optimisation techniques. In fact, the performances of the gas dynamic do not always present the same trends, which can influence the spring system of linear engines. For that reason, the displacement, velocity and acceleration also need to be studied.

Figure 4.5.17 shows a predicted and designed displacement of a linear engine at a frequency 16.67 Hz. The equality of frequency is shown at 1000 rpm, or 1 m/sec in this engine. However, the oscillation of the predicted trend is about 29.99 mm at the TDC and only 26.95 mm for the design oscillation.

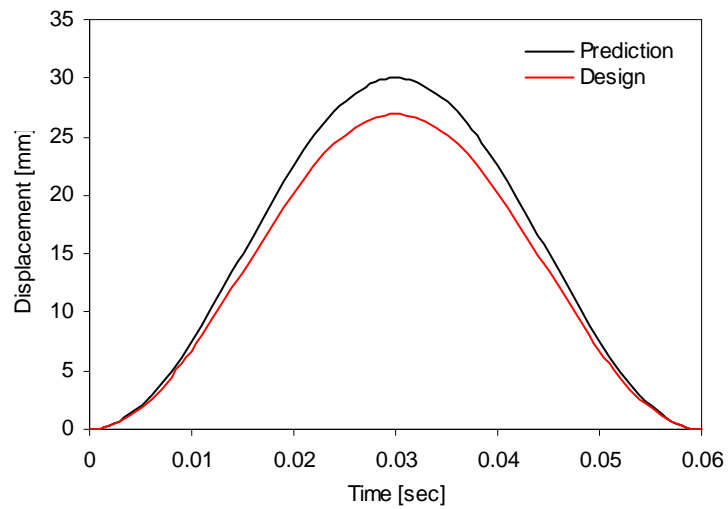


Figure 4.5.17: Displacement trend of predicted and designed linear engines at 16.67 Hz

Figure 4.5.18 shows the displacements of the predicted and designed linear engine at a frequency of 66.67 Hz. The trend is similar to that of the frequency of 16.67 Hz and is only different in terms of the values. The displacement of the predicted value is 29.7 mm and 27.4 mm for the designed value. The design displacement result is smaller than the prediction. This occurs because the combustion pressure is not high enough to compress the spring until maximum elevations at speeds of both 16.67 Hz and 66.67 Hz.

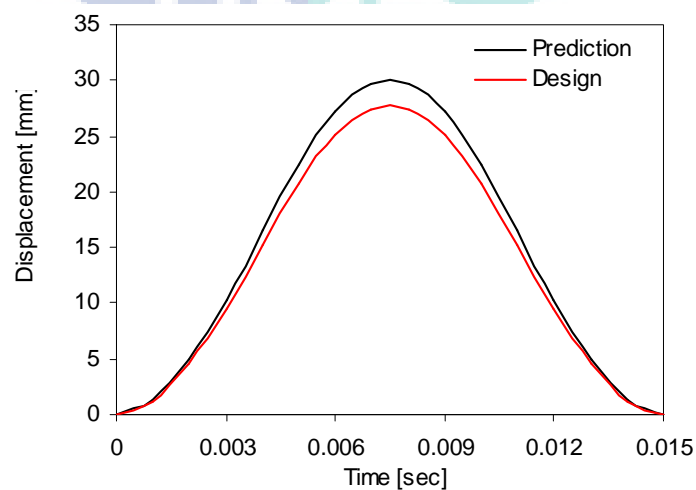


Figure 4.5.18: Displacement trend of predicted and designed linear engines at 66.67 Hz

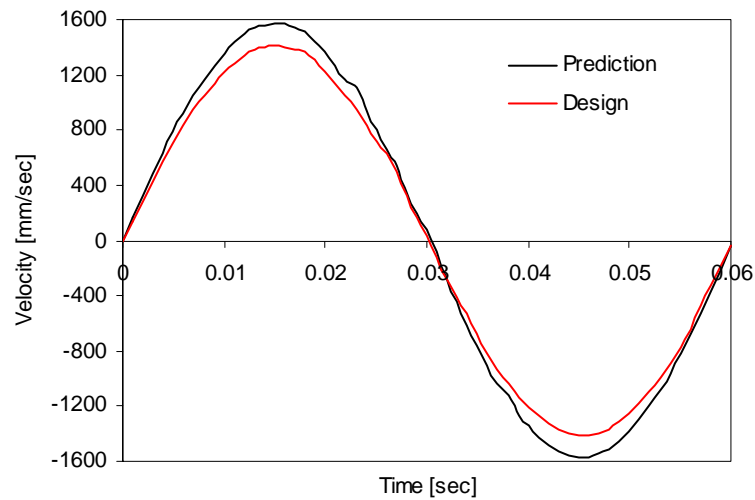


Figure 4.5.19: Velocity of predicted and designed linear engines at a frequency of 16.67 Hz

Figures 4.5.19 and 4.5.20 show the velocity of the predicted and designed engine results at frequencies of 16.67 and 66.67 Hz respectively. Both figures have the same trend, the designed trend is smaller than predicted. Unlike the acceleration figure, the velocity trend was not influenced by friction. The predicted maximum velocity at a frequency of 16.67 Hz is 1536.24 mm/sec, and is 1404.22 mm/sec for the designed result.

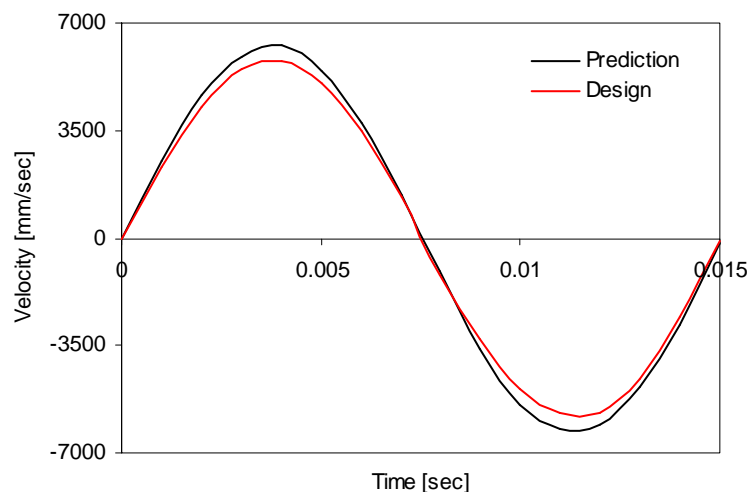


Figure 4.5.20: Velocity of predicted and designed linear engines at a frequency of 66.67 Hz

The difference in maximum piston velocity for these two types of engine is 132.02 mm/sec. The velocity at the middle, TDC and BDC are zero. Negative velocity is mean on the bottom quadrant. Negative and positive values are dependent on the placement of the coordinates. However, the velocity is the same value with at the top site. The maximum velocities at a frequency of 66.67 Hz, for both the predicted and designed engines, are 6263.05 mm/sec and 5765.6 mm/sec, respectively. The difference in the maximum velocity of the predicted and designed engines is about 497.45 mm/sec. By increasing the frequency of linear engines, the velocity of the piston also increases. The difference in the maximum velocity of both engines also increases.

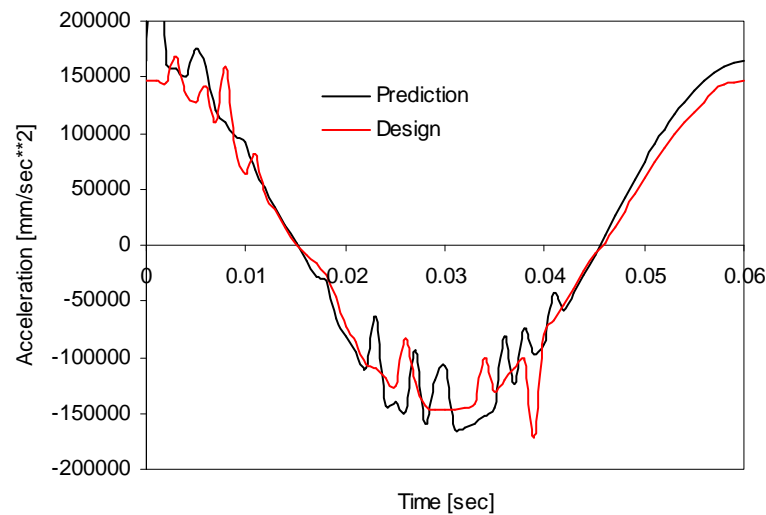


Figure 4.5.21: Acceleration trend of predicted and designed linear engines at a frequency of 16.67 Hz.

Different piston acceleration trends between the predicted and designed models are difficult to study. Figure 4.5.21 shows the acceleration of engines at a frequency of 16.67 Hz. It can be seen that the acceleration trend at the BDC and TDC fluctuates and is unsystematic. Figure 4.5.22 presents the acceleration trend at a frequency of 66.67 Hz. Although the figure shows unsystematic fluctuation, it can be seen that the acceleration of the predicted engines is higher than in the designed engines, especially at the BDC. Compared to the acceleration produced at 16.67 Hz, the trend in the acceleration at a frequency of 66.67 Hz shows the characteristics more clearly.

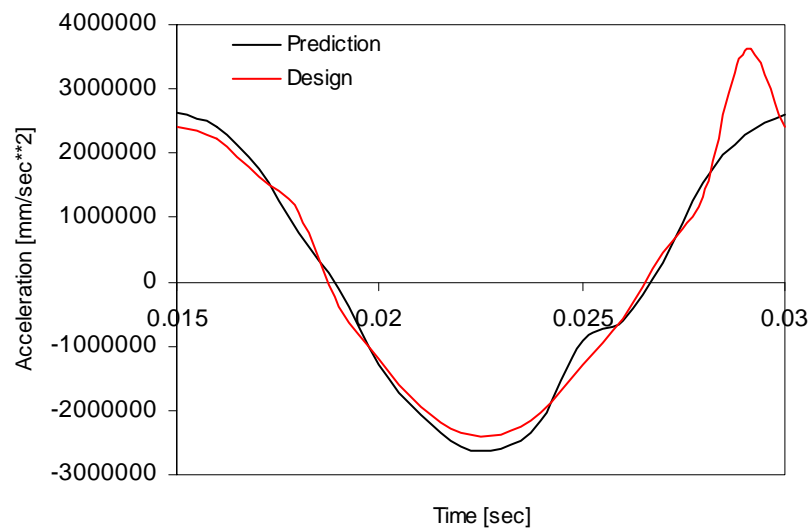


Figure 4.5.22: Acceleration trend of predicted and designed linear engines at a frequency of 66.67 Hz

4.5.2.4 Discussion

Based on basic consideration studies, the differences between conventional and linear engine characteristics are very clear in all motions such as displacement, velocity and acceleration. Most of researchers present similar results in that conventional and linear engines have different characteristics (Mikalsen & Roskilly, 2008A; Fredriksson & Denbratt, 2004; Qingfeng, Xiao & Huang, 2008). However the displacement trend is similar in both engines. The results of this work are closer to the results obtained by Fredriksson and Denbratt (2004) and Qingfeng, Xiao and Huang (2008). Although both engines show similar trends in piston velocity, the characteristics of the top piston velocity of linear engines are not dramatically different to the characteristics of the conventional engine. It might be that, in this comparison, both conventional and linear engines have the same characteristics for a single cylinder. Other researchers, however, have studied dual piston engines. In the case of conventional engines, it was found that the piston velocity trend has the same trend and the same characteristics as this research.

The piston acceleration of both engines also have similar trends, but some researchers have found that both engines have different characteristics (Fredriksson & Denbratt, 2004; Qingfeng, Xiao & Huang, 2008; Mikalsen & Roskilly, 2008B). The

high acceleration at the TDC and BDC is similar in both conventional and linear engines. However, for linear engines the piston acceleration at the TDC is slimmer but a little bit fatter at the BDC compared to that in conventional engines. It may be that conventional engines are influenced by the combustion process, spark timing (starting at 20° BTDC) and the burning of fuels on elapse time with turbulence flame propagation. On the other hand, the return cycle of linear engines is compressed by springs which have a strong stiffness (depending on the design of the spring geometry); as a result, there is consistent piston acceleration at the TDC and BDC.

Friction very strongly affects the characteristics of linear engines with spring systems. Friction does not influence the displacement and velocity trend of the piston. However, acceleration characteristics, especially at the TDC and BDC, are strongly impacted on. Figures 4.5.13 and 4.5.14 clearly show the influence of friction on the acceleration characteristics. Figures 4.5.21 and 4.5.22 also introduce unsystematic trend characteristics caused by friction. Both characteristics are unclear since the engine runs at high speeds and the capacity of the software only reaches 1000 frames per second. It was not sufficient to simulate high frequency engine movement because there were much unrecorded data.

Friction also influences the piston movement. From a visual linear motion study, it is clear that a piston moves as shown in Figure 4.5.16. The rotary motion is strongly correlated with angular momentum. Figure 4.5.15 clearly shows that the angular momentum is very strong influenced by friction. However, the angular momentum rotates the piston by 90 degrees at 5000 frames. Accordingly, below the piston pinhole, there is a window of the inlet scavenging port. If the piston rotates 90 degrees then there no mixture will be supplied to the combustion chamber, which results in the engine misfiring and not run. This appears to be evidence that the designed linear engine may not work properly and that the spring system needs to be modified, especially the connection with the piston.

The design of the spring geometry is strongly influenced by the motion of a linear engine. A smaller piston displacement would influence both the compression ratio and scavenging. In this work, displacements on a certain frequency could not work properly. Frequencies of 16.67 Hz and 66.67 Hz resulted in the displacements being reduced to 26.95 mm and 27.4 mm, respectively. Such displacements could affect the scavenging of the mixture and also decrease the pressure ratio. If a displacement

decreases then the scavenging port window is also smaller and that influences the combustion process. If there is not enough fuel to burn then a smaller combustion pressure is produced; as a result there is smaller thrust force to push the piston. It is possible that a misfire will occur for a small displacement. Decreasing the pressure ratio also influences the combustion process. Therefore, decreasing the displacement very strongly influences the overall linear engine performance.

4.5.3 Summary

This chapter has observed the effect of the spring system design on the linear engine performance and piston dynamics. Subchapter 4.5.1 discusses the influence of the spring system on engine performance, while subchapter 4.5.2 discusses the influence of the spring system on piston dynamics.

The effect of the spring design as a return cycle of two-stroke spark ignition linear engines on their combustion process and performance has been studied in this research. The combustion process and performance are compared with the predicted results. In general, at three focused speeds, the combustion and performance decrease. However, even with a decrease in combustion and performance, at a speed of 1 m/sec the engine still promises to run well. On the other hand, at speeds of 4.1 m/sec and 4.6 m/sec, misfiring will occur because the deflection of the spring decreases significantly.

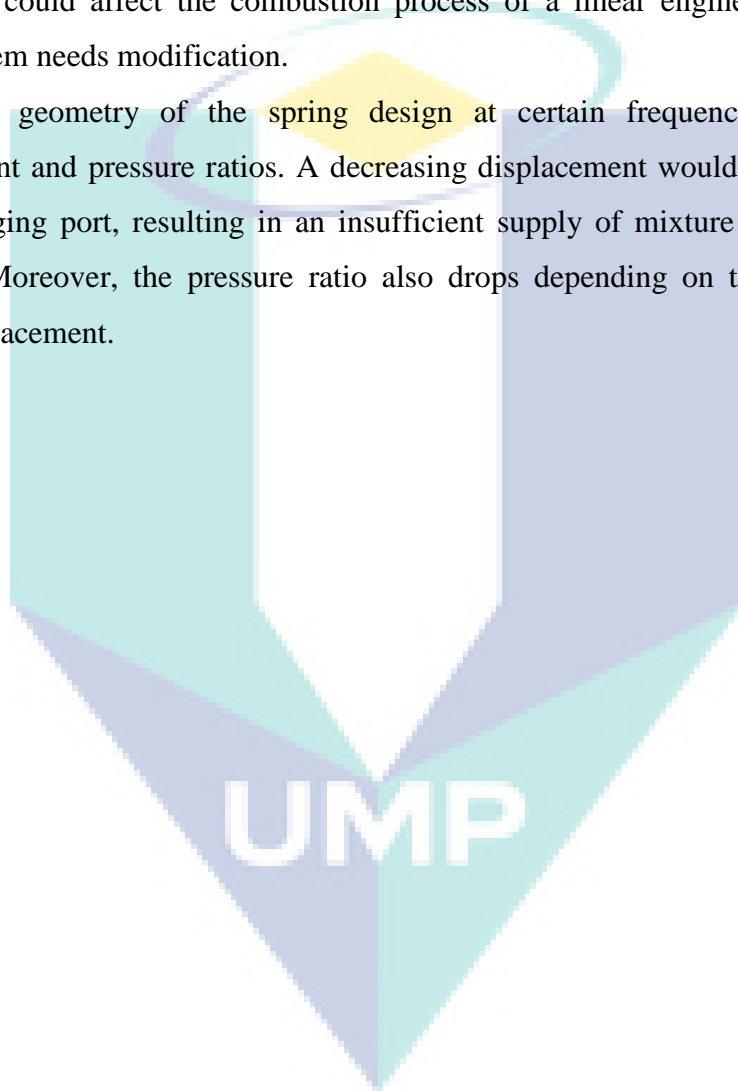
Of the 12 different speeds, only 6 work properly. Although the range in speeds decreases, compared to the speeds in conventional engines the maximum power output is still higher. The final design result of the power output is 1.03 kW at 3.6 m/sec.

The motion analysis of a single cylinder in a high-speed spark ignition linear engine with a spring system as a return cycle has been investigated. 3-D conventional and linear engine models have been used to simulate piston motion, while GT-Power has been used to simulate the combustion pressure as input for the thrust forces. The geometry of the spring has been optimised with multilevel optimisation using a spreadsheet. SolidWorks has been used to design and assemble the model, while Cosmos is utilised to simulate motion analysis. According to the basic considerations, it showed a clear difference in motion between conventional and linear engines. Acceleration characteristics are very different. Conventional engine characteristics are inconsistent since there is a longer period at the TDC, and then dramatically banded

down to the BDC. On the other hand, the acceleration characteristic of a linear engine is consistent from the TDC to the BDC.

The friction force has a strong influence on the piston acceleration, especially in the TDC and BDC zones due to the extremely fluctuating trends. Moreover, the piston has a rotary motion which would influence the scavenging process. This is alarming for a two-stroke engine with a conventional scavenging piston control system. The pure free-piston could affect the combustion process of a linear engine. In this case, the spring system needs modification.

The geometry of the spring design at certain frequencies influences the displacement and pressure ratios. A decreasing displacement would reduce the area of the scavenging port, resulting in an insufficient supply of mixture to the combustion chamber. Moreover, the pressure ratio also drops depending on the decrease in the piston displacement.



4.6 DESIGN MODIFICATION

A pure free-piston engine that is designed based on a modified conventional engine has a problem with the scavenging process. The most commonly used conventional two-stroke engine configurations are those with fixed scavenge and an exhaust port in the cylinder liner that is opened and closed by a moving piston. For a conventional engine, the piston movement is fixed at a rotary position, so that the scavenging process is not disturbed. In the case of a free-piston linear engine, the movement of the piston is not only an oscillating motion but also a rotation on the z-ordinate. This movement disturbs the scavenging process of the mixture. Therefore, it is necessary to modify the spring system as a return cycle for an excellent scavenging process.

Two scenarios have been proposed in this study, the first is the modification of the piston, and the second is modifying the connecting rod. Piston modification is removed by cutting the bottom part of the piston skirt. The objective is for the piston to revolve on the z-ordinate so that it does not disturb the scavenging process. While modification of the connecting rod is achieved by locking the rod in order to restrain the movement of angular momentum.

Modifying the piston and connecting rod would have some effect on the structural strength. Therefore, the modifications of the components need to be studied in terms of the material strength. In the case of the piston, analysis would be affected by heating as well as by pressure from combustion on the top surface. Hence, the thermal-structure of the stress needs to be observed. The connecting rod is analysed in terms of structural stress alone.

4.6.1 Scenario of Design Modification

Figure 4.6.1 presets the design configuration of a linear engine with a spring system. Figure 4.6.1(A) shows the linear engine design configuration, Figure 4.6.1(B) is the design of the spring system and Figure 4.6.1(C) is the design of the connecting rod.

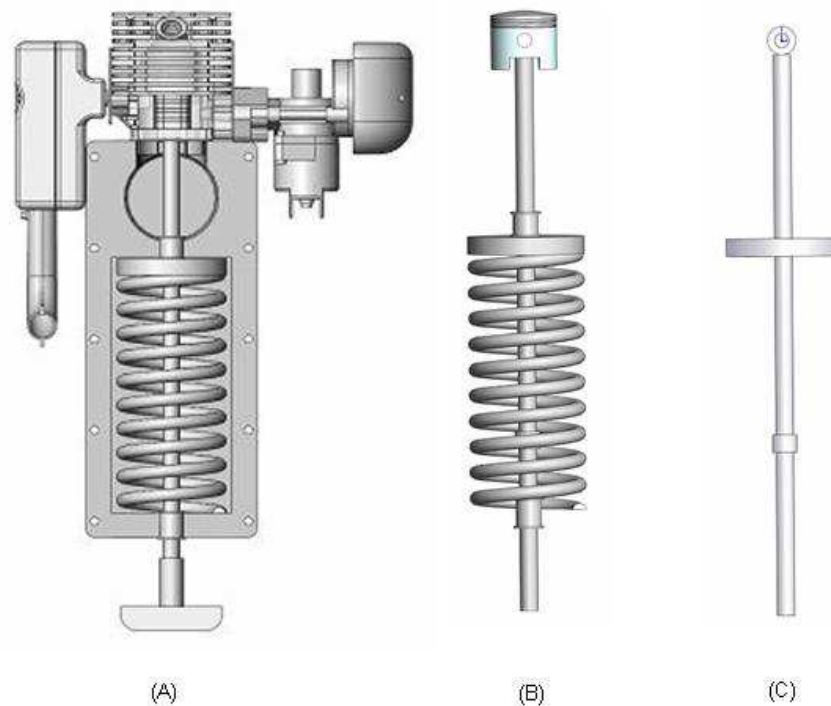


Figure 4.6.1: Design configuration of linear engine before modification.

Figure 4.6.1 showed the design configuration of a spring system before modification. The pure free-piston linear engine is modified from a conventional engine since it cannot work properly. The free-piston is influenced by friction between the piston ring and cylinder liner. The piston moves in an oscillating manner and also rotates on the z-ordinate. This piston movement interferes with the scavenging of the mixture which causes a failure in combustion. Therefore, a modification of the spring system is required. The first scenario is to modify the piston by cutting the bottom of the skirt, as shown in Figure 4.6.2. The second scenario is to add a lock on the connecting rod as shown in Figure 4.6.3. Stress analysis should be conducted before a proper spring system is chosen as an alternative modification.

An integral part of the engine design process is to ensure that the product has sufficient reliability and durability. Reliability refers to the useful life of an engine. For the engine system, this is the average life until overhaul. For most major engine components, it includes the expectation to reuse the components when the engine is overhauled. Reliability also includes infant mortality and unforeseen problems that require attention during the engine's operating life. Engine design and development

must include a validation processes to ensure that the durability and reliability expectations are met.

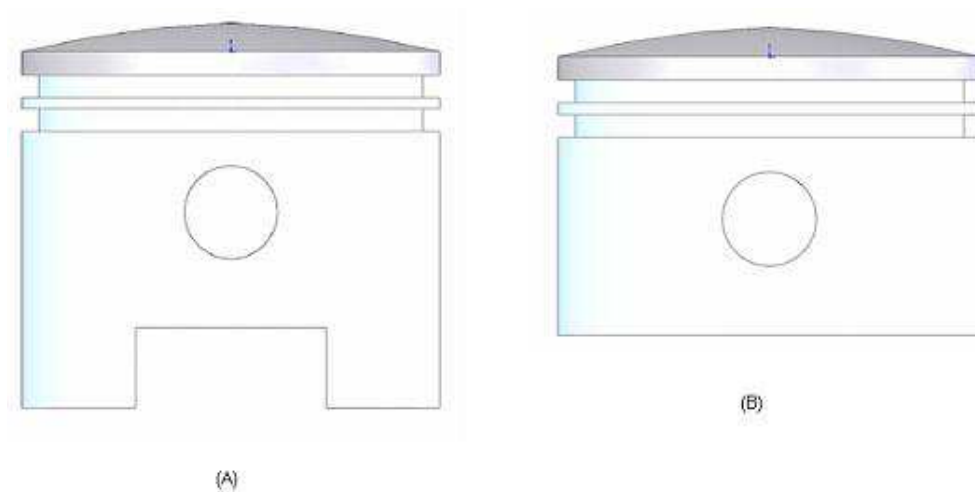


Figure 4.6.2: (A) Original piston. (B) Modified piston

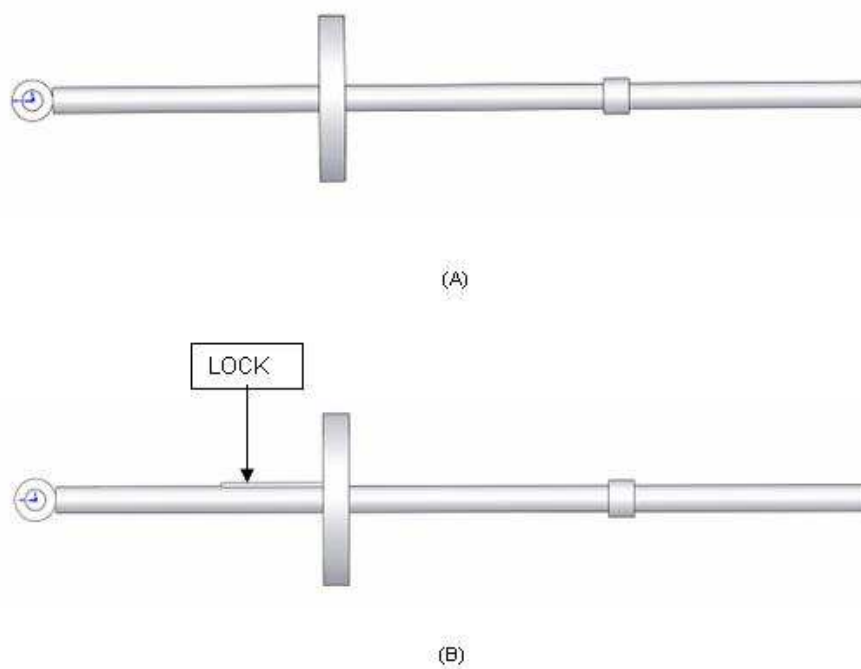


Figure 4.6.3: (A) Original connecting rod. (B) Modified connecting rod.

The modified piston should be as durable and reliable as the original one. The piston is a major component of the engine and must perform its functions without problems during the engine's useful life. The skirt cutting at the bottom part of the piston would affect thermal distribution. It also would have an impact on the thermal stress of the piston. It is expected that the piston will not be damaged prematurely. According to durability and reliability concepts, it is expected that if an engine is overhauled, the piston will not be replaced but will be reused. This is the goal of the study when looking at the modification of the piston.

In contrast with the modifications to the piston, the connecting rod is designed for a linear engine. Therefore, the modification of the connecting rod will concentrate on its structure. Its thermal stress need not be studied since the modified connecting rod is far from the location of the combustion chamber. It is estimated that the greatest stress will occur in the pinhole hose.

4.6.2 Modification Analysis Methods

For the analysis of both piston and connecting rod, the finite element method has been adopted. Structure and thermal stress have been used to analyse the piston. However, the analysis of the thermal stress is unnecessary in the case of the connecting rod. The modification models such as piston and connecting rod have been compared with the original model design. Three pieces of software have been adopted in the research, namely GT-Power, SolidWorks, and Algor. GT-Power has been used to conduct data source processing, SolidWorks has been used to build the models and assembly, and Algor has been used to solve and analyse the problems.

For thermal stress analysis, the piston has been analysed separately. However, the connecting rod has been assembled with the piston and piston pin. The objective is to treat the load analysis similarly to the piston analysis. The analysis steps begin with building the mathematical model, building the finite element model, solving the finite element model, and analysing the results. Figure 4.6.4 shows the flowchart for the stress analyses.

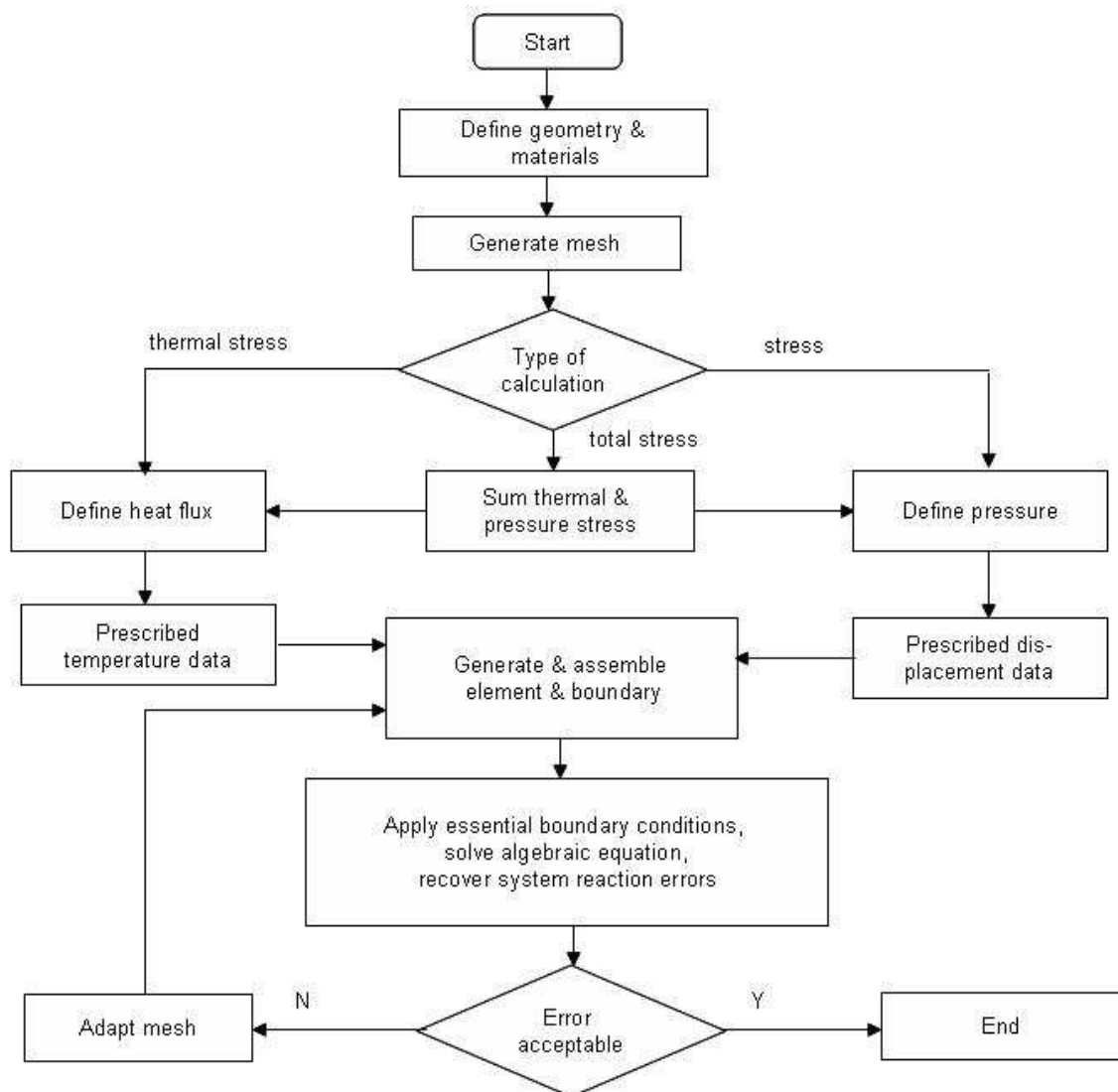


Figure 4.6.4: Flowchart for stress analyses

The first step is to build the mathematical model. It starts with the building of the geometry of the model parts in SolidWorks, and then assembling the components. The components are piston, pin, and connecting rod. The parts included the piston and the modified connecting rod. The geometry should be discretised into correct, and reasonably small, finite element meshes. The requirement of the mesh ability has very important implications. It must ensure that the CAD geometry will indeed mesh, and that the produced mesh provides correct solutions for stress and thermal stress.

Meshing builds an element model through a process of discretisation. The modelling of mesh is set to automatic mode, in which the shape of the meshes is a

combination of bricks and tetrahedral. The form of analysis is a static stress with linear material model. However, the thermal stress process analysis consists of two basic steps: (i) analysis of the temperature distribution with steady state heat transfer in which the temperature results are directly input as loads into the structural analysis to determine the stress caused by the temperature loads, and (ii) defining materials, loads, constraints, and analysed.

4.6.2.1 Basics of Finite Element Techniques and Software

An actual mechanical component in a continuous elastic structure is called a continuum. Finite-Element Analysis (FEA) divides or discretises the structure into small but finite, well-defined, elastic sub-structures (elements). By using polynomial functions, together with matrix operations, the continuous elastic behaviour of each element is developed in terms of the elements of material and geometric properties. Loads can be applied within the element (gravity, dynamic, thermal, etc), on the surface of the elements, or at the nodes of the elements. The element's nodes are the fundamental governing entities of the element, since the nodes connect one element to the other elements, and they are the location at which the elastic properties of the element are eventually established. Hereabout, boundary conditions are assigned and it is where the force (contact or body) is ultimately applied.

Due to the complicity of the spring system, including piston, pin, and connecting rod configuration, it is difficult to complete it using a basic (manual) technique. It is not only less effective, but also provides inaccurate approximations of the closed solution. There are a great many numerical techniques used in engineering applications for which the digital computer is very useful. Computer-Aided Design (CAD) connected with FEA software could help to solve these problems. There are also a number of commercial CAD and FEA programs. One of them is SolidWorks for CAD and Algor for FEA. In actual fact, SolidWorks is not only used for CAD but also used to conduct some numerical analyses. It is connected with the Cosmos software, which includes Cosmos-Motion, Cosmos-Works, and Cosmos-Flow. In this study, the stress and thermal stress analyses used Algor, since the combination between the bricks and tetrahedral shapes have been adopted for meshing. Cosmos-Works is not used since its

element geometries are limited to meshes of tetrahedral shapes which offer fewer opportunities to solve the problems.

4.6.2.2 Governing Equations

Governing equations related to this research include heat transfer, elasticity, and finite elements. For the modification of the design components of the spring system study, a steady state condition is used. However, the load is adopted from the prediction of engine performance at maximum pressure load at maximum torque. The concept of FEA starts from the unknowns in finite element problems. The unknowns are referred to as degrees of freedom (DOF). Types of DOF include displacement and temperature, which are required in this particular study. The basic stress and strain equations shown below are adopted from Algor (2005):

$$\sigma = \frac{F}{A} \quad (4.6.1)$$

$$\varepsilon = \frac{\sigma}{E} \quad (4.6.2)$$

$$\delta = \frac{FL}{AE} \quad (4.6.3)$$

To analyse a pre-stressed system (a material that has already been loaded and stressed before it is loaded again, such as an interference-fit system), the initial strain must be modelled. The easiest way to model an initial strain is to induce a thermal stress that will produce the desired strain. (Even if the strain in the real-world system was actually created by some circumstance other than thermal stress, the FEA modelling technique remains the same). If the amount of the existing strain and the properties of the material are known, then the necessary temperature difference can be calculated.

The basic equation for thermal stress states that the strain (ϵ) is equal to the product of the coefficient of thermal expansion (α) and the temperature difference (ΔT). The equation is shown below:

$$\epsilon = \alpha \Delta T \quad (4.6.4)$$

To solve this equation for the temperature differences, the equation below is used:

$$\Delta T = \frac{\epsilon}{\alpha} \quad (4.6.5)$$

Equations (4.6.1) to (4.6.5) are basic equations for the stress and thermal stress calculations. However, for 3-D problems, it is necessary to present finite element formulations of (1) the Poisson equation governing 3-D heat transfer and (2) 3-D elasticity equations (Reddy, 2006). Heat transfer from an engine piston crown was carried out using three different by Esfahanian, Javaheri and Gaffarpour (2006). Dechaumpai and Lim (2006) presented the finite element formulations, and these computer programs solved the heat transfer and thermal stress problems of an engine piston.

4.6.2.2.1 Heat Transfer Analysis

3-D heat transfer analysis is considered by the Poisson equation as given below:

$$-\frac{\partial}{\partial x} \left(k_x \frac{\partial T}{\partial x} \right) - \frac{\partial}{\partial y} \left(k_y \frac{\partial T}{\partial y} \right) - \frac{\partial}{\partial z} \left(k_z \frac{\partial T}{\partial z} \right) = g \quad \text{in } \Omega \quad (4.6.6)$$

Subjected to boundary conditions of the form:

$$T = \hat{T} \quad \text{on} \quad \Gamma_1, \quad (4.6.7A)$$

$$k_x \frac{\partial T}{\partial x} n_x + k_y \frac{\partial T}{\partial y} n_y + k_z \frac{\partial T}{\partial z} n_z + \beta(T - T_\infty) = \hat{q} \quad \text{on} \quad \Gamma_2 \quad (4.6.7B)$$

where k_x, k_y , and k_z are the conductivities of an orthotropic solid in the three coordinate directions, g is the internal heat generation per unit volume in a 3-D domain Ω , \hat{T} and \hat{q} are specified functions of the position on the portions Γ_1 and Γ_2 , respectively, of the surface Γ of the domain (see Figure 4.6.5), β is the convection coefficient, and T_∞ is the ambient temperature.

The weak form of Equation (4.6.6) can be developed in relation to the domain element (Ω_e), which is given as the following equations:

$$0 = \int_{\Omega_e} w \left[-\frac{\partial}{\partial x} \left(k_x \frac{\partial T}{\partial x} \right) - \frac{\partial}{\partial y} \left(k_y \frac{\partial T}{\partial y} \right) - \frac{\partial}{\partial z} \left(k_z \frac{\partial T}{\partial z} \right) - g \right] dx \quad (4.6.8A)$$

$$= \int_{\Omega} \left[k_x \frac{\partial w}{\partial x} \frac{\partial T}{\partial x} + k_y \frac{\partial w}{\partial y} \frac{\partial T}{\partial y} + k_z \frac{\partial w}{\partial z} \frac{\partial T}{\partial z} - wg \right] dx + \oint_{\Gamma^e} \beta w T ds - \oint_{\Gamma^e} w (q_n + \beta T_\infty) ds \quad (4.6.8B)$$

where w is the weight function.

The interpolation function form can be assumed as a finite element as:

$$T = \sum_{j=1}^n T_j^e \Psi_j^e(x, y, z) \quad (4.6.9)$$

Through the element Ω_e in Figure 4.6.5 and then substituting $w = \Psi_i^e$ and Equation (4.6.9) into (4.6.8), the finite element model as formulated below is obtained.

$$K^e T^e = f^e + Q^e \quad (4.6.10A)$$

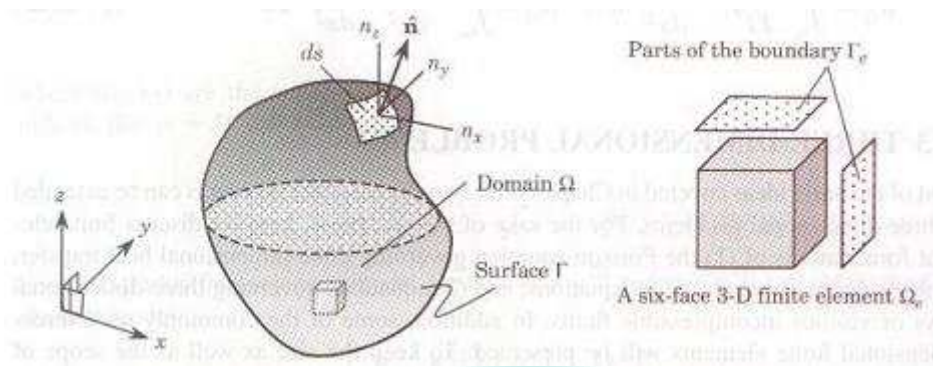


Figure 4.6.5: A 3-D domain Ω , its boundary Γ with unit normal \hat{n} , and a typical 3-D finite element (Reddy, 2006)

$$K_{ij}^e = \int_{\Omega_e} \left(k_x \frac{\partial \Psi_i^e}{\partial x} \frac{\partial \Psi_j^e}{\partial x} + k_y \frac{\partial \Psi_i^e}{\partial y} \frac{\partial \Psi_j^e}{\partial y} + k_z \frac{\partial \Psi_i^e}{\partial z} \frac{\partial \Psi_j^e}{\partial z} \right) + \oint_{\Gamma^e} \beta \Psi_i^e \Psi_j^e ds \quad (4.6.10B)$$

$$f_i^e = \int_{\Omega_e} g \Psi_i^e dx \quad (4.6.10C)$$

$$Q_i^e = \oint_{\Gamma^e} (q_n + \beta T_\infty) \Psi_i^e ds \quad (4.6.10D)$$

Equations 4.6.6 to 4.6.10 are adopted from Reddy (2006). More detailed information can be read in that particular reference.

4.6.2.2.2 Elasticity Analysis

Elasticity is a part of solid mechanics that is associated with the stress and deformation of a solid body. Linearisation elasticity is concerned with small deformations that obey Hooke's law. The equilibrium condition for a 3-D elastic body is governed by the differential equation. Stress-strain relationships can be written using a generalised form of Hooke's law. Strain-displacement relations are also part of the finite element models in 3-D elasticity problem development. The governing equations below are elasticity formulas for calculating stress, and in our research are coupled with thermal or total stress, which have been adopted from Reddy (2006).

Strain-displacement relationships of 3-D equations are written below:

$$\begin{aligned}\varepsilon_{xx} &= \frac{\partial u_x}{\partial x}, & \varepsilon_{yy} &= \frac{\partial u_y}{\partial y}, & \varepsilon_{zz} &= \frac{\partial u_z}{\partial z}, \\ 2\varepsilon_{xy} &= \frac{\partial u_x}{\partial y} + \frac{\partial u_y}{\partial x}, & 2\varepsilon_{xz} &= \frac{\partial u_x}{\partial z} + \frac{\partial u_z}{\partial x}, & 2\varepsilon_{yz} &= \frac{\partial u_y}{\partial z} + \frac{\partial u_z}{\partial y}\end{aligned}\quad (4.6.11A)$$

In the finite element formulation it can be written as:

$$\varepsilon = Du, \varepsilon = \begin{Bmatrix} \varepsilon_{xx} \\ \varepsilon_{yy} \\ \varepsilon_{zz} \\ \varepsilon_{xz} \\ \varepsilon_{yz} \\ \varepsilon_{xy} \end{Bmatrix}, D^T = \begin{bmatrix} \frac{\partial}{\partial x} & 0 & 0 & \frac{\partial}{\partial z} & 0 & \frac{\partial}{\partial y} \\ 0 & \frac{\partial}{\partial y} & 0 & 0 & \frac{\partial}{\partial z} & \frac{\partial}{\partial x} \\ 0 & 0 & \frac{\partial}{\partial z} & \frac{\partial}{\partial x} & \frac{\partial}{\partial y} & y \end{bmatrix} \quad (4.6.11B)$$

The equation of motion below is developed from the stress equilibrium equation

$$\begin{aligned}\frac{\partial \sigma_{xx}}{\partial x} + \frac{\partial \sigma_{xy}}{\partial y} + \frac{\partial \sigma_{xz}}{\partial z} + f_x &= \rho \frac{\partial u_x}{\partial t^2} \\ \frac{\partial \sigma_{xy}}{\partial x} + \frac{\partial \sigma_{yy}}{\partial y} + \frac{\partial \sigma_{yz}}{\partial z} + f_y &= \rho \frac{\partial u_y}{\partial t^2} \\ \frac{\partial \sigma_{xz}}{\partial x} + \frac{\partial \sigma_{yz}}{\partial y} + \frac{\partial \sigma_{zz}}{\partial z} + f_z &= \rho \frac{\partial u_z}{\partial t^2}\end{aligned}\quad (4.6.12A)$$

Equations of motion can be written in finite element formulation as follows:

$$D^T \sigma + f = \rho \ddot{u} \quad (4.6.12B)$$

where f_x, f_y , and f_z denote the components of the body force vector (measured in unit volume) along the x, y and z directions, respectively. ρ is the density of the material, and the formulas for σ, f , and u are shown below:

$$\sigma = \begin{Bmatrix} \sigma_{xx} \\ \sigma_{yy} \\ \sigma_{zz} \\ \sigma_{xy} \\ \sigma_{xz} \\ \sigma_{yz} \end{Bmatrix}, \quad f = \begin{Bmatrix} f_x \\ f_y \\ f_z \end{Bmatrix}, \quad u = \begin{Bmatrix} u_x \\ u_y \\ u_z \end{Bmatrix} \quad (4.6.12C)$$

Stress-strain relations

$$\begin{Bmatrix} \sigma_{xx} \\ \sigma_{yy} \\ \sigma_{zz} \\ \sigma_{xy} \\ \sigma_{xz} \\ \sigma_{yx} \end{Bmatrix} = \begin{bmatrix} c_{11} & c_{12} & c_{13} & 0 & 0 & 0 \\ c_{12} & c_{22} & c_{23} & 0 & 0 & 0 \\ c_{13} & c_{23} & c_{33} & 0 & 0 & 0 \\ 0 & 0 & 0 & c_{44} & 0 & 0 \\ 0 & 0 & 0 & 0 & c_{55} & 0 \\ 0 & 0 & 0 & 0 & 0 & c_{66} \end{bmatrix} \begin{Bmatrix} \varepsilon_{xx} \\ \varepsilon_{yy} \\ \varepsilon_{zz} \\ 2\varepsilon_{xz} \\ 2\varepsilon_{yz} \\ 2\varepsilon_{xy} \end{Bmatrix} \quad \text{or } \sigma = C\varepsilon \quad (4.6.13)$$

where c_{ij} ($c_{ji} = c_{ij}$) are the elasticity of the material constant for an orthotropic medium with material principal directions (x_1, x_2, x_3) that coincide with the coordinates (x, y, z) used to describe the problem. c_{ij} can be expressed in terms of the engineering constants $(E_1, E_2, E_3, \nu_{12}, \nu_{13}, \nu_{23}, G_{12}, G_{13}, G_{23})$ for an orthotropic material.

Accordingly, in order to study the structural and thermal stresses with finite elements, it is necessary to consider the boundary conditions (Noda, Hetnarski & Tanigawa, 2003). When the stress is prescribed over the entire boundary surface, the problem is called a first boundary-volume problem. When the displacement is prescribed over the entire boundary surface, the problem is called a second boundary-volume problem. According to Reddy (2006), the first boundary-volume problem is called the natural boundary and the second boundary-volume problem is called an essential boundary. Natural boundary conditions are:

$$\begin{aligned}
 t_x &\equiv \sigma_{xx}n_x + \sigma_{xy}n_y + \sigma_{xz}n_z \\
 t_y &\equiv \sigma_{xy}n_x + \sigma_{yy}n_y + \sigma_{yz}n_z \\
 t_z &\equiv \sigma_{xz}n_x + \sigma_{yz}n_y + \sigma_{zz}n_z
 \end{aligned}
 \quad \text{on } \Gamma_\sigma \quad (4.6.14A)$$

In finite element formulation, it can be written as:

$$\bar{t} \equiv \bar{\sigma} n = \hat{t} \text{ on } \Gamma_\sigma, \quad n = \begin{Bmatrix} n_x \\ n_y \\ n_z \end{Bmatrix}, \quad \bar{\sigma} = \begin{bmatrix} \sigma_{xx} & \sigma_{xy} & \sigma_{xz} \\ \sigma_{xy} & \sigma_{yy} & \sigma_{yz} \\ \sigma_{xz} & \sigma_{yz} & \sigma_{zz} \end{bmatrix} \quad (4.6.14B)$$

Essential boundary conditions are:

$$u_x = \hat{u}_x, \quad u_y = \hat{u}_y, \quad u_z = \hat{u}_z \quad \text{on } \Gamma_u \quad (4.6.15A)$$

In finite element formulation, it can be written as:

$$u = \hat{u} \quad \text{on } \Gamma_u \quad (4.6.15B)$$

where (n_x, n_y, n_z) denote the components of the unit normal vector on the boundary Γ ; Γ_σ and Γ_u are disjoint portions of the boundary; \hat{t}_x, \hat{t}_y and \hat{t}_z denote the components of the specific traction vector; and \hat{u}_x, \hat{u}_y and \hat{u}_z are the components of the specified displacement vector. Only one element of each pair, (u_x, t_x) , (u_y, t_y) and (u_z, t_z) may be specified at a boundary point.

The principle of virtual displacement for the 3-D elasticity problems can be expressed in vector form as follows:

$$0 = \int_{\Omega_e} \left[(D\delta u)^T C(Du) + \rho u^T \ddot{u} \right] dx - \int_{\Omega_e} (\delta u)^T f dx - \oint_{\Gamma_e} (\delta u)^T t ds \quad (4.6.16)$$

The finite element approximation is assumed to be in the form:

$$u = \begin{Bmatrix} u_x \\ u_y \\ u_z \end{Bmatrix} = \Psi \Delta, \quad w = \delta u = \begin{Bmatrix} w_1 = \delta u_x \\ w_2 = \delta u_y \\ w_3 = \delta u_z \end{Bmatrix} = \Psi \delta \Delta \quad (4.6.17)$$

where:

$$\Psi = \begin{bmatrix} \Psi_1 & 0 & 0 & \Psi_2 & 0 & 0 & \dots & \Psi_n & 0 & 0 \\ 0 & \Psi_1 & 0 & 0 & \Psi_2 & 0 & 0 & \dots & \Psi_n & 0 \\ 0 & 0 & \Psi_1 & 0 & 0 & \Psi_2 & 0 & \dots & 0 & \Psi_n \end{bmatrix} \quad (4.6.18)$$

$$\Delta = \{u_x^1 \quad u_y^1 \quad u_z^1 \quad u_x^2 \quad u_y^2 \quad u_z^2 \quad \dots \quad u_x^n \quad u_y^n \quad u_z^n\}^T$$

Substituting Equation (4.6.17) into the statement of virtual work equation (Equation (4.6.16)) then provides the finite element model of a 3-D elastic body:

$$M^e \ddot{\Delta} + K^e \Delta = F^e + Q^e \quad (5.6.19)$$

where:

$$K^e = \int_{\Omega_e} B^T C B dx,$$

$$M^e = \int_{\Omega_e} \rho \Psi^T \Psi dx$$

$$F^e = \int_{\Omega_e} \Psi^T f dx,$$

$$Q^e = \oint_{\Gamma_e} \Psi^T t ds \quad (4.6.20)$$

The element mass matrix M^e and stiffness matrix K^e are of the order $3n \times 3n$ and the element load vector F^e and the vector of internal forces Q^e is of the order $3n \times 1$, where n is the number of nodes in the finite element.

4.6.2.3 Model and Discretisation

The two models used in this study are the piston with its modification and the connecting rod with its improvement. To obtain an excellent formulation, the piston has been analysed separately, along with the connecting rod. Due to the large geometry and complexity of the model, it is difficult to analyse the problem and the results are inaccurate. For facilitating load placement, the connecting rod is analysed in the assembly system together with the pin and piston. Figures 4.6.6 and 4.6.7 show the models used in the research. Figure 4.6.6(A) shows the original piston model and its modification model is shown in Figure 4.6.6(B). Figures 4.6.7(A) and 4.6.7(B) present the models of the connecting rod and its improvement.

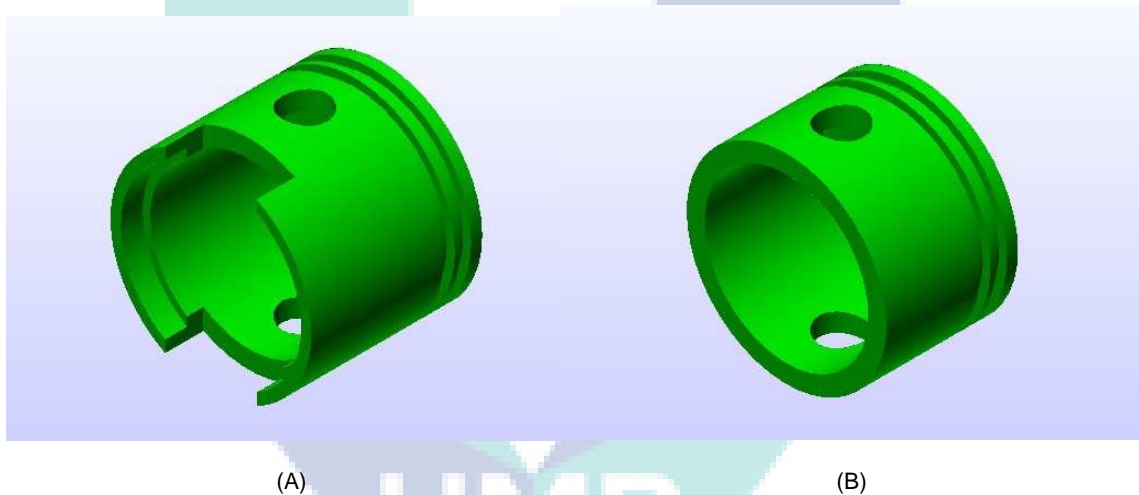
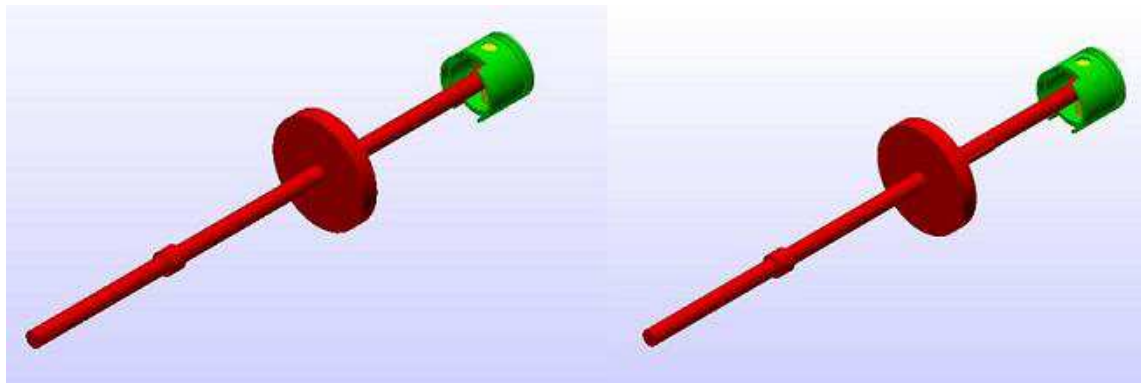


Figure 4.6.6.: Piston models. **(A):** Original model. **(B):** Modification model.



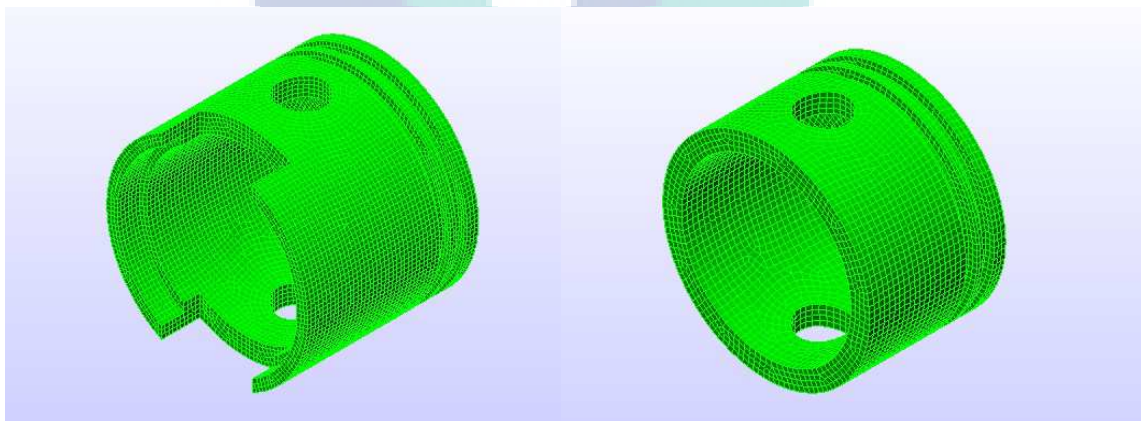
(A)

(B)

Figure 4.6.7: Connecting rod with pin and piston models.

(A): Original model. (B): Improved model.

The models of the piston are analysed by thermal-structural analysis methods. This method has been chosen because the piston is influenced by the process of combustion from the combustion chamber. The purpose of this study is to examine the material strength of the modified piston. Therefore, the maximum load is selected at a piston speed of 2 m/s at 2000 rpm. Steady state analysis has been chosen for all studies, including the mechanical, thermal, and total stress of the piston models.



(A)

(B)

Figure 4.6.8: Piston mesh generated in Algor FEMPRO.

(A): Mesh of original piston. (B): Mesh of modified piston.

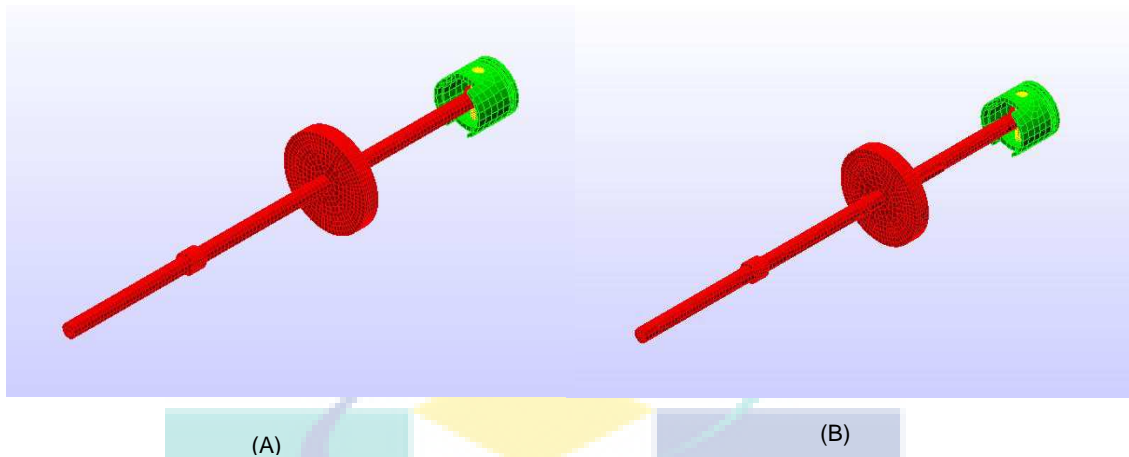


Figure 4.6.9: Connecting rod mesh assembly with piston and pin.

(A): Mesh of original design. (B): Mesh of improved design.

Table 4.6.1: Solid mesh statistics

No.	MODELS	Mesh model settings	Elements				
			Tetrahedron	Pyramid	Wedge	Brick	Total
1	Original piston model	0.30	15054	8971	2034	16264	42323
2	Modified piston model	0.25	12988	8412	2418	17798	41616
3	Connecting rod original model	1.53	3123	931	86	307	4447
4	Connecting rod improved model	1.53	4497	1368	117	386	6368

In accordance with the finite element method used, the models have been meshed with Algor commercial software. The mesh types are a mixture of bricks, wedges, pyramids, and tetrahedral elements. The solid mesh statistics of the models are shown in Table 4.6.1. Figures 4.6.8 and 4.6.9 present the discretisation results (mesh) of the models. The model mesh setting of the original piston was solid 0.30, and for the

modified version was 0.25. The connecting rods were set at 1.53. All settings have been chosen for the smallest mesh element error.

Small engine pistons and connecting rod are made of aluminium (Heywood, 1989). High performance engines often use forged pistons to improve strength. Most piston alloys are eutectic to hypereutectic alloys of aluminium and silicon (Hoag, 2006). Based on the literature, the original piston is approximated as an aluminium alloy. The connecting rod is also designed using aluminium alloy. From Algor's material library, the materials chosen are aluminium 6061-T6 and 6061-T651. The material design characteristics are shown in Table 4.6.2.

4.6.3 Results from the Analysis of the Modification

The structural stress analysis of the original piston and its modification have been conducted at maximum torque, in which the pressure is maximised. The pressure data has been adopted from the highest PV diagram. The pistons have been analysed using stresses through combustion pressure effects, and thermal stresses via temperature distribution at the piston crown. The combination of stresses from the pressure and temperature of the combustion chamber have also been applied. The remaining results are related to the structural stress of the connecting rod and its improvement. All the results from this section can be seen in Appendix E.

Table 4.6.2: Material design characteristics

Material Model: Aluminium 6061-T6; 6061-T651		
No	Definitions	Characteristics
1	Material Source	ALGOR Material Library
2	Material Description	None
3	Mass Density	0.000000027 Ns ² /mm/mm ³
4	Modulus of Elasticity	68900 N/mm ²
5	Poisson's Ratio	0.33
6	Shear Modulus of Elasticity	26000N/mm ²
7	Thermal Coefficient of Expansion	2.360000E-005 1/°C

4.6.3.1 Structural Stress of Pistons.

Figures 4.6.10 and 4.6.11 are examples of the structural stresses in the original piston and its modification. Broadly speaking, the structural stresses in both pistons showed the same trend. The difference is only in the value of the stress occurring. Structural stress on the original piston is higher than the structural stress of its modification. The structural stress on the original piston is between 0.084–137.9 N/mm², while the structural stress on the modified piston is between 0.168–130.16 N/mm². The stresses near the pin-holes are greater than the stresses in other regions. Ring grooves at the top of the pin-hole regions also experienced very strong stresses. The piston crown regions also receive high stresses; nevertheless, the highest stresses occur at the inner part of the ring grooves at the upper regions of the pin-holes. This can be more clearly seen in Figures 4.6.10(B) and 4.6.11(B). More detailed information can be seen in the figures, of a variety of views, in Appendix E. Structural stress analysis on the piston in this section is only conducted for the pressure load on the combustion chamber.

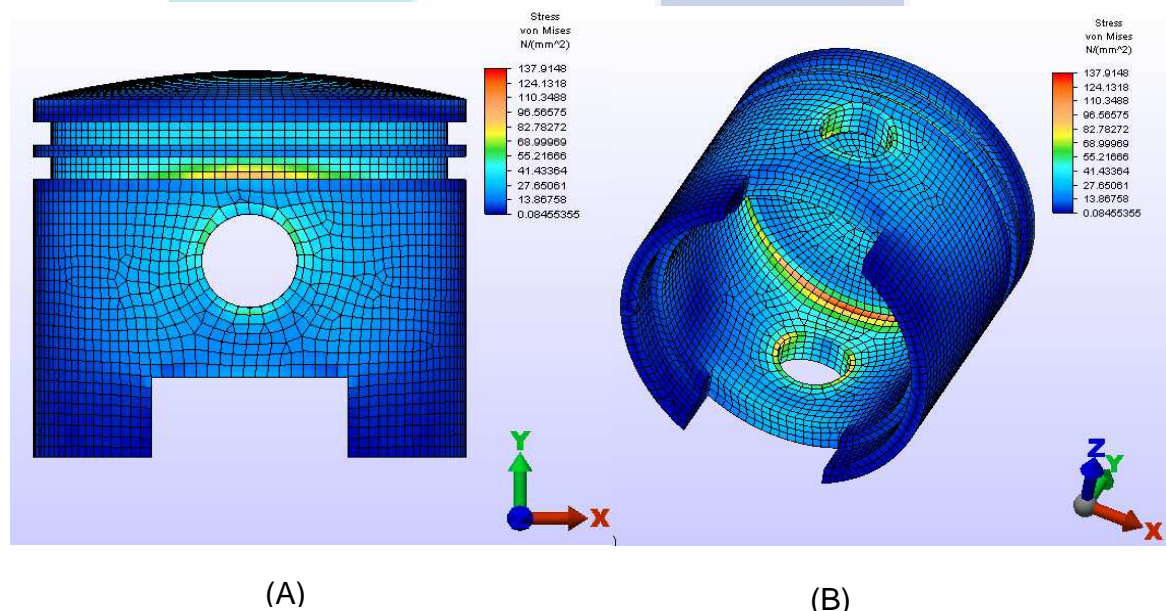
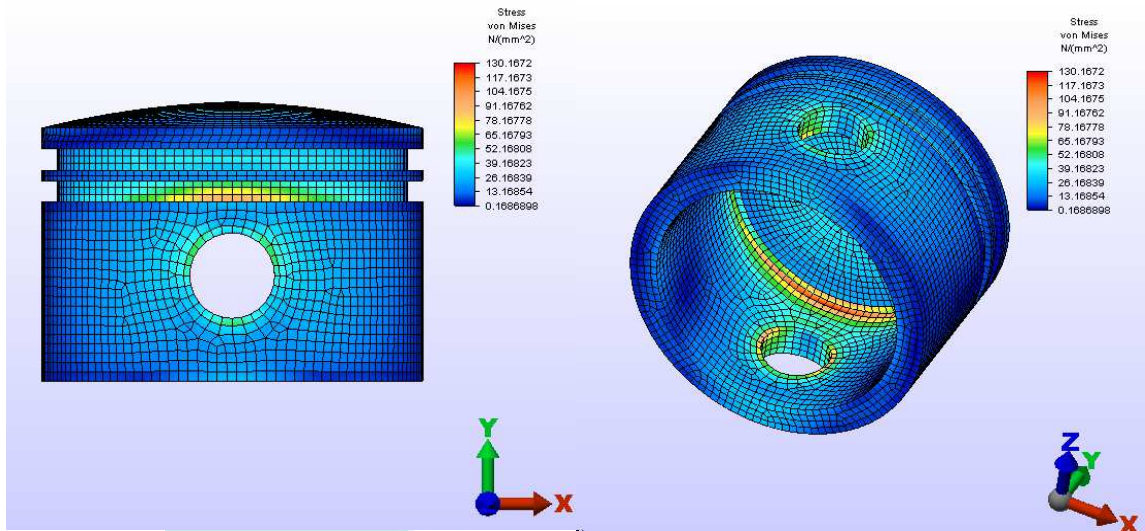


Figure 4.6.10: Structural stress analysis of the original piston.

(A): Front view of the stress analysis of the original piston.

(B): Inner view of the stress analysis of the original piston.



(A)

(B)

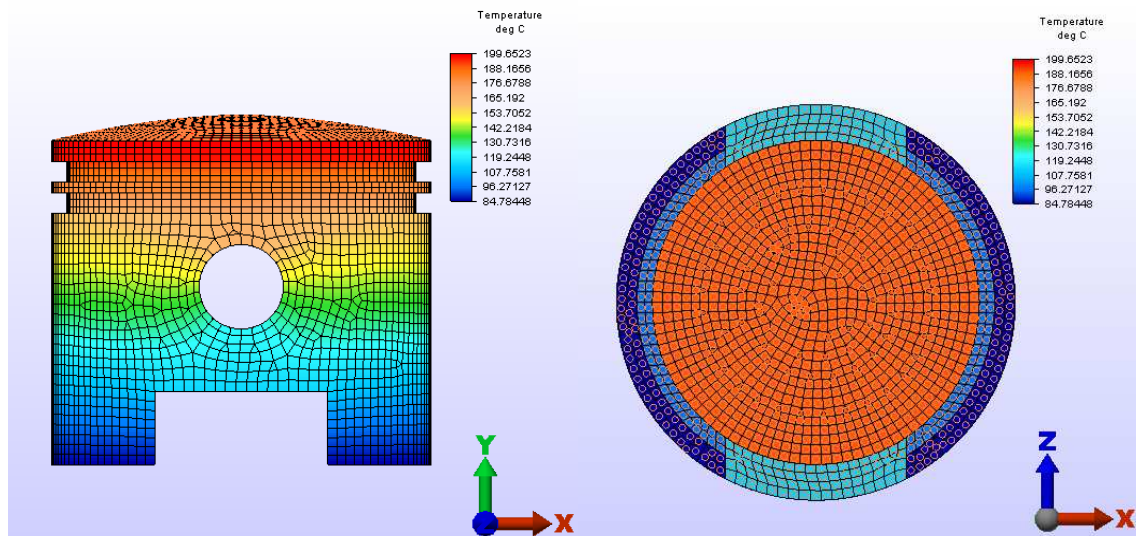
Figure 4.6.11: Structure stress analysis of the piston modification.

A: Front view of the stress analysis of the modified piston.

B: Inner view of the stress analysis of the modified piston.

4.6.3.2 Thermal Stress in Pistons

Contraction of the material would cause thermal expansion, and this would produce thermal stress. Thermal stress effects can be simulated by coupling a steady state heat transfer analysis and a linear static stress structural analysis. Heat transfer analysis is performed to determine the temperature distribution, and the temperature results become data input as loads in the structural analysis to determine the stresses and displacement caused by the temperature loads. In the following sections, the results of the analysis of the thermal stress of the pistons are presented.



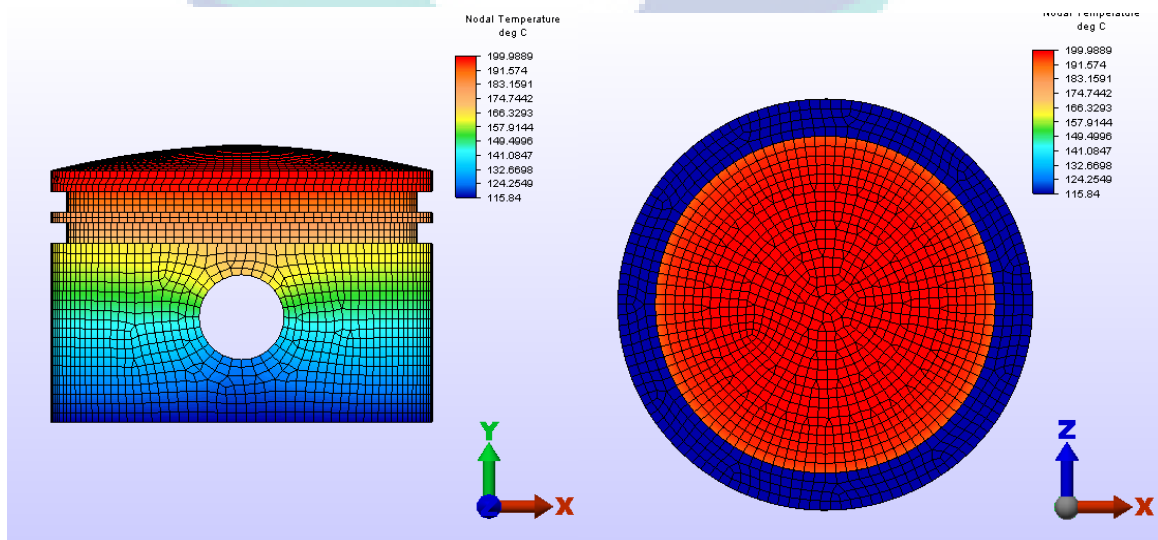
(A)

(B)

Figure 4.6.12: Thermal distribution of original piston.

(A): Front view of thermal distribution of original piston.

(B): Bottom view of thermal distribution of original piston.



(A)

(B)

Figure 4.6.13: Thermal distribution of modified piston.

(A): Front view of thermal distribution of modified piston.

(B): Bottom view of thermal distribution of modified piston.

Figure 4.6.12 shows the thermal distribution of the original piston. The thermal distribution at the front view is shown in Figure 4.6.12(A) and from the bottom view in Figure 4.6.12(B). The highest temperature distribution is at the regions of piston crown, and it gradually decreases to the bottom of the piston skirt. The highest temperature is 199.65°C and the lowest is 84.78°C . A similar trend can be seen in the modified piston. However, the distribution temperature is between $115.84\text{--}199.98^{\circ}\text{C}$.

Temperature distribution leads to thermal stresses. The thermal stress caused by the temperature distribution on the pistons is shown in Figures 4.6.14 and 4.6.15. Thermal stresses that occur in the original piston are not too high. The range of stresses is between $0.028\text{--}27.47\text{ N/mm}^2$. Regions of larger stresses are at the bottom of the piston crown and ring grooves. However, the greatest stress occurs at the first ring groove region. Figure 4.6.14 clearly illustrates the occurrence of thermal stress in the original piston.

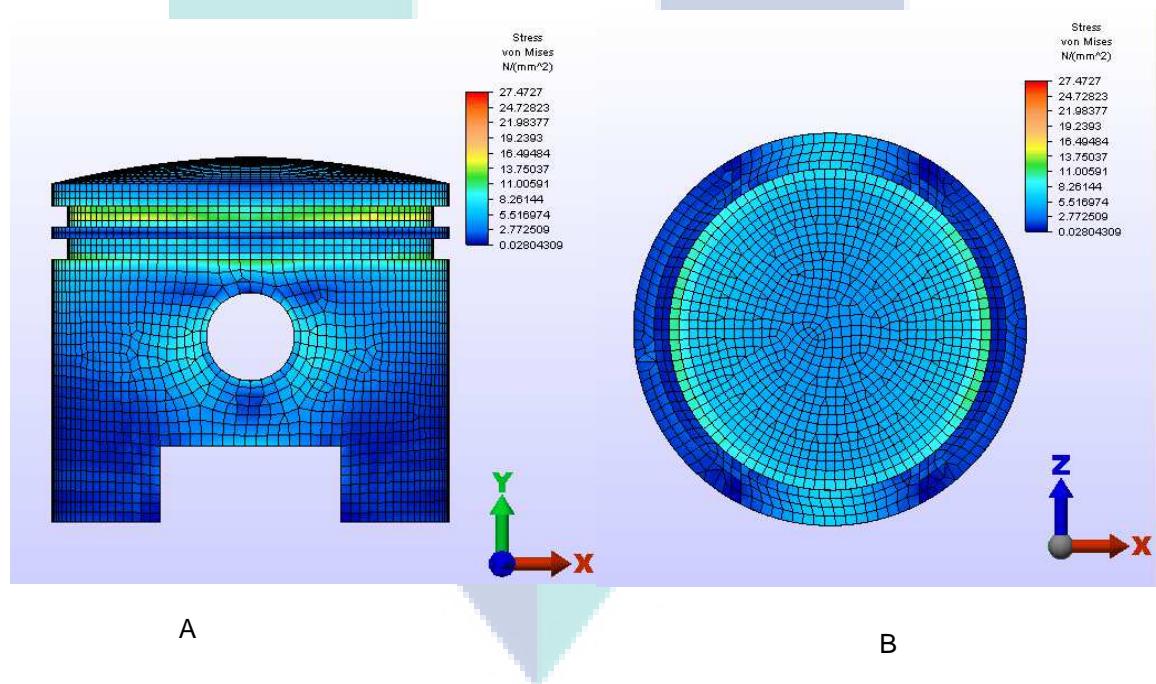


Figure 4.6.14: Thermal stress of original piston.

A: Front view of thermal stress of original piston.

B: Bottom view of thermal stress of original piston.

Figure 4.6.15 shows the thermal stress of a modified piston. The stresses occurring are higher than the stresses in the original piston. However, the stress is

distributed in the range of 0.16–48.17 N/mm². The regions of stress scatter from the base of the piston crown, which is close to the skirt, until the first ring groove. Similar to the thermal stress in the original piston, the thermal stresses in the modified version are not as high as the stresses caused by structural stress.

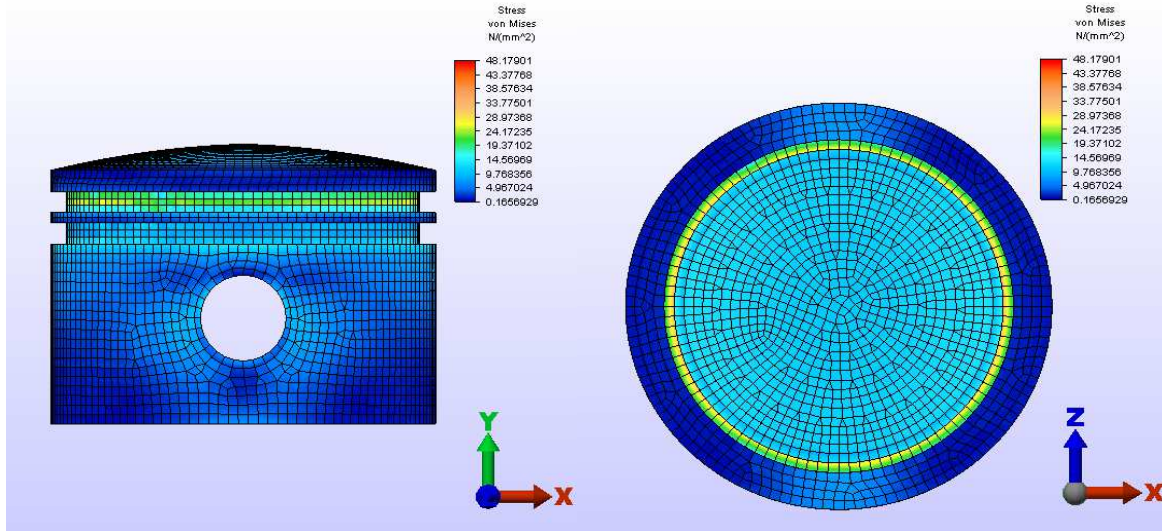


Figure 4.6.15: Thermal stress of modified piston.

A: Front view of thermal stress of modified piston.

B: Bottom view of thermal stress of modified piston.

4.6.3.3 Thermal-Structural Stress of Pistons

The thermal-structural (total) stress is a combination of the pressure and temperature of combustion from the combustion chamber. This effect is manifested from the released heat of the combustion on the internal combustion engine. Using Algor FEMPRO, the combined thermal-structural stress can be simulated. Figures 4.6.16 and 4.6.17 present the thermal-structural stress of the original and modified pistons.

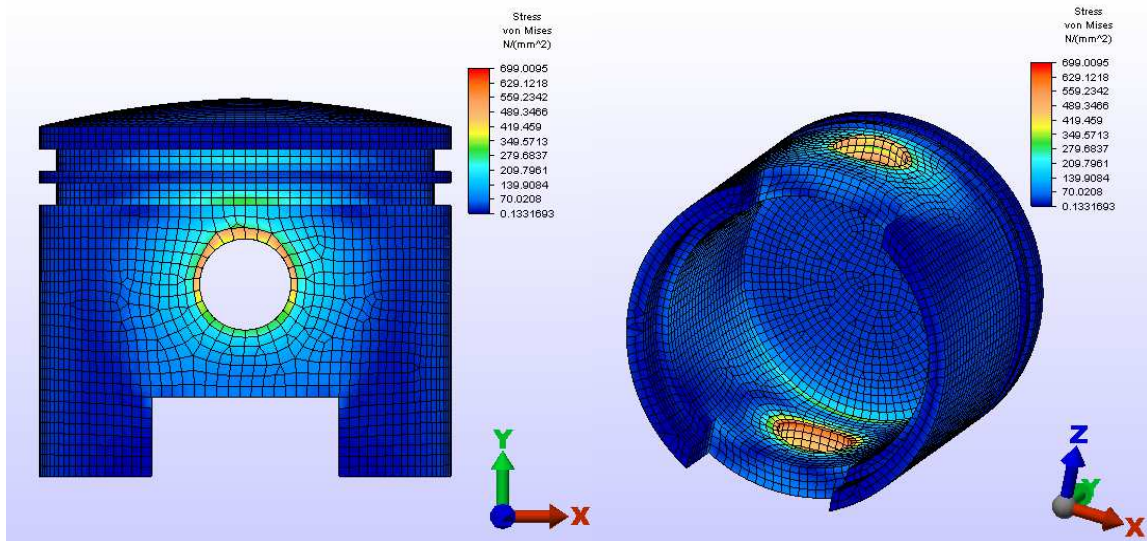


Figure 4.6.16: Thermal-structural stress of original piston.

A: Front view of thermal-structural stress.

B: Isometric view of thermal-structural stress.

The combination of thermal and pressure loads due to the released heat of the combustion process affect different phenomena. For the original piston, the stress range is 0.13–699.0 N/mm². Higher stresses occur near the pin-hole regions and at the second ring groove in the upper side of the pin-hole region. The highest stresses are at the top of pin-hole region. Figures 4.6.16(A) and 4.6.16 (B) highlight in colour the highest stress location, that is at the pin-hole region.

The trend of thermal stresses in the modified piston is similar to the thermal stresses of the original piston. The difference lies in the value of stress generated. The range of stress is between 0.93–714.87 N/mm². In the case of thermal-structural stress, the total stress of the modified piston is larger than the total stress of the original one. The largest stress is located on the inner lip of the pin-holes.

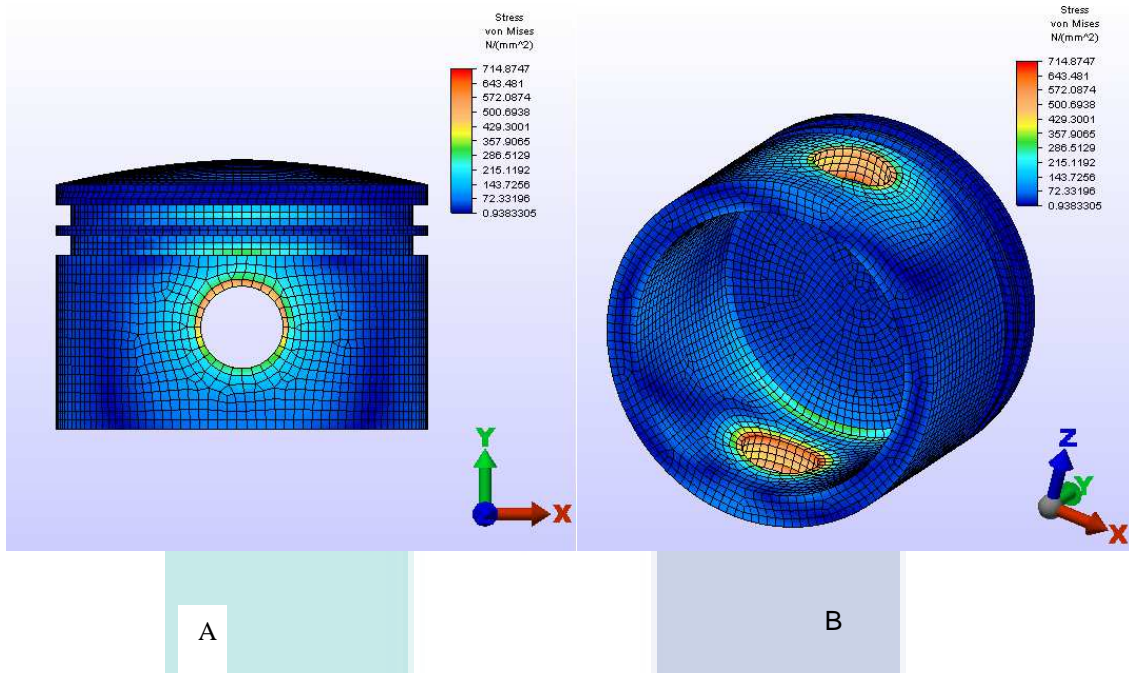


Figure 4.6.17: Thermal-structural stress of modified piston
A: Front view of thermal-structural stress of modified piston.
B: Isometric view of thermal-structural stress of modified piston.

4.6.3.4 Structural Stress of Connecting Rod

The improvement in the connecting rod design is to add a lock, as shown in Figure 4.6.3(B). The effect of combustion temperature on the stress has been ignored, because it is very small. The results of the structural stress analysis are shown in Figures 4.6.18 and 4.6.19. Figure 4.6.18 shows the structural stress for the original design of the connecting rod, and Figure 4.6.19 presents the structural stress of the improved design of the connecting rod.

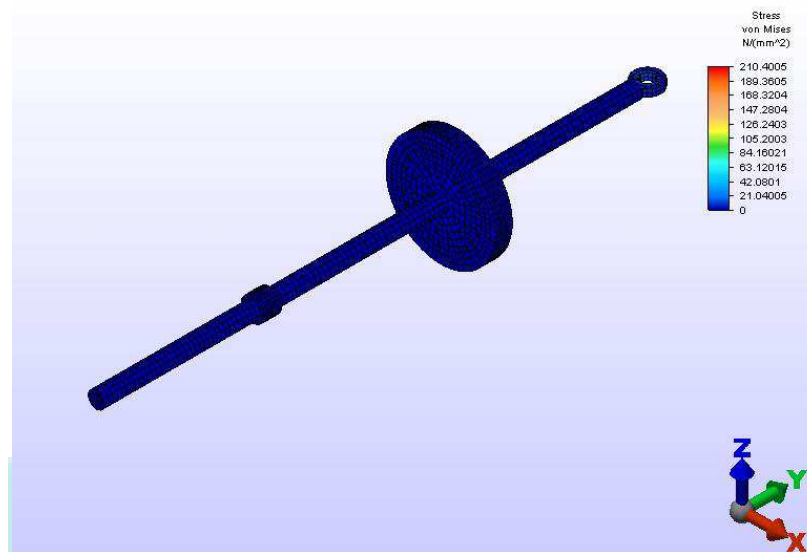


Figure 4.6.18: Structural stress of the original design of the connecting rod.

Stress distribution in the original design of the connecting rod is between 0–210.4 N/mm². The regions around the pin-hole show larger stresses than any other region. At node 9547, on element number 6596, the highest stress of 210.40 N/mm² is located. While the stresses on other elements are 29.68, 23.21, 14.94, 18.46, 141.16, 14.27, 24.92, 28.58, 20.61, 13.83, 17.62 N/mm², which occurs at the sequence of elements of 6407, 6408, 6582, 6589, 6594, 6595, 6596, 6598, 6599, 6600, 6603, and 6604, respectively.

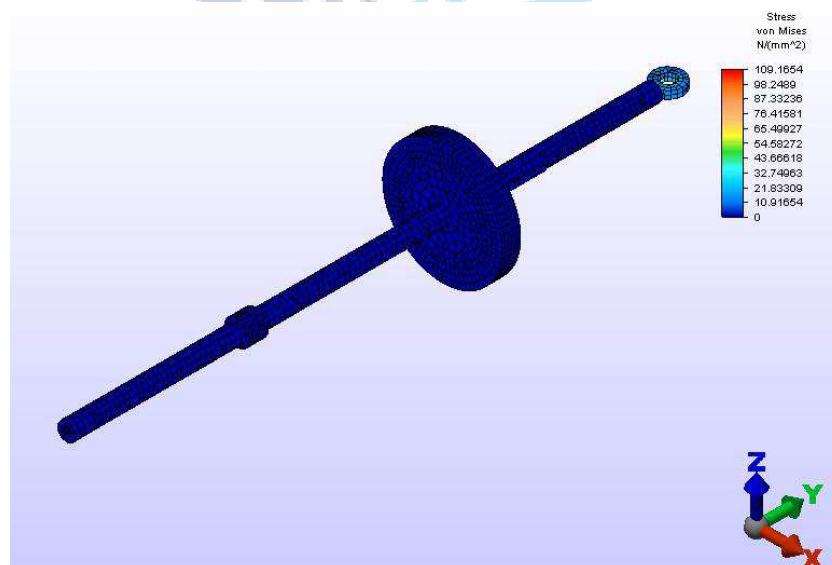


Figure 4.6.19: Structural stresses in the modified connecting rod.

Higher structure stresses in the modified connecting rod are found at the pin-hole region. The stresses over the whole pin-hole region are larger compared to other regions, but the greatest stress occurs at node 9777 (the actual location is on the inner side). At node 9777, there are eight elements, one of which (element number 10,204).experienced the highest stress of 109.16 N/mm^2 . While the stresses for the other elements are 14.72, 9.02, 48.24, 28.98, 12.0, 16.59, 14.72 N/mm^2 . Those stresses occurred at elements 10200, 10201, 10202, 10203, 10205, and 10206 respectively.

4.6.4 Discussion

Two scenarios for the modification of the spring system of a linear engine have been analysed. The results of the analysis have been compared with the original design. However, stress analysis results show a significant difference. By reducing the bottom of the piston skirt, the maximum stress increases, although the value of the increased stress is still allowed.

The thermal and structural stresses are also analysed separately in the piston analysis. The aim is to determine the contribution to the stress of pressure and temperature. The thermal-structural stress is the end result of the total stress caused by the combustion process in the combustion chamber. The structural stress is more dominant compared with the thermal stress in the thermal-structural stress effects (Heywood, 1989).

With reference to the maximum thermal-structural stress, both original piston and modified versions show similar trends. The inside of the pin-hole is the most critical region. These results are in accordance with Hoag (2006), who reported that the stress concentration is located on the inside of the hole on the piston pin and the connecting rod journal.

In practice, the length of the piston skirt is taken as 0.65 to 0.8 times the diameter of the cylinder bore (San, 2008). Following the formula for the original piston, the length of the skirt is 0.68 times the diameter of the cylinder bore; nevertheless, after modification, the length of skirt becomes 0.48 times the diameter of the cylinder bore. In the end, the design of the piston and ring have changed, and the area and weight of

the piston have been significantly reduced. In modern piston designs, the area of the oil film under shear and the inertia loads contribute to the effective pressure (Ferguson, 1986).

The thermal-structural stress can be eliminated by removing the pin connection system when creating a new design. The linear motion does not require a turning movement, and so the fixed connection system design is more efficient. Considering the spring system design as a whole, which includes the piston, a more optimum design will be obtained.

Modifying the connecting rod is more profitable, because by adding the lock the structural stress is smaller. The most critical area is located at the connecting rod journal. The highest stress only occurred at one element of the eight elements that support a node. Thus, the resultant average stress is small. Therefore, at the surface of the connecting rod, the colours which indicating a high stress are not visible. Almost the entire surface is blue. This phenomenon indicates that the average stress that occurs is not too large. In "inquire" of the element, some nodes have zero stress. This indicates that the critical region is only at the journal of the connecting rod.

4.6.5 Summary

The structural aspects of a single cylinder high-speed spark ignition linear engine with a spring system as the return cycle have been modified and analysed. The results show that there is a clear difference between the design and the modification of the piston. Both modification schemes, such as removing the bottom of the piston skirt and adding a lock to the connecting rod, have advantages and disadvantages. Based on the thermal-structural stress analysis, both modifications are acceptable for the modification of a system with a spring mechanism as the return cycle.

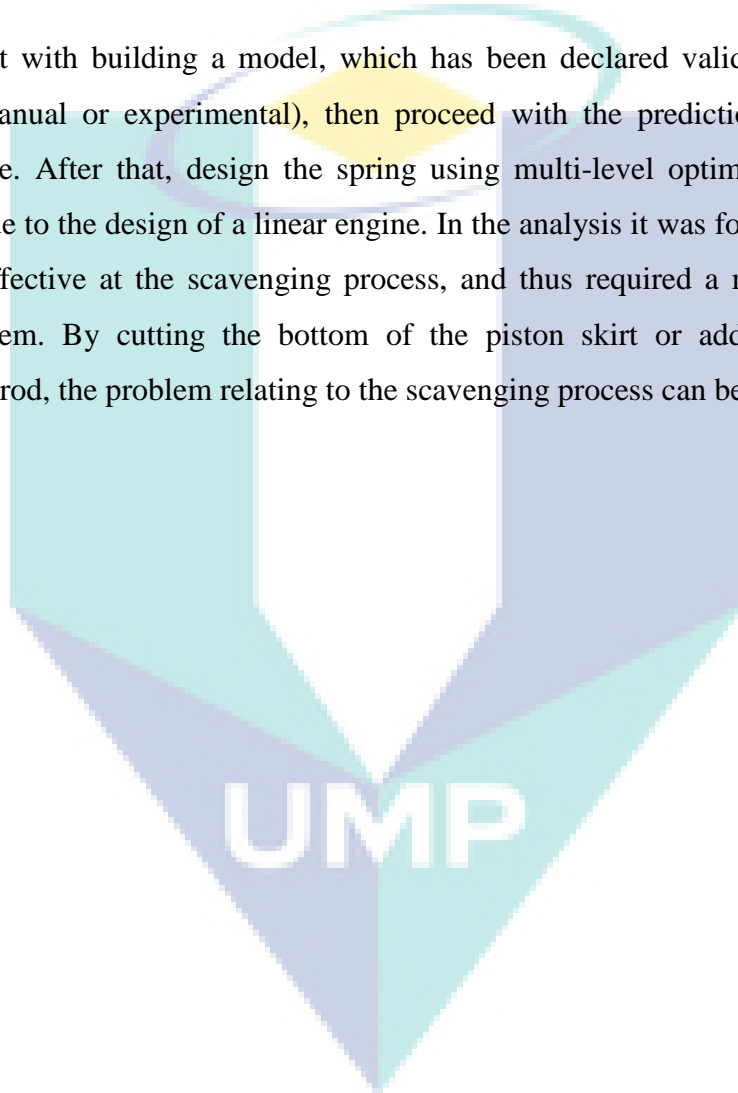
The first scenario proposes cutting the bottom of the piston skirt. It is more efficient because removing the area of the skirt results in less friction. The disadvantage is the high stress placed on the pin-hole regions that may damage the system more quickly.

The second scenario examines adding a lock to the connecting rod. Its purpose is not to reduce structural stress, which tends to be smaller. However, adding the lock will create more friction, although the value is not significant. By adding the lock, the spring

system movement is more stable, and it will not disturb the combustion process. The second scenario is therefore recommended. Designing the spring system as a whole, including the piston, is a discourse that needs to be realized. This system would be excellent provided the linear generator does not require stable linear motion.

4.7 CONCLUSION

Start with building a model, which has been declared valid after a validation process (manual or experimental), then proceed with the prediction of the engine's performance. After that, design the spring using multi-level optimisation techniques, and continue to the design of a linear engine. In the analysis it was found that the engine was less effective at the scavenging process, and thus required a modification of the spring system. By cutting the bottom of the piston skirt or adding a lock to the connecting rod, the problem relating to the scavenging process can be overcome.



CHAPTER 5

CONCLUSION AND RECOMMENDATIONS

5.1 INTRODUCTION

Design and simulation of a single cylinder high-speed SI linear engine has been carried out in this research. The discussion begins with the prediction of the engine's performance and compares it with the original engine. The result of the predicted performance is important data for the optimisation of the spring as well as a reference for studying the performance of the new linear engine design. After completing the preliminary design of the linear engine, an analysis and modification of its weaknesses are carried out. The process has been conducted step-by-step as indicated in each chapter. The conclusions of the study are as follows.

5.2 CONCLUSIONS

The prediction of the combustion pressure at variable speeds is very important data in this research. Although the area of maximum pressure is fairly different, it is still possible to design springs as a return cycle in a linear engine. The combustion pressure performance result is complicated. This is because the pressure is affected by many variables.

The design of a spring for a single cylinder spark ignition linear engine has been carried out, and a multilevel optimisation approach is an excellent technique to adopt. Shot-peened, chrome-vanadium alloy steel wire SAE 6150 of 7 mm diameter is an excellent spring design on cold process. The spring works excellently on dynamic load services and it satisfies all safety level requirements. Moreover, it also provides the best operating work at certain speeds and loads. Incomplete deflection of the spring could have an impact on the combustion process, including the scavenging port not opening properly and the pressure ratio decreasing.

The combustion process and performance are compared with the simulation. In general, at the three focused speeds, the combustion and performance decreased. Although there is a decrease in the combustion and performance, at a speed 1 m/sec the spring is still working quite well. On the other hand, at speeds of 4.1 and 4.6 m/sec the combustion misfires because the deflection of the spring significantly decreases. From 12 speed variables, only 50% of them allow the spring to work properly. The speed range of the linear engine is between 1 m/sec to 3.6 m/sec. Although the range of speeds of the engine is lower than the range of a conventional engine, the maximum power output is still higher. The final design result is 1.03 kW at 3.6 m/sec.

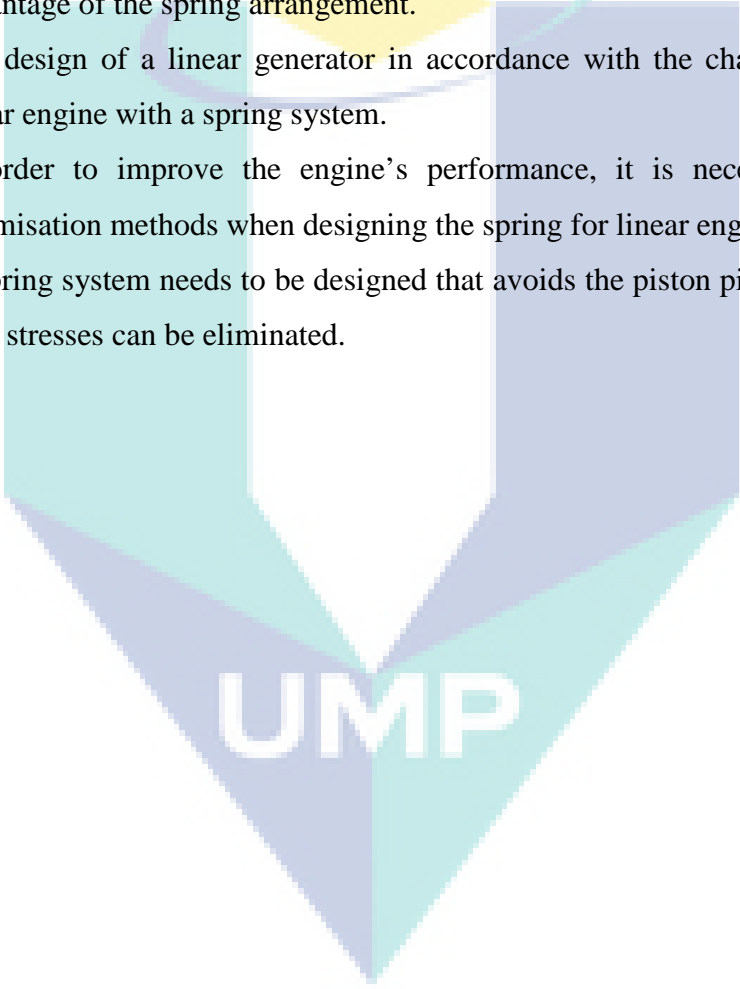
Motion analysis of a single cylinder of a high-speed spark ignition linear engine with a spring system as the return cycle has been investigated. Friction forces have a strong influence on piston acceleration. The TDC and BDC zones are locations where there is a pronounced fluctuation. Moreover, the piston has a rotary motion and influences the scavenging process. That purely free piston could affect the combustion process of the linear engine. In the case of this research, a modification of spring system needs to be done.

Modification of the spring system of a single cylinder spark ignition linear engine is necessary. According to thermal-structural stress analysis, scenarios such as removing the bottom of the piston skirt and adding a lock to the connecting rod could be adopted. The advantage of cutting the bottom of the piston skirt is it is more efficient because subtracting the area of the skirt incurs in less friction. The highest thermal stress occurs at pin-hole regions, in these areas the piston is damaged more quickly. Adding a lock at the connecting rod is a way of reducing structural stress. However, adding the lock provides more friction, although the amount is not significant. By adding the lock, the movement of the spring system will not disturb the combustion process. When installing the lock, the linear generator does not disrupt the system.

5.3 RECOMMANDATIONS FOR FUTURE RESEARCH

There are still many things that need to be developed for the design of a linear engine with spring system. Engine performance improvement is first on the agenda before developing a linear engine. These recommendations are as follows:

1. An ignition system for linear engines with a spring system needs to be developed. The system should be a simple ignition system which can take advantage of the spring arrangement.
2. The design of a linear generator in accordance with the characteristics of the linear engine with a spring system.
3. In order to improve the engine's performance, it is necessary to develop optimisation methods when designing the spring for linear engines.
4. A spring system needs to be designed that avoids the piston pin-holes so that the high stresses can be eliminated.

The logo for UMP (Université de Moncton) is a large, downward-pointing arrow shape. It is composed of four triangular sections meeting at a central point. The top-left and bottom-right sections are light blue, while the top-right and bottom-left sections are a slightly darker shade of blue. The letters 'UMP' are printed in a bold, white, sans-serif font across the center of the arrow.

UMP

REFERENCE

- Achten, P.A.J., van den Oever, J.P.J., Potma, J., and Vael, G.E.M., 2000, Horsepower with Brains: The Design of the Chiron Free Piston Engine, *SAE Technical paper* 2000-01-2545
- Achten, P.A.J., 2009, A Series Hydraulic Hybrid Drive Train, Off-Highway Directory, www.ifps.org | www.fluidpowerjournal.com (16 December 2009)
- Agrwal, G.K. 1978. Helical torsion springs for minimum weight by geometric programming, *Journal of Optimization and Applications*: Vol. 25, No. 2, pp:307-310
- Ahn, G.Y., Jeong, K.Y., 2004, Optimization of the spring design parameters of a circuit breaker to safety the specified dynamic characteristics, *International Journal of Precision Engineering and Manufacturing* Vol.5, No. 4, pp: 43-49
- Aichlmayr, H.T., 2002. *Design Considerations, Modeling, and Analysis of Micro-Homogeneous Charge Compression Ignition Combustion Free-Piston Engines*, PhD Thesis, The University of Minnesota.
- Aichlmayr, H.T., Kittelson, D.B. and Zachariah, M.R. 2002 A. Miniature free-piston homogeneous charge compression ignition engine-compressor concept—Part I: performance estimation and design considerations unique to small dimensions, *Elsevier Science, Chemical Engineering Science* 57, pp: 4161 – 4171
- Aichlmayr, H.T., Kittelson, D.B. and Zachariah, M.R. 2002 B. Miniature free-piston homogeneous charge compression ignition engine-compressor concept—Part II: modeling HCCI combustion in small scales with detailed homogeneous gas phase chemical kinetics, *Elsevier Science, Chemical Engineering Science* 57, pp: 4173 – 4186
- Algor. 2005. *Finite Element Analysis in Practice*. Algor. Pittsburgh. USA
- Allais, E., “Free-Piston Engine with Operatively Independent Cam”, U.S. Patent Application No. 416,959, Application filed September 9, 1982; U.S. Patent No. 4,480,599, Patent issued November 6, 1984.

- Annen, K.D., Stickler, D.B., and Woodroffe, J., 2003. Linearly-oscillating miniature internal combustion engine (MICE) for portable electric power, AIAA 2003-1113, 41st *Aerospace Sciences Meeting and Exhibit* 6-9 January, Reno, Nevada
- Annen, K.D., David B. Stickler, D.B., Woodroffe, J., 2008. Miniature Internal combustion Engine-generator for high energy density portable power, 26th *Army Science Conference*, December 1-4
- Ariffin, A.K., Mohamed, N.A.N., Fonna, S., 2006. Simulation of Free Piston Linear Engine Motion with Different Intake and Exhaust Port Positions. *Jurnal Kejuruteraan* 18, UKM, Malaysia pp 97-106
- Arshad, W.M., Backstrom, T., Thelin, P., Sadarangani, C., 2002, Integrated free-Piston generators: An Overview, Proceeding of the Nordic Workshop on Power and Industrial Electronics, http://www.ee.kth.se/php/modules/publication/2002/IR-EE-EME_2002_0021
- Arshad, W.M., Thelin, P., Bäckström, T., and Sadarangani, C. 2003, "Alternative electrical machine solutions for a free piston generator", *The Sixth International Power Engineering Conference (IPEC2003)*, Singapore, 27 - 29 November,
- Arshad, W.M., 2003, *A low-leakage linear transverse-flux machine for a free-piston generator*, Ph.D. thesis, ISBN 91-7283-535-4, TRITA-ETS-2003-08, ISSN 1659-674x, ISRN KTH/EME/ R 0304-SE.
- Arsie, I., Pianese, C., Rizzo, G., Flora, R., Serra, G., 1998, Development and validation of a model for mechanical efficiency in a spark ignition engine, *Society of Automotive Engineer* 99P-284
- Atkinson, C., Petreanu, S., Clark, N., Atkinson, R., McDaniel, T., Nandkumar, S., Famouri, P., "Numerical Simulation of a Two-Stroke Linear Engine-Alternator Combination," *SAE Technical Paper* 1999-01-0921, 1999.
- Atkinson, R.J., Nandkumar, S., Atkinson, C.M., and Petreanu, S., 1999, Development of linear alternator-engine for hybrid electric vehicle applications, *IEEE transactions on vehicular technology*, Vol. 48. No. 6, pp.1797- 1802

- Balling, R.J., Safieszcznski-Sobieski, J. 1994. An Algoritm for solving the system-level problem in multilevel optimization, *NASA Contractor report* 195015, ICASE Report No. 94-96, pp:1-23
- Baumuller, A., and E. Schmierder, E., 2001. Field-test and market introduction of a 10 kW stirling engine as CHP-and Solar-Module, 10th *International Stirlig engine conference* 2001 (10th ISEC), 24-26 September 2001, Osnabruck, Germany, pp 106-113
- Bos, M. 2007. *Validation Gt-Power Model Cyclops Heavy Duty Diesel Engine*, MSc. Thesis Reportnumber WVT 2007, The Technical University of Eindhoven
- Brandhorst, H.W., 2007. Development of a 5 kW Free-Piston Stirling Space Convertor, *AIAA Technical Conference*.
- Braun, A. T. and Schweitzer, P. H., 1973. The Braun Linear Engine. *SAE Technical Paper* 730185.
- Bruening, D., Garnet, T., Amarashinghe, S., 2003, An infrastructure for adaptive optimization, *International Symposium on Code Generation and Optimization*, pp:265-275
- Buck, E.S., 1991. Two plus two stroke opposed piston heat engine, U.S. Patent Application No. 4,996, 953, Application filed, March 5, 1991
- Cawthorne W.R., Famouri, P., Chen, J., Clark, N.N., McDaniel, T.I., Atkinson, R.J., Nandkumar, S., Atkinson, C.M.,and Petreanu, S., 1999. Development of a Linear Alternator–Engine for Hybrid Electric Vehicle Applications, *IEEE Transaction on Vehicular technology*, Vol 48, No. 6, pp. 1797-1802
- Cawthorne, W.R., Famouri, P., Clark, N., 2001. Integrated design of linear alternator/engine system for HEV auxiliary power unit, *IEEE*, 0-7803-709, pp. 267-274
- Cawthorne, W.R. Parviz Famouri, P. Chen, J. Clark, N.N. McDaniel, T.I. Atkinson, R.J. Nandkumar, S. Atkinson, C.M. and Petreanu, S. 1999. Development of a Linear Alternator–Engine for Hybrid Electric Vehicle Applications, *IEEE TRANSACTIONS ON VEHICULAR TECHNOLOGY*, VOL. 48, NO. 6, pp. 1797-1802

- Chen, A., Arshad, W.M., Thelin, P., Zheng, P., 2004, Analysis and Optimization of a Longitudinal Flux Linear Generator for Hybrid Electric Vehicle Applications, *IEEE VTS Vehicle Power and Propulsion Symposium*, VPP 04, France October
- Clark, N., Nandkumar, S., Atkinson, C., Atkinson, R., McDaniel T., and Petreanu, S., 1998. Modeling and development of a linear engine, *ASME Spring Conference, Internal Combustion Engine Division* **30** (2), pp. 49–57.
- Clark, N., Nandkumar, S., Famouri, P. 1999. Fundamental Analysis of a Linear Two-Cylinder Internal Combustion Engine. *SAE Technical Paper* 982692.
- Clark, N., McDaniel, T., Atkinson, R., Nandkumar, S., Atkinson, C., Petreanu, S., Tennant C., Famouri, P., Modeling and Development of a Linear Engine,” ICE-Vol. 30-2 *Proceeding of the Spring Technical Conference of the ASME Internal Combustion Engine Division*, Book No. G1074B, 1998.
- Clark, N., Nandkumar, S., Atkinson, C., Atkinson, R., McDaniel, T., Petreanu, S., Famouri, P., “Operation of a Small Bore Two-Stroke Linear Engine,” *ASME 98- ICE-120*, 1998.
- Christopher M.A., Petreanu, S., Clark, N.N., Atkinson, R.J., McDaniel, T.I., Nankumar, S., and Famouri ,P. 1999. Numerical Simulation of a Two-Stroke Linear Engine_Alternator Combination, *SAE Technical Paper Series*, 1999-01-0921
- Dechaumphai, P., Lim, W. 1996. Finite Element Thermal-Structural Analysis of Heated Products, *Thamasai International Journal of Science and Technology*, Vol. 1, Issue 01.
- Del Llano-Viscaya, L., Rubio-Gonzalez, C., Mesmacque, G., Cervantes-Hernandez, T., 2006, Multiaxial fatigue and failure analysis of helical compression springs, *Elsevier, Engineering Failure Analysis* **13**, pp: 1303-1313
- Derek B., Garnet, T. And Amarasinghe, S. 2003. An Infrastructure for Adaptive Dynamic Optimization, *IEEE International Symposium an Code Generation and Optimization*, 265-275
- Deutsch, P., Vysoky, O., 2006. In-cycle thermodynamic model of linear combustion engine, *Proceedings of the 2006 IEEE International Conference on Control Applications* Munich, Germany, October 4-6,

- Esfahanian, V., Javaheri, A., Ghaffapour, M. 2006. Thermal Analysis of an SI Engine Piston Using Different Combustion Boundary Condition Treatments, *Science Direct, Applied Thermal Engineering* 26, pp: 277-287
- Fahs, B., Bose, S., Crum, M., Slechta, B., Spadini, F., Tung, T., Patel, S.J., Lumetta, S.S. 2001. Performance characteristic of a hardware mechanism for dynamic optimization, *Proceeding of the 34th ACM/IEEE International Symposium on Microarchitecture*, 2001, pp:16-27
- Farmer, H. O., 1947. Free-Piston Compressor-Engines." *Proceedings of the Institution of Mechanical Engineers*, vol. 156, pp. 253-271
- Fathallah, A.Z.M., Bakar, R.A., 2009, Prediction Studies for the Performance of a Single Cylinder High Speed Spark Ignition Linier Engine with Spring Mechanism as Return Cycle, *American J. of Engineering and Applied Science*, 2 (4) pp720-727
- Ferguson, C.R. 1986. *Internal combustion engine applied thermosciences*. New York. Jon Wiley & Sons
- Ferguson, C.R., Kirkpatrick, A.T., 2001, *Internal combustion engine applied thermosciences*, 2nd Ed, Jon Wiley & Sons.
- Flynn, G. Jr., 1957, "Observations on 25,000 Hours of Free-Piston-Engine Operation", *SAE Transactions*, Volume 65, pp 508-515.
- Fonna,S., Mohammed, N.A.N. Arifin., A.K., 2005. Cycle effect inversigation of free piston linear engine, *National Seminar on Computational & experimental Mechanic (CEM)*, bangi, Malaysia may 17-18, pp:249-257
- Fredriksson J., and Denbratt I., 2004, Simulation of two-stroke free piston engine, *SAE series publication* 2004-01-1871
- Frey, D. N., Klotsch, P., Egli, A., 1957. "The Automotive Free-Piston-Turbine Engine", *SAE Transactions*, Volume 65, pp 628-634.
- Galitello K.A., 1989. Two stroke cycle engine, U.S. Patent Application No. 4,876, 991, Application filed, October 31, 1989
- Gamma., T., 2004, GT-Power manual, Version 6.1, *Gamma Technologies*

- Goldsborough S.S., Van Blarigan, P., 2003, Optimizing the Scavenging System for a Two-Stroke Cycle, Free Piston Engine for High Efficiency and Low Emissions: A Computational Approach, *SAE Technical paper* 2003-01-0001
- Gotoh, T. Imaizumi, T. 2000. Optimization of force action line with new spring design on the macpension for riding comfort, *SAE Technical Paper Series*, 2000-01-0101
- Hansson J., Lekssel M., Carlsson F., 2005, Minimization power pulsation in a free piston energy converter, *proceedings of the 11th European Conference on power electronics and Applications (EPE05)*, Dresden, Germany.
- Hansson J., Leksell M., Carlsson F., Sadarangani C., 2005, Operation Strategies for a free piston energy Converter, *proceeding of the fifth International Symposium on Linear Drivers for Industry Applications (LDIA05)*, Kobe-Awaji, Japan
- Hansson J., Leksell M., 2006, Performance of a Series Hybrid electric vehicle with a free-piston energy converter, *Proceedings of the 2006 IEEE Conference on Vehicle Power and Propulsion (VPPC2006)* Windsor, UK.
- Hansson, J., Leksell, M., Carlsson, F., 2005, Minimizing Power Pulsations in a Free Piston Energy Converter, *Proceedings of the 11th Europea Confrence Power Electronic and Applications (EPE05 September 2005)*
- Heintz, R. P., 1989 ‘Free-Piston Engine Pump’, U.S. Patent Application No. 150,390, Application filed May 16, 1980; U.S. Patent No. 4,369,021, Patent Issued January 18, 1983.
- Henry W. Brandhorst, H.W. and Chapman, P.A. 2008. New 5k Wfree-piston Stirling space convertor developments, *Science direct, Acta Astronautica* 63 (2008) 342 – 347
- Heywood, J.B. 1988. *Internal combustion engine fundamentals*. USA: McGraw-Hill.
- Hibi, A., Ito, T., 2004. Fundamental test results of a hydraulic free piston internal combustion engine, *Proc. Instn Mech. Engrs* Vol. 218 Part D: J. Automobile Engineering
- Hoag, K.L. 2006. *Vehicular Engine Design Powertrain*. New York. Springer Wien.
- Hoshino, T., 2003. Preliminary test results on 200 We free-piston stirling engine converter, *AIAA 2003-6094, 1st International Energy Conversion Engineering Conference* 17-21 August, Portsmouth, Virginia.

- Houdyschell, D., 2000, *A Diesel Two-Stroke Linear Engine*, Master thesis in Mechanical Engineering, Department of Mechanical and Aerospace Engineering, West Virginia University
- Hu, Y., Hibi, A., 1990. Hydraulic free piston Internal combustion Engine (Outline of the Fundamental test apparatus with Oppose Pistons), *JSME* 56, 89-1131 B Series pp 343-346
- Hu, Y., Hibi, A. 1990. Hydraulic free piston Internal combustion Engine (Experiment Investigation on the Fundamental test apparatus with Opposed piston), *JSME* 56, 89-1372 B Series pp 339-344
- Iliev, M. D., Kervanbashiev, S. S., Karamanski, S. D., Makedonski, F. M., “Method And Apparatus For Producing Electrical Energy From A Cyclic Combustion Process Utilizing Coupled Pistons Which Reciprocate In Unison”, U.S. Patent Application No. 431,119 (CUV “Progress”), Application filed September 30, 1982; U.S. Patent No. 4,532,431 (CUV “Progress”), Patent Issued July 30, 1985.
- Innas, 2010, Two cars: same weight, same size, same engine, same traction, same performance, was download in May 6, 2010, available at: <http://www.innas.com/Assets/files/Hydriddbrochure.pdf> (10 January 2010)
- Issakson S, 2002. Simulation of a Two-Stroke Compression Ignition Hydraulic Free Piston Engine, *GT-Suite user conference, October 30*
- Jakob F and I. Denbratt, 2004. Simulation of two-stroke free piston engine, *SAE Technical paper series*, 2004-01-1871
- Juvinall, R.C. and Marshek, K.M. 2006, *Fundamental of Machine Component Design*, John Wiley & Sons Asia, 4th Ed, ISBN: 13978-0-471-74285-2, pp: 290-339 and 469-492
- Klemann, A.P., Dabadie, J.C., Henriot, S., 2004. Computational Design Studies for a High Efficiency and Low-Emissions Free Piston Engine Prototype, *SAE Technical paper series*, 2004-01-2928
- Kos, F. J., 1991. “Computer Optimized Hybrid Engine”, U.S. Patent Application No. 556,872, Application filed July 20, 1990; U.S. Patent No. 5,002,020, Patent Issued March 1991.

- Kowalewicz, A., 1984, *Combustion systems of high-speed piston I.C. engine*, Elsevier Science Publishers, Amsterdam, the Netherlands
- Kwankaomeng, S. 2008. *Design of a free-piston stirling engine-pump*, PhD Thesis, University of Wisconsin-Madison
- Lane, N.W., Beale, W.T., 1997, Free-piston Stirling design features, *8th International Stirling Engine Conference*, May 27-30, University of Ancona, Italy
- Larrowe, V.L. and M.M. Spancer, 1958. *Analog computer simulation of a free-piston engine*, The University of Michigan, Industry program of the college of engineering, IP-239
- London, A. L. and Oppenheim, A. K., 1952. The Free-Piston Engine Development-Present Status and Design Aspects. *Transactions of the ASME*, vol. 74, no. 2, pp. 1349-1361. *Based upon ASME Technical Paper 52-S-17.*
- Martin Goertz, M., Peng, L., 2000. Free Piston Engine Its Application and Optimization, *SAE Technical Paper Series*, 2000-01-0996
- Mikalsen, R., and Roskilly, A.P., 2008. The design and simulation of a two-stroke free-piston compression ignition engine for electrical power generation, *Science Direct, Applied Thermal Engineering* 28, pp. 589-600
- Mikalsen, R., and Roskilly, A.P., A review of free-piston engine history and applications, Science Direct, *Applied Thermal Engineering* 27 (14–15) (2007), pp. 2339–2352
- Mikalsen, R., Roskilly, A.P., 2008, Coupled Dynamic-multidimensional modeling of free-piston engine combustion, *Applied Thermal Engineering* 85, Science Direct, 89-95
- Nankumar S., 1998, *Two stroke Linear Engine*, MSME Thesis, The College of Engineering and Mineral Resources, West Virginia University.
- Nandkumar, S., 1998, *Two-Stroke Linear Engine*, Master thesis in Mechanical Engineering, Department of Mechanical and Aerospace Engineering, West Virginia University
- Němeček, P., Vysoký, O., 2007, Control of two-stroke free-piston generator, was down loaded in April, 12, 2010, available at:
http://www3.fs.cvut.cz/web/fileadmin/documents/12241-BOZEK/publikace/2007/2007_076_01.pdf

- Nerstrom, J. S., "Two-Cycle Internal Combustion Engine Including Means For Varying Cylinder Port Timing", U.S. Patent Application No. 376,705 (Outboard Marine Corporation), Application filed May 10, 1982; U.S. Patent No. 4,516,540 (Outboard Marine Corporation), Patent Issued May 14, 1985.
- Nik A.M.N., A.K. Ariffin, S. Fonna, 2006, Simulation of a Two-Stroke Spark Ignition Free Piston Linear Motion, *Jurnal Teknologi*, 44 (Jun) 2006, Universiti Teknologi Malaysia, 27-40
- Noda, N., Hetnarski, R.B., and Tanigawa, Y.2003. *Thermal Stress*. New York: Taylor and Francis, 2nd Ed.
- Noren, O.B. and R.L. Erwin, 1958. The future of the free-piston engine in commercial vehicles, *SAE Transactions* **66**, pp. 305–314.
- Parades, M., Sarfor, M., Masclet, C., 2001, An optimization process for extension spring design, *ELSEVIER, Comput. Methods Appl. Engrg.* 191, pp:783-797
- Pascara, R.P. 1928. Motor compressor apparatus. US Patent 1,657,641
- Pascara, R. P., 1941. Motor Compressor of the Free Piston Type." U. S. Patent 2,241,957.
- Petele, M. 2009. Spring Calculation,
<http://www.mitcalc.com/doc/springs/help/en/springs.htm> , Copyright 2003-2009, all rights reserved.
- Petreanu, S., 2001, *Conceptual analysis of a four-stroke linear engine*, Doctor of Philosophy thesis in Mechanical engineering, Department of Mechanical and Aerospace Engineering, West Virginia University
- Pohl S.K., Markus Graf, M., 2005. Dynamic Simulation of a Free-Piston Linear Alternator in Modelica, *Proceedings of the 4th International Modelica Conference*, Hamburg, March 7-8,
- Porterio. J.L. 2010. Spring design optimization with fatigue, Master Science Thesis, Mechanical Engineering, University of South Florida.
- Qingfeng L, J. Xiao, Z. Huang, 2008. Simulation of a Two-Stroke Free-Piston Engine for Electrical Power Generation, *Energy & Fuels* 22, pp: 3443–3449
- Rao, S.S., 1996, *Engineering optimization theory and practice*, 3rd Ed, John Wiley and Sons.

- Reddy, J.N. 2006. *An Introduction to the Finite Element Method*, McGraw Hill, 3rd Ed, International Edition, Singapore.
- Rittmaster, P. A., Booth J. L. 1980. Hydraulic Engine”, U.S. Patent Application No. 110,771, Application filed January 9, 1980; U.S. Patent No. 4,326,380, Patent Issued April 27, 1982.
- Ruzicka, M., Doubrava, K., 2005, Loading regimes and designing helical coiled springs for safe fatigue life, *RES. AGR.ENG*, 51,(2) pp:50-55
- Saiful A.Z., M.N. Karsiti., B.S. Iskandar., A.R.A. Aziz, 2008, Starting of Free-Piston Linear Engine-Generator by Mechanical Resonance and Rectangular Current Communication, *IEEE Vehicle and Propulsion Conference (VPPC)*, September 3-5, Harbin, China,
- San, M.N. 2008. Design and Kinematics Analysis of Piston. *GMSARN International Conference on Sustainable Development: Issues and Project for the GMS*
- Slaby, J.G., 1984., Overview of NASA Lewis Research Center Free-Piston Stirling Engine Activities, *Nineteenth Intersociety Energy Conversion Engineering Conference cosponsored by the ANS, ASME, SAE, IEEE, AIAA, ACS, and AIChE* San Francisco, California, August 19-24
- Stone, R. 1997. *Introduction to internal combustion engines*. USA: Society of Automotive Engineers, Inc.
- Underwood, A.F, 1957. The GMR 4-4 “HYPREX” engine – A concept of the free-piston engine for automotive use, *SAE Transactions* **65**, pp. 377–391.
- Van Blarigan, P., Paradiso, N., and Goldsborough, S. S., 1998. Homogeneous Charge Compression Ignition with a Free Piston: A New Approach to Ideal Otto Cycle Performance, *SAE Technical Paper* 982484.
- Van Blarigan, P., 2001. Free-Piston Engine. U. S. Patent 6,199,519.
- Van Blarigan, P., 1999. Homogeneous charge compression ignition with a free piston: a new approach to ideal Otto cycle performance, *Proceedings of the 1999 U.S DOE Hydrogen Program Review* NREL/CP-570-26938

- Van Blarigan, P., Paradiso, N., and Goldsborough, S.S., 1998, Homogeneous Charge Compression Ignition with a Free Piston: A New Approach to Ideal Otto Cycle Performance, SAE Technical Paper 982484
- Van Blarigan, P., 1999, Homogeneous Charge Compression Ignition with a Free Piston: A New Approach to Ideal Otto Cycle Performance, *Proceedings of the 1999 U.S DOE Hydrogen Program Review* NREL/CP-570-26938
- Van Blarigan, P., 2002, Advanced Internal Combustion Electric generator, Proceedings of the 2002 U.S. DOE Hydrogen Program Review NREL/CP-610-32405
- Wood, J.G., Lane N.W., and Beale, W.T., 2001, Preliminary Design of a 7 kWe Free-Piston Stirling Engine with Rotary Generator Output, *the proceedings of the 10th International Stirling Engine Conference (10th ISEC)*, 24 - 27 Sept. 2001, Osnabrück/ Germany
- Wood, J.G., and Lane, N., 2004, Advanced Small Free-Piston Stirling Convertors for Space Power Applications, *American Institute of Physics*, <http://proceedings.aip.org/proceedings/confproceed/699.jsp>
- Yamada, Y., Saitoh, T., Ishida, M. Uzumachi, K., Suzuki, H., Teratoko, K., 2000, Improve fatigue strength of valve springs and sheet springs by application of a new fine shot peening technology, *SAE Technical Paper series*, 2000-01-0791,